



STUDY REPORT No.58 (1996)

FIELD TESTING OF HOUSE TIMBER PILE FOUNDATIONS UNDER LATERAL LOADING

Stuart J. Thurston

The work reported here was funded jointly by the Building Research Levy
and the Foundation for Research, Science and Technology from
the Public Good Science Fund.

FIELD TESTING OF HOUSE TIMBER PILE FOUNDATIONS UNDER LATERAL LOADING

BRANZ Study Report SR 58

S.J. Thurston

REFERENCE

Thurston, S.J. 1996. Field Testing of House Timber Pile Foundations Under Lateral Loading. Building Research Association of New Zealand. Study Report SR 58, Judgeford, Wellington.

KEYWORDS

Piles; Foundations; Timber; Earthquake; Seismic; Wind; Racking; Cyclic; Tests; Experimental; Houses; Residential Buildings; Bracing; Design Loads.

ABSTRACT

Cyclic lateral load tests were performed on several representative pile systems used to brace New Zealand houses. Anchor, braced, fixed-head normal and driven piles as defined within the light timber framing standard (NZE 3604) were tested in soils which were close to the minimum bearing strength allowed by NZS 3604 including clay, silt, sand and peat. The report includes test details and measurements. For each pile and soil type, non-linear equations were fitted to the measured hysteretic peaks. Wind design strengths were obtained directly from these equations. Earthquake design strengths were obtained from simulation by time history computer analysis using a model of the measured pinched hysteresis loops.

Preface

This study forms the second phase of an investigation into the wind and earthquake racking resistance of timber piles used under New Zealand houses. The first phase (see BRANZ Study Report No 46) investigated the basis for the design values specified in the New Zealand Standard NZS 3604 and also included some laboratory testing. This second phase reports on site measurements of the lateral strengths of piles when cast into the ground. Time history computer analytical simulation was used to determine earthquake static design loads from the averaged measured pinched hysteresis loops.

Acknowledgments

The author acknowledges financial support for this project from the Building Research Levy and the Public Good Science Fund of the Foundation for Research, Science and Technology. The author wishes to thank Mr Keith Morgan of Kapiti Timber Traders for allowing his property to be used for pile testing; Mr John Reelick of Timberlink Connectors for their donation of pile connectors and Mr Don Macintyre of James Hardie and Co Ltd for the donation of fibre-cement sheets, permission to reference commercial test results, and permission to reproduce a diagram from their foundation brochure.

Readership

This report is intended for structural engineers, architects, designers, manufacturers and others researching the earthquake and wind resistance of low-rise buildings.

Contents

Page No.

1.	INTRODUCTION.....	2
1.1	Wind and Earthquake Design and Performance of New Zealand House Foundation Systems.....	2
	House Pile Types Evaluated in this Report	3
1.2	Preliminary Investigation into Lateral Load Resistance of House Pile Foundation Systems.....	6
1.3	Pile Lateral Load Capacity in Soil.....	6
1.4	Outline of Report	7
2.	BRIEF LITERATURE SURVEY	9
3.	STRENGTH REQUIREMENTS FOR HOUSE CONNECTION TO PILES	10
4.	TEST PROGRAM	14
4.1	Introduction.....	14
4.2	Site Locations and Soil Conditions.....	16
4.3	General Test Details.....	20
	4.3.2 Anchor Pile Tests	23
	4.3.3 Braced Pile Tests	25
	4.3.4 Shear Pile Tests	33
	4.3.5 Driven Pile Tests	37
5.	RESULTS	39
5.1	Anchor Piles.....	39
	5.1.1 Data Reduction	39
	5.1.2 Experimental Observations	39
5.2	Braced Piles	44
	5.2.1 Data Reduction	44
	5.2.2 Experimental Observations	44
5.3	Shear Piles	46
	5.3.1 Data Reduction	46
	5.3.2 Experimental Observations	46
5.4	Driven Piles	48
	5.4.1 Data Reduction	48
	5.4.2 Experimental Observations	48
6.	DERIVATION OF DESIGN LOADS	49
6.1	Design Philosophy	49
6.2	Derivation of Average Parent Curves	49

FIGURES	Page No.
Figure 1. House Behaviour Under Earthquake Loading Assumed in NZS 4203.....	3
Figure 2. Actual House Pile Foundation Stable Hysteresis Loops at Large Deflections.....	4
Figure 3. Seismic or Wind Forces on an Anchor Pile.....	4
Figure 4. Soil Pressures on Piles with a Restrained Pile Head	5
Figure 5. Derivation of Element Design Loads.....	8
Figure 6. Horizontal Load Transfer From Ground to House	10
Figure 7. Design Forces at Top of Braced Pile From SANZ (1990)	12
Figure 8. Design Forces at Top of Braced Pile from Johnstone (1994).....	13
Figure 9. Lateral Loading of Shear Piles.....	14
Figure 10. Sheet Bracing of Normal Piles (James Hardie and Coy, 1994).....	15
Figure 11. Location of Test Piles	16-18
Figure 12. Relationship between Scala Penetrometer Soundings and Depth in the Soil.....	19
Figure 13. Relationship between Shear Vane Strength and Depth in the Soil.....	20
Figure 14. Anchor Pile Test Details	21
Figure 15. General Photographs of Test Arrangement.....	22
Figure 16. Photographs of Anchor Pile Tests	24
Figure 17. Braced Pile Test Details.....	26-28
Figure 18. Photographs of Braced Pile Tests	29-32
Figure 19. Photographs of Shear Tests.....	35-36
Figure 20. Test Set-up and Photograph of Driven Pile Tests.....	38
Figure 21. Failure of Group 1 Anchor Pile J4.....	40
Figure 22. Failure of Group 1 Anchor Pile J3.....	41
Figure 23. Failure of Pile W13 in Flexure	42
Figure 24. Failure of Footing at Pile M1 (photograph taken after the soil was dug away).....	43
Figure 25. Damage and Deformations Observed in Braced Pile Tests.....	45
Figure 26. Photographs of Horizontal Sliding Movement of Shear Piles in the Ground	47-48
Figure 27. Relationship Between Deflection and Assumed Damping Ratio For Anchor Piles.....	54
Figure 28. Predicted Force Versus Deflection For Anchor Pile Under NZA Earthquake (T = 0.4 seconds, damping ratio = 5%)	54
Figure 29. Relationship Between Deflection and Assumed Damping Ratio for Various Shapes of Hysteresis Loops For Anchor Piles of Period 0.4 Seconds.....	55

6.3	Earthquake Design Loads	50
6.3.1	Background to NZS 3604 Earthquake Design Loads	50
6.3.2	Pinched Hysteresis Loops	50
6.3.3	Pinched Hysteretic Loop Matching	51
6.3.4	NZA Artificial Earthquake Record	51
6.3.5	Determination of Maximum Seismic Mass.....	51
6.3.6	Summary of Procedure to Obtain Pile Seismic Design Loads	52
6.3.7	Verification of PhylMas	52
6.3.8	Assumptions Inherent in Earthquake Load Analysis	53
6.4	Wind Design Strengths	55
6.5	Additional Factors	56
6.6	Comparison with Current NZS 3604 Loadings	57
6.7	Comparison with SR 46.....	58
7.	SUMMARY AND CONCLUSIONS.....	59
8.	REFERENCES.....	60
Appendix A.	Sample Hysteresis Loops	62
Appendix B.	Parent Curves	68
Appendix C.	Best Fit Curves.....	86
Appendix D.	Fitting PhylMas Loops to Experimental Data.....	94
Appendix E.	Earthquake and Wind Pile Design Loads.....	100
Appendix F.	Soil Properties	106
Appendix G.	Proprietary Products Used	128
Appendix H.	Test Hysteresis Loops (Separate Volume)	

1. INTRODUCTION

1.1 Wind and Earthquake Design and Performance of New Zealand House Foundation Systems

New Zealand timber framed houses built this century have generally performed well under extreme wind and severe earthquake loading. Earthquake damage has been limited to collapse of unreinforced brick chimneys (and to a lesser extent brick veneers), failure of some forms of pile foundations and, in a few instances, racking failure of lower storey walls (Cooney, 1979). Wind damage is usually limited to failure of roof systems (sheeting and framing). Foundation failures have usually been attributed either to inadequate joint detailing or to failure to provide a load path through which lateral loads can be transmitted from the structure to the ground. These issues were partially addressed in the 1978 edition of the non-specific light timber framed code (SANZ, 1978). Engineering principles have been more rigorously applied in the 1990 edition (SANZ, 1990). However, as no major earthquake has occurred in densely populated areas since the 1931 Napier earthquake, modern construction has not been well tested.

Most new New Zealand houses are designed and built in accordance with the standard for Light Timber Frame Buildings not Requiring Specific Design - NZS 3604:1990 (SANZ, 1990). This standard specifies the earthquake and wind lateral load resistance required for a particular house foundation system as a function of the house geometry and weight. The standard also provides design strengths for various foundation configurations; e.g., the earthquake strength of an anchor pile is given as 70 BU (ie 3.5 kN). A house designer must provide a foundation system such that the sum of the foundation element strengths equals or exceeds the lateral forces specified by the standard. Although the designer need not consider the effects of torsion or the effect of combining foundation elements of different stiffnesses, the standard does place some limitation on the distribution of foundation elements to partially address these problems.

The assumptions and philosophy used to derive design loads for NZS 3604 (SANZ, 1990) are outlined by Thurston and King (1992) and Thurston (1993). This standard developed an engineering rationale for the complete design process, from derivation of design loads through to provision of load-resisting elements with a traceable load path from the loaded element through to the foundations. It has long been acknowledged, however, that timber framed buildings have greater resilience than expected by the application of strict engineering principles. Such reserve strength comes from their system behaviour, which ensures that load sharing and composite action occurs under wind or earthquake loading. This enhances overall building performance. In addition, houses have many "non-structural" elements which contribute significantly to their strength. However, whilst true for the part of the house above floor level, piled foundation systems are unlikely to have significant reserve strength due their lack of redundancy.

The earthquake and wind loadings specified in NZS 3604 (SANZ, 1990) were derived from a draft version of the loadings standard NZS 4203 (SNZ, 1992a) and assume a building of natural period (T) of 0.4 seconds and a structural ductility (μ) of 4, ie

assuming that the building performs in an elasto-plastic manner as shown in Figure 1. However, at large seismic deflections, timber systems such as houses exhibit pinched hysteretic behaviour similar to that shown in Figure 2. The concept of a single natural period or a ductility ratio is not applicable to such systems. The difference between the hysteresis loop shape assumed within NZS 4203 and thus by NZS 3604 (Figure 1) and the real shape (Figure 2) should be taken account of when deriving design values for bracing elements. Thurston (1993) noted that NZS 3604 effectively assumes a ductility (μ) of 2 for braced and anchor piles, (ie less ductile than the value of $\mu = 4$ assumed in NZS 3604) and reduced the assumed pile design resistance accordingly.

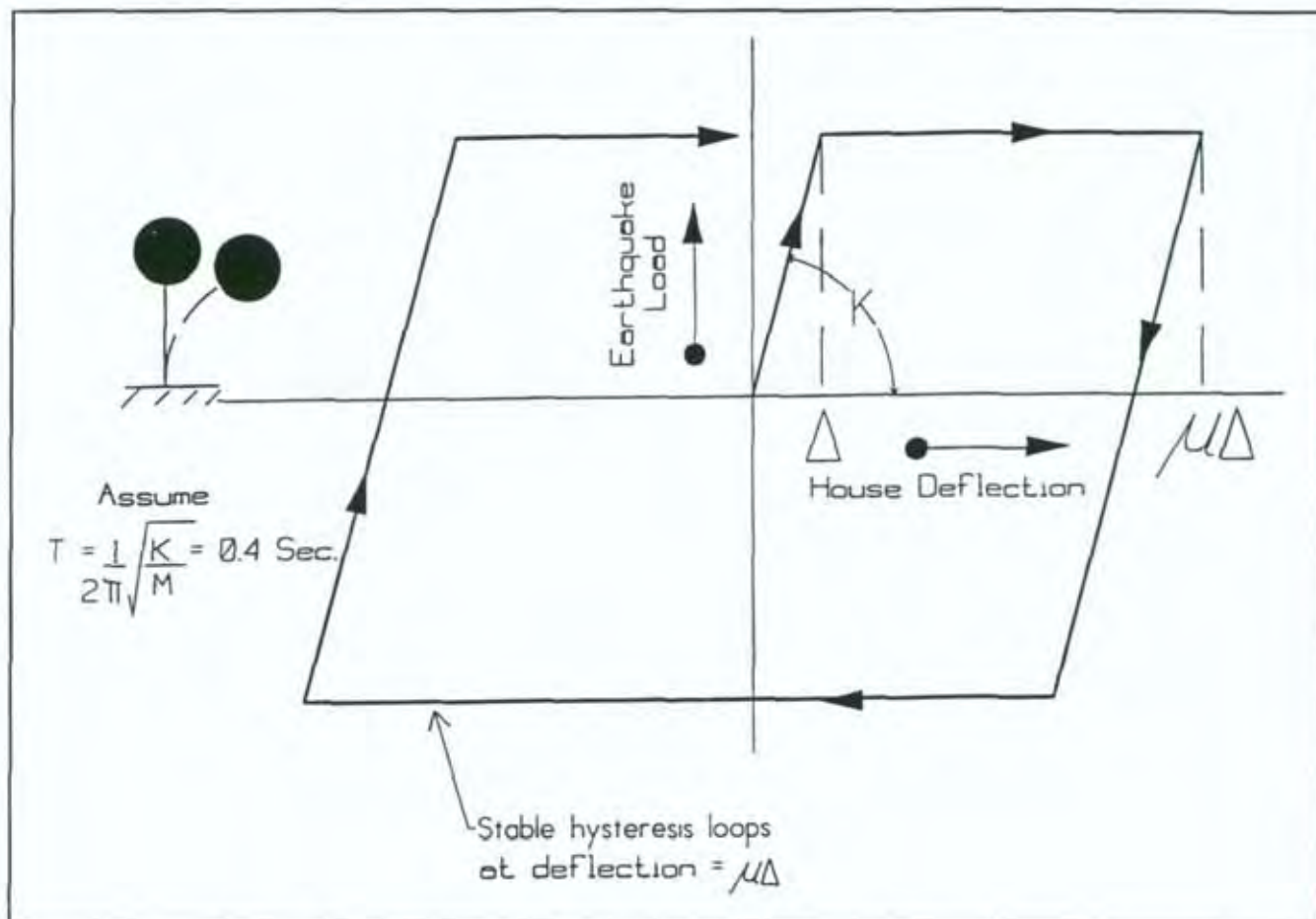


Figure 1. House Behaviour Under Earthquake Loading Assumed in NZS 4203

House Pile Types Evaluated in this Report

Four types of timber piles were tested. The first three are fully defined in NZS 3604 (SANZ, 1990), namely anchor piles, braced piles and driven piles. The fourth type was a "normal pile" with the top rotationally restrained and is referred to as a "shear pile" in this report for reasons described in the paragraph below. A "normal" pile is also described in NZS 3604.

Free-standing house piles are designed to transfer both vertical and horizontal forces from the house into the soil. The horizontal forces originate mainly from earthquake or wind loads whereas the vertical forces usually come from the weight of house and contents although they can also be caused by earthquake or wind loads. To transfer horizontal forces, piles act as vertical cantilevers and usually resist both a moment and a shear force at the soil level, as

shown in Figure 3. However, in some situations the pile is rotationally restrained at the top and only transfers shear forces in the soil. A braced pile, or pile fastened to sheet bracing, approaches this horizontal shear transfer situation as indicated in Figure 4. Under lateral load a normal pile with the top rotationally restrained shears through the soil as shown in Figure 4 and so has been referred to as a "shear pile".

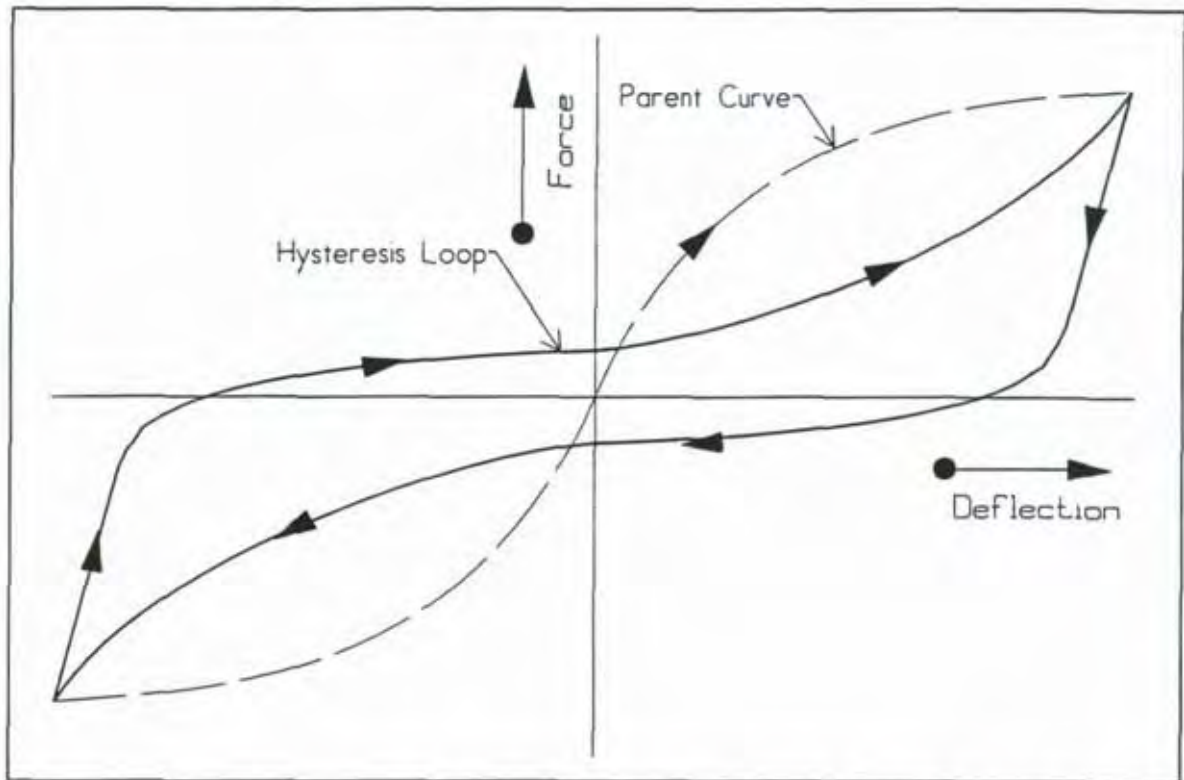


Figure 2. Actual House Pile Foundation Stable Hysteresis Loops at Large Deflections

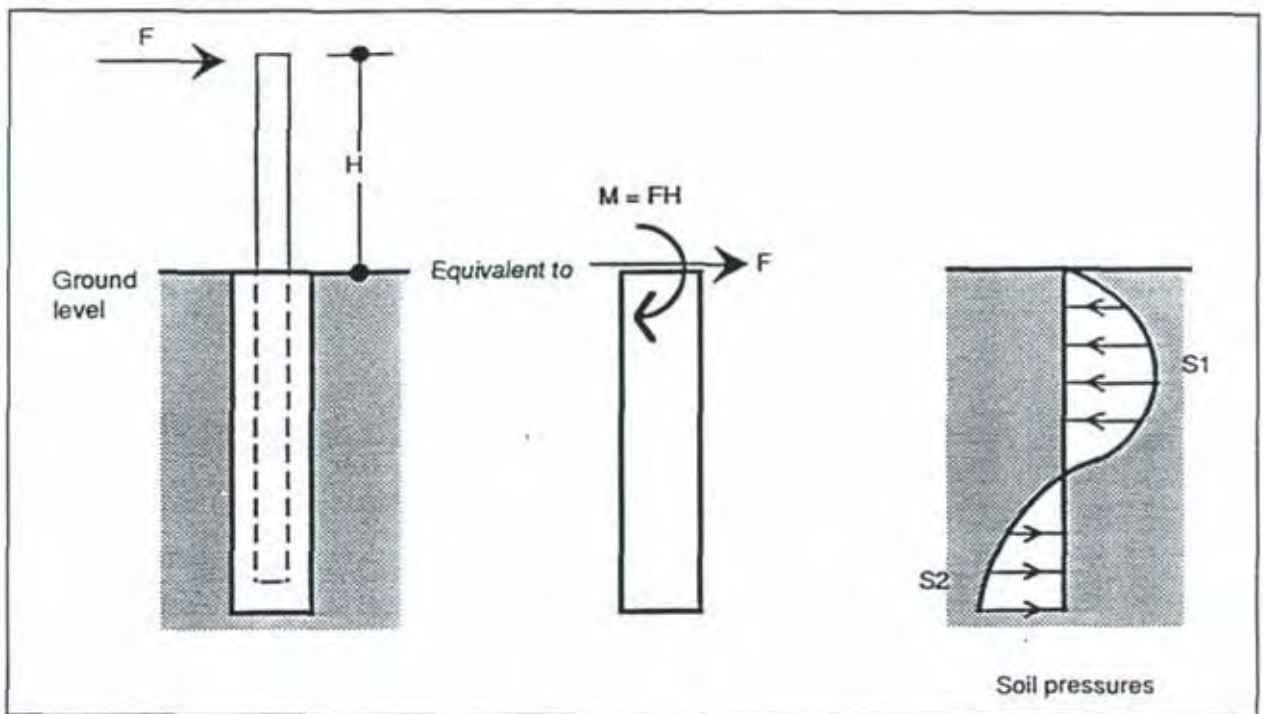


Figure 3. Seismic or Wind Forces on an Anchor Pile

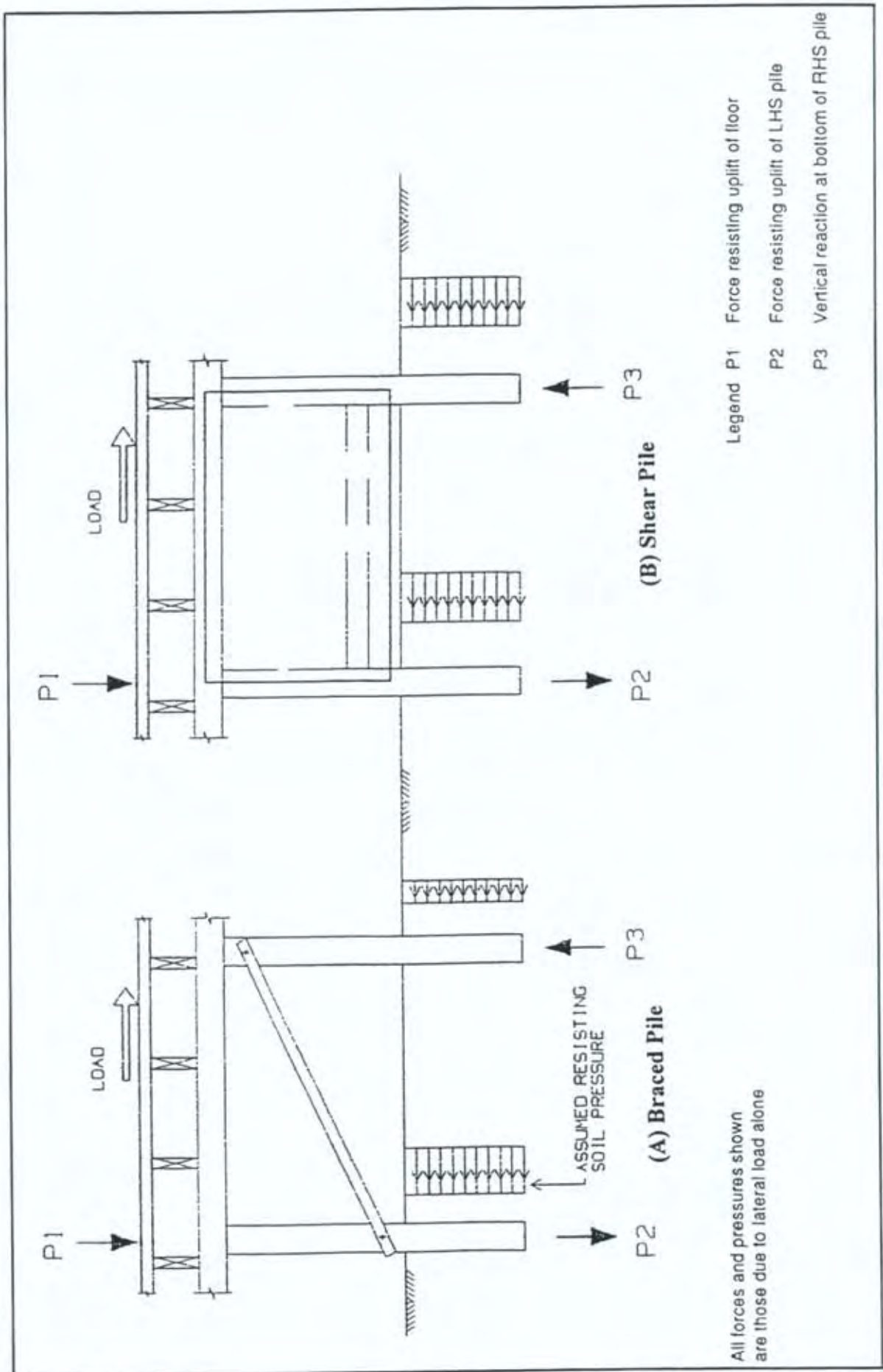


Figure 4. Soil Pressures on Piles with a Restrained Pile Head

Minimum concrete footing sizes around timber piles required by NZS 3604 (SANZ, 1990) are given in Table 1. The concrete footings may have either a round or square section.

Table 1 - Minimum Footing Sizes from Table 4.5 of SANZ (1990)***

Pile Type	Depth (mm)	Side (mm)
Ordinary Pile	300*	275**
Braced Pile	450	350
Anchor Pile	900	350

* No concrete required for first 100 mm of pile depth

** For pile beneath one storey load bearing wall

*** Sizes may increase for greater bearer and joist spans and for buildings of more than one storey

1.2 Preliminary Investigation into Lateral Load Resistance of House Pile Foundation Systems

Thurston (1993) provided a preliminary investigation into the lateral strength of house pile foundation systems. He outlined the assumptions and philosophies used by the NZS 3604 Standards Committee during preparation of this standard (SANZ, 1990). A literature review was given, from which it was concluded that although some information was available on the lateral strength of long, relatively slender piles, there was little available on the strength and resistance mechanisms developed by the short, very squat piles that constitute the bulk of the New Zealand house pile systems (depth in the ground/pile diameter < 2.6). A limited number of laboratory test results were presented (where the soil was represented by yielding steel springs) from which tentative revised design strengths were derived. Field testing was recommended. This study follows from these recommendations.

1.3 Pile Lateral Load Capacity in Soil

For testing to be of general application, the soil conditions should be the weakest consistent with the scope of application of the intended use (namely, clause 3.1.1(a) of NZS 3604:1990). This clause requires the soil to have a safe (vertical) bearing strength of 100 kPa beneath the pile. The standard allows this to be ascertained either by observation of the performance of nearby buildings, or by Scala Penetrometer soundings at the pile founding depth. The maximum penetration allowed from this testing is 25 mm/blow. For this Scala Penetrometer strength, Stockwell (1977) suggests that an appropriate allowable vertical bearing pressure is 125 kPa (using a safety factor of 3), and that the soil is likely to be either stiff clay, uniform compact sand or well graded loose sand.

NZS 3604 places no limitation on soil strength over the depth of the pile. Yet it is this upper soil zone which determines pile lateral load resistance. If the piles pass through a layer of peat or very soft clay before being founded in a firmer soil, then the lateral pile

stiffness will be significantly reduced. The actual soil strength will vary extensively from season to season (due to moisture content changes) as well as place to place throughout New Zealand.

Although long pile design is usually governed by deflection (Works and Development Corporation, 1990), short pile design is usually limited by soil strength. If house piles deform excessively in the ground during an earthquake, there is a danger that building services may rupture and P-Delta effects may become significant. It is suggested that a certain degree of damage to building services is acceptable during major earthquakes, although only minimal or no damage should occur during minor (say, serviceability level) earthquakes. General pipework damage and reticulation problems usually make services inoperative after large earthquakes. It should also be noted that if a foundation is very flexible it will significantly alter the building response period, thereby inducing some form of "base isolation" and earthquake forces are consequently reduced.

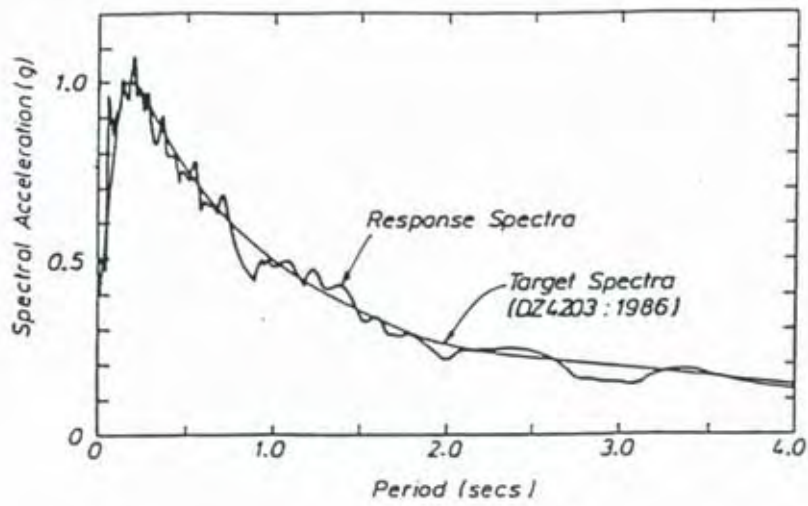
It is important that suitable ultimate and serviceability limit state deflection criteria for foundations be determined (eg that ground floor deflection does not exceed 60 mm under the NZS 3604 [strength] design load to avoid pile overturning and does not exceed 8 mm under the NZS 3604 [serviceability] design load to avoid damage to building services). Serviceability criteria for pile foundation design will also be needed to ensure excessive vibrations do not occur at serviceability loads.

1.4 Outline of Report

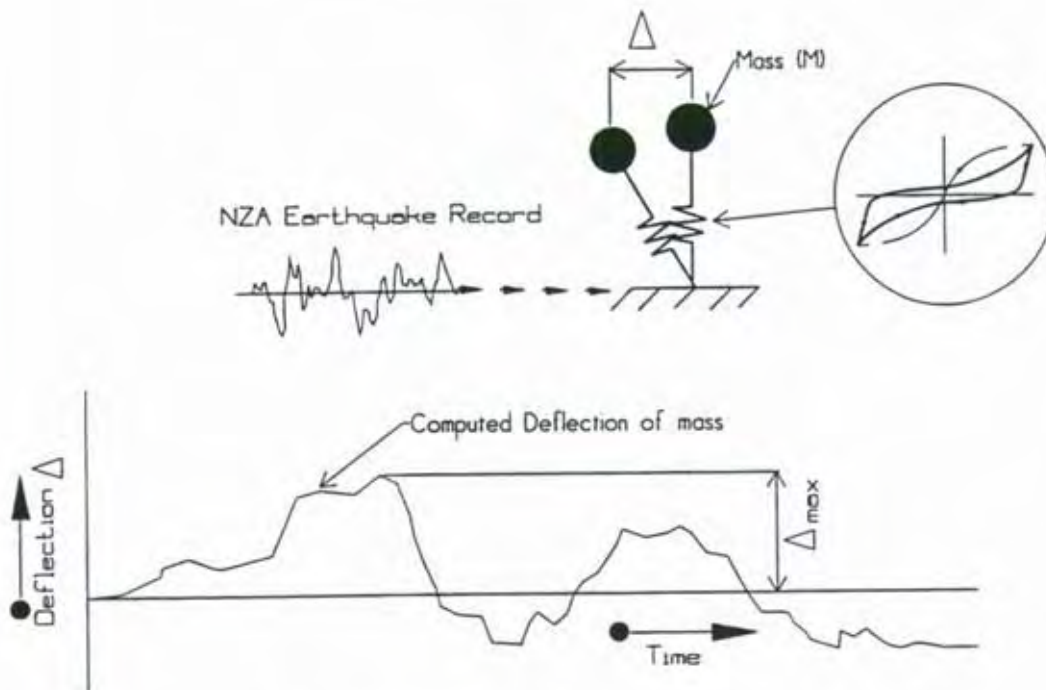
A brief literature survey is presented and a discussion provided on the design forces specified by NZS 3604 (SANZ, 1990) for connections between the top of piles and the house above. A series of anchor piles, braced piles and shear piles founded in clay, sandy-silt and sand were tested under incrementally increasing reversed cyclic lateral loading. The soil in each case was close to the minimum bearing strength allowed by NZS 3604, as described in Section 1.3. Full test details are provided. This report then presents the methodology required to derive design loads for such piles thus:

- Regression analysis was used to find the best fit parent curve to the measured hysteresis loops (see Figure 2) for each pile and soil type. This enabled an "average" set of hysteresis loops for each pile and soil type to be obtained.
- The pile wind design loads for each group were determined directly from the best fit parent curve and the maximum acceptable deflection.
- The earthquake design loads for each group were determined by time history computer analysis using the NZA acceleration record (Andrino and Carr, 1991), the test data and the maximum acceptable deflection as is schematically illustrated in Figure 5.

In addition to obtaining design loads for the various pile groups, this report also investigated the performance of piles in soft peat (particularly driven piles). Design loads for driven piles in low strength clay soils can be estimated from data measured by Cocks et al (1975) using the same methodology detailed in this report.



(a) Comparison of NZA Response Spectra and Design Spectra



(b) Computer Analysis

Figure 5. Derivation of Element Design Loads

2. BRIEF LITERATURE SURVEY

Thurston (1993) carried out a literature survey on the lateral load capacity of New Zealand house piles. Further literature which has come to hand is below. This includes several analysis methods that could be applicable to anchor piles. However, each of these methods only provides an approximation to real behaviour and requires estimation of soil properties. Hence, for the single solution required for anchor piles in minimum strength soil, recourse to experimental testing as described in this report provides the most reliable method.

Czerniak (1957) summarised the "rule-of-thumb" methods which may be used for estimating the lateral resistance of squat piles (those with an aspect ratio of less than 10). Note, anchor piles have an aspect ratio of 2.6. He developed equations for predicting the pile strength from first principles, assuming a parabolic distribution of soil pressure, and assumed that soil resistance increases linearly with depth.

Vallabhan and Alikhanlou (1982) summarised various analysis methods for squat piles. They showed that pile skin friction and the forces and moments at the bottom of the pile were significant and could not be ignored. The discrete spring model proposed provided good agreement with their experimental data.

Pender (1993) provided an extensive summary of design of pile foundations. However, although this provided useful background information, the emphasis was on long slender piles and has little applicability to house piles.

Dowrick et al. (1994) reported a reassessment of damage to houses in the 1931 Napier earthquake. He noted that a significant proportion of the damage was due to a lack of sub-floor pile bracing. This substructure weakness has been better addressed in modern houses. The average damage ratio in this intense shaking was stated to be 8% and was greater on rock and firm sites than on soft ground, which is contrary to conventional wisdom.

3. STRENGTH REQUIREMENTS FOR HOUSE CONNECTION TO PILES

Figure 6 depicts a pile resisting a horizontal earthquake or wind force F_H . This force must be transmitted from the house to the ground. In this report pile design strengths were derived on the basis of soil failure for the minimum strength soil as defined in NZS 3604 (SANZ, 1990). Thus force F_H may be significantly greater than the pile design strength, F_D , if the pile is founded in soil which is stronger or has a greater capacity than assumed in the design, ie:

$$F_H/F_D = R_{OS} \text{ may be } >1 \dots\dots\dots (1).$$

Modern design philosophy is to select a preferred failure mechanism and design against other less desirable mechanisms by ensuring higher strengths for these mechanisms. The preferred failure mechanism is either soil failure around a pile or a ductile bolted joint failure (ie failure of the brace-bolted connection in a braced pile). Soil failure from lateral earthquake loading usually results in the soil being pushed away from the pile sides and this cavity can be easily repaired by filling with concrete slurry. Failure of the connection between house and pile or pile timber flexural failure and splitting are undesirable failure mechanisms as these failure modes may be brittle, difficult to repair and may result in loss of gravity load-carrying capacity.

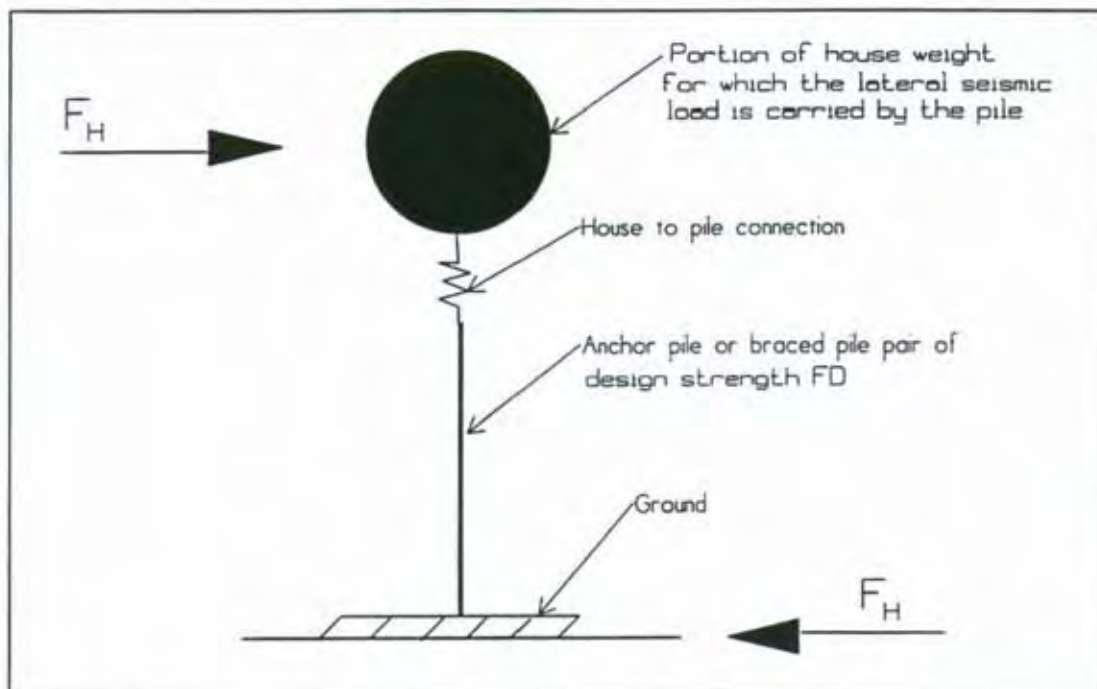


Figure 6. Horizontal Load Transfer From Ground to House

The design house-to-pile connection strength (FH in Figure 6) can be calculated from $FH = FD * ROS$. The choice of a suitable value of ROS in equation 1 will depend on many factors, including the effect of failure of the pile-to-house connection, ease of repair, relative cost of providing additional strength, etc. There may be a different factor for wind and earthquake. The rest of this section discusses the actual values of ROS provided in NZS 3604 (SANZ, 1990).

Generally, NZS 3604 requires the house-to-pile connection to have a capacity of 12 kN, although this is discussed in more detail below. The capacity is defined in the standard as being the 5% lower probability limit of the maximum loads of a series of test specimens. In his proposed test procedure, Thurston (1993) interpreted this as being the lower 5 percentile of the average residual maximums (ie average of push-plus-pull loads) after 4 cycles of loading. The author now considers that it is acceptable to base this on the first cycle of loading.

The intention of the Timber Pile and Pole Standard (NZS 3605, 1992b) is that 95% of the 140 mm diameter and 125 mm square house anchor piles have a bending strength of at least 7.2 kNm. For a 600 mm high anchor pile this implies a lateral load strength of $7.2/0.6 = 12$ kN. (This assumes that the anchor pile timber failure occurs at the soil surface, as at greater depths the required pile concrete surround strengthens the pile.) Thus the horizontal load design strength of both the house-to-pile connection and pile timber flexural strength is 12 kN.

The wind design strength of braced and anchor piles given in NZS 3604 is $160 B_u = 8$ kN. Thus the value of $ROS = 12/8 = 1.5$ for wind.

The earthquake design strength of braced and anchor piles in NZS 3604 is $70 B_u = 3.5$ kN. If the failure mechanism is in the house-to-pile connection then Thurston (1993) recommends that design loads be based on $\mu = 1.5$. (Note that for nominally elastic timber systems the ductility recommended in NZS 4203 [SNZ, 1992a] is $\mu = 1.25$). Reference to NZS 4203 shows that the design loads for $\mu = 1.5$ are twice the design loads for $\mu = 4$. (Note, $\mu = 4$ is the basis for the design loads in NZS 3604.) Thus the design earthquake would have a force of $3.5 \times 2 = 7$ kN at failure of the house-to-pile connection, which gives a value of $ROS = 12/7 = 1.7$.

The 12 kN house-to-pile connection force discussed above should be in the same direction as the load resistance provided by the bracing element. Thus the two 6 kN requirements of SANZ, 1990, shown circled in Figure 7 can be questioned.

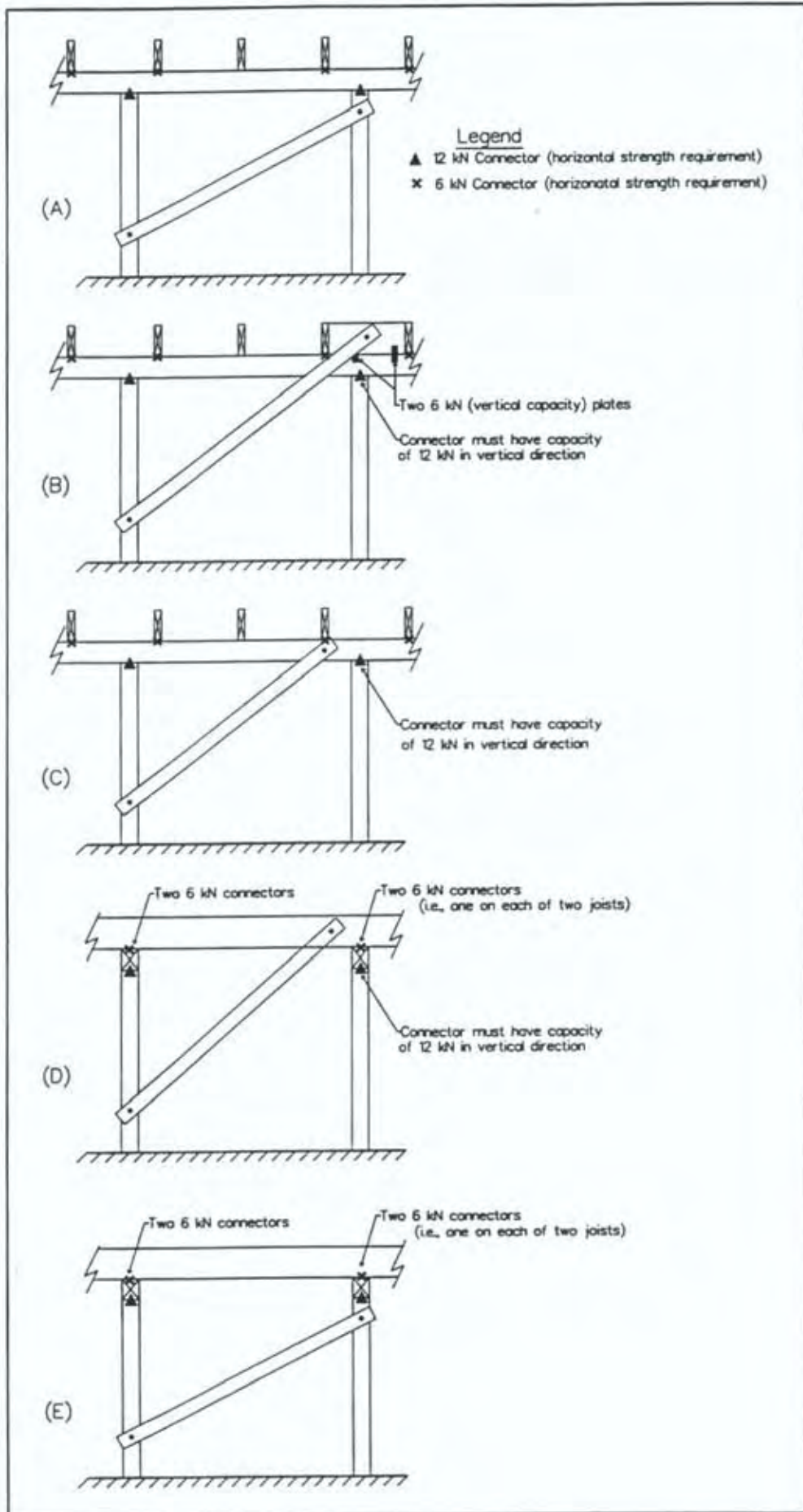


Figure 8. Design Forces at Top of Braced Pile from Johnstone (1994)

4. TEST PROGRAM

4.1 Introduction

The strengths of various house pile foundation systems were tested under cyclic horizontal loading in clay, peat, sandy-silt and sand.

The radiata pine timber piles were of 122 mm square cross section and were cast in a concrete footing, except for the driven piles which were round (150 mm diameter cross section). The new piles used in this project had been treated to level H5. Four pile types were tested, all of which complied with NZS 3604 (SANZ, 1990), namely - anchor piles, braced piles, ordinary piles and driven piles (see Figures 14, 17, 9 and 20). The first three were unrestrained at the top and were loaded as simple cantilevers using a horizontal load applied approximately 600 mm above the soil line. A schematic diagram of this loading and induced soil pressures is given in Figure 3. In contrast, the top of the ordinary pile was restrained against rotation and was loaded close to the soil line, as shown in Figure 9. A schematic diagram of this loading on a real structure is given in Figure 4(b). These ordinary piles consequently remained close to vertical and only transferred shear forces in the soil. They are referred to as shear piles in this report to differentiate their seismic behaviour from the low-strength rocking action expected from ordinary piles without this top rotational restraint. The tops of these piles were prevented from rotating by nailing them to sheet cladding in much the same manner as recommended by a cladding manufacturer (James Hardie and Coy, 1994) and shown in Figure 10.

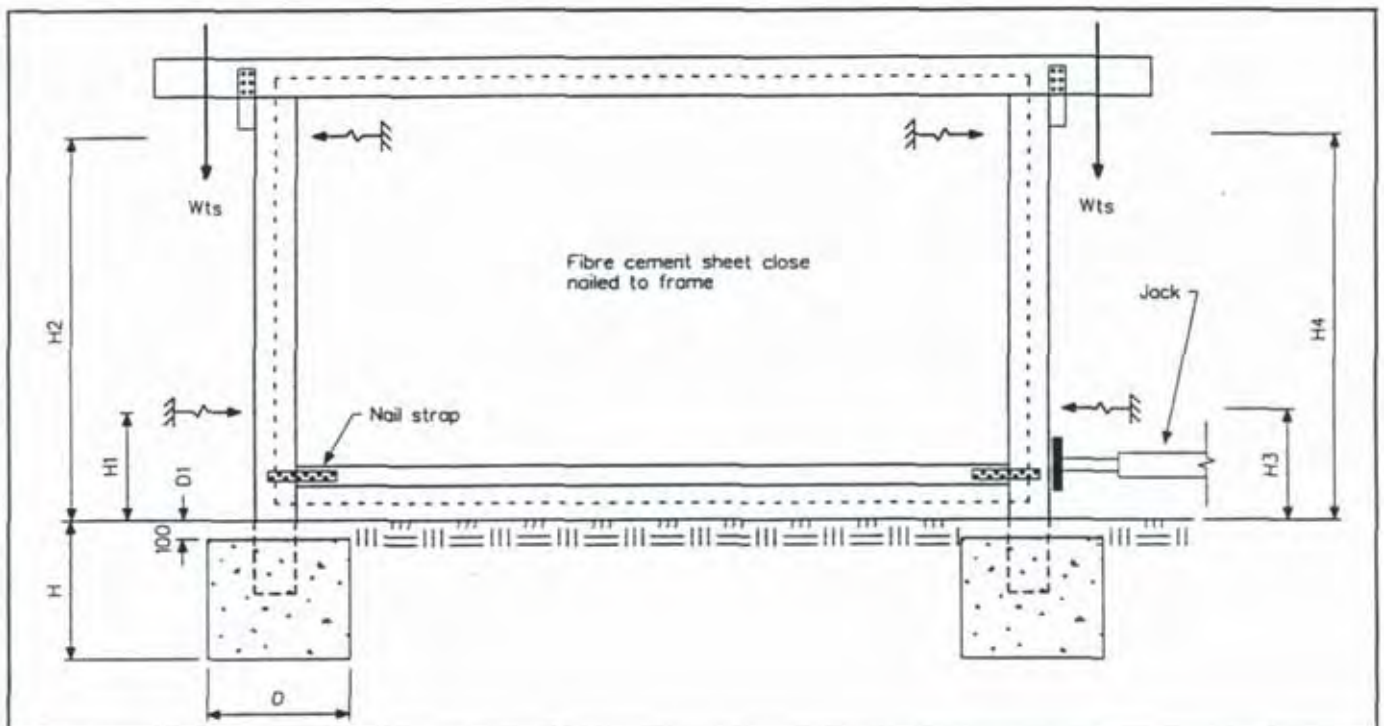


Figure 9. Lateral Loading of Shear Piles

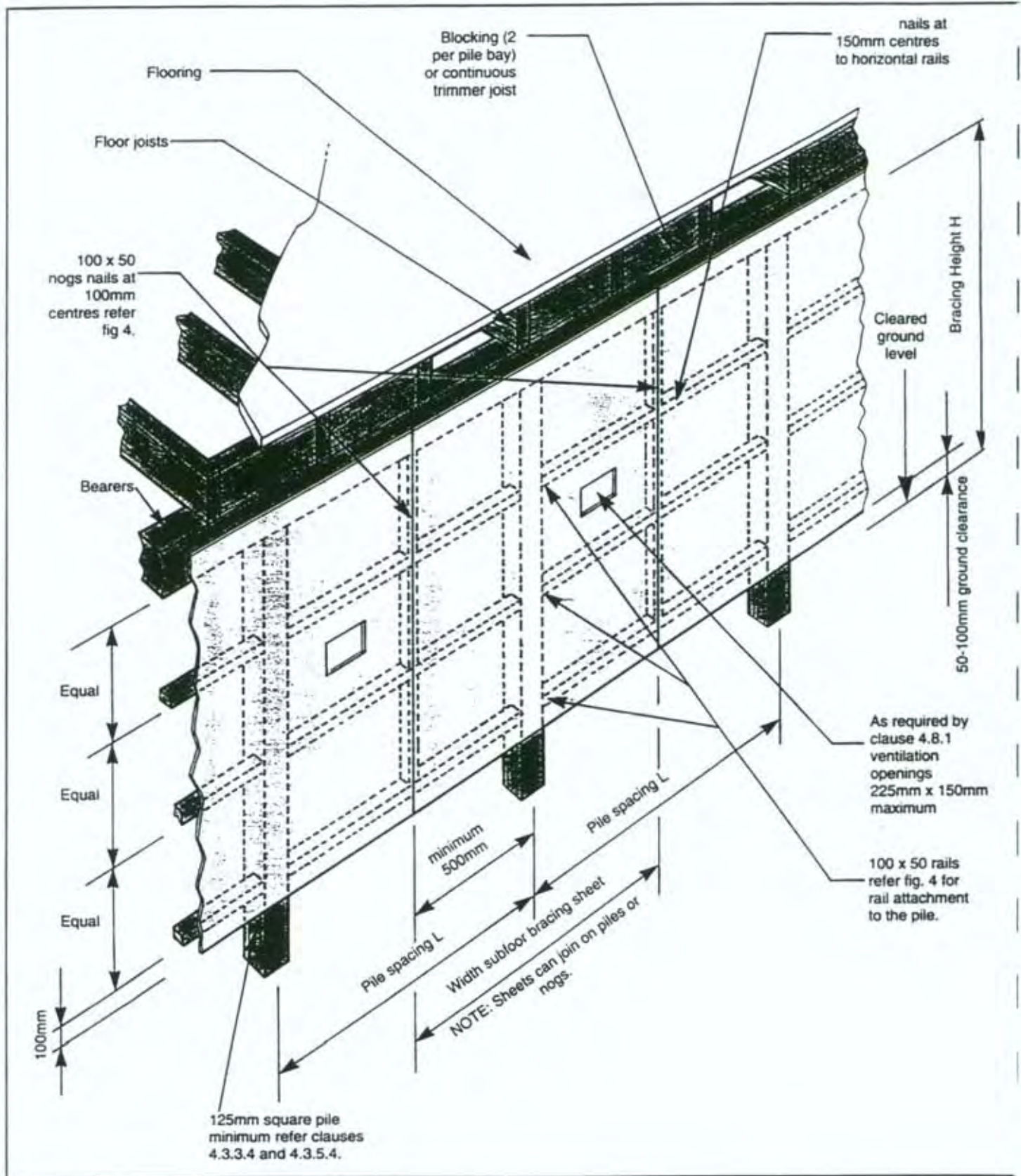


Figure 10. Sheet Bracing of Normal Piles (James Hardie and Coy, 1994)
 (Reproduced with permission of James Hardie Industries)

4.2 Site Locations and Soil Conditions

Two sites were used for the tests. The piles were installed in a total of five groups (two at the first location and three at the second location) and labelled using a grid reference system as shown in Figure 11 (eg the pile in the north west corner of Group 1 is labelled as Pile J1 as it is at the intersection of Grids J and 1. The pile foundation system in Group 1 was installed at BRANZ in 1983 as an educational display for the building industry and some details do not comply with SANZ (1990), such as the dimension requirements of Clause 4.7.6.3. However, test observations suggested that the lack of compliance with SANZ did not affect the results. Pile Groups 2-5 were installed by a contractor between 1 and 3 months before testing. Pile Group 2 was installed close to Group 1 as shown in Figure 11 (b). Pile Groups 3-5 were located a field in Kapiti.

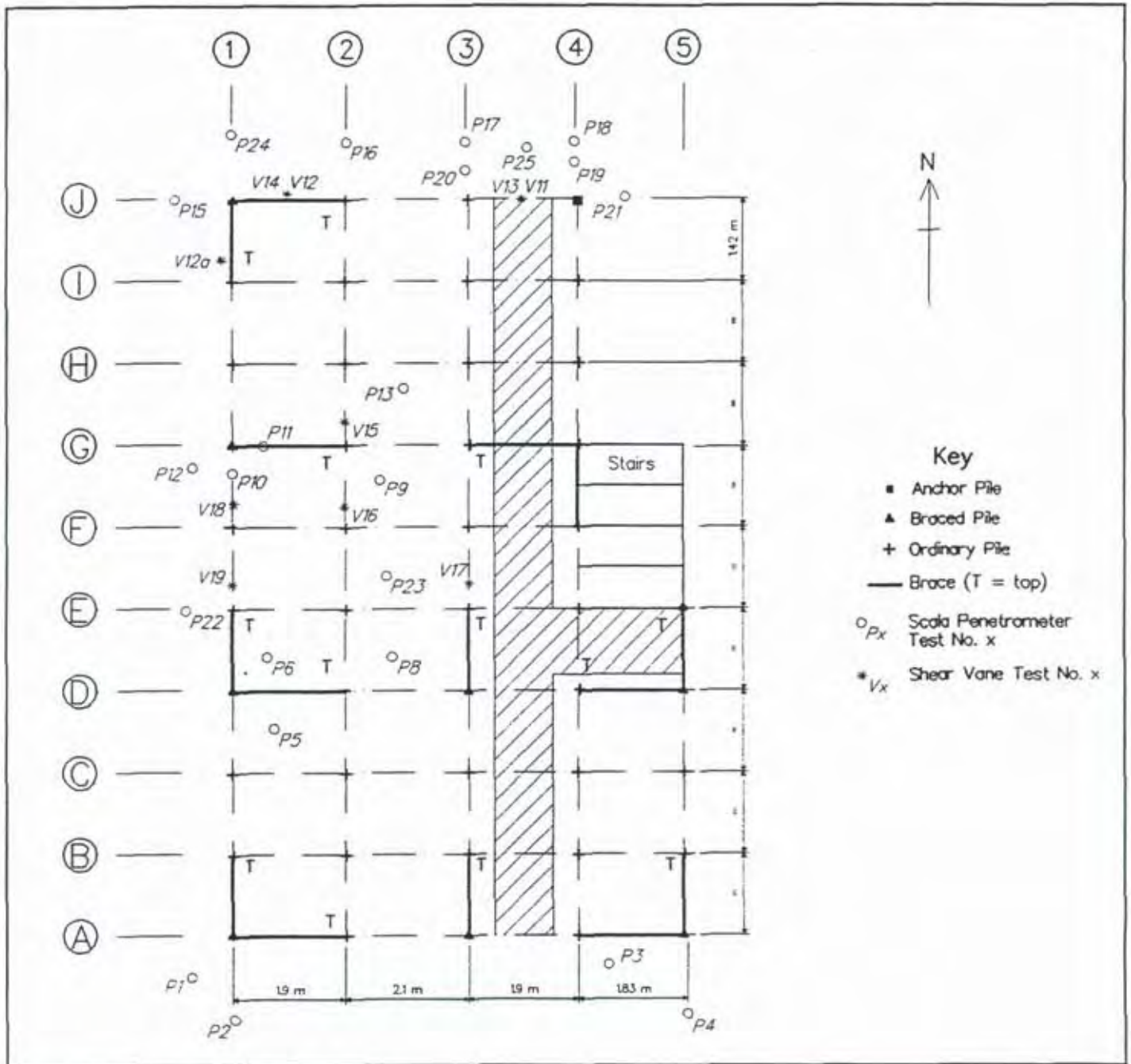


Figure 11. Location of Test Piles
(a) BRANZ SITE - Group 1

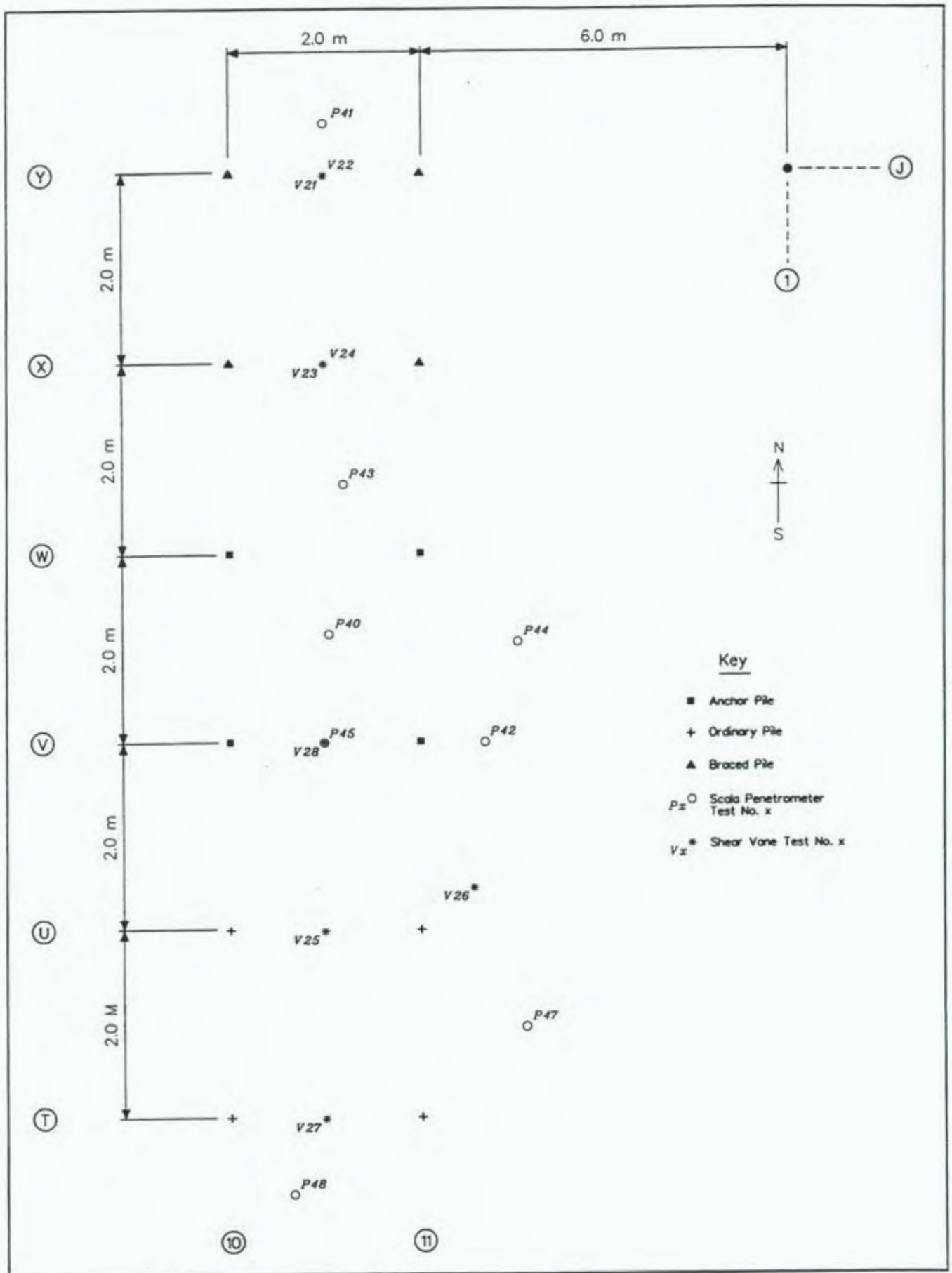


Figure 11. Location of Test Piles
(b) BRANZ SITE - Group 2

Pile Groups 1 and 2 were at a clay site, while Group 3 was in peat, Group 4 in sandy silt and Group 5 was in a small knoll of beach sand. (see Appendix F).

The soil “strength” was measured using Scala Penetrometer soundings and shear vane tests at the locations shown in Figure 11. These tests are identified by a prefix of P for the penetrometer test and V for the vane tests. The subscript X is an identifying location number. Plots of Scala Penetrometer soundings and shear vane strengths are plotted against depth within the soil in Appendix F.

Averaged Scala Penetrometer soundings over 300 mm depth increments at each sampled location are given in Tables F1-F5 of Appendix F for Groups 1-5 respectively. NZS 3604 (SANZ, 1990) requires soundings to be 25 mm or less below pile founding depth. Overall averages for each group are plotted in Figure 12. These show that the clay and sandy-silt soil strengths were generally of slightly lower strength than required by NZS 3604 for normal and braced piles with founding depth 300 and 450 mm respectively but were closer to the limit for anchor piles (founding depth 900 mm). The peat was extremely soft. Scala Penetrometer testing is not really applicable to sand but was included for completeness.

Shear vane test results measured near mid-depth of successive 300 mm depth increments at each sampled location are given in Tables F7-F11 of Appendix F for Groups 1-5 respectively. Overall averages for each group are plotted in Figure 13. The averages shown for clay will be on the low side since the instrument was only capable of reading to 234 kPa and many of the readings in the clay exceeded this value. Shear vane testing is not really applicable to sand but was included for completeness.

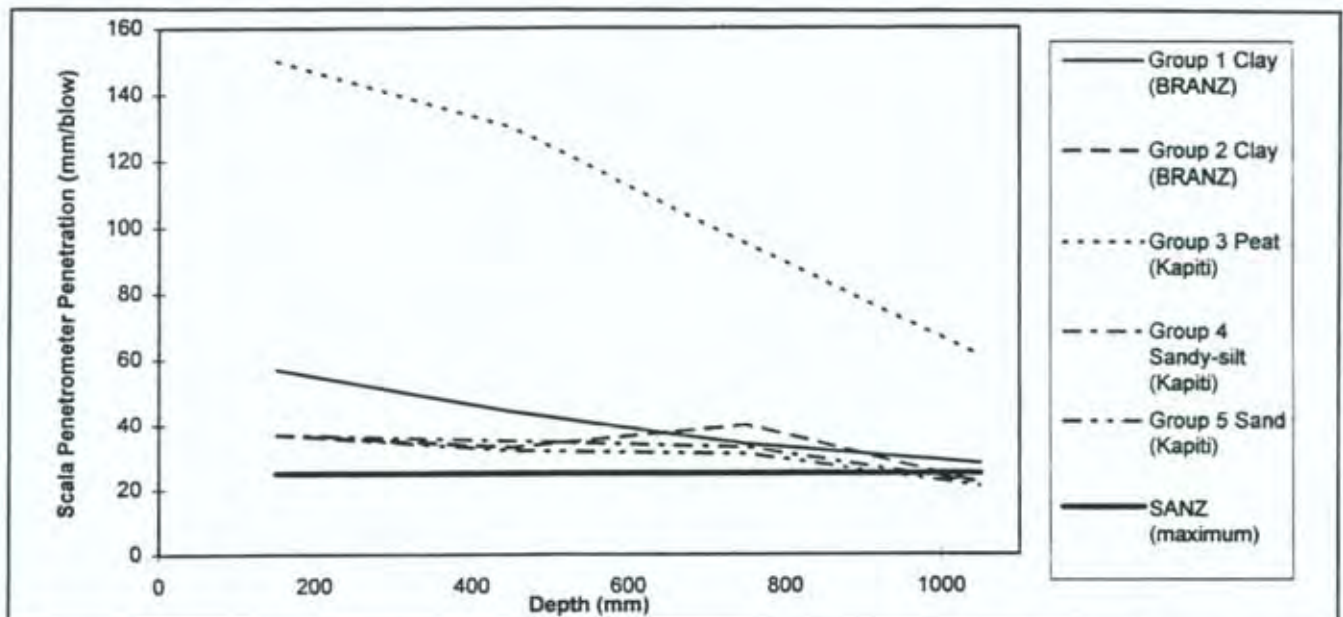


Figure 12. Relationship between Scala Penetrometer Soundings and Depth in the Soil

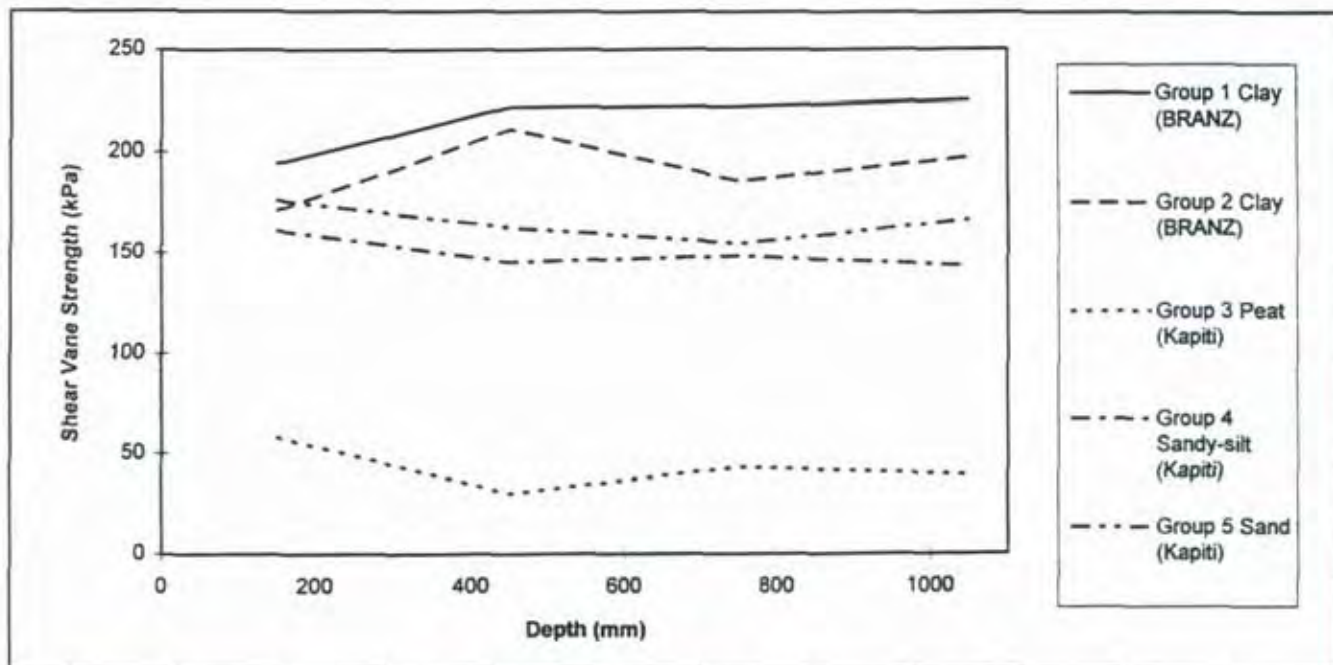


Figure 13. Relationship between Shear Vane Strength and Depth in the Soil

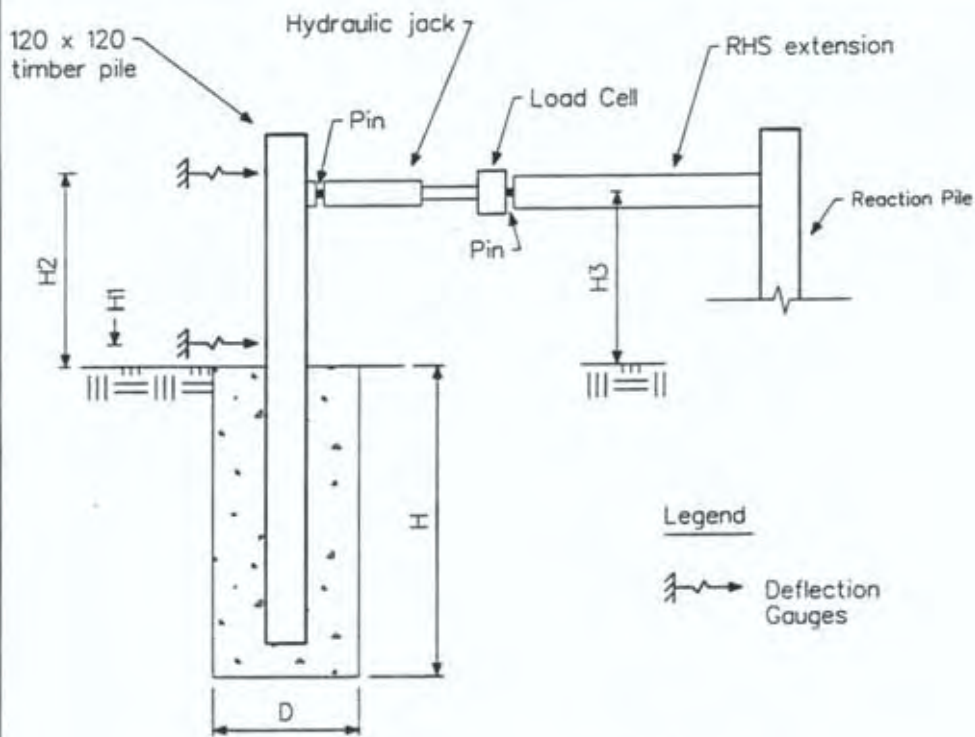
4.3 General Test Details

A hydraulic jack (operated via a hand pump) was used to apply horizontal load to piles being tested, as shown in the general test arrangement depicted in Figures 14 and 15. One end of the jack was fastened to the test pile while the other was fastened to a reaction pile. The test and reaction piles were both subjected to the same force (thus in many instances the reaction pile was actually a second test pile). This enabled one test to be used to measure the stiffness of two test piles. Load was generally measured using a 45 kN load cell although a 22 kN load cell was used in some of the early tests.

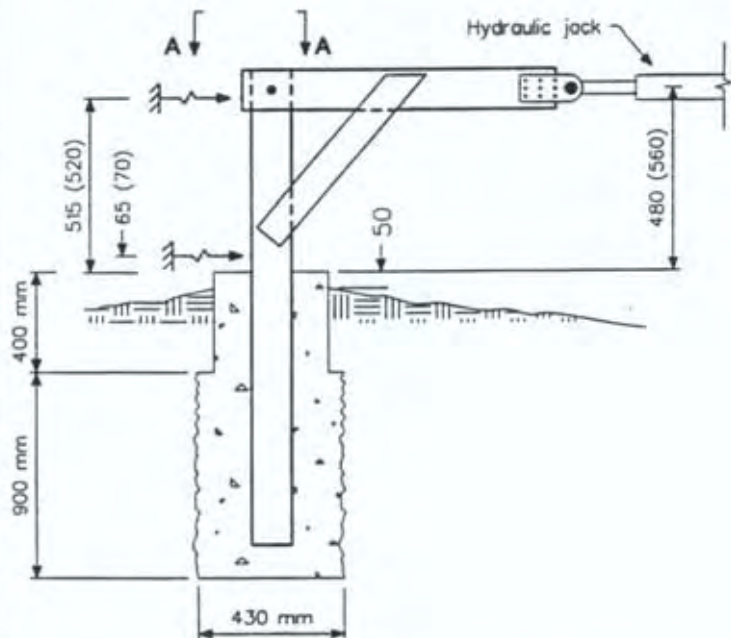
The load cells were calibrated to within BS 1610 (BSI, 1985) Grade 1.0 accuracy, which ensured that the monitored load was within 1% of the nominal load.

Horizontal and vertical pile deflections were measured using linear potentiometers reading to an accuracy of 0.5% of the nominal deflection. The test load and displacement readings were recorded using an IBM-compatible "Notebook" PC running a software programme to record data in real-time mode. Data was sampled at 5 hertz, averaged, and recorded at 1 hertz. This data was subsequently processed and plotted using a spreadsheet program (see Appendix H).

Piles were tested using a pseudo-static reverse-cyclic loading regime to provide indicative behaviour of that which is expected to occur with large earthquake or wind loading. A single cycle was used at each load and this load level was incrementally increased during subsequent cycles until failure occurred. The load increments varied with the type of pile being tested (but may can be readily determined from the hysteresis plots presented in Appendix H). Load increments were between 1 and 1.5 kN for all piles, except the shear piles where the increment was usually approximately 3 kN.



(a) Schematic View of Anchor Pile Tests Group 2,3,4,5



(b) Schematic View of Anchor Pile Tests Group 1 (Piles J3 and J4)

Note: Values in brackets are dimensions at Pile J3 relative to concrete at J3 others are at J4

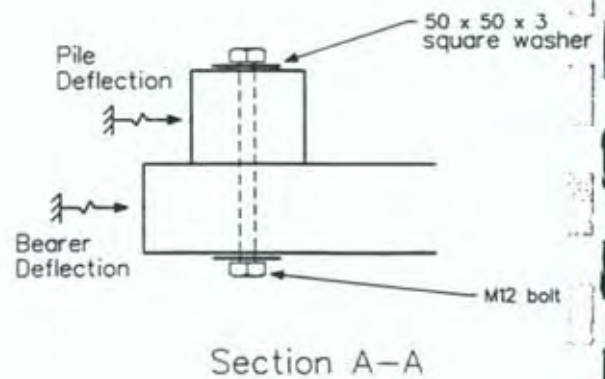
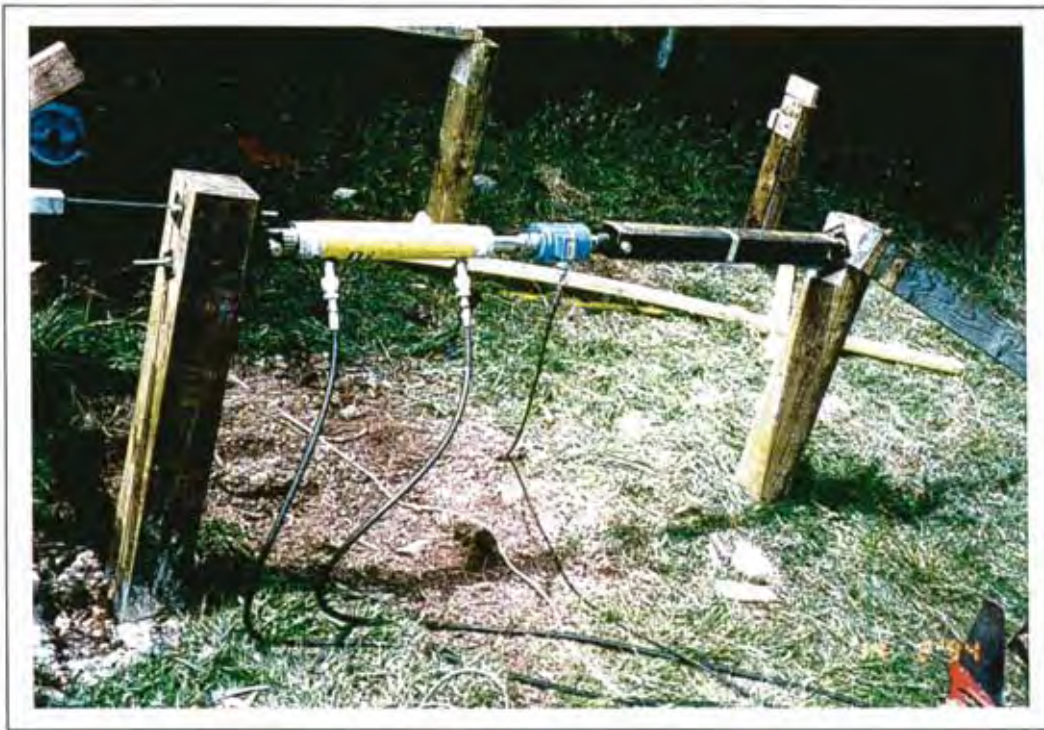


Figure 14. Anchor Pile Test Details



(a) Test Loading of Anchor Pile (LHS) While Reacting Against "Another" Pile



(b) Pile Instrumentation

Figure 15. General Photographs of Test Arrangement

4.3.2 Anchor Pile Tests

The general test arrangement for anchor piles is shown in Figure 14. Load was applied directly to the pile in most instances, as shown in Figure 14(a), and through bearers bolted to the piles, as shown in Figure 14(b) for piles J3 and J4 of Group 1. Horizontal deflections were measured at two heights for each test, as shown in Figure 14. Average pile footing dimensions are given in Table 4 and instrumentation locations are given in Table 5. A light "nailed" brace was added, as shown in Figure 14(b), to prevent the development of an unstable loading mechanism. This would not have affected the load on the pile but would have slightly reduced the horizontal force on the bolt. General details of testing can be seen in the photographs of Figures 15 and 16.

Table 4. Measured Anchor Pile Footing Average Dimensions

Group	D (mm)	H (mm)
1	430 sq	900 *
2	430 Ø	900
3	430 Ø	920
4	430 Ø	940
5	400 Ø	900

Legend

Ø = diameter of round pile in bored hole

sq = side of approximately square cross section in hand-dug hole

* Additional block cast on top 400 mm deep and 340 mm square section - see Figure 14 (b)

Table 5. Instrumentation of Anchor Piles

Pile Label	Group No.	Soil	Plot No. ***	Maximum Pile Deflection (mm) **	H ₁ (mm) ****	H ₂ (mm) ****	H ₃ (mm) ****
J4*	1	Clay	18	47	65	515	480
J3*	1	Clay	14,19	87	70	520	560
W13	2	Clay	36	40	150	675	700
V13	2	Clay	38	33	140	730	700
W10	2	Clay	42	55	67	632	658
V10	2	Clay	40	40	108	685	658
M1	4	Sandy-silt	96	93	140	900	900
M2	4	Sandy-silt	98	130	110	920	920
M3	4	Sandy-silt	100	55	130	820	820
M4	4	Sandy-silt	102	52	130	915	910
P1	5	Sand	110	58	185	850	700
P2	5	Sand	112	76	160	830	800
H50	3	Peat	84	120	80	860	800
H51	3	Peat	86	95	60	850	850

Legend

* Piles were loaded through a bolted joist connection. The remainder of the piles were loaded directly

** Maximum pile deflection where stable hysteresis loops were obtained.

*** Plot numbers used in Appendix H.

**** Location of instrumentation - see Figure 14.



Figure 16. Photographs of Anchor Pile Tests
(a) Group 1 - Anchor Piles



Figure 16. Photographs of Anchor Pile Tests
(b) Group 5 Anchor Piles

The anchor pile footings in Table 4 are close to the minimum specified by NZS 3604 (SANZ, 1990). This standard requires the concrete footings to be 900 mm deep and a minimum of 350 square section (see Table 1).

The two piles in Group 1 were modified soon after their installation in 1983 by casting an additional block on top of the existing anchor pile and moulding the soil around this block. (This was only discovered when investigating the footing after the pile test.) The larger pile size would have increased the total soil resistance, although this soil was very soft.

4.3.3 Braced Pile Tests

Three types of braced pile test arrangement were used, as shown in Figures 17 and 18, and summarised in Table 6. Types 1 and 2 were used for braced piles within the construction platform in Group 1 while Type 3 was used for Group 2. No braced pile tests were performed at the less accessible Group 3, 4 and 5 sites because these tests required a large number of "weights", as discussed below. It was anticipated that the strength of braced piles would be governed by the bolted brace connection rather than the soil so the choice of site was not considered to be a major test parameter requiring investigation.

Table 6. Instrumentation and Brace Details, Braced Piles (Clay)

Pile Label	Pile Type	Gr. No.	Plot No.	Max. Pile Defl. (mm)*	Brace Top Connect	Brace Angle Deg.	H1 (mm)**	H2 (mm)**	H3 (mm)**	H4 (mm)**
A1 - A2	1	1	1	78	Joist	34.4	290	1490	1500	1310
A4 - A5	1	1	4	45	Joist	33.5	60	1485	1490	1332
D1 - E1	2	1	6	72	Pile	31.8	190	1260	-	1160
I1 - J1	2	1	8	60	Bearer	23.9	160	1210	-	910
G1 - G2	1	1	29	65	Joist	27.0	210	1100	1225	-
G3 - G4	2	1	32	52	Pile	16.0	-	920	330	1110
J1 - J2	1	1	26	32	Joist	21.4	230	1140	970	780
X10 - Y10	3	2	50	140	Bearer	41.1	110	1260	50	1200
X13 - X13	3	2	43	100	Pile	31.9	125	1300	100	1145

Legend

* Maximum pile deflection where stable hysteresis loops were obtained.

** Location of instrumentation - see Figure 17.

Pile footing details are shown in Figure 17. NZS 3604 recommends that the pile footing be a minimum of 450 mm deep with a square section of sides 350 mm or a round section of diameter 350 mm (See Table 1). The Type 1 and 2 piles were built to SANZ (1978) (a previous edition of NZS 3604) which allowed a smaller footing for the pile to which the top end of the brace was attached. The more critical footing (for the pile at the lower end of the

brace) was 50 mm shallower but had sides 50 mm wider than required by NZS 3604. The footing for the Type 3 brace was slightly deeper and the pile footing had a larger diameter than required by NZS 3604. However, variations from NZS 3604 minimum footing sizes were not considered to be critical as it was expected that the braced pile behaviour would be governed by the brace bolted connection.

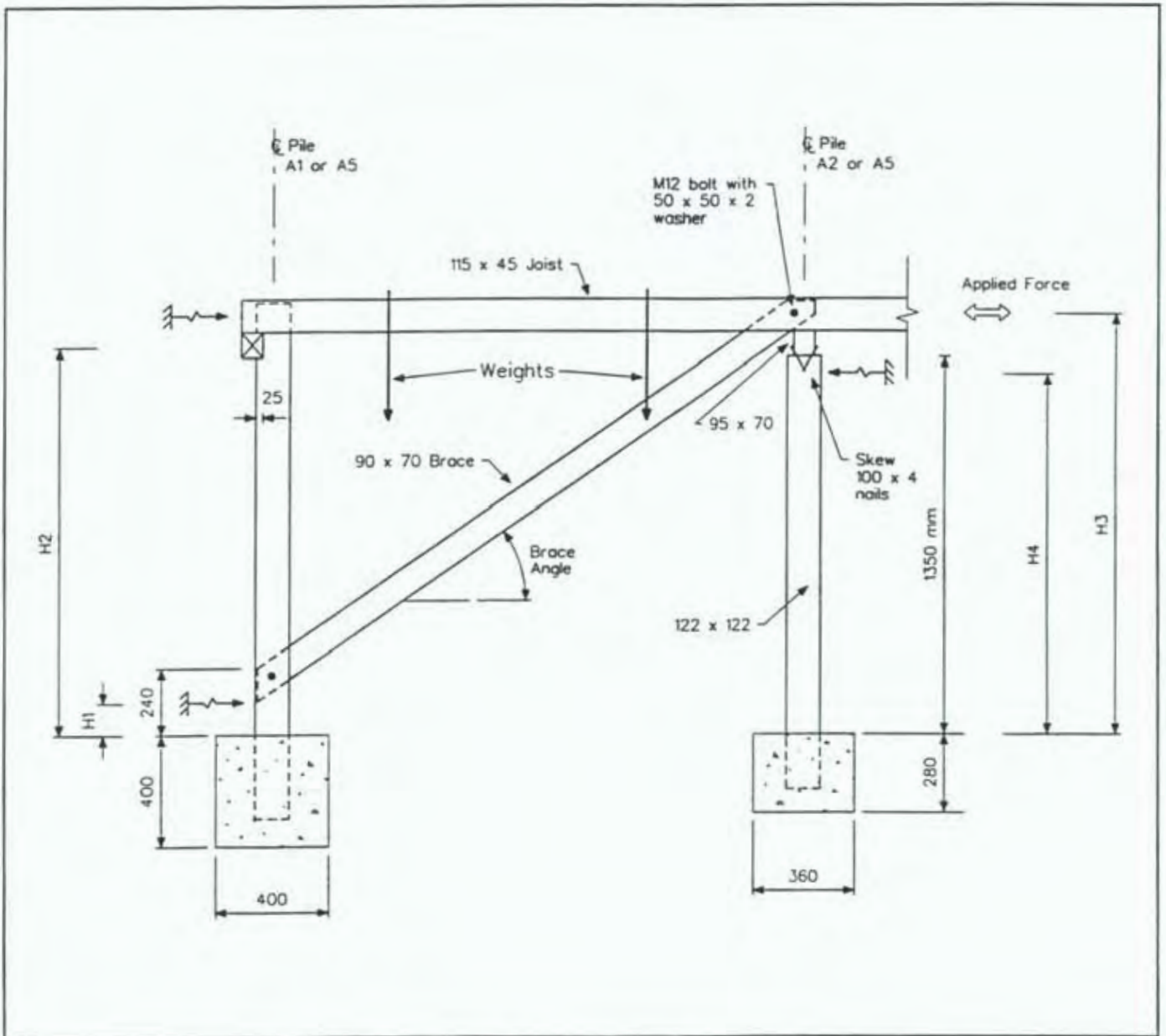


Figure 17. Braced Pile Test Details
a) Type 1 Brace Test

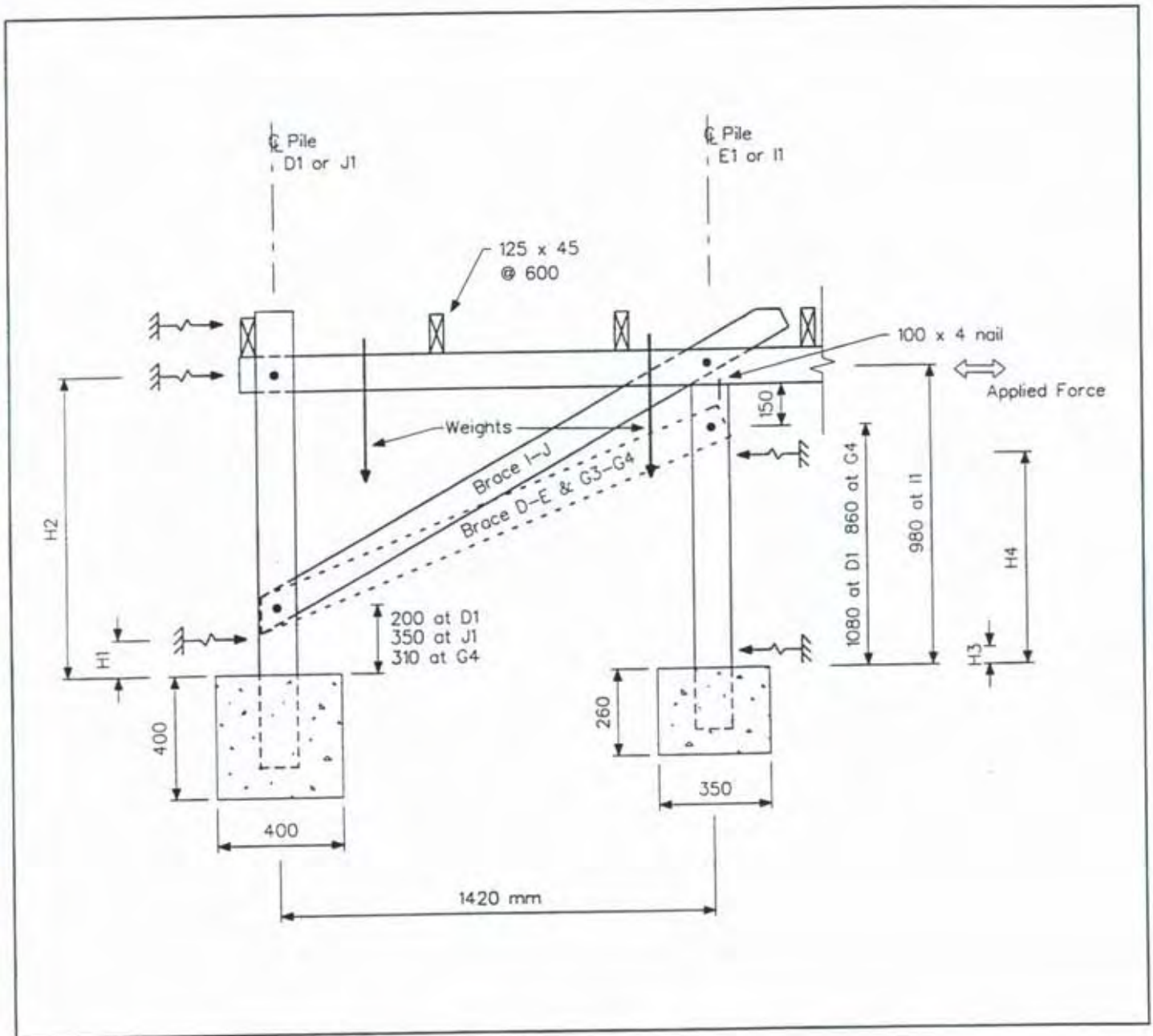
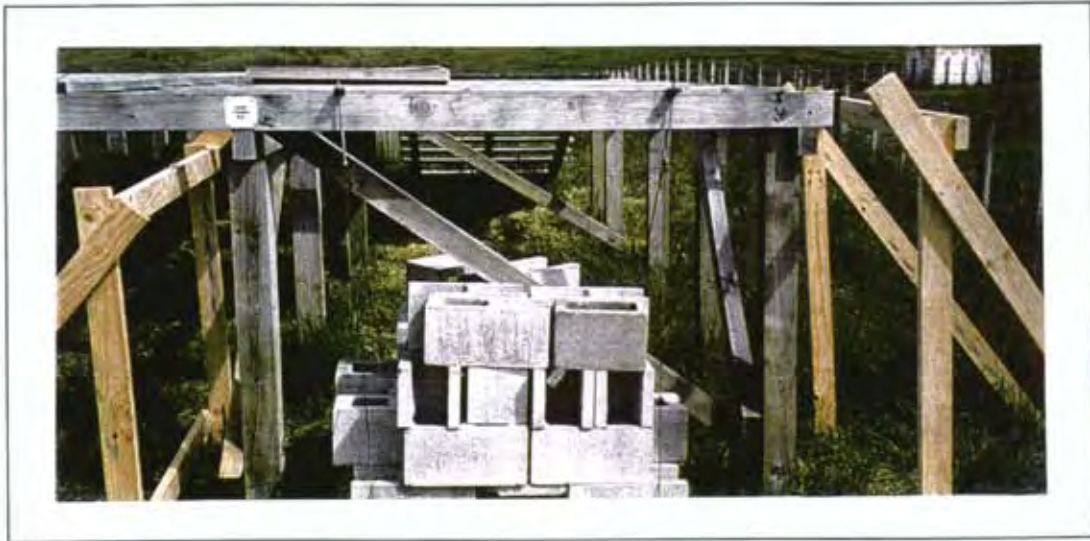


Figure 17. b) Type 2 Brace Test



(a) Test Set-up at Brace A4-A5



(b) Connection of Brace to Joist (Short length packer sandwiched between)



(c) Type 1 Test J1 - J2

Figure 18. Photographs of Braced Pile Tests



(d) Test II - J1



(e) Test D1 - E1

Figure 18. Photographs of Braced Pile Tests

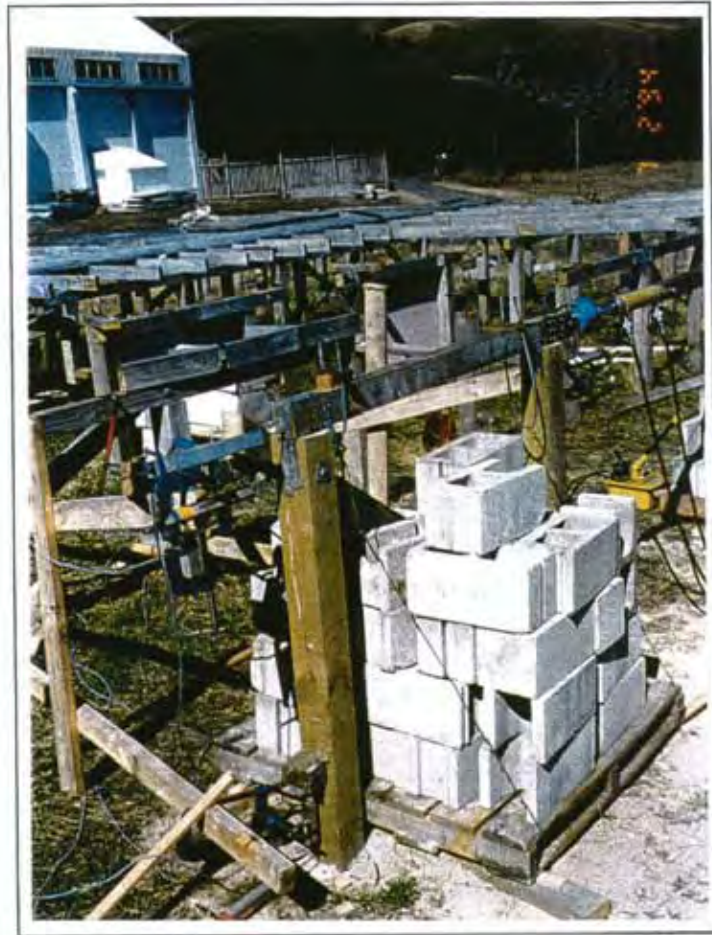


Test X10-Y10



Test X10-Y10

Figure 18. Photographs of Braced Pile Tests



Test X13 - Y13

Figure 18. Photographs of Braced Pile Tests

Weights were suspended from the bearers to simulate gravity load from the house, as shown in Figures 17 and 18. Without these weights the lateral force would cause rocking about one concrete footing so that the other end lifted out of the ground at a relatively low lateral force level. The weights were greater than those from a house (on a tributary area basis) because stiff walls above the lifting pile would transfer a larger proportion of house weight to this pile and unload other piles. (It is possible that braced piles not located beneath a wall may punch through the floor, but this was not investigated in the tests described in this report.)

The vertical load system was required to apply a small restraining force at low lateral loads but only allow small vertical pile uplift movement at greater lateral loads. This was achieved using concrete blocks, as shown in Figure 18. (For clarity only the line of action is shown in Figure 17.) Thirty blocks (giving a total weight of approximately 5 kN) were placed on a timber pallet between the test braced piles. The pallet was placed on timber packers so the weight was supported on the ground at least 300 mm away from the concrete footings. The pallet was suspended from the bearer or joist using wires (tightened only sufficiently to remove initial slackness from the wires).

A hydraulic jack (reacting against a second pile system) was used to apply horizontal load to the bearer or joist running between the braced piles, as shown in Figure 18. Instrument position details are given in Table 6.

4.3.4 Shear Pile Tests

Pile foundation systems usually resist horizontal load by acting as cantilevers within the soil. An alternative system has been demonstrated in the BRANZ laboratory (Thurston, 1992) whereby a sheet restrains rotation of the pile top and allows a small shallow pile footing to be used (see Figure 10). Under lateral wind and earthquake loading the pile remains vertical and shears through the ground. High bracing strengths were derived from this configuration. A number of piles were tested using this configuration to measure the strength of the various soils under this (shear mode) translation.

Table 7. Instrumentation of Shear Piles

Pile Label	Soil Group	Soil Type	Plot No.	Max. Pile Defl. (mm)*	Weights per pile (kN)**	H1 (mm) ***	H2 (mm) ***	H3 (mm) ***	H4 (mm) ***
C2-D2	1	Clay	73	32	-	260	-	280	960
E2-F2	1	Clay	71	34	-	130	-	80	1040
T10-U10	2	Clay	63	40	1.36	220	1200	310	1090
T13-U13	2	Clay	57	31	1.36	330	1200	320	1060
G50-F50	3	Peat	89	68	0.54	130	1130	210	1205
G51-F51	3	Peat	93	100	0.54	200	1110	200	1130
M3-M4	5	Sandy-silt	105	40	0.80	110	1180	70	1130
P3-P4	5	Sand	117	18	0.80	95	840	245	775

Legend

* Maximum pile deflection where stable hysteresis loops were obtained.

** Weights initially supported on ground.

*** Location of instrumentation - see Figure 9.

Table 8. Measured Shear Pile Footing Average Dimensions*

Group	D(mm)	H(mm)
1	350 sq	300
2	250 sq	320
3	250 sq	320
4	250 sq	320
5	280 sq	330

Legend

* No concrete for first 100 mm of pile depth

Test set up details are shown in Figures 9 and 19. To ensure the piles were loaded in close to pure translation mode the load was applied close to the ground and the pile top was restrained from rotating by nailing fibre cement sheets (Type TX - see Appendix G) to the piles and framing. Weights up to a total of 2.5 kN were used to prevent the entire system from rocking, in the same manner as for the braced pile system described above. Generally these weights rested on the ground and only imposed significant vertical load onto the bearer (between the piles) as the piles attempted to uplift. However, in some tests (as noted in Table 7), the weights were hung directly from the bearer. The maximum weight (per pile) was 1.36 kN, which was small relative to the total (horizontal) force the shear pile systems resisted (see Table 7).

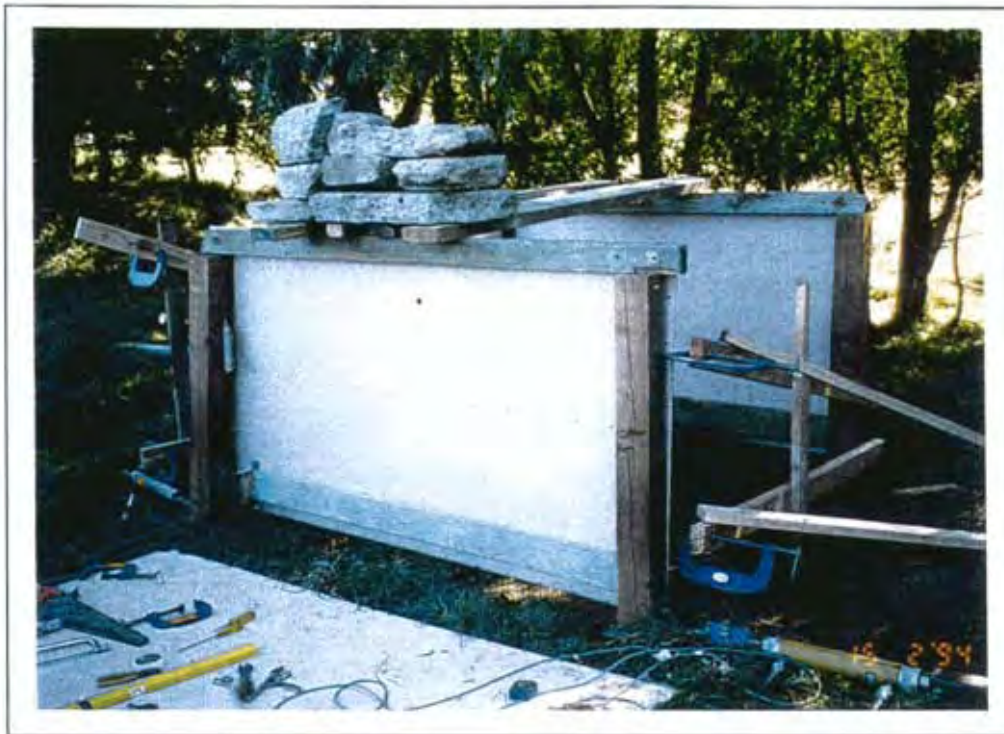


Figure 19. Photographs of Shear Tests
(a) Tests in Peat Group 3



Figure 19. Photographs of Shear Tests
(b) Tests in Clay Group 1



Figure 19. Photographs of Shear Tests
(c) General Views Group 1 & 2
36

Deflections were measured at two heights at each end of the shear pile pairs shown in Figures 9 and Table 7. Measured pile footing dimensions are given in Table 8. These were approximately the same as the minimum dimensions detailed in Table 1.

4.3.5 Driven Pile Tests

The 150 mm diameter round piles were driven to a depth of 1.5 m into soft peat which merged into dark organic silt at about 1.1 metres depth. A jack was attached between pairs of piles to apply horizontal load to both as shown in Figure 20. Deflections were measured at two levels for each driven pile as defined in Table 9.

Table 9 - Instrumentation of Driven Piles (Peat - Group 3)

Pile Label	Plot N ^o .	Max. Pile Defl. (mm)	H ₁ (mm) *	H ₂ (mm) *
I50	78	72	140	800
J50	77	78	130	130
I51	82	88	150	950
J51	83	90	200	870

Legend

* Location of instrumentation - see Figure 20.

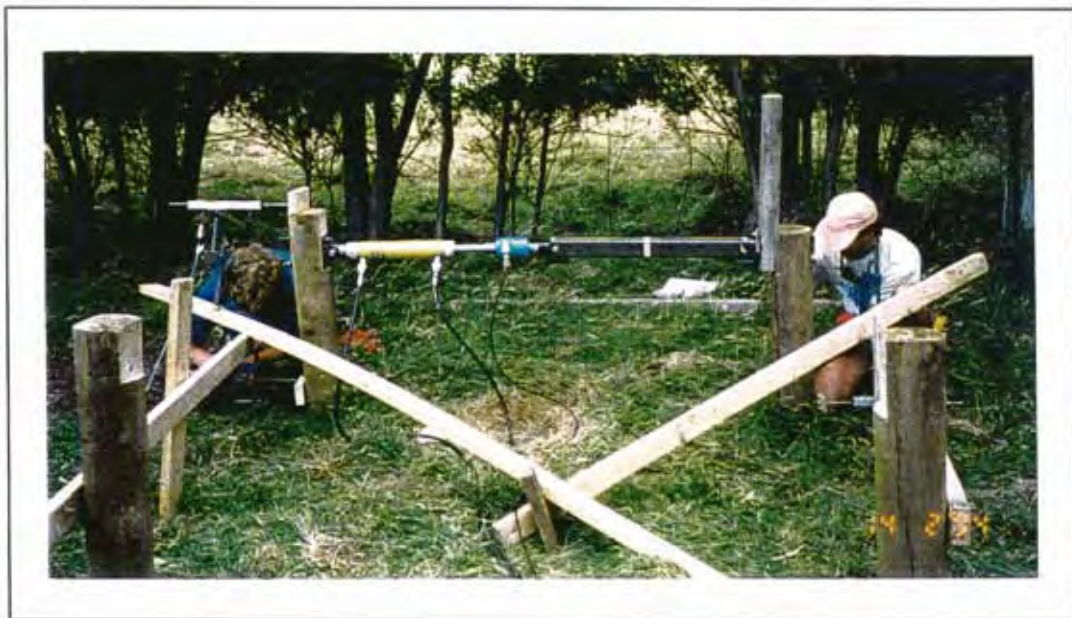
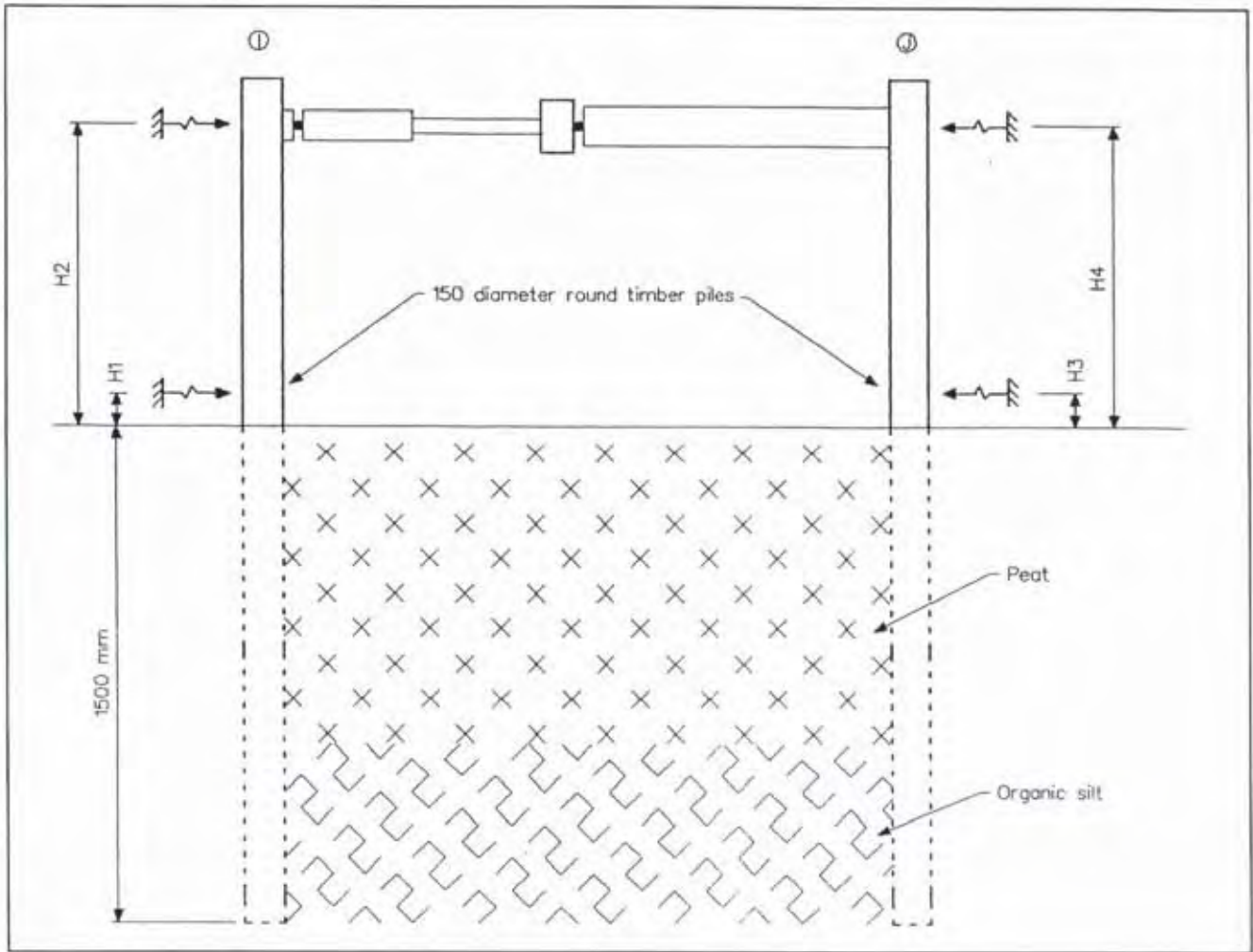


Figure 20. Test Set-up and Photograph of Driven Pile Tests

5. RESULTS

Plots of the load-deflection history (hysteresis loops) for each pile are given in Appendix H. Typical plots are reproduced in Appendix A as the large number of plots in Appendix H required it to be published as a separate document.

Points on the parent curve (often called a back-bone or envelope curve) were extracted from the hysteresis loop peaks for each pile. The parent curve was plotted using a series of straight lines joining the hysteretic peaks. These curves were factored for the four pile types as described below and are given in Appendix B. These have been used to compare results from different tests.

5.1 Anchor Piles

Representative hysteresis loops for anchor piles in clay, peat, sandy-silt, and sand are given in Appendix B. The maximum deflections for which stable hysteresis loops were obtained in the 14 anchor pile tests are given in Table 5. The hysteresis loops are given in Appendix H and the pile location in Figure 11.

5.1.1 Data Reduction

The horizontal force was applied to each pile at a different height and the pile deflections were also measured at different heights. The parent curves were normalised to a common height of 600 mm to enable them to be compared with each other. Deflections were linearly interpolated (or extrapolated) from measured deflections and loads were factored using the following expression (see Figure 14 for symbols):

$$Factor = \frac{H_3 + 0.6H}{600 + 0.6H} \dots\dots\dots (2)$$

This approximate formula assumes the soil stress can be represented by a rectangular stress block Thurston (1993).

The normalised Parent Curves are given in Appendix B.

The loading and deflection measurements heights were close to 900 mm for the anchor piles in peat, so parent curves for this soil were normalised to 900 mm rather than 600 mm.

5.1.2 Experimental Observations

Pile Pair J3-J4

At a load of 6.1 kN pile J4 split at the top, as shown in Figure 21(a). The vertical split passed through the bolt hole as a result of the horizontal load being applied to the pile through the bolt. The split was contained using plates and a G-clamp to enable greater forces to be applied. However, at 13.8 kN a second split developed, as shown in Figure 21(b) and the test was terminated. Complete vertical splitting of the concrete footing was also noted.

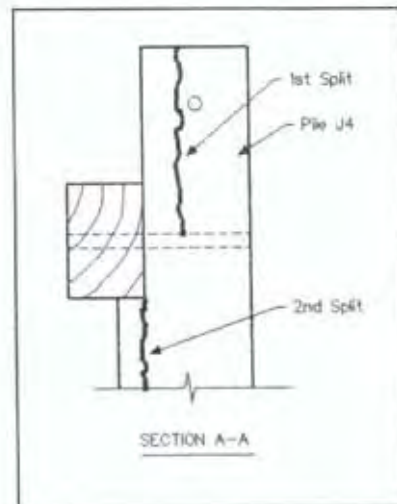
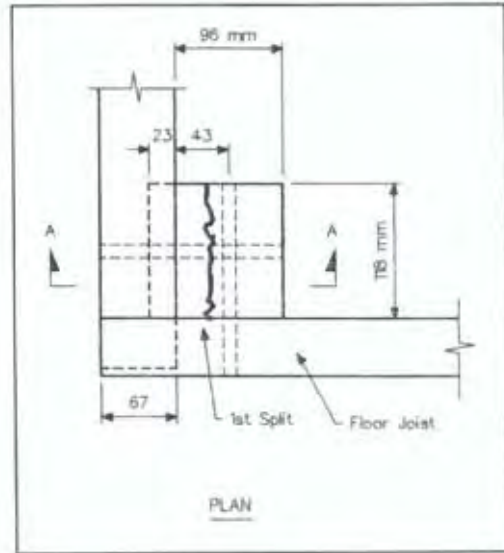


Figure 21. Failure of Group 1 Anchor Pile J4

Pile J3 was used as a reaction pile when testing the pile pair J1-J2 (see Plot 19). The pile failed in flexure at the bearer rebate notch at 8.96 kN load (see Figure 22[b]). The damaged pile was repaired using plates and a G-clamp to enable the test to continue.

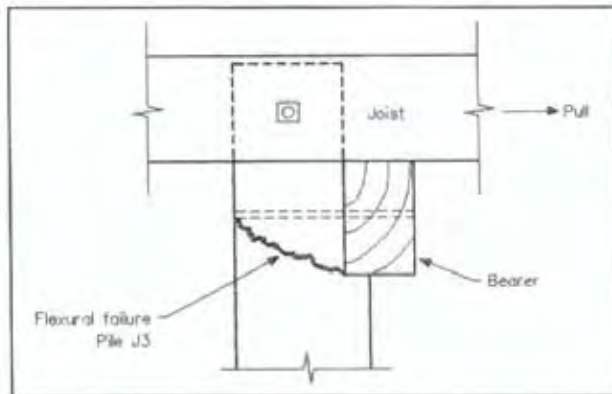


Figure 22. Failure of Group 1 Anchor Pile J3

The parent curve was not influenced by the failures discussed above because the deflection measurements were outside the failure regions. The major deformation mechanism was rocking of the pile footing in the ground.

Pile Pair V13-W13

The piles rocked in the ground until, at a load of 8.6 kN (ie at a bending moment of 6.0 kNm), pile W13 failed in flexure at the interface of pile and concrete footing (see Figure 23). Cracking noises were first heard at pile W13 at a load of 7.6 kN.



Figure 23. Failure of Pile W13 in Flexure

Cracking noises also emitted from pile V13 and a small horizontal crack was detected at interface of pile and concrete footing.

Pile Pair V10-W10

Pile W10 failed in flexure at the footing/pile interface at a load of 5.5 kN (bending moment of 3.6 kNm).

Pile Pair M1-M2

Both pile footings split at approximately 10 kN load, as shown in Figure 24. (Note that this photograph was taken when digging out the pile to measure its depth.) Only the last 3 cycles



Figure 24. Failure of Footing at Pile M1 (photograph taken after the soil was dug away)

Pile Pair M3-M4

Pile M3 failed in flexure at the interface with the concrete footing at a bending moment of 7.4 kNm.

Pile Pair P1-P2

The pile footings rocked in the sand, with no concrete or timber failure.

Piles H50 and H51

As for pile pair P1-P2. At test completion compression of the piles against the peat had left 50 mm gaps each side of the soil surface.

Summary

Of the 14 anchor piles tested, pile flexural failure occurred in 5 instances and pile splitting failure occurred in one instance (where the load was introduced through the bolted joist connection). Otherwise the pile rocked within the soil in a stable and ductile manner.

5.2 Braced Piles

Representative hysteresis loops for braced piles are given in Appendix B. The maximum deflections for which stable hysteresis loops were obtained in the nine braced pile tests are given in Table 6. The hysteresis loops are given in Appendix H and the three pile types shown in Figure 17.

5.2.1 Data Reduction

During the current and previous (Thurston, 1993) testing it was noted that the main failure and deformation mechanism of braced piles occurred in the bolted connection between the brace and pile. The shear force applied to the bolt is $F/\cos\theta$ where F is the horizontal load and θ is the angle the brace makes with the horizontal. The brace loads were normalised to their maximum brace angle (namely $\theta = 45^\circ$). As the braces were at various angles (see Table 6) horizontal forces were factored by:

$$\text{Factor} = \cos\theta / \cos 45^\circ$$

Deflections were linearly interpolated (or extrapolated) from measured deflections to give the deflection at the top brace bolt.

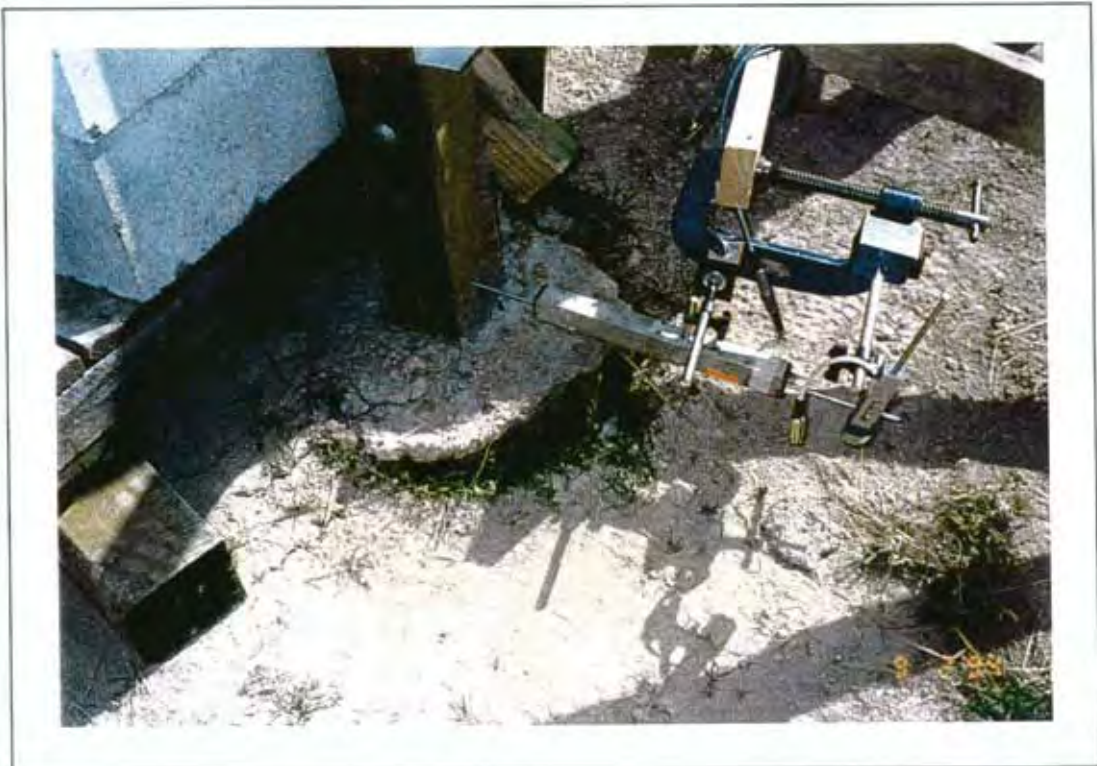
5.2.2 Experimental Observations

Pile Pairs A1-A2, A4-A5

The brace was connected between the pile and joist, as shown in Figure 17(a). Only the last two cycles of test data were recorded (see Plots 1 and 4), because of a computer malfunction. The deformation appeared mainly to be twisting of the pile and joist about the pile axis and slip of the lower end of the brace relative to the pile. The pile footings rocked freely in the ground. At close to maximum loads, the pile at the lower brace end began to lift out of the ground (Figure 25[b]), the bearers began to separate from the pile and the bearers rocked on their supports. At test completion the brace bolts were deformed to a flat "S" shape (Figure 25[a]), especially at the lower end of the brace, and the bolt hole had elongated by approximately 15 mm at the interfaces between the brace and pile and by 8 mm between the brace and joist.



(a) Deformed Bolt



(b) Pile Uplift

Figure 25. Damage and Deformations Observed in Braced Pile Tests

Pile Pairs D1-E1, I1-J1 and G1-G2, G3-G4 and J1-J2

No failures occurred. Observations were similar to those for pile pairs A1-A2 and A4-A5.

Pile Pair X13 - Y13

The test load was applied to a bearer connected to the braced piles by Type TL connectors. Although these connectors deformed significantly during testing, they did not fail. Near the end of the test the pile at the lower end of the brace cracked near the footing to one third of the pile depth at a 45° angle. Unfortunately, due to a computer malfunction, only the last two cycles of data recording were retained (Plot 43).

Pile Pair X10-Y10

Several cracking noises were heard but only fine cracks were detected in the piles.

5.3 Shear Piles

Representative hysteresis loops for shear piles are given in Appendix B. The maximum deflections for which stable hysteresis loops were obtained in the eight shear pile tests are given in Table 7. The hysteresis loops are given in Appendix H and pile locations are given in Figure 11.

5.3.1 Data Reduction

The load measured during the test was the load resisted by two piles. Hence, this load has been divided by two to produce the Parent Curves given in Appendix B.

5.3.2 Experimental Observations

The piles sheared horizontally in the ground, as shown in Figure 26. This compressed the soil on either side of the pile so when the pile was restored to its initial position a void was created on either side. This void was partially filled by natural sand movement in Pile Pairs P3-P4. No damage occurred to the piles in any test.



(a) Test (Group 3)



(b) Clay (Group 1)

Figure 26. Photographs of Horizontal Sliding Movement of Shear Piles in the Ground



(c) Jacking Location on Shear Piles

Figure 26. Photographs of Horizontal Sliding Movement of Shear Piles in the Ground

5.4 Driven Piles

Representative hysteresis loops for driven piles are given in Appendix B. The maximum deflections for which stable hysteresis loops were obtained in the four driven pile tests in soft peat are given in Table 9. The hysteresis loops are given in Appendix H and pile locations are given in Figure 11.

5.4.1 Data Reduction

To enable results to be compared, the parent curves were normalised to a height of 900 mm using the method described in Section 5.2.1 (with the 600 mm dimension replaced by 900 mm).

5.4.2 Experimental Observations

The piles deformed the peat soil around the piles as they rocked from side to side under the cyclic loading. No other damage occurred.

6. DERIVATION OF DESIGN LOADS

6.1 Design Philosophy

Design for wind generally requires the structure to be strong and stiff to resist face loadings resulting from wind pressures during severe storms. The unidirectional nature of such applied forces is reflected in laboratory test methods (eg Reardon, 1980) which verify the suitability of structural elements by racking representative specimens in one direction only (monotonic loading). Strength and stiffness are measured from plots of the applied load and the corresponding specimen deflection.

Seismic design generally requires stiff lateral load-resisting elements to prevent damage during (relatively frequent) low intensity earthquakes. The design criterion for high intensity earthquakes is for the structure to survive the earthquake without collapse, although damage is anticipated (and acceptable).

It is uneconomic to design structures to respond elastically (ie without damage) during a high intensity earthquake so most designers prefer the system to deform inelastically in a controlled manner while avoiding collapse (Dowrick, 1977). This is reflected in laboratory test methods, such as the BRANZ P21 test procedure (King and Lim, 1990), which racks timber framed walls to ultimate limit state deflections.

6.2 Derivation of Average Parent Curves

The experimental test data consisted of a set of hysteresis loops for each pile and soil type. Design values are subsequently derived using "average" loops. As a first step in obtaining these average loops, equations for a best fit to the parent curves were derived.

Appendix B presents parent curves for each pile type in various soil conditions. The relationship given in Equation 3 was fitted to the parent curves for each pile type and soil condition by minimising the difference between the predicted and measured loads using the Excel solver. Appendix C presents the solutions obtained.

$$P = \frac{A\Delta}{B + \Delta^C} \dots\dots\dots(3)$$

Where: P = Pile horizontal load (kN)
Δ = Pile horizontal deflection (mm)
A,B,C are best fit constants

A complete load deflection response for a typical test pile from each pile type and soil condition was selected and the loads were (slightly) factored so that the parent curve in the first quadrant fitted closely to that of the best fit solution of equation 3 for corresponding piles. These slightly factored sets of hysteresis loops were then designated the "average" for that pile type and soil condition.

6.3 Earthquake Design Loads

6.3.1 Background to NZS 3604 Earthquake Design Loads

Earthquake design loads in the non-specific design code NZS 3604 (SANZ, 1990) were derived from a draft version of the loadings standard NZS 4203 (SNZ, 1992a) for a building with a period of 0.4 seconds and ductility $\mu = 4$. From equation 4.6.2 (a) of NZS 4203, the seismic design force, V , on a building of mass M is given by:

$$V = C_h(T,\mu) \times S_p \times R \times Z \times L_u \times M \times g \dots\dots\dots(4)$$

where: $C_h(T,\mu)$ = Basic seismic hazard coefficient for period T and ductility μ
 S_p = Structural performance factor
 R = Risk factor for a structure
 Z = Zone factor
 L_u = Limit state factor for ultimate limit state
 g = Acceleration due to gravity

Taking $R = L_u = 1$, $S_p = 0.67$, $g = 9.81 \text{ m/sec}^2$, $Z = 1.2$ (Wellington) and $C_h(T,\mu) = 0.27$ (for $T = 0.4$ seconds, $\mu = 4$ and "intermediate" soils), then:

$$V = 0.217 \times M \times g \dots\dots\dots(5)$$

Thus if it can be shown that a pile performs satisfactorily under the design earthquake when it is required to restrain a seismic mass m , then an appropriate design load for that pile can be derived from equation 5 with the mass M replaced by the mass m . For instance, if $m = 1200 \text{ kg}$, then

$$V = 0.217 \times 1200 \times 9.81 = 2554 \text{ N} = 2.554 \text{ kN} = 51 \text{ BU}$$

The above calculation converts a force in kN to BU (Bracing Units) using the identity of $1 \text{ kN} = 20 \text{ BU}$ as defined by NZS 3604.

6.3.2 Pinched Hysteresis Loops

It is difficult to assess both "yield" and "effective ductility" for structures or elements with pinched hysteresis loops (Deam and King, 1994). An alternative design method, based on displacement, may be employed instead. Dean et al. (1986) showed that slackness from the pinching of the loops appears to increase the natural period of oscillation. As the maximum accelerations of most earthquake records decrease as the period increases, this effectively reduces the maximum force in the structural element. This force reduction occurs without "fat" hysteretic loops normally associated with absorption of seismic energy. Dean et al., 1986, showed that the displacement demand with slackness is similar to that with elastic and elastoplastic behaviour. Slackness is also thought to isolate the mass from high ground acceleration pulses of short duration. The maximum displacement of a tested bracing element may be used to determine the mass able to be restrained by the bracing element using this envelope curve, without requiring the yield force or ductile capacity of the bracing element to be defined.

6.3.3 Pinched Hysteretic Loop Matching

To perform time-history analysis, the hysteretic loop approximations require fitting to measured test hysteresis loops. The elastoplastic response is a poor approximation and is consequently difficult to fit to the hysteresis loops. Stewart's (1987) approximation is better but still requires curves to be approximated with straight lines. A bar and spring model (Deam, 1994) gives the best match but is difficult to fit because of the large number of generating parameters.

Deam (1994) further developed the bar and spring model into the computer program PhylMas. PhylMas enables the generating parameters to be quickly adjusted to match test specimen hysteresis loops by graphically superimposing generated and test hysteresis loops on the computer screen. The parameters are varied by movement of the computer's mouse and the generated loops are updated almost instantaneously. Appendix C shows the excellent match between the smooth hysteresis loops generated by PhylMas and those from the testing described in this report.

6.3.4 NZA Artificial Earthquake Record

An artificial earthquake record was generated at the University of Canterbury (Andriono and Carr, 1991) to match the 1986 edition of the draft loadings standard NZS 4203 (SNZ, 1992a) uniform risk acceleration spectrum (Figure 5). The uniform risk spectrum in the final edition of NZS 4203 (SNZ, 1992a) incorporated a structural performance factor and revised the zone factors to retain the same shape and accelerations as the 1986 draft uniform risk acceleration spectrum. The original artificial earthquake record was factored to give the design accelerations for Wellington (which was within "Zone A", hence the record is known as "NZA"). This record may contain more spectral energy than a real earthquake because it matches the envelope of a range of earthquakes. Thus it is likely to be more demanding than any individual earthquake record and the results so derived will generally be conservative.

6.3.5 Determination of Maximum Seismic Mass

Non-linear time-history analyses were performed with PhylMas for every "average" set of pile hysteresis loops using the NZA earthquake record. The determination of these "average" loops is described in Section 6.2.

PhylMas is able to produce acceleration and displacement response spectra by performing a series of time-history analyses, incrementing the natural period before each analysis. For this relationship the period (T) was related to the initial stiffness, k , of the element and the restrained mass, m , by Equation 6 (Paz, 1985):

$$T = 2\pi\sqrt{\frac{m}{k}} \dots\dots\dots(6)$$

Thus if the maximum deflection to which a pile can be safely cycled is stipulated, then the period (T) corresponding to this deflection can be determined directly from the

displacement response spectra provided by PhylMas, and hence the restrained mass, m , can be calculated using Equation 6.

6.3.6 Summary of Procedure to Obtain Pile Seismic Design Loads

A modified version of Deam and King's (1994) procedure was used to obtain seismic design loads for the tested piles. This used the following steps:

1. Adjust the PhylMas model parameters so a match is obtained with the PhylMas model loops and the "average" test hysteresis loops as derived in Section 6.2. Appendix D shows the excellent agreement obtained.
2. Use PhylMas to generate displacement response spectra for the NZA earthquake records for the PhylMas model parameters derived in Step 1.
3. The mass m able to be restrained by the element may then be calculated from Equation 6 using the natural period T and the stiffness k from the hysteresis loop match in step 1.
4. The pile design load is obtained directly from Equation 5 using the mass m from Step 3.

Using the above procedure the plots in Appendix E relating earthquake design load and maximum displacement were derived for various pile type and soil conditions. The maximum acceptable pile deflections were estimated from the maximum measured deflections given in Tables 5, 6, 7 and 9. Pile earthquake design strengths can then be obtained directly from the plots in Appendix E. It may be appropriate to further factor these pile earthquake strengths before the values are disseminated for design purposes as discussed in Section 6.5.

NZS 4203:1992a gives the serviceability design earthquake as one sixth of the ultimate limit state earthquake. The deflections of the piles at this level of earthquake (assuming they were restraining their full design level mass) were calculated using PhylMas and are given in Table 10. It can be seen that these deflections are generally less than the 8 mm limit sometimes taken as the maximum serviceability earthquake deflection (eg King and Lim, 1990 for walls). A limit of 15 mm may be more appropriate for foundation control. The serviceability level earthquake deflections were particularly low for the shear piles and high for the braced piles and piles in peat.

6.3.7 Verification of PhylMas

Stewart (1987) compared the time history of deflections of a shear wall subjected to an El Centro type earthquake with predictions from his theoretical model. Deam (1994) verified that PhylMas was providing realistic results by comparing Stewart's experimental and theoretical data with predictions from PhylMas.

6.3.8 Assumptions Inherent in Earthquake Load Analysis

The methodology outlined in Section 6.3.7 implicitly assumes that the entire building is founded on the same type of piles and the building does not twist - ie all piles deflect the same amount. The influence of a mixed-pile foundation system on the design loads derived using the methodology needs to be investigated.

The methodology also assumes the building superstructure deformation is very small compared to the foundation deformation. This is because the model used a single degree of freedom (DOF) system. For a one-storey building a more accurate model would be a two-mass model with the top mass (representing the roof and the upper half of the walls) being supported on springs having lateral stiffnesses representing wall racking stiffnesses. Flexibility of the superstructure will increase the effective building fundamental period and hence is expected to lower the foundation seismic shear forces. Thus the assumption of a rigid superstructure (ie a single degree of freedom oscillator) used in the above analysis is likely to be conservative.

The effects of the above assumptions will be investigated in a future research project.

PhylMas was used to study the relationship between damping ratio and element deflection using the standard anchor pile hysteresis loops determined using the procedure in Section 6.3.7. Figure 27 shows that predicted deflections are sensitive to assumed damping ratios. Stewart (1987) used a damping ratio of 10% to obtain best agreement between predictions and measurements for shear walls. Deam (1994) found best agreement was obtained with a damping ratio of 14% for this same data. From Figure 27 the deflections reduce by 35% when the damping ratio of an anchor pile with natural period 0.4 seconds is increased from 5% to 12%. Figure 28 shows a typical plot of force versus deflection from one of the dynamic analysis runs. Figure 29 shows that there is little difference between the predicted deflection of elastic, elastoplastic and pinched hysteresis loops for piles with natural period 0.4 seconds and damping above 10%, although greater deflections are predicted for the pinched hysteresis loop case where damping is less than this value. (The yield force for the elastoplastic analysis was taken as 8 kN for this analysis - see Figure 28.)

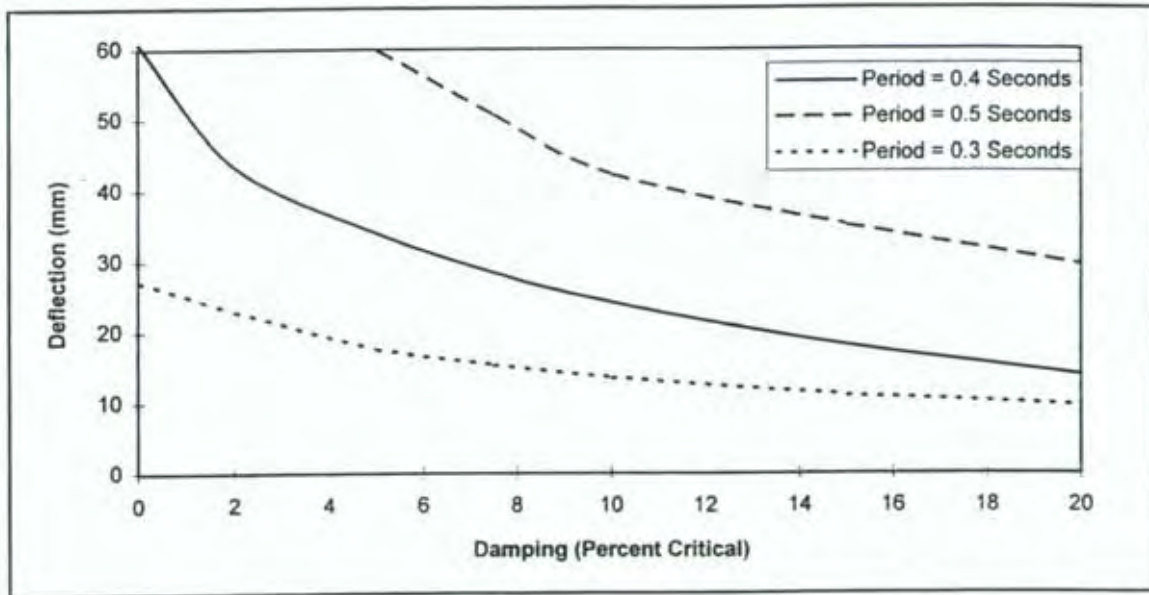


Figure 27. Relationship Between Deflection and Assumed Damping Ratio For Anchor Piles

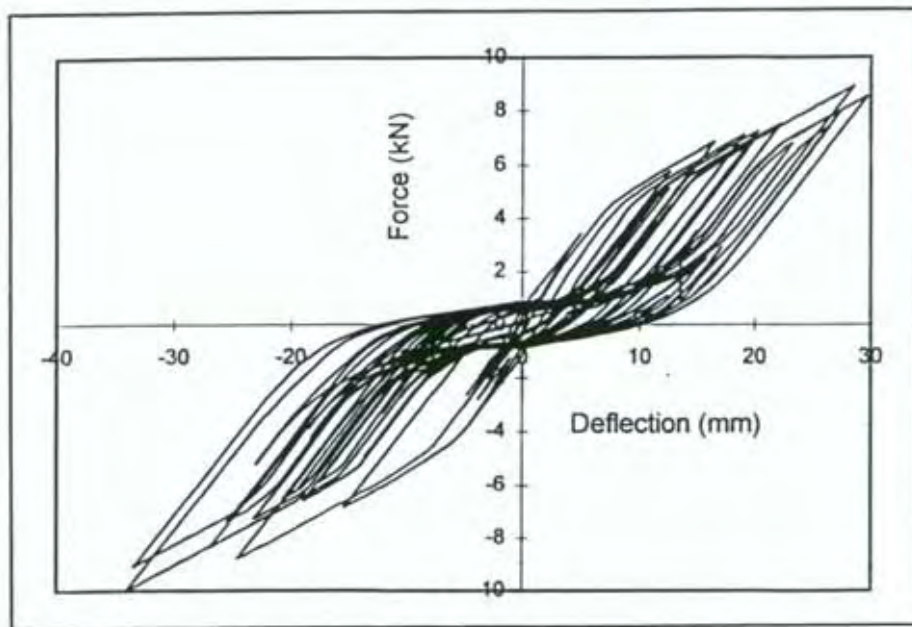


Figure 28. Predicted Force Versus Deflection For Anchor Pile Under NZA Earthquake (T = 0.4 seconds, damping ratio = 5%)

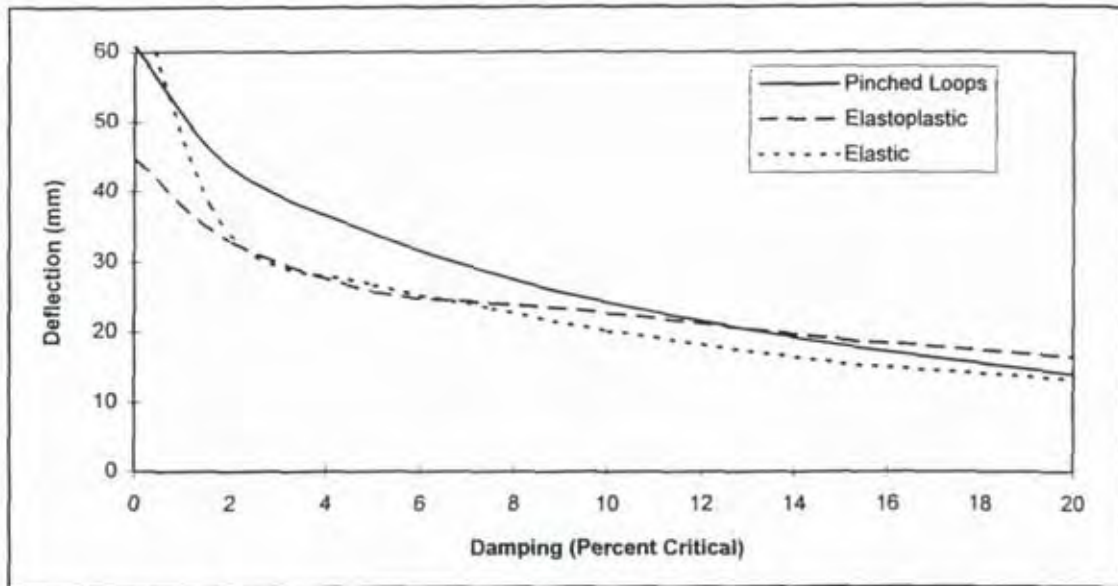


Figure 29. Relationship Between Deflection and Assumed Damping Ratio for Various Shapes of Hysteresis Loops For Anchor Piles of Period 0.4 Seconds

6.4 Wind Design Strengths

Wind design strengths in Table 10 were determined directly from 0.9 times the force predicted from the best fit equations (Section 6.2) at the displacement given in Table 10. The factor of 0.9 is intended to account for strength loss due to the buffeting action of the wind and is the same factor used by King and Lim (1990). It may be appropriate to factor these pile wind strengths before the values are disseminated for design purposes as discussed in Section 6.6.

NZS 4203 (NZS 1992a) gives the serviceability limit state wind actions as $(0.93/0.75)^2 = 0.65$ times the ultimate limit state wind actions. The deflections of the piles at the serviceability wind (assuming they will be loaded to their full design level in an ultimate limit state wind) are also given in Table 10. With the exception of the shear piles, the serviceability wind deflections in Table 10 are generally in excess of a 15 mm limit (tentatively suggested as being an appropriate limit by the writer). The largest deflections were calculated for braced piles and piles in peat, sandy-silt or sand. Serviceability level winds are expected to have a 5% probability of occurring every year (SNZ, 1992a). Hence it may be more appropriate to base wind loads for some piles on serviceability criteria to limit vibration and other problems at serviceability level loadings. However, at serviceability loads a real building may be stiffer than predicted from the tests because gravity load may provide some rotational fixity at the pile top and the additional restraint present with "normal" piles is usually ignored in the analysis.

**Table 10. Pile Earthquake and Wind Design Strengths
(to be used with NZS 3604 loadings)**

Pile Type	Soil Condition	Serv. Displ.		Maximum ULS Displ. † (mm)	Design Forces	
		EQ (mm)	Wind (mm)		EQ BU**	Wind BU**
Anchor	Clay	6.5	15.5	40	137	200
	Peat	10.0	17.8	80‡	72	90
	Sand/Silt	8.6	36	60	207	243
Braced	Clay	7.3	23	60	162	180
	Clay	16.7	34.5	90*	245	226
Shear	Clay	4.3	7.25	30	412	362
	Peat	3.9	12.1	40	113	171
	Sandy-silt	2.4	7.25	30	354	446
	Sand	6.0	2.88	17	138	161
Driven	Peat	8.9	38	80‡	93	101

Legend

† Deflections were limited to 60 mm for 600 mm high piles.

‡ Deflections were limited to 80 mm for 900 mm high piles.

* Greater deflection for braced piles which will be more than 900 mm high.

** 20 BU (bracing Units) are defined as equal to 1 kN in NZS 3604.

6.5 Additional Factors

Design values given in Table 10 may require modification for the following reasons:

- Wall systems in most buildings have a greater bracing strength than that traditionally included in design. This redundancy does not usually exist to the same extent in piled foundations (which can be very simple systems). To provide the same degree of security in an overload situation, it may be appropriate to reduce the design loads in Table 10. This in effect will result in stronger foundation systems being built.
- Values in Table 10 may require reduction to account for possible building torsion and combining foundation elements of different stiffness etc. The effect of other assumptions outlined in Section 6.3.8 (such as assumed damping ratio) may also necessitate changes to the design values.

- Values in Table 10 assume a strength reduction factor of 1.0. A lower value may be appropriate.
- Values in Table 10 are based on average strengths. It may be appropriate to reduce the design values to the lower 5 percentile.
- Values in Table 10 are based on the ductile load resisting mechanisms present in the measured hysteresis loops. The effects of brittle failure have not been taken into account. Three of the fourteen anchor piles fractured, three footings split, and the mechanism transferring load into the piles was shown to result in pile splitting at pile scarfings. This should be taken into account either by reducing design values in Table 10 or by changing construction practice to ensure these other failures will not occur.

The design values did not take into account serviceability criteria (such as the service load deflections given in Table 10) which may be critical, especially for braced piles. Braced piles may be constructed taller than those tested which will increase the lateral load deflections. On the other hand most braces are at less than 45 degrees which will result in higher design load and stiffness.

- The pile footing dimensions and actual soil conditions (as detailed in this report) did not always match the minimum requirements of the non specific design code NZS 3604 (SANZ, 1990).
- Wind design loads in NZS 3604 were derived using the limit state multiplier $M_{1S} = 1.0$ given in a draft version of NZS 4230 (SNZ, 1992a). When NZS 4203 was finally published, the value published was $M_{1S} = 0.93$. Thus the wind loads in NZS 3604 were $(1.0/0.93)^2 = 16\%$ greater than would have been obtained directly from NZS 4203. To balance this it may be appropriate to increase the wind resistances given in Table 10 by 16%.

6.6 Comparison with Current NZS 3604 Loadings

NZS 3604 (SANZ, 1990) stipulates anchor and braced pile earthquake design loads to be 70 BU and wind design loads to be 160 BU. These cannot be compared with values for peat soils given in Table 10 because peat soils are outside the scope of NZS 3604. Values (other than for peat) in Table 10 indicate the standard is unduly conservative for the earthquake design loads, but quite reasonable for wind design loads. The table also indicates that unacceptable pile deflections may occur during serviceability level wind actions. However, BRANZ has received few complaints in this regard, which indicates that other factors (such as given in Section 6.5) may stiffen piled foundations at these lower loads.

6.7 Comparison with SR 46

Two braced pile sets were tested in the laboratory and reported in BRANZ Study Report 46 (Thurston, 1993). The braces in each instance were at approximately 45° to the horizontal. In the first test the brace went from pile to pile and the load resisted averaged 6.2 kN at 60 mm deflection and 8.3 kN at 100 mm deflection. In the second test the brace went from pile to bearer and the load resisted was 5.9 kN at 60 mm deflection and 8.3 kN at 100 mm deflection. However, the best fit curve to the braced pile test results in the current test series indicates a load resistance of 10.0 kN at 60 mm deflection. The difference between field and laboratory tests is attributed to the following three effects:

- (1) Laboratory pile specimens were more than 50% taller than the pile sets in the field and hence it is more reasonable to compare to loads at 60 mm in the field (10.0 kN) with that at 100 mm deflection in the laboratory (8.3 kN).
- (2) The braced pile twisted in the laboratory due to eccentricity between brace and pile, adding flexibility to the system. This was not present in the field as the concrete footing in soil resisted this twisting action.
- (3) The method used to restrain pile uplift in the field may have provided a small amount of strength enhancement to these piles.
- (4) Braced piles cast in concrete will have some base fixity imposed by the surrounding soil and therefore can be expected to be stronger than those tested in the laboratory which were pinned at the base.

7. SUMMARY AND CONCLUSIONS

Cyclic lateral load tests were performed in the field on several pile systems used to brace New Zealand houses and the data collected was used to derive suitable earthquake and wind design loads. The piles were founded in clay, silt and sand soils which had close to the minimum bearing strength allowed by NZS 3604 (SANZ, 1990).

The results indicated that the design wind loads recommended in NZS 3604 for braced and anchor piles were reasonable, although deflections at the serviceability wind loads were unacceptably high. However, it was considered that actual house deflection at this loading may be lower, for various reasons cited. The earthquake design loads recommended in NZS 3604 were significantly lower than derived from the test data.

Design wind and earthquake loads were also derived from the test data for "shear" piles - (ie piles rotationally restrained at the top) by nailing sheet bracing to the piles. This appears to be an effective method of bracing piles against lateral loads. As these pile systems were initially very stiff, the earthquake and wind serviceability limit deflections were very low. This system even provided useful levels of earthquake and wind resistance when used in soft peat soils.

The lateral load resistance of anchor and driven piles in peat was relatively low. However, the test piles had low initial stiffnesses which consequently may result in unacceptably large deflections at the serviceability wind loads.

There were two instances of brittle fracture of the bolted connection between a bearer and anchor piles. The piles themselves fractured in three instances and the concrete pile footings also fractured in three instances. These non-ductile failure mechanisms were not considered in the method used to derive design loads.

Braced pile systems can experience considerable deformations without shedding load. However, their flexibility may result in annoying vibrations or movements which are discernible to a house occupant. Damage to building services may occur at relatively low horizontal loads.

Earthquake design loads were successfully obtained from the field-measured hysteresis loops using a computer package PhylMas, developed jointly by BRANZ and Canterbury University. This was used to perform a time-history simulation using an earthquake record which closely fitted the design acceleration spectrum given in NZS 4203 (SNZ, 1992a).

The braced pile systems tested in the field were stronger than those tested in the Laboratory. The difference was attributed to the greater height of the laboratory system and the zero base fixity used in the laboratory tests.

8. REFERENCES

Andrino, T. and Carr, A. J. 1991. A Simplified Earthquake Resistant Design Method for Base Isolated Multistorey Structures. Bulletin N.Z. National Society of Earthquake Engineering. Vol 24, No. 3 238-250. Wellington, New Zealand.

British Standards Institute, 1985. Materials Testing Machines and Force Verification Equipment. BS 1610. London.

Cocks, D.E, Lapish, E.B. and Compton, M.J. 1975. Driven Short Timber Pile Foundations for Light Timber Frame Construction. Cocks, Lapish & Compton, Takanini, New Zealand.

Czerniak, E. (1957) Resistance to Overturning of Single Short Piles. Journal of the Structural Division of ASCE Volume 83, No. ST2 March, 1957, Page 1188-1.

Cooney, R.C. 1979. The Structural Performance of Houses in Earthquakes. Bulletin N.Z. National Society of Earthquake Engineering. Vol 12, No. 3 223-237. Wellington, New Zealand.

Deam, B.L. 1994. Equivalent Ductility for Residential Timber Buildings. Building Research Association of New Zealand, Unpublished Report. Judgeford, New Zealand.

Deam, B. and King, A. 1994. The Seismic Behaviour of Timber Structures. Pacific Timber Engineering Conf. Pages 215-221, Vol 1. Gold Coast, Australia.

Dean, J.A., Stewart, W.G. and Carr, A.J. 1986. The Seismic Behaviour of Plywood Sheathed Shearwalls. Bulletin, New Zealand National Society for Earthquake Engineering 19(1): 48-63.

Dowrick, D.J. 1977. Earthquake Resistant Design. John Wiley & Sons, Chichester.

Dowrick, D.J. Roades, D.A., Babor, J. and Beetham, R.D. 1994. Damage Ratios and Microzoning Effects for Houses in Napier at the Centre of the Magnitude 7.8 Hawke's Bay, New Zealand, Earthquake of 1931. Bulletin of the New Zealand National Society for Earthquake Engineering, Vol 27, No. 4, December.

Greensill, B.N. 1990. Master of Engineering Science Thesis. An Investigation of Short Bored Piers Subjected to Combined Uplift and Lateral Loads. James Cook University of North Queensland.

Graham, K.J. 1991. Master of Engineering Science Thesis. An Investigation of Combined Uplift and Lateral Load Resistance of Short Bored Piles. James Cook University of North Queensland.

James HardIE and Coy, 1994. Subfloor Bracing Systems. James Hardie Building Products. June, 1994. Auckland.

Johnstone, P. 1994. Pers. comm.

Johnstone, P. 1995. Pers. comm.

- King, A.B. and Lim, K.Y.S. 1990. Supplement to P21: An Evaluation Method of P21 Test Results for use with NZS 3604:1990. Technical Recommendation No. 10. Building Research Association of New Zealand, Judgeford, New Zealand.
- Paz, M. 1985. Structural Dynamics. Van Nostrand Reinhold Company. New York.
- Pender, M.J. 1993. Aseismic Pile Foundation Design Analysis. Bulletin N.Z. National Society of Earthquake Engineering. Vol 26, No. 1 49-160. Wellington, New Zealand.
- Reardon, G.F. 1980. Recommendations for the Testing of Roofs and Walls to Resist High Wind Forces. Technical Report No. 5, Cyclone Testing Station, James Cook University, Queensland.
- Standards Association of New Zealand. 1978. Code of Practice for Light Timber Frame Buildings not Requiring Specific Design. NZS 3604. Wellington, New Zealand.
- Standards Association of New Zealand. 1990. Code of Practice for Light Frame Timber Buildings Not Requiring Specific Design. NZS 3604. Wellington, New Zealand.
- Standards New Zealand. 1992a. General Structural Design Loadings for Buildings. NZS 4203. Wellington, New Zealand.
- Standards New Zealand. 1992b. Specification for Timber Piles and Poles for Use in Buildings. NZS 3605. Wellington, New Zealand.
- Stewart, W.G. 1987. The Seismic Design of Plywood Sheathed Shearwalls. Thesis submitted in partial fulfilment of PhD Degree, University of Canterbury, Christchurch, New Zealand.
- Stockwell, M.J. 1977. Determination of Allowable Bearing Pressures Under Small Structures. New Zealand Engineering 32(6) 132-135. Wellington, New Zealand. 15 June, 1977.
- Thurston, S.J. and King, A.B. 1992. Bracing Requirements for NZS 3604:1990 Limit State Code. Proceedings of the Institute of Professional Engineers Annual Conference, 561-570. Christchurch, New Zealand.
- Thurston, S.J. 1992. Report on Bracing Ratings for Various Foundation Systems Using "Harditex" Sheets. Report STR 216. Judgeford, New Zealand. Restricted Document.
- Thurston, S.J. 1993. Design Strength of Various House Pile Foundation Systems. Building Research Association of New Zealand, Study Report SR 46. Judgeford, New Zealand.
- Vallabhan, C.V.G. & Aliktianlou, F. (1982) Short Rigid Piers in Clay. Journal of the Geotechnical Engineering Division, ASCE Volume 108 No. GT10 October, 1982, Page 1255.
- Works Consultancy Services 1990. From Theory to Practice in Pile Design. Internal Technical publication TSC 1990/48. Wellington, New Zealand.

Appendix A Sample Hysteresis Loops

A.1 Introduction

This Appendix contains a typical applied load versus deflection hysteresis plot for each pile type and soil type as summarised in Table A.1. All measured plots are provided in Appendix H which is a separate volume to this report. Locations of applied load and measured deflection are fully described in Section 4 of the main report.

Table A.1 Plots Given in this Appendix

Pile type	Soil Type	Pile Label	Plot Number	Figure
Anchor	Clay	W13	36	A1
	Peat	H50	86	A2
	Sandy-silt	M4	102	A3
	Sand	P2	112	A4
Braced	Clay	X10	50	A5
Shear	Clay	T10	63	A6
	Peat	G50	89	A7
	Sandy-silt	M5	105	A8
	Silt	P4	117	A9
Driven	Peat	J50	77	A10

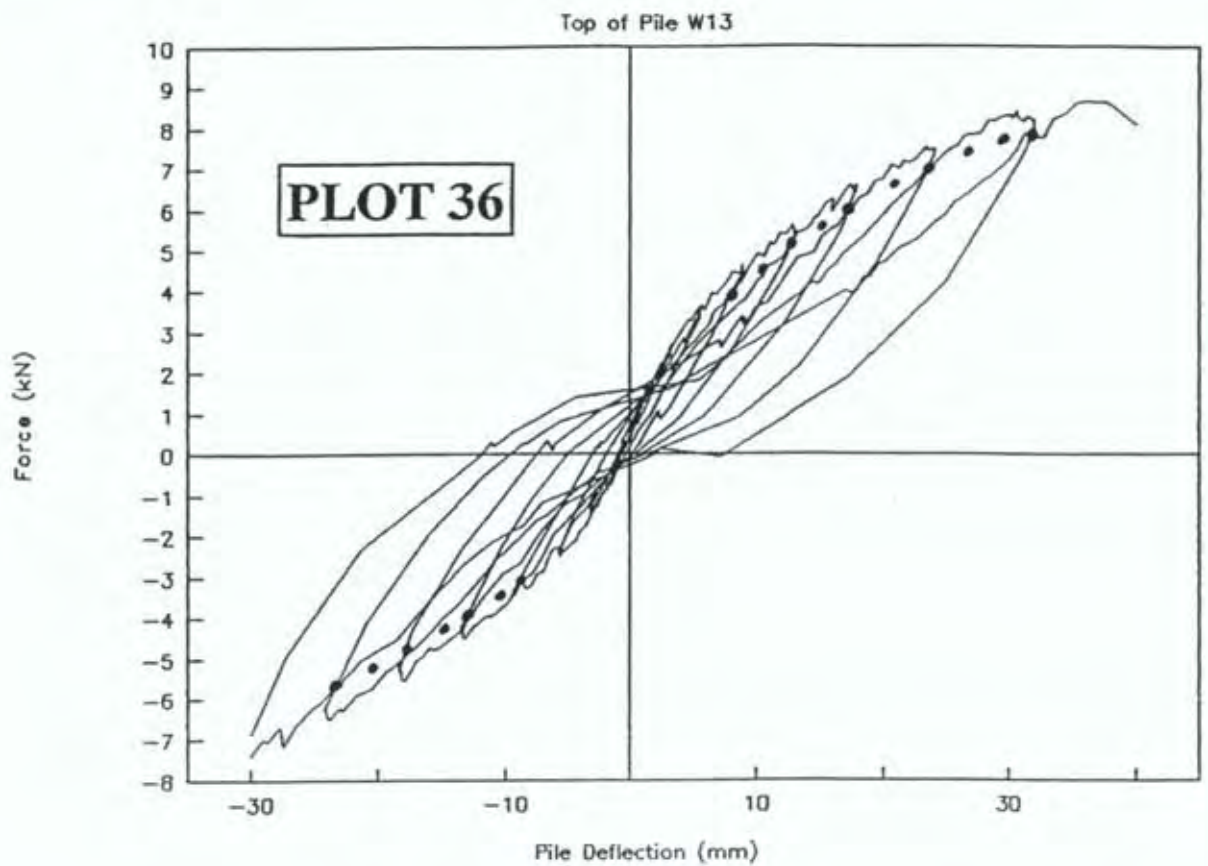


Figure A.1 Typical Measured Hysteresis Loops for Anchor Piles in Clay

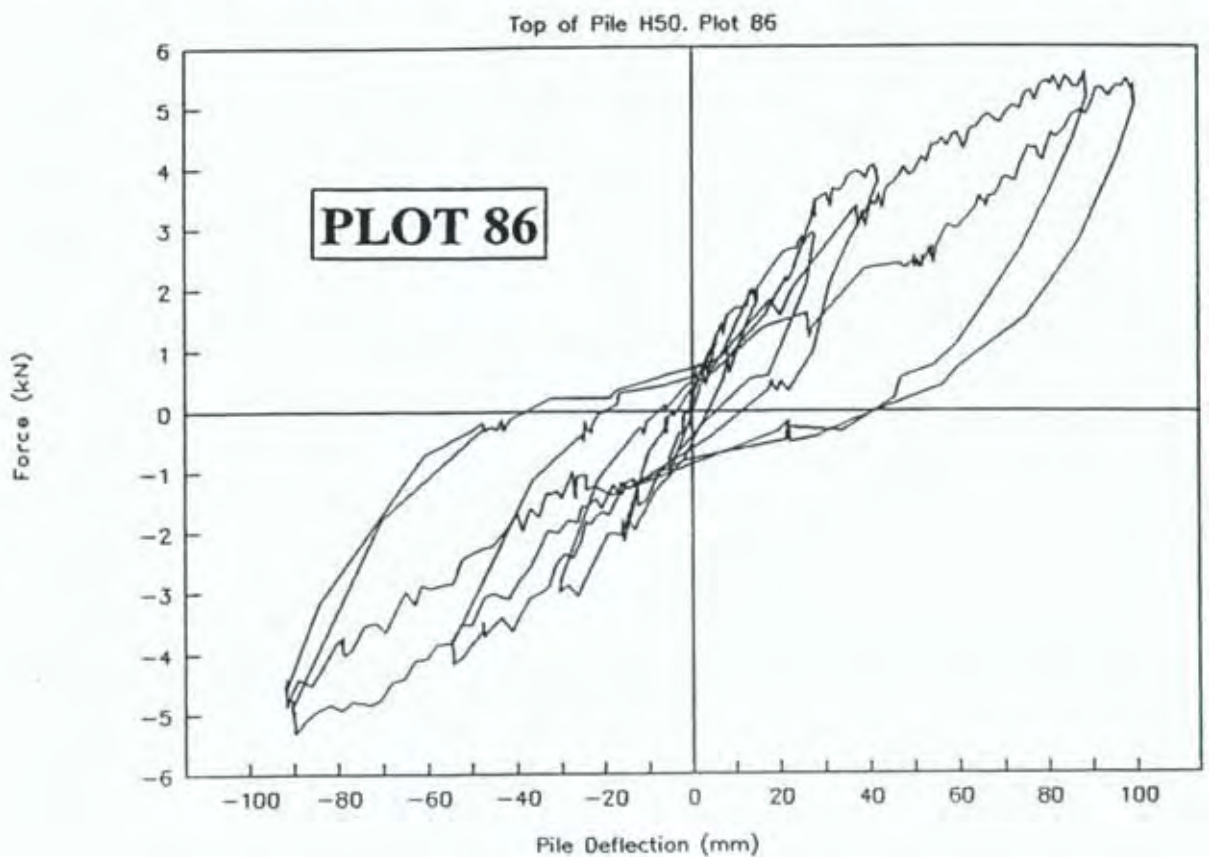


Figure A.2 Typical Measured Hysteresis Loops for Anchor Piles in Peat

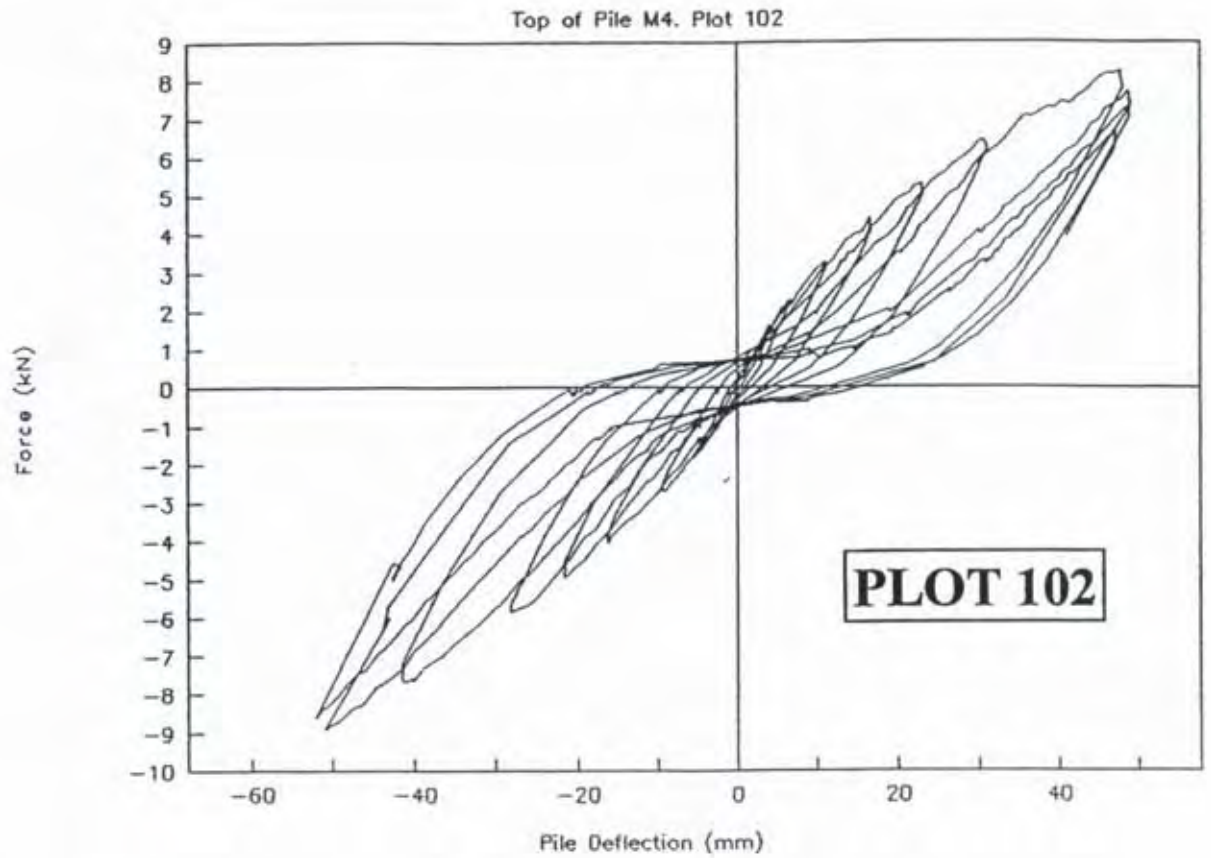


Figure A.3 Typical Measured Hysteresis Loops for Anchor Piles in Sandy-Silt

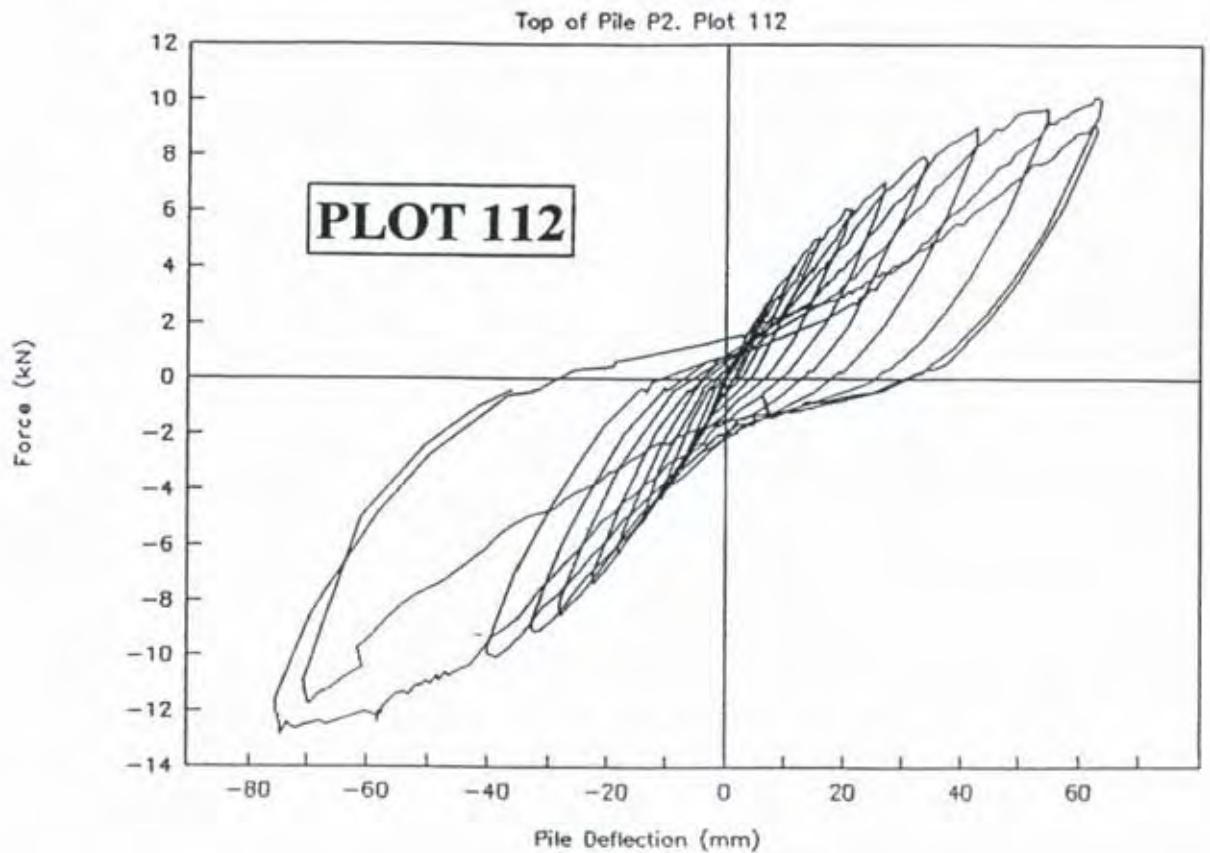


Figure A.4 Typical Measured Hysteresis Loops for Anchor Piles in Sand

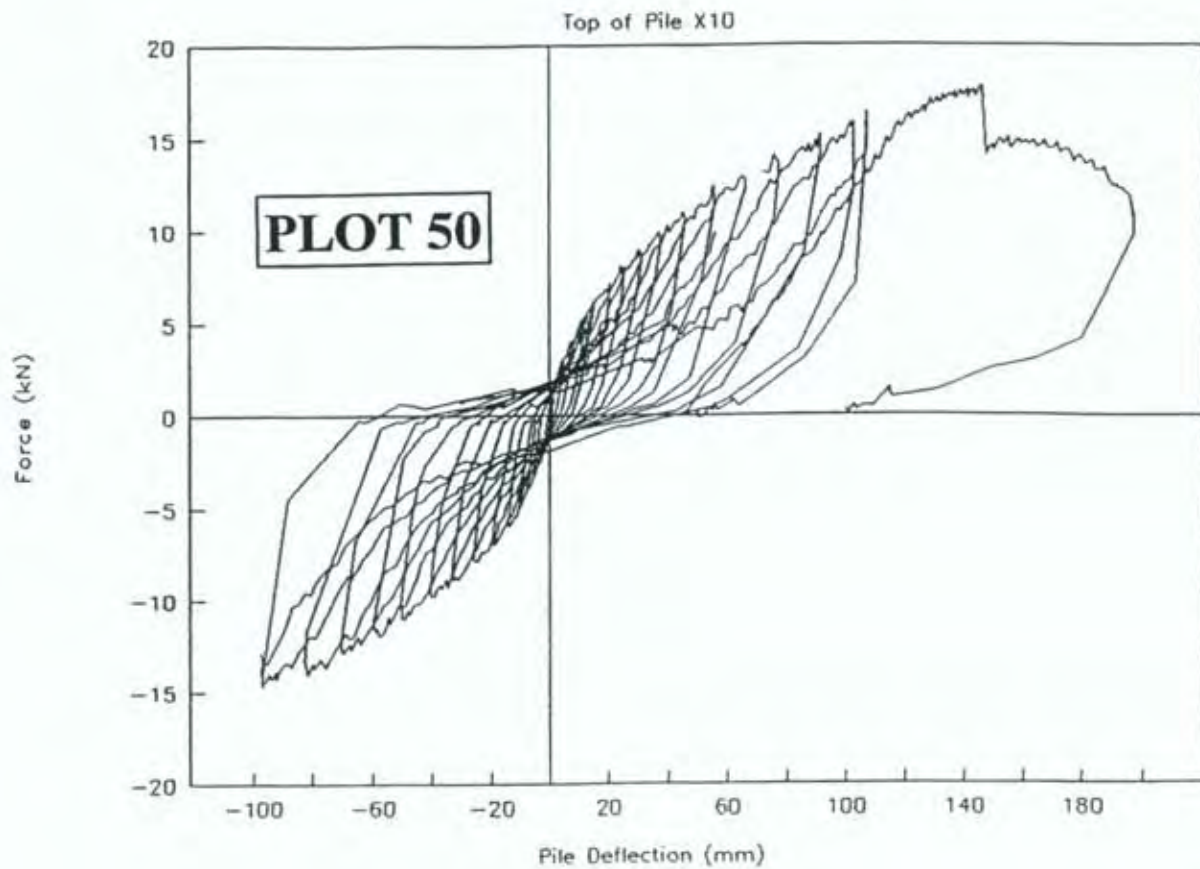


Figure A.5 Typical Measured Hysteresis Loops for Braced Piles in Clay

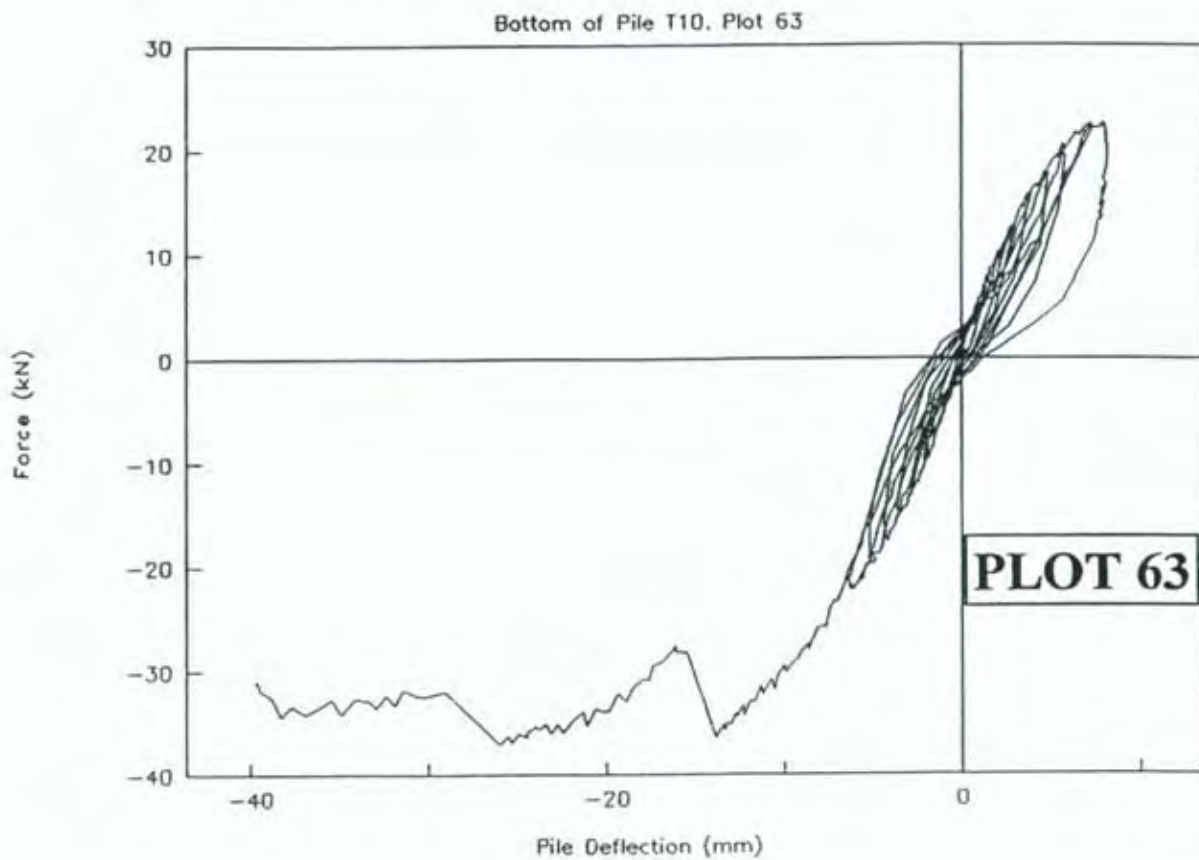


Figure A.6 Typical Measured Hysteresis Loops For Shear Piles in Clay

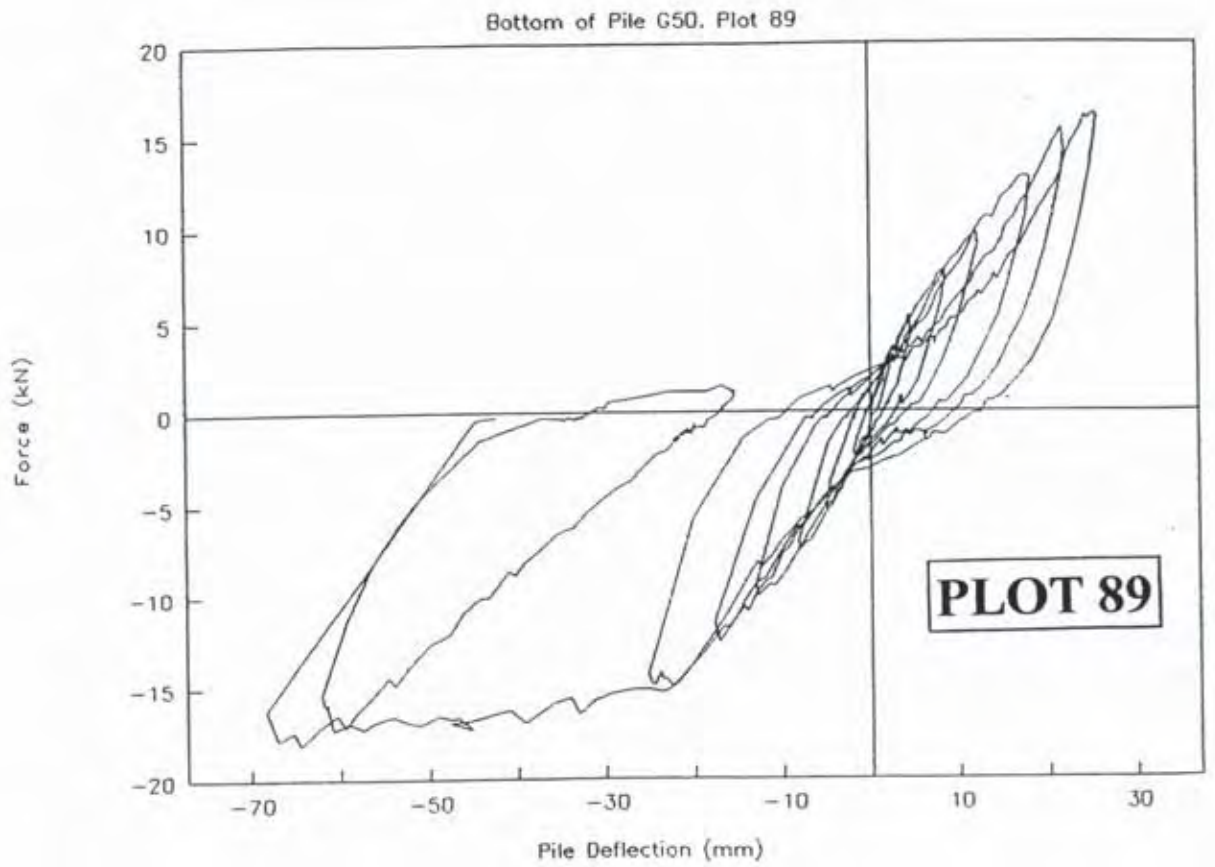


Figure A.7 Typical Measured Hysteresis Loops for Shear Piles in Peat

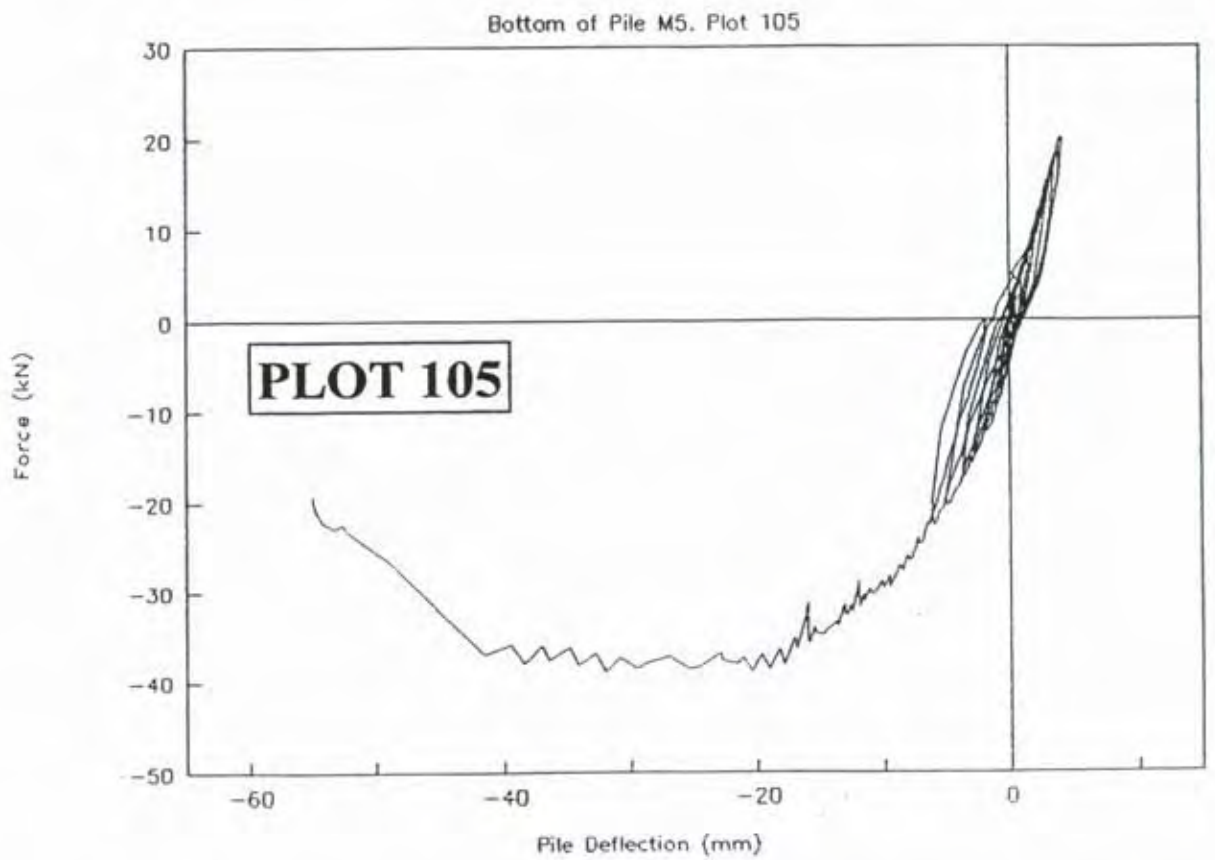


Figure A.8 Typical Measured Hysteresis Loops for Shear Piles in Sandy-Sil

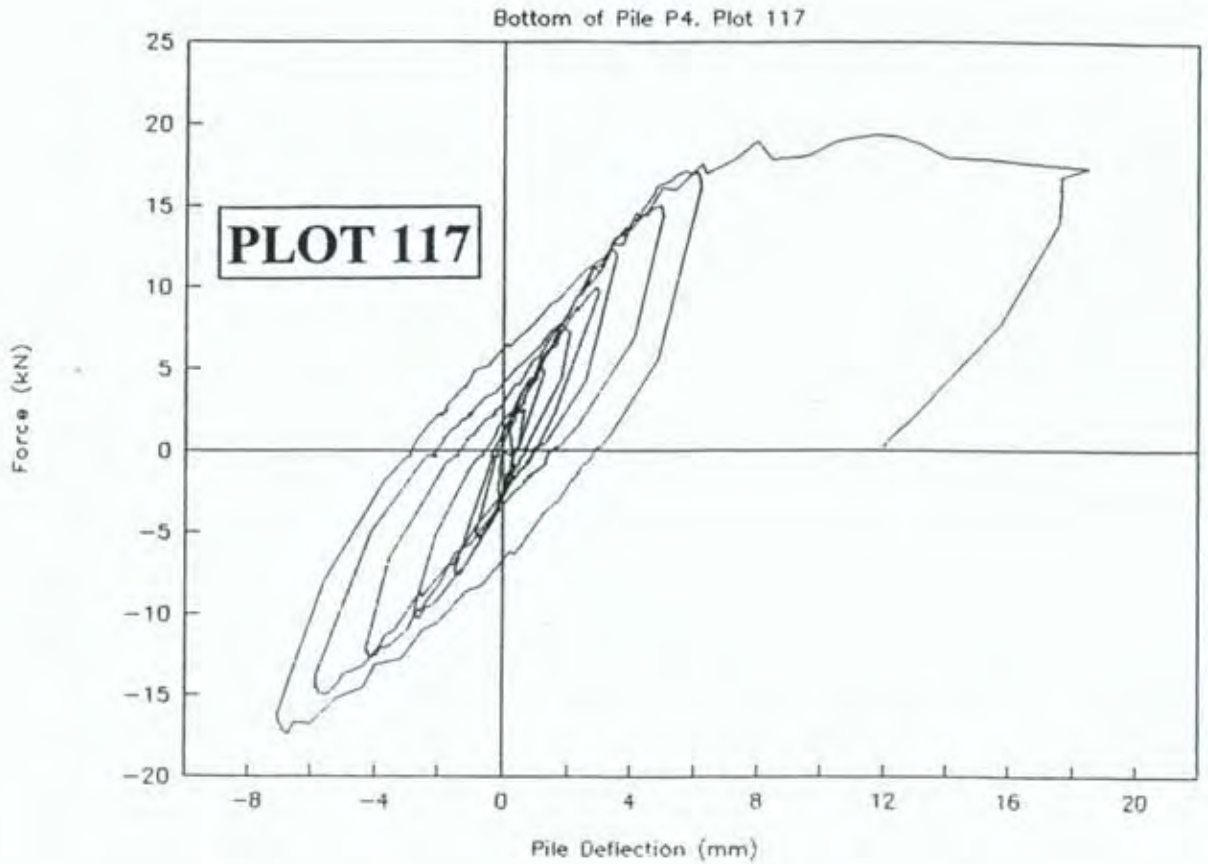


Figure A.9 Typical Measured Hysteresis Loops for Shear Piles in Sand

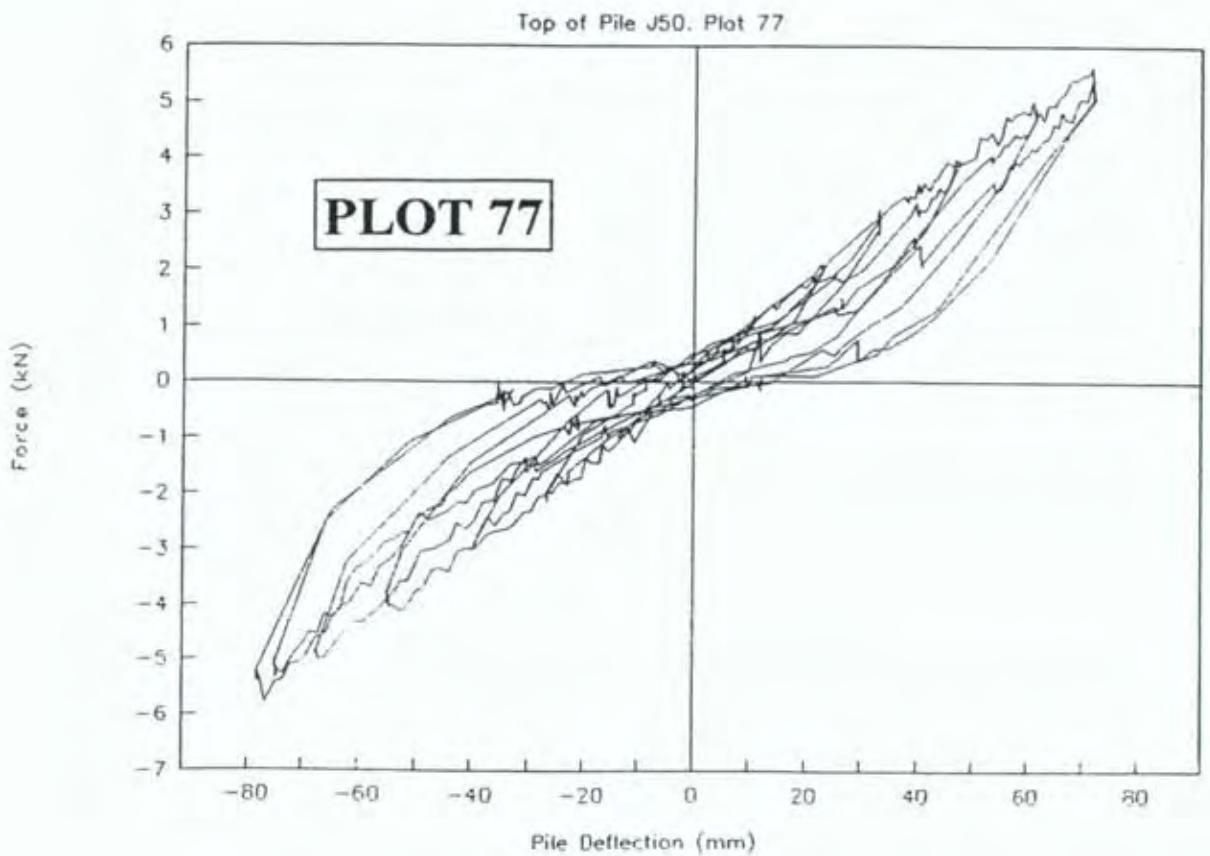


Figure A.10 Typical Measured Hysteresis Loops for Driven Piles in Peat

Appendix B Parent Curves

B.1 Introduction

The piles were pushed and pulled backwards and forwards using gradually increasing loads. The load and deflection monitored at each load reversal point (ie the maximum load and deflection the piles had been subjected to up to that time) are called hysteretic peaks. The actual test regimes used can be seen in the plots in Appendix A or H. The coordinates of the load and deflection at each hysteretic peak were extracted from the data. A plot consisting of a series of straight lines joining these hysteretic peaks is called a parent curve. The parent curves given in this Appendix have been factored as discussed in Section 5.

B.2 Obtaining Backbone Curve for Anchor Piles in Clay

Figure B.1 presents parent curves for anchor piles tested in soft clay which have been factored to represent results for load and deflection being applied/recorded at 600 mm above ground level as discussed above. This graph consists of curves in the first and third quadrants. The curves in the first and third quadrants have been averaged to produce an average absolute parent curve in the first quadrant, and this is plotted in Figure B.2. Where the load resisted by the pile in one direction is greater than in the other direction, there is a transition from the averaged to single curve and the average absolute parent curve plot may exhibit a sharp discontinuity at this point.

A series of dots have been placed on the hysteresis loops in Figure A.1 where the loading curve reaches the maximum deflection of the preceding cycle. A curve joining these points is called the "repeat curve". The difference between the parent curve and the Repeat Curve gives a measure of the degree of degradation of the system and has also been used in the dynamic analysis simulation. Figure B.3 compares the first quadrant repeat curves for anchor piles in soft clay.

B.3 Obtaining Other Backbone Curves

Plots giving the backbone curves for (parent, first quadrant parent and repeat curves) for the other piles were processed as described.

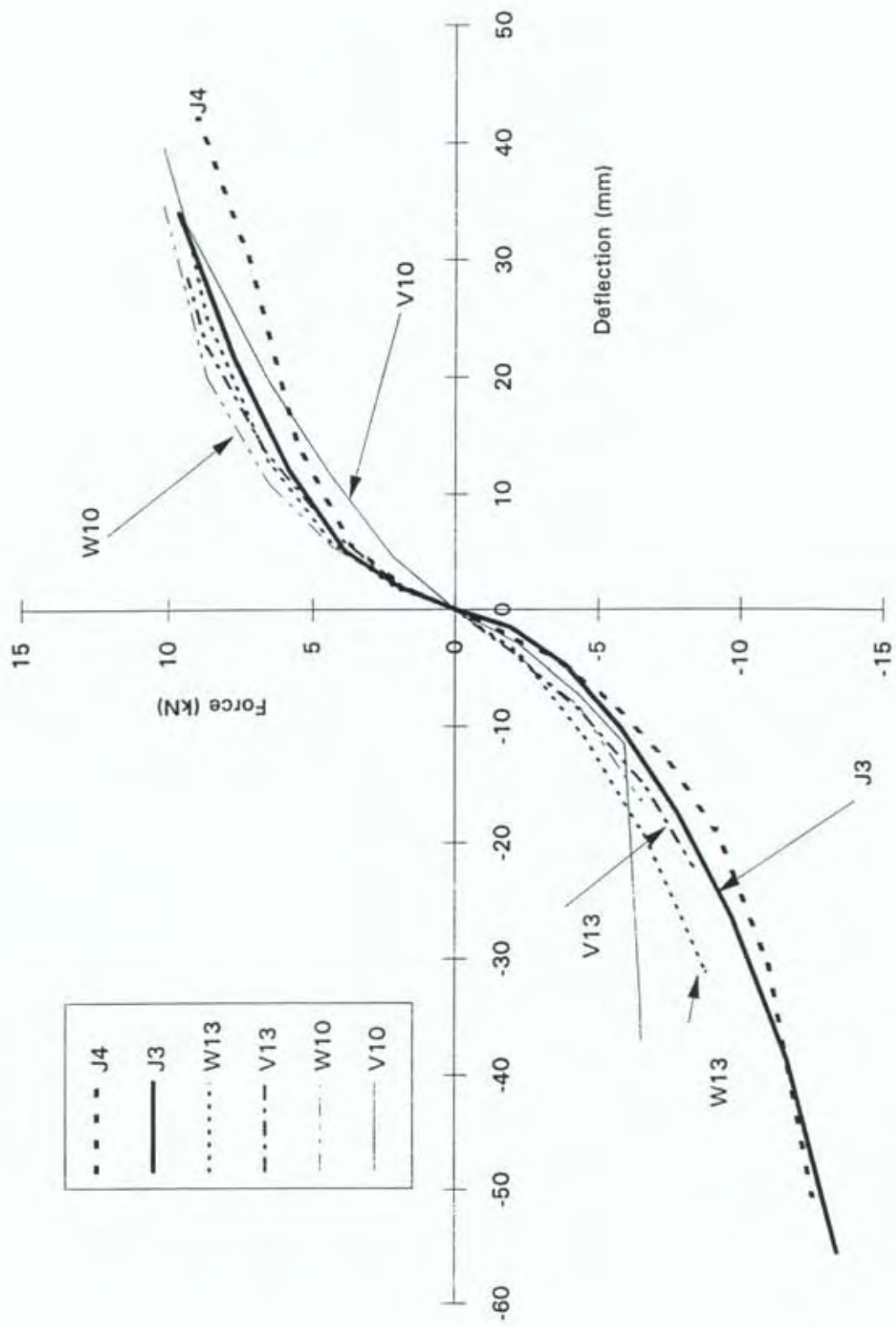


Figure B.1 Complete Parent Curves for Anchor Piles in Clay

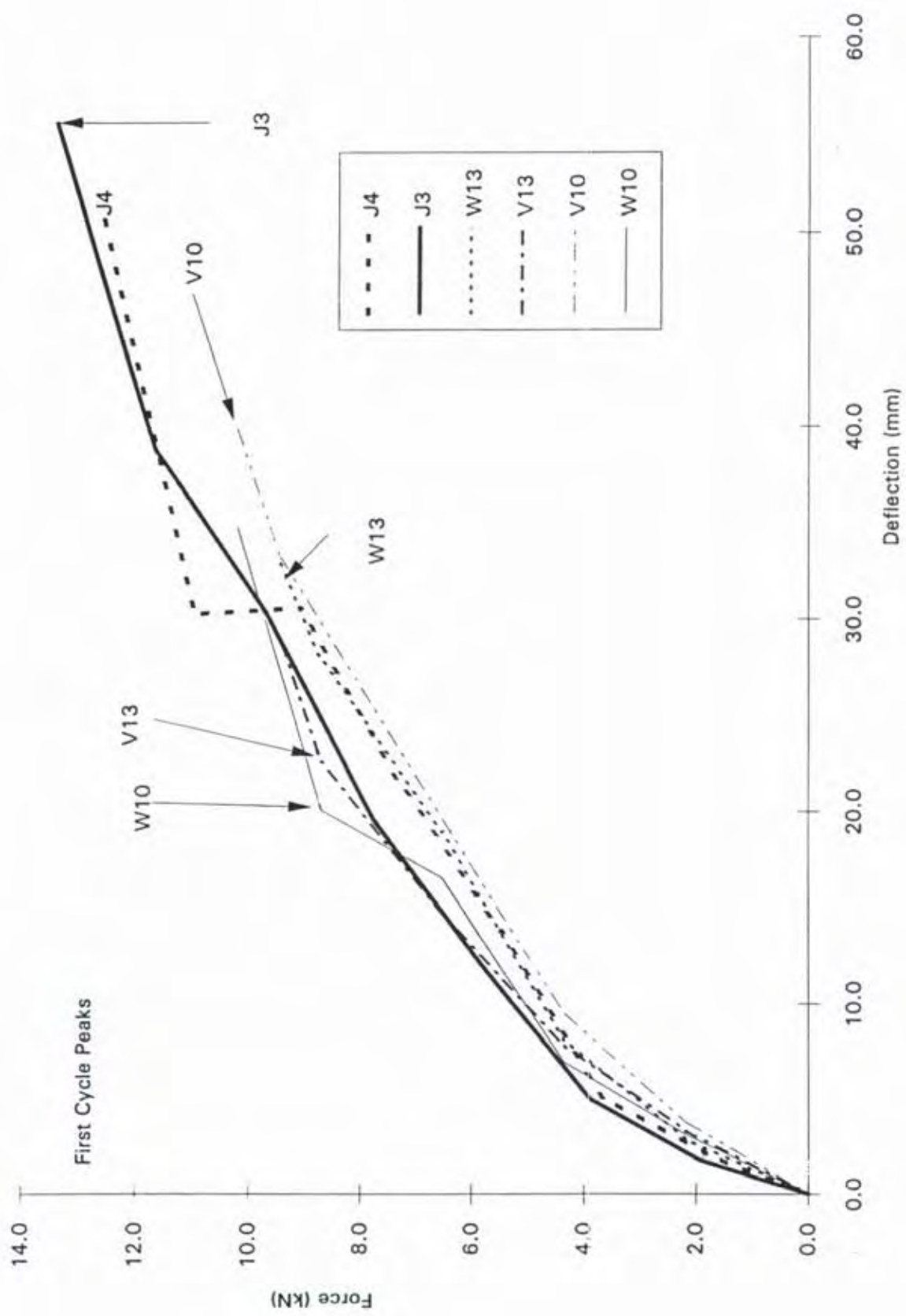


Figure B.2 First Quadrant Parent Curves for Anchor Piles in Clay

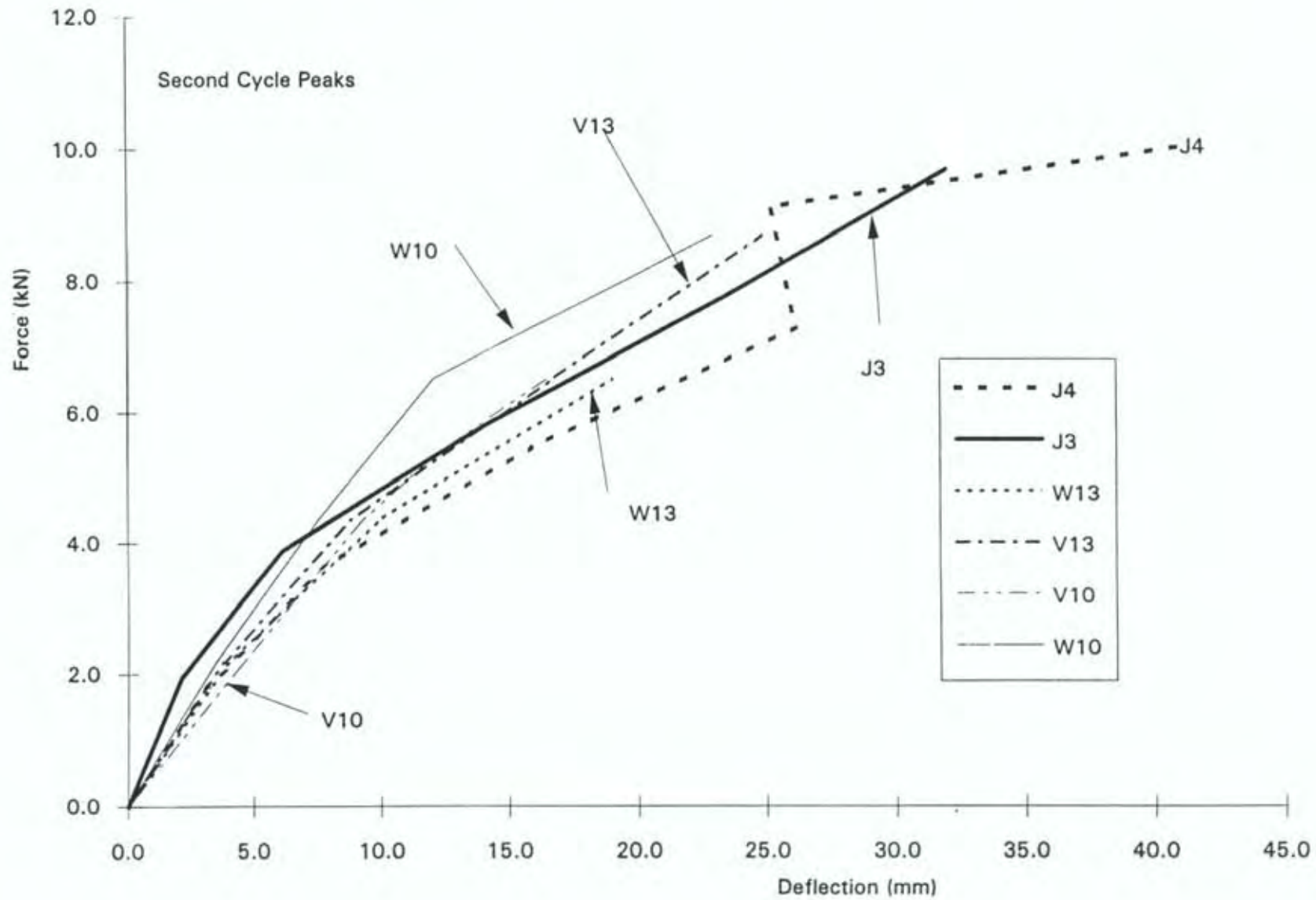


Figure B.3 Repeat Curves for Anchor Piles in Clay

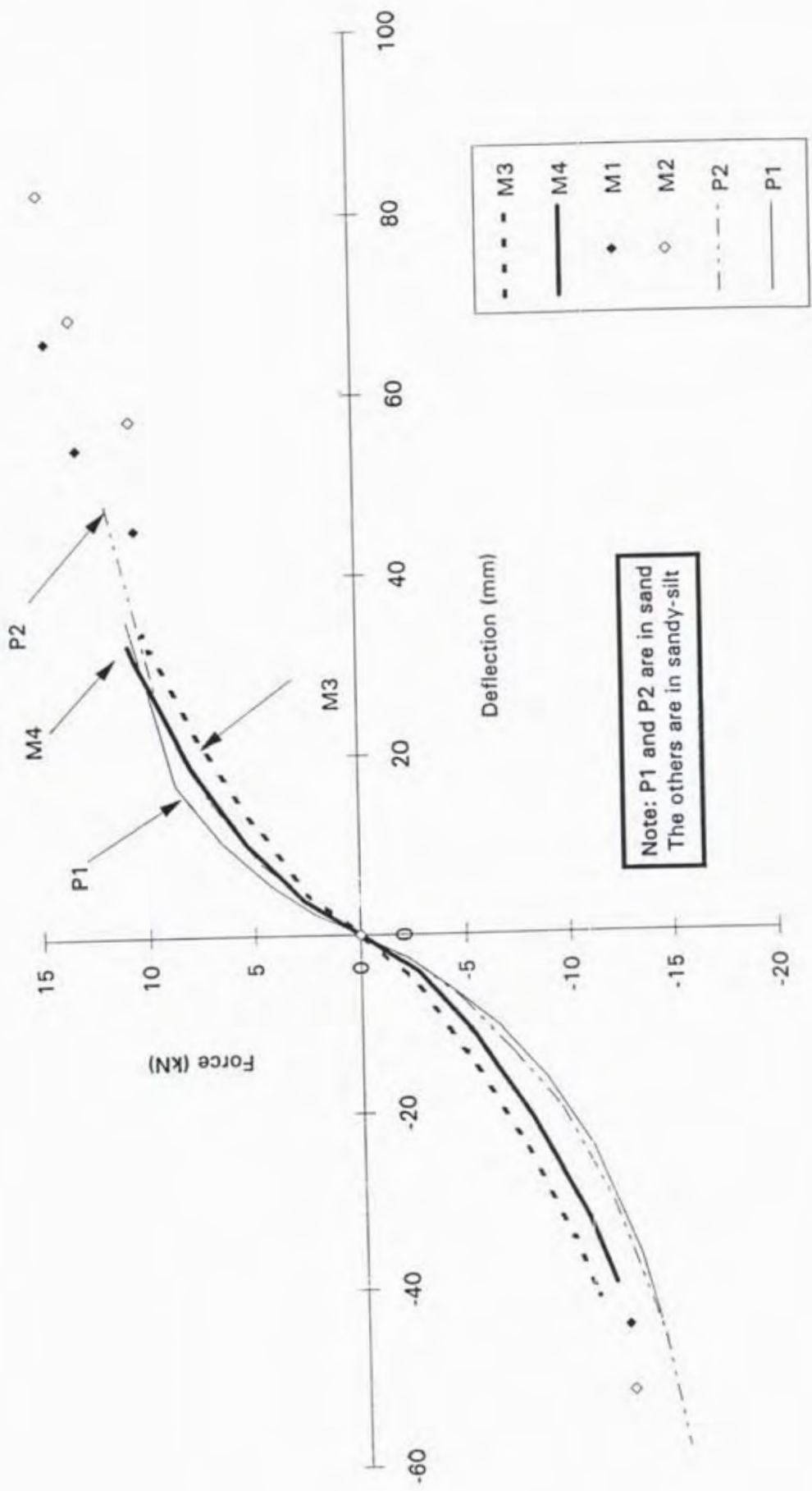
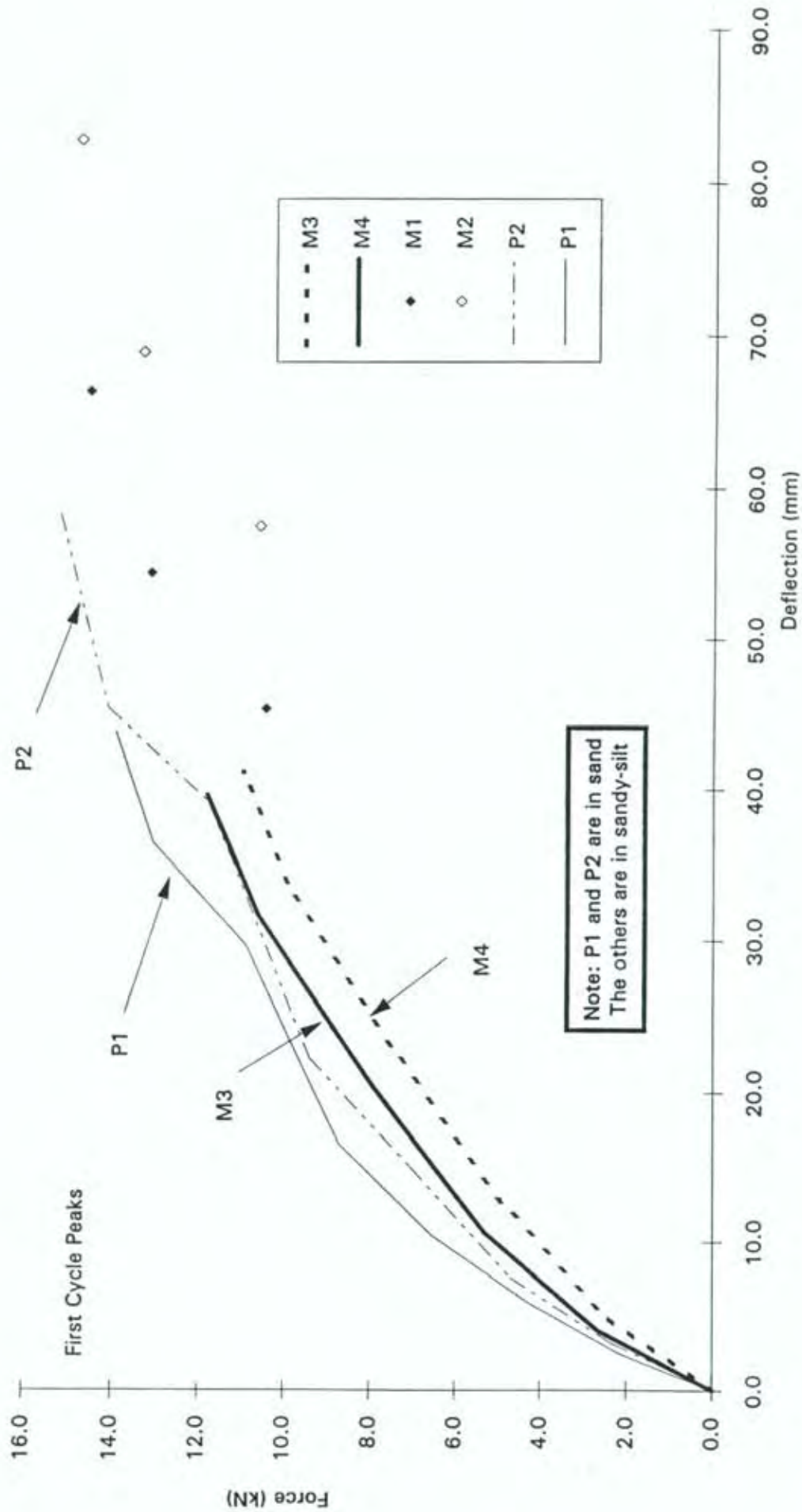


Figure B.4 Complete Parent Curves for Anchor Piles in Sandy-Silt and Sand



Note: P1 and P2 are in sand
The others are in sandy-silt

Figure B.5 First Quadrant Parent Curves for Anchor Piles in Sandy-Silt and Sand

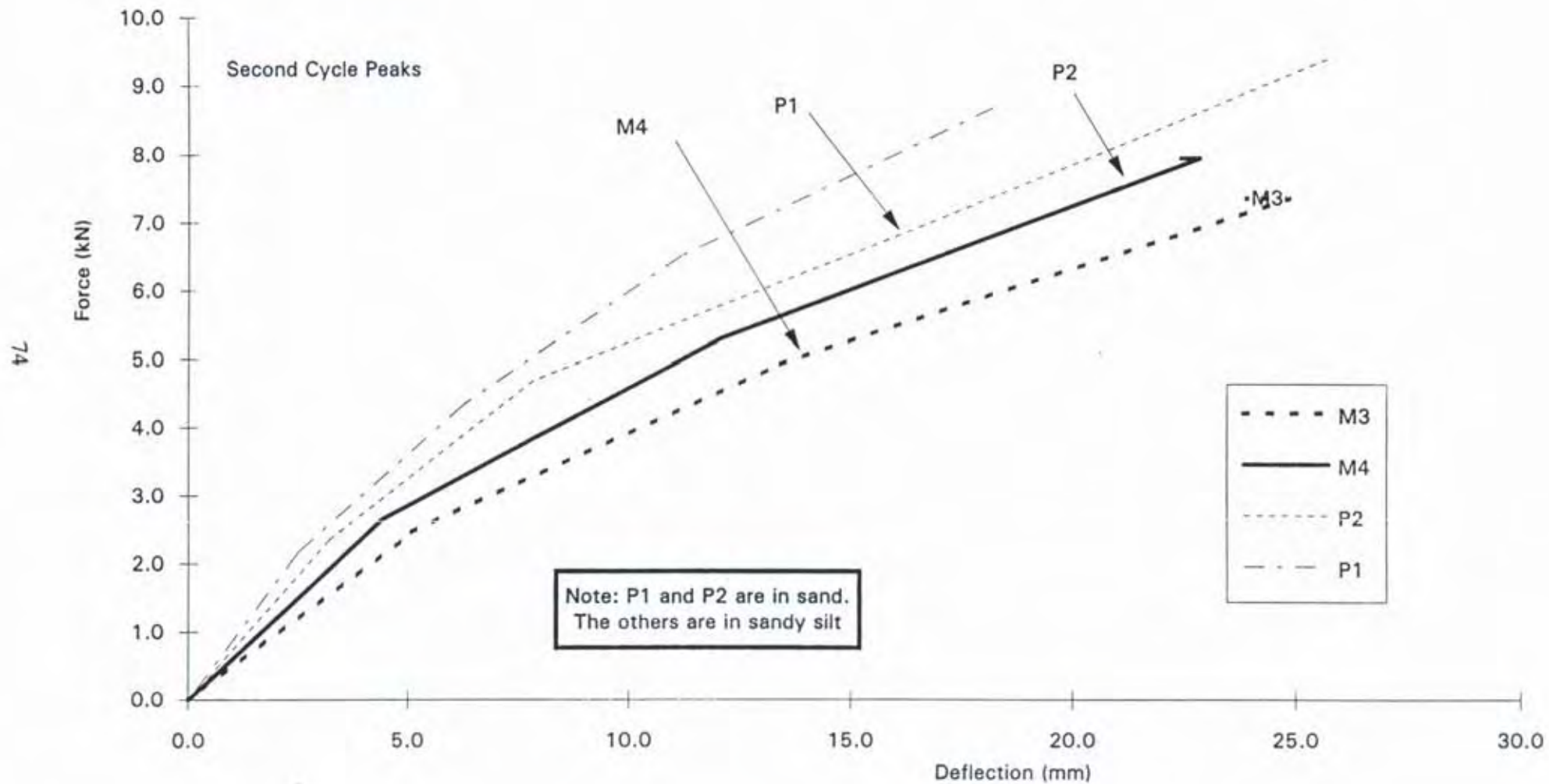


Figure B.6 Repeat Curves for Anchor Piles in Sandy-Silt and Sand

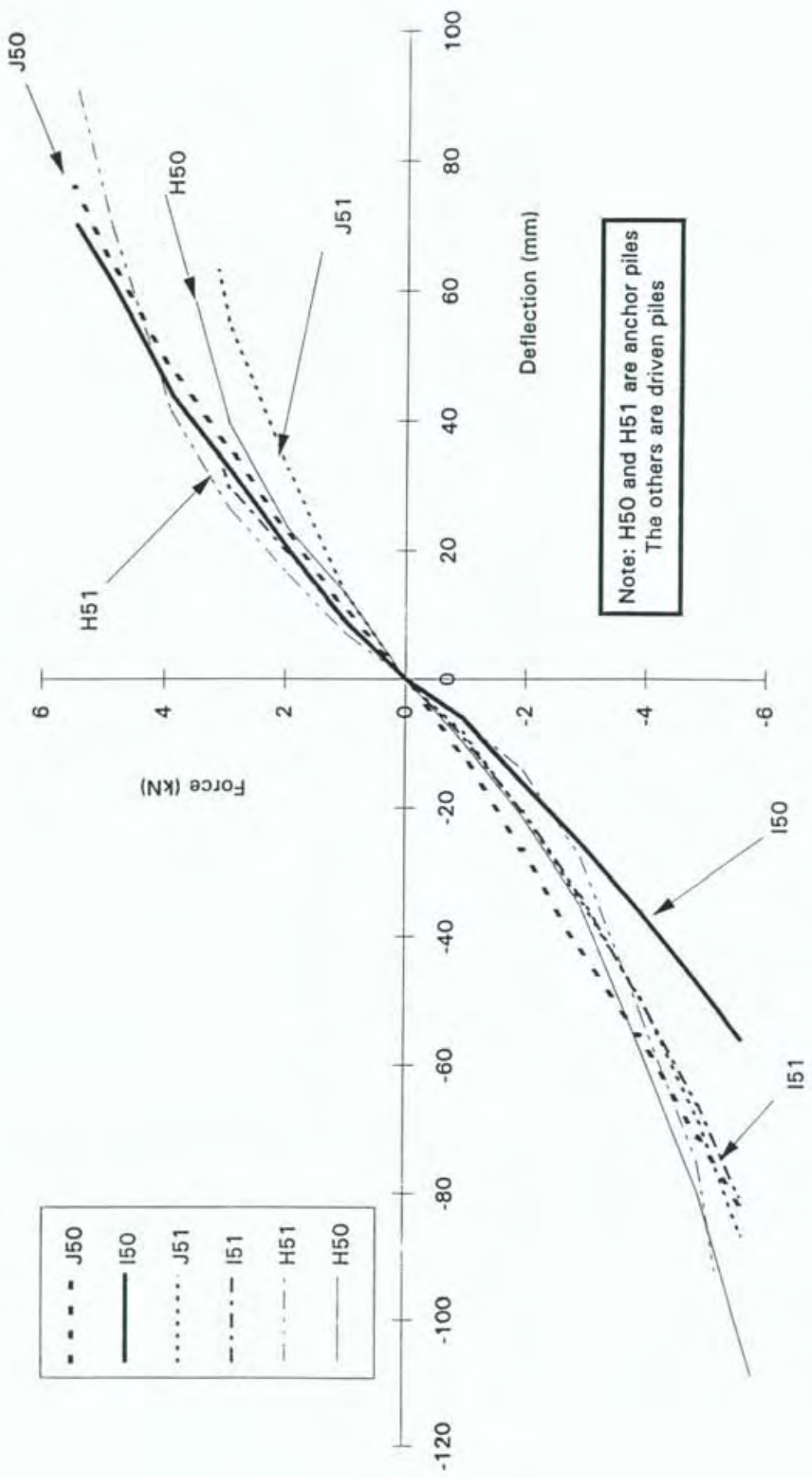


Figure B.7 Complete Parent Curves for Anchor and Driven Piles in Peat

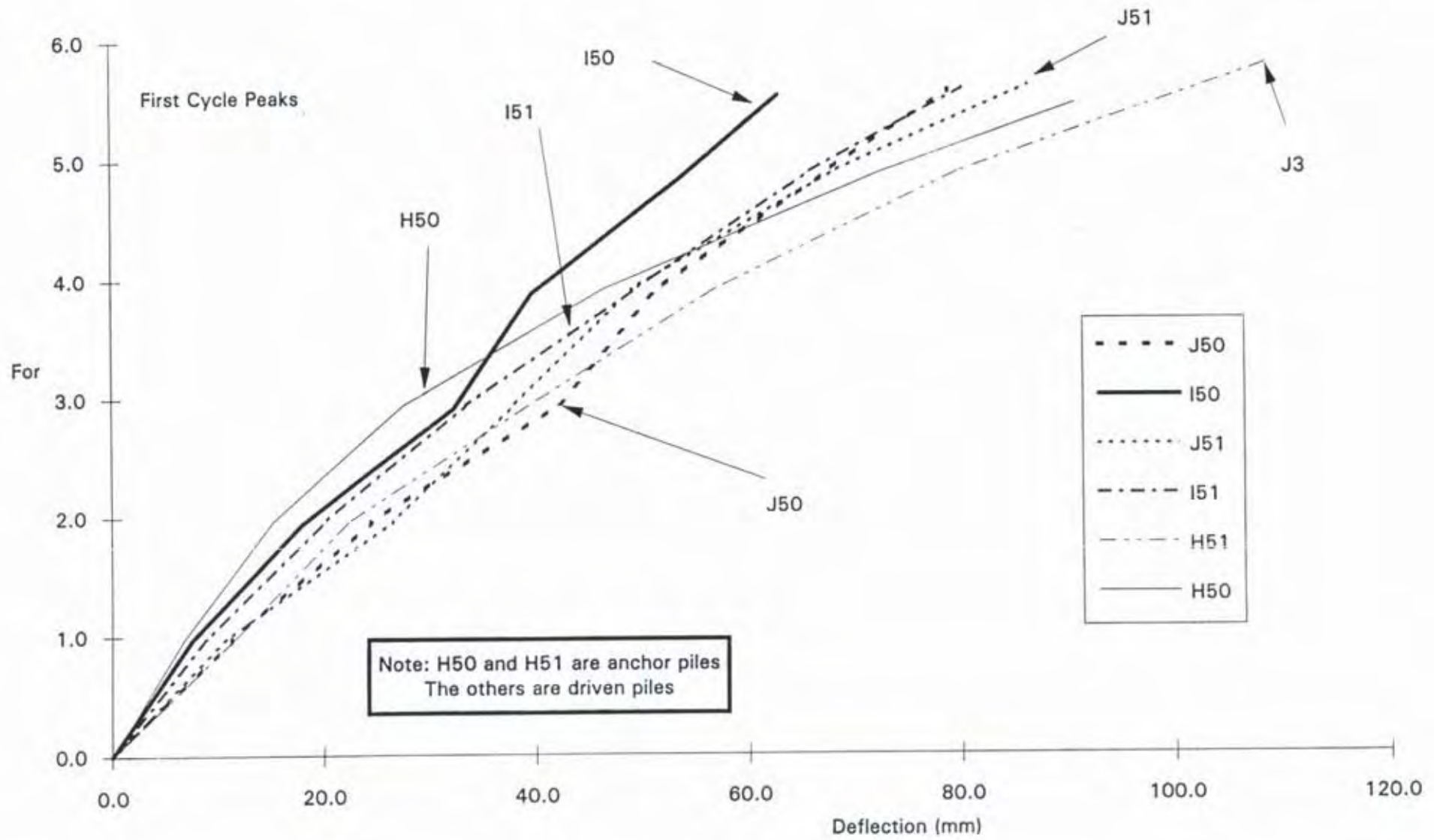


Figure B.8 First Quadrant Parent Curves for Anchor and Driven Piles in Peat

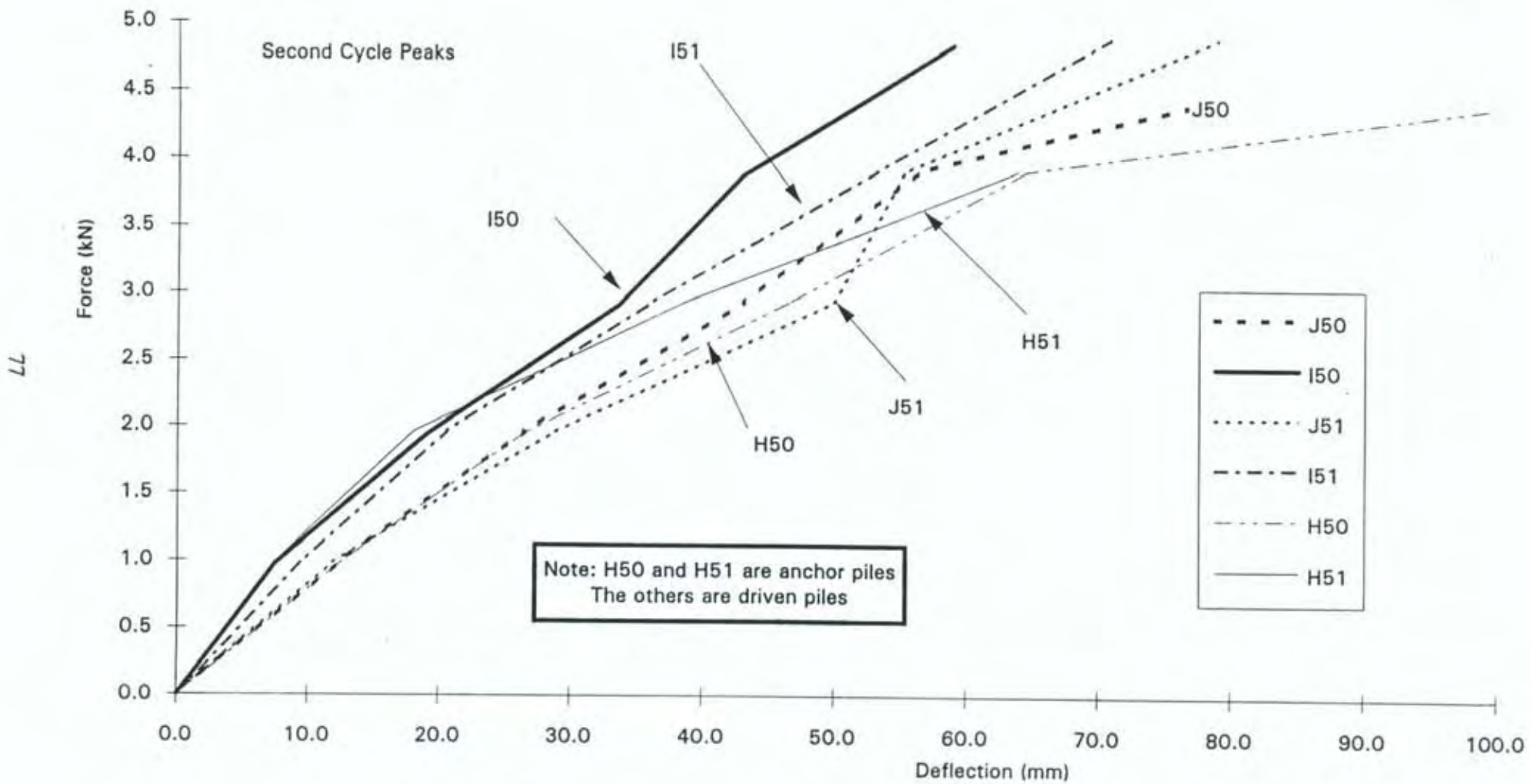


Figure B.9 Repeat Curves for Anchor and Driven Piles in Peat

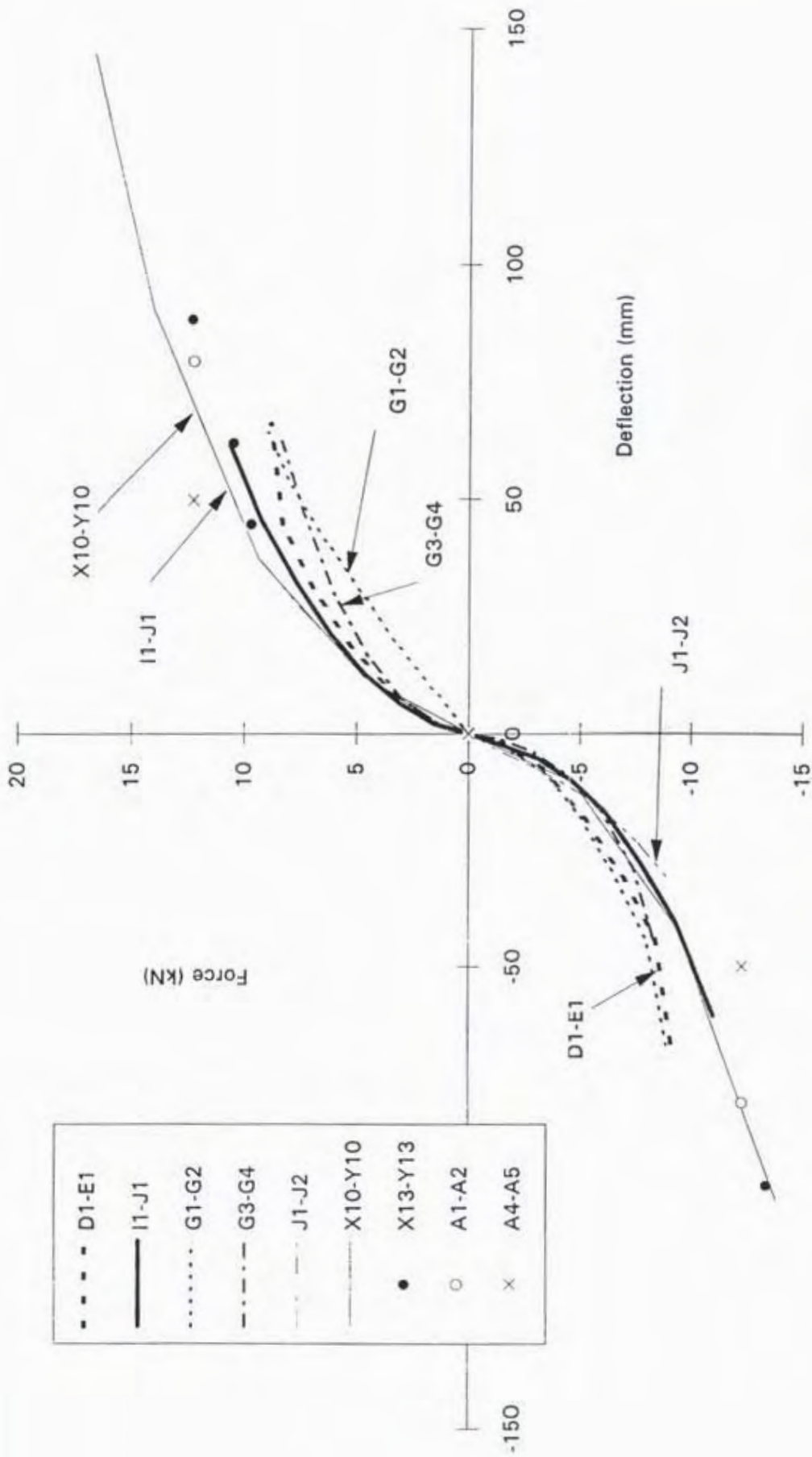


Figure B.10 Complete Parent Curves For Braced Piles in Clay

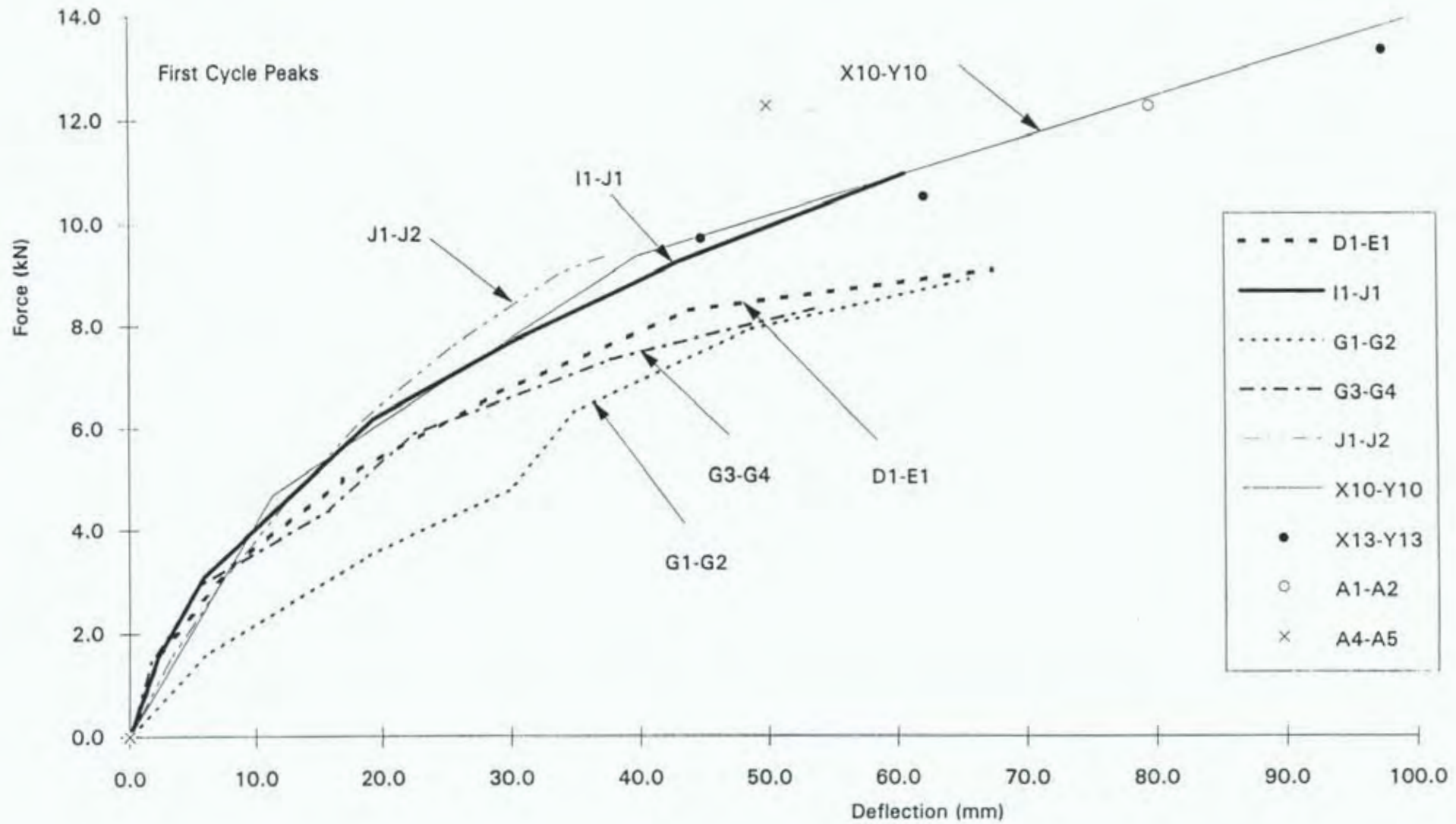


Figure B.11 First Quadrant Parent Curves for Braced Piles in Clay

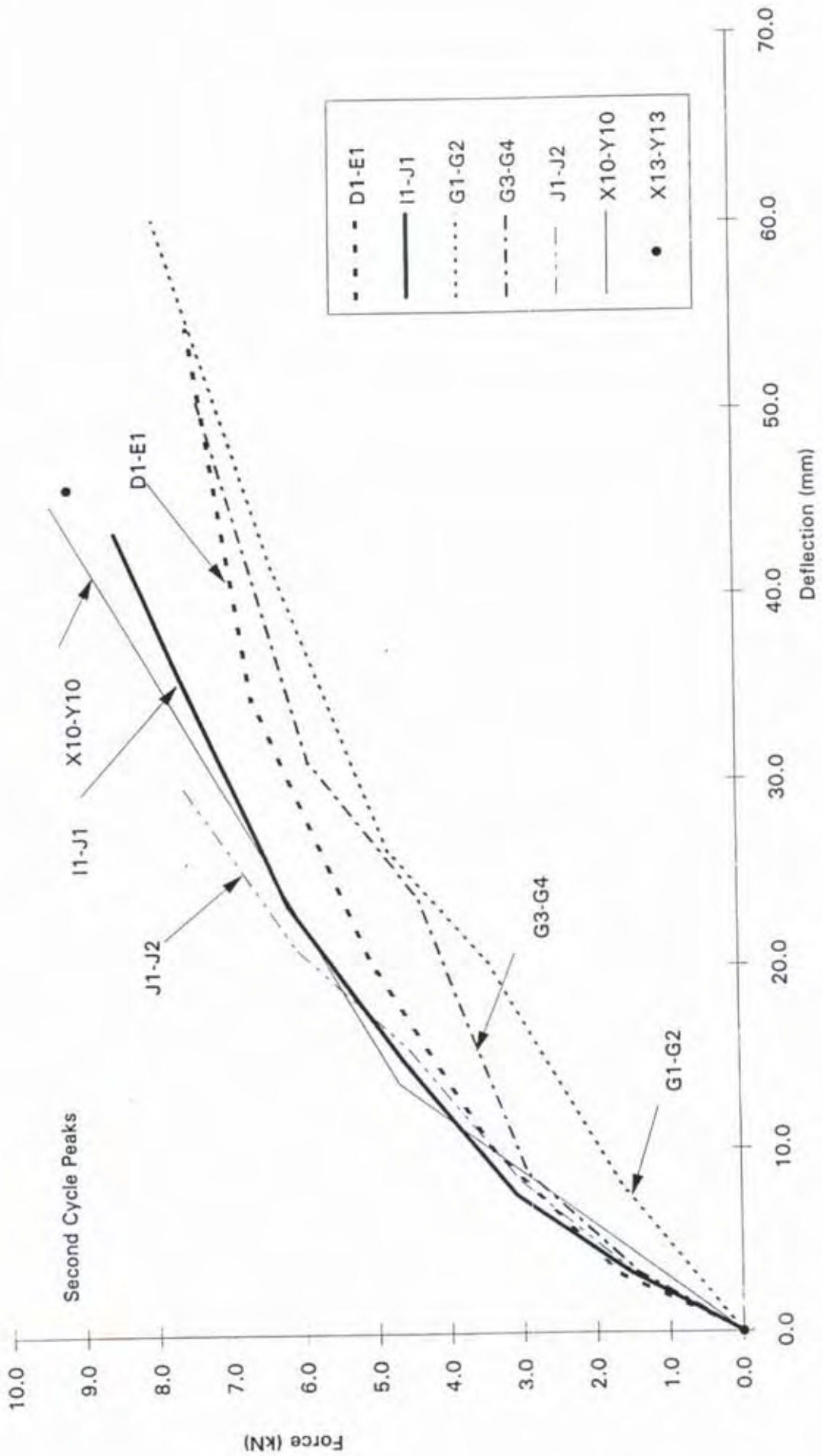


Figure B.12 Repeat Curves for Braced Piles in Clay

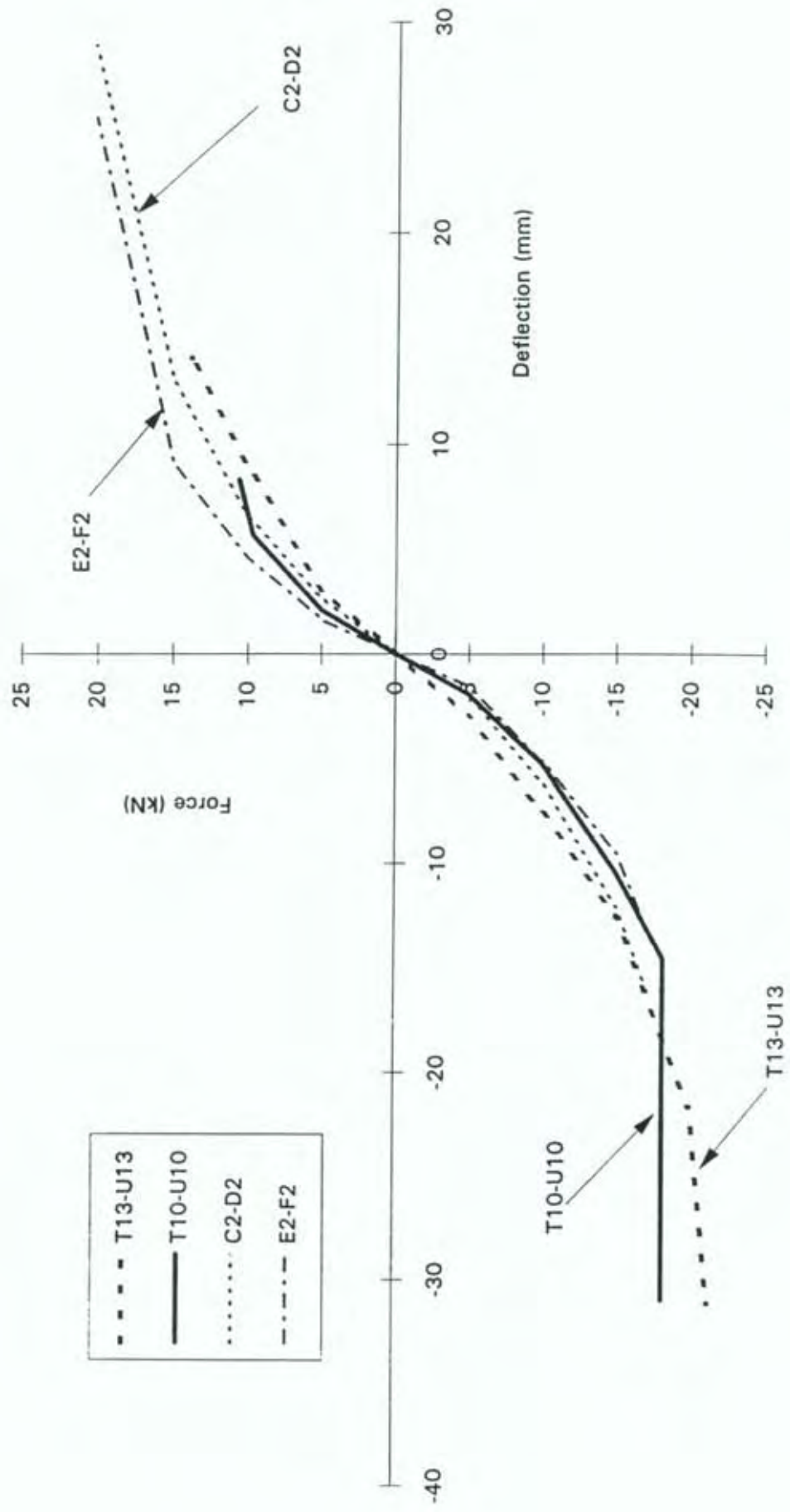


Figure B.13 Complete Parent Curves for Shear Piles in Clay

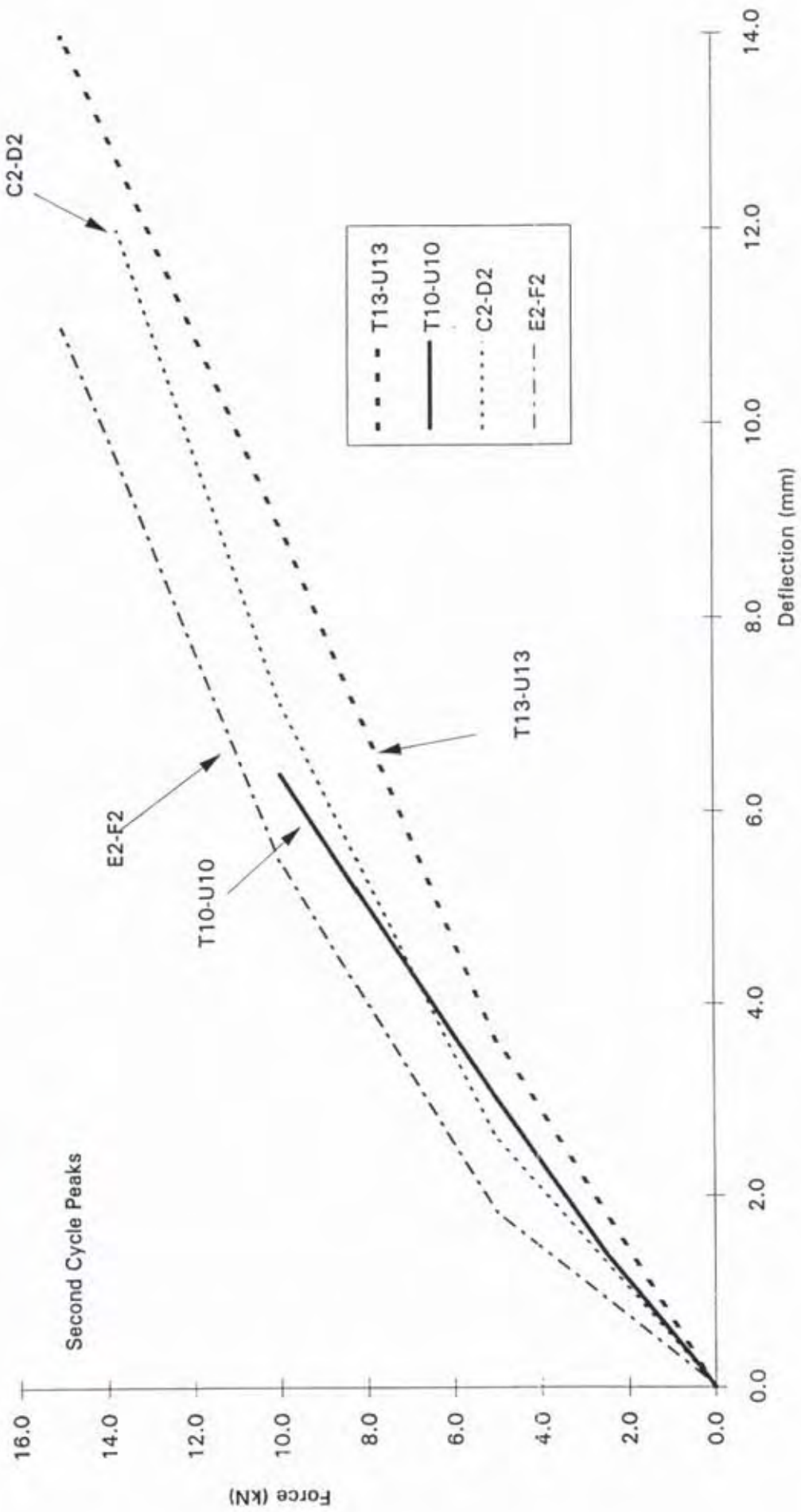


Figure B.14 First Quadrant Parent Curves for Shear Piles in Clay

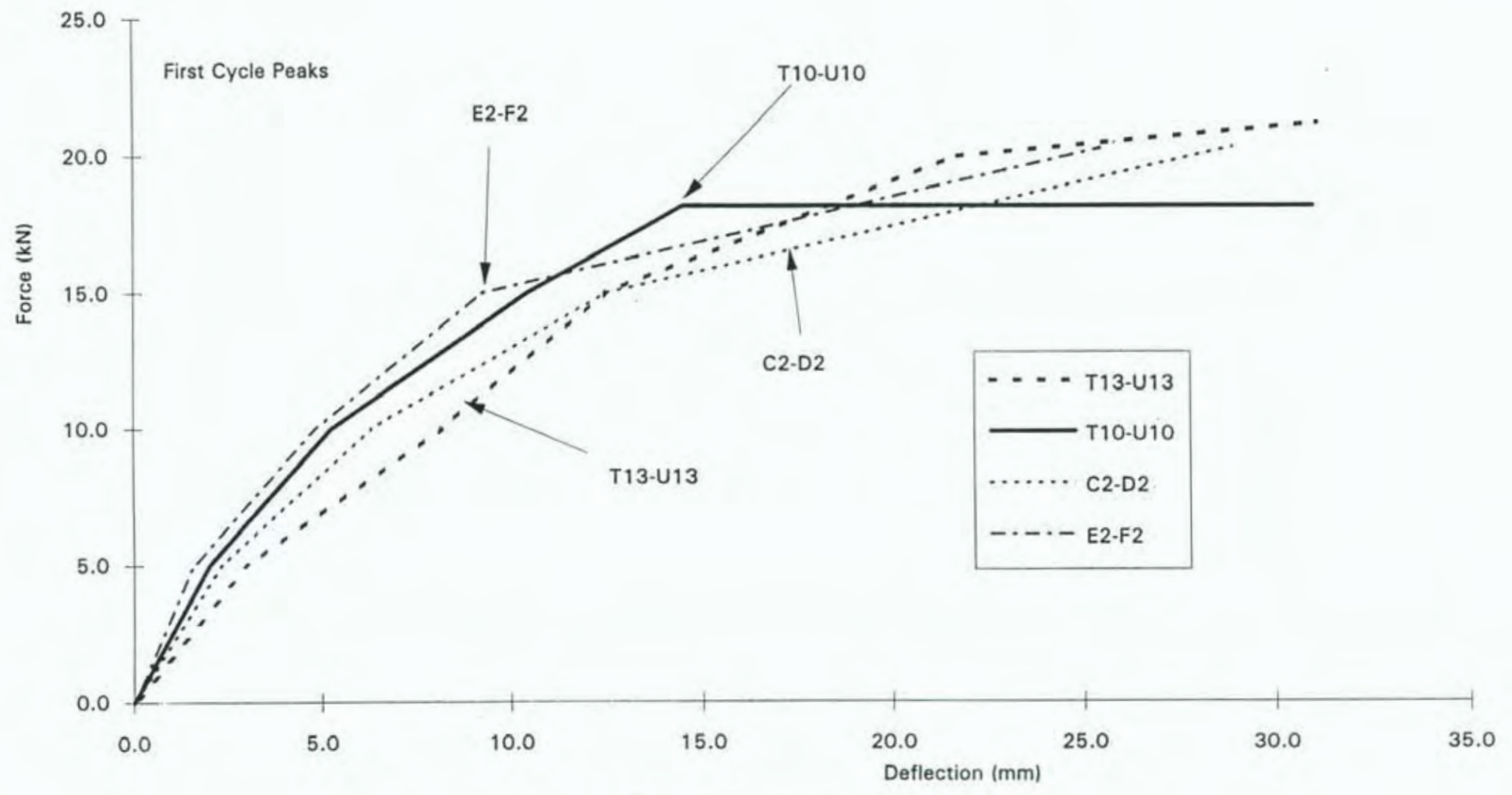


Figure B.15 Repeat Curves for Shear Piles in Clay

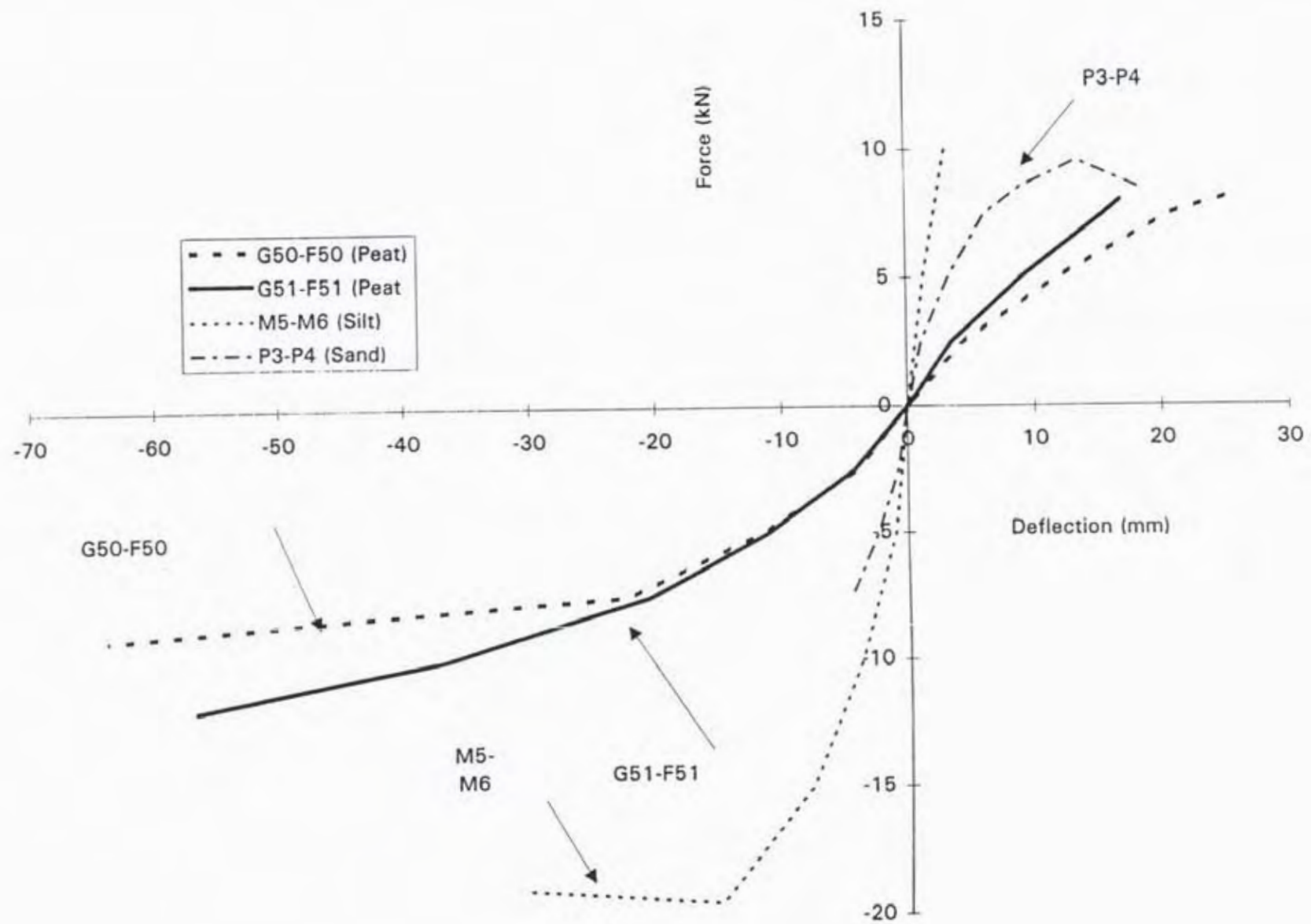


Figure B.16 Complete Parent Curves for Shear Piles in Peat, Sandy-silt and Sand

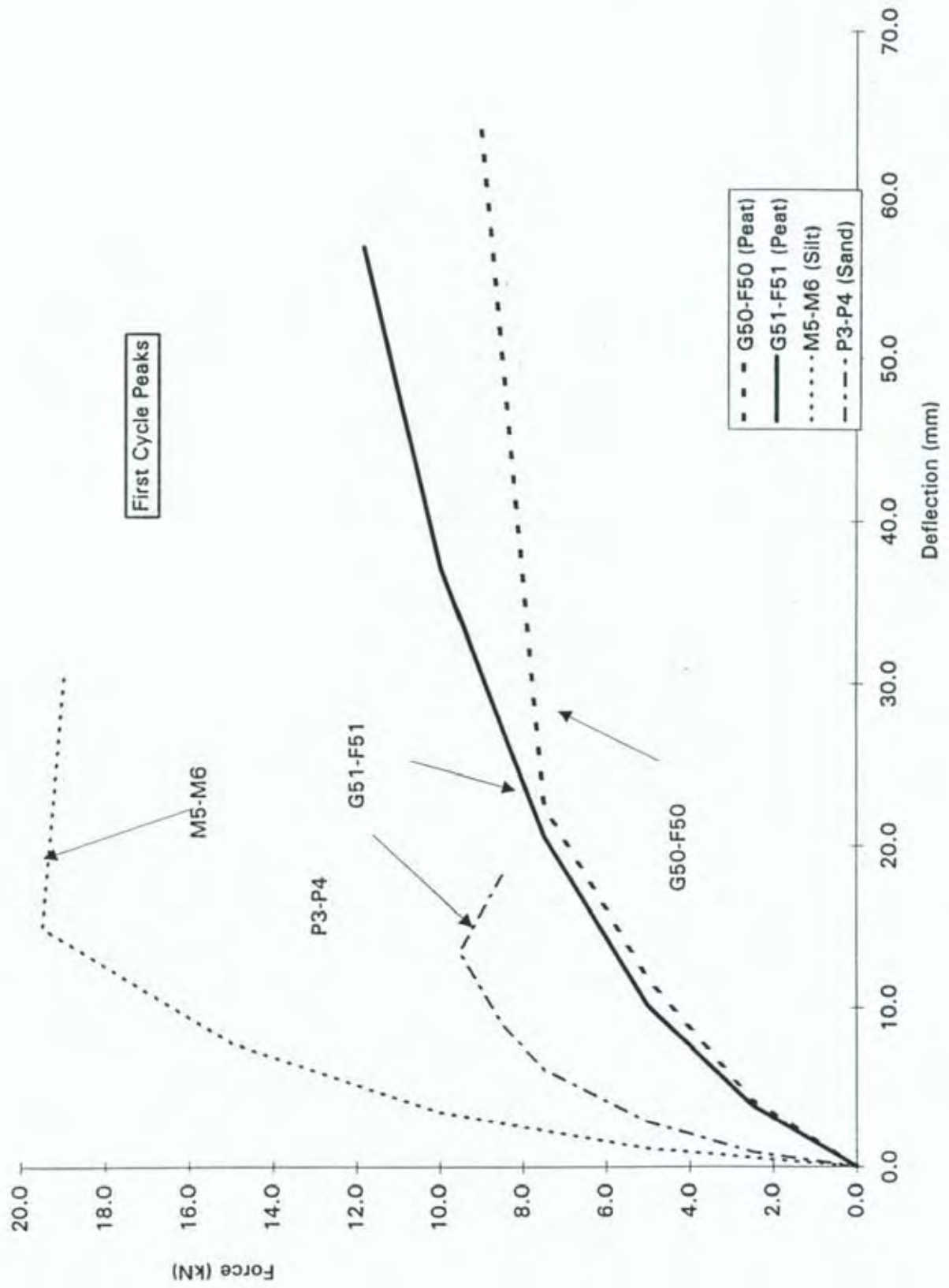


Figure B.17 First Quadrant Parent Curves for Shear Piles in Peat, Sandy-silt and Sand

Appendix C Best Fit Curves

C.1 Introduction

The method used to derived best fit equations to the parent curves for each pile and soil type are described in Section 6.2. This involved fitting a non-linear equation to the experimental data and solving for the constants A, B and C that provided the best fit. The values of A, B and C so found are given in Table C.1.

A comparison of the best fit curves and the parent curves for each pile and soil type are given in this Appendix. Generally all parent curves for a particular pile and soil type were similar and the best fit curves derived fitted the data well.

Table C.1 - Coefficients For Best Fit Equation

Pile Type	Curve Type	Group No	Soil Type	Regressional Coefficients		
				A	B	C
Anchor	Parent	1 & 2	Clay	2.065	0.8903	0.5099
Anchor	Repeat	1 & 2	Clay	10.22	13.80	0.8835
Anchor	Parent	4 & 5	Silt/Sand	19.28	25.60	1.000
Anchor	Repeat	4 & 5	Silt/Sand	12.56	14.91	0.9603
Anchor	Parent	3	Peat	3.949	27.02	0.8179
Anchor	Repeat	3	Peat	38.41	377.6	1.341
Braced	Parent	1 & 2	Clay	0.9161	- 0.2002	0.4251
Braced	Repeat	1 & 2	Clay	13.67	31.12	1.038
Shear	Parent	1 & 2	Clay	92.33	42.53	1.339
Shear	Parent	3	Peat	13.78	17.95	1.000
Shear	Parent	4	Silt	12.91	1.845	0.7715
Shear	Parent	5	Sand	28.16	11.47	1.320
Driven	Parent	3	Peat	1584	17071	1.969
Driven	Repeat	3	Peat	14.51	140.8	1.034

Anchor Piles in Clay

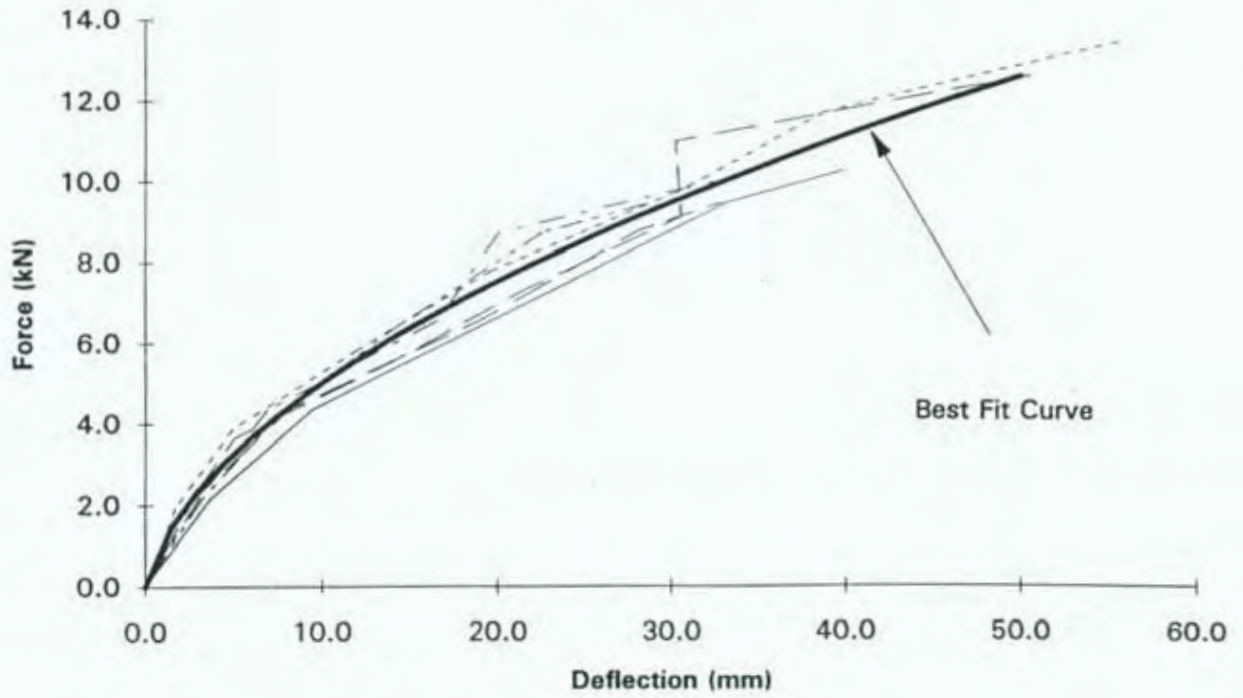


Figure C.1 Comparison of Best Fit Curve and Parent Curves for Anchor Piles in Clay

Anchor Piles in Clay Repeat Loops

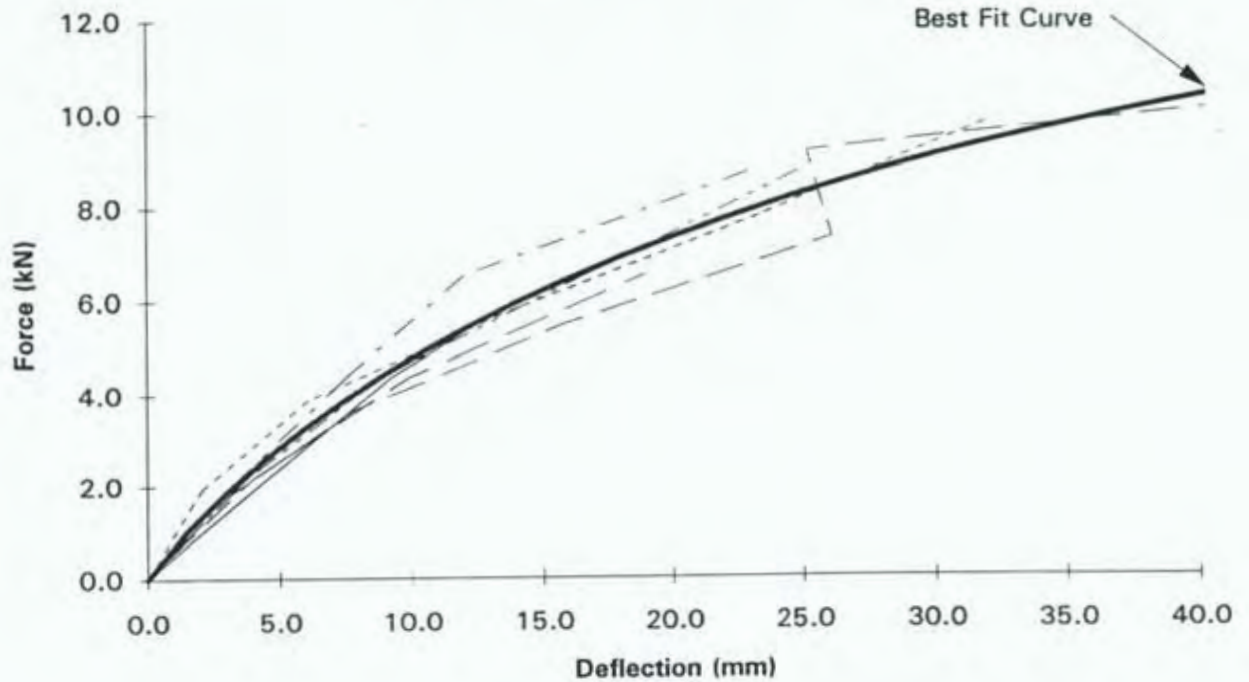


Figure C.2 Comparison of Best Fit Curve and Repeat Curves for Anchor Piles in Clay

Anchor Piles in Peat

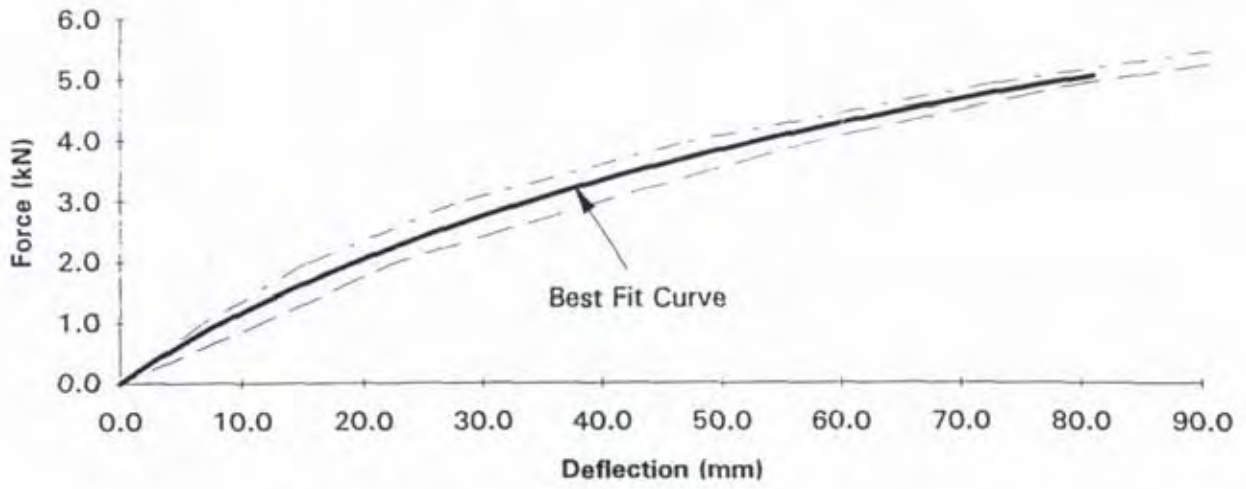


Figure C.3 Comparison of Best Fit Curve and Parent Curves for Anchor Piles in Peat

Anchor Piles in Peat Repeat Loops

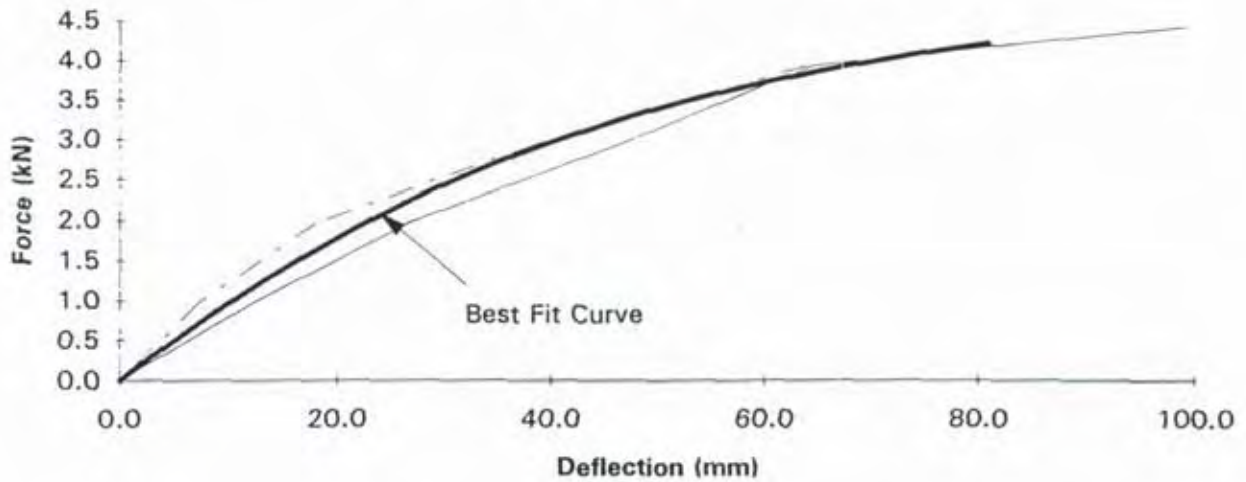


Figure C.4 Comparison of Best Fit Curve and Repeat Curves for Anchor Piles in Peat

Anchor Piles in Sand/Silt

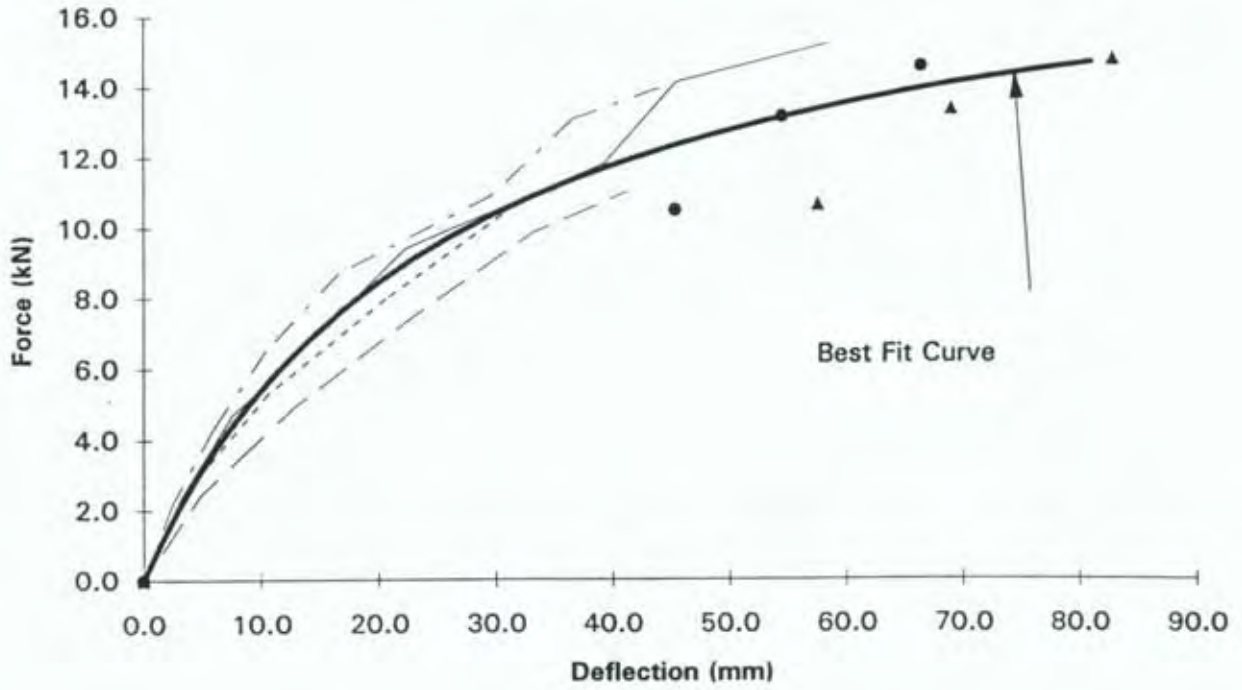


Figure C.5 Comparison of Best Fit Curve and Parent Curves for Anchor Piles in Sand/Si

Anchor Piles in Sand/Silt Repeat Loops

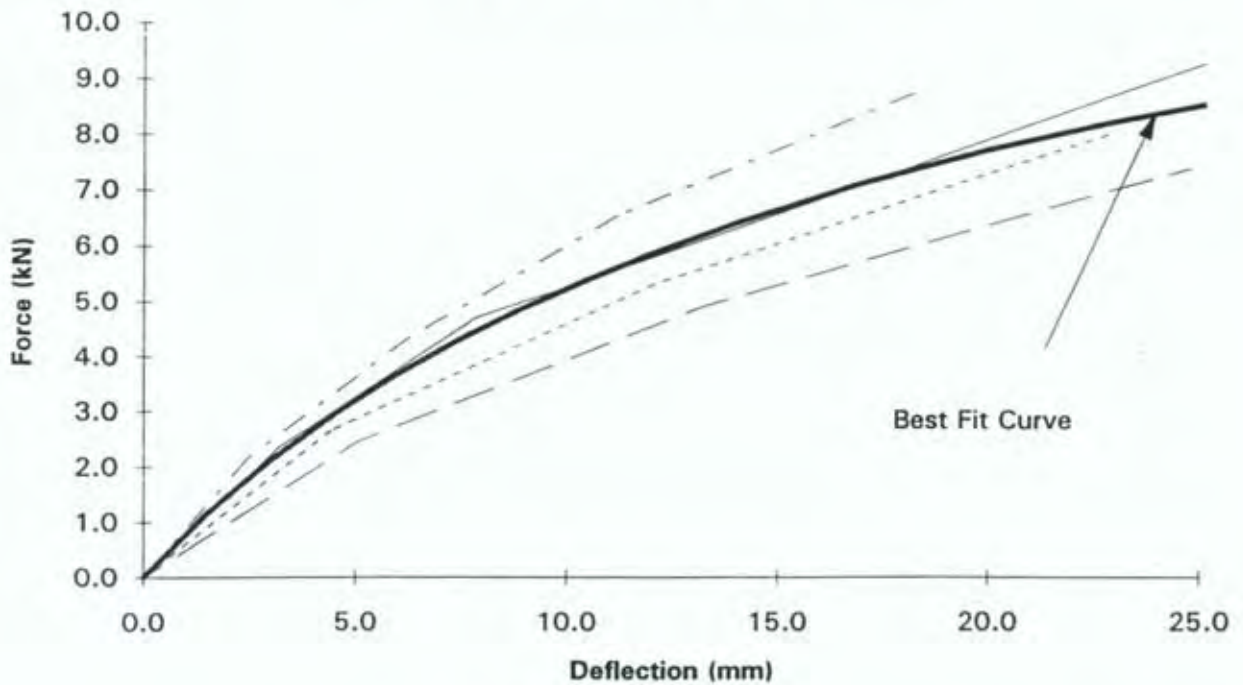


Figure C.6 Comparison of Best Fit Curve and Repeat Curves for Braced Piles in Sand/Si

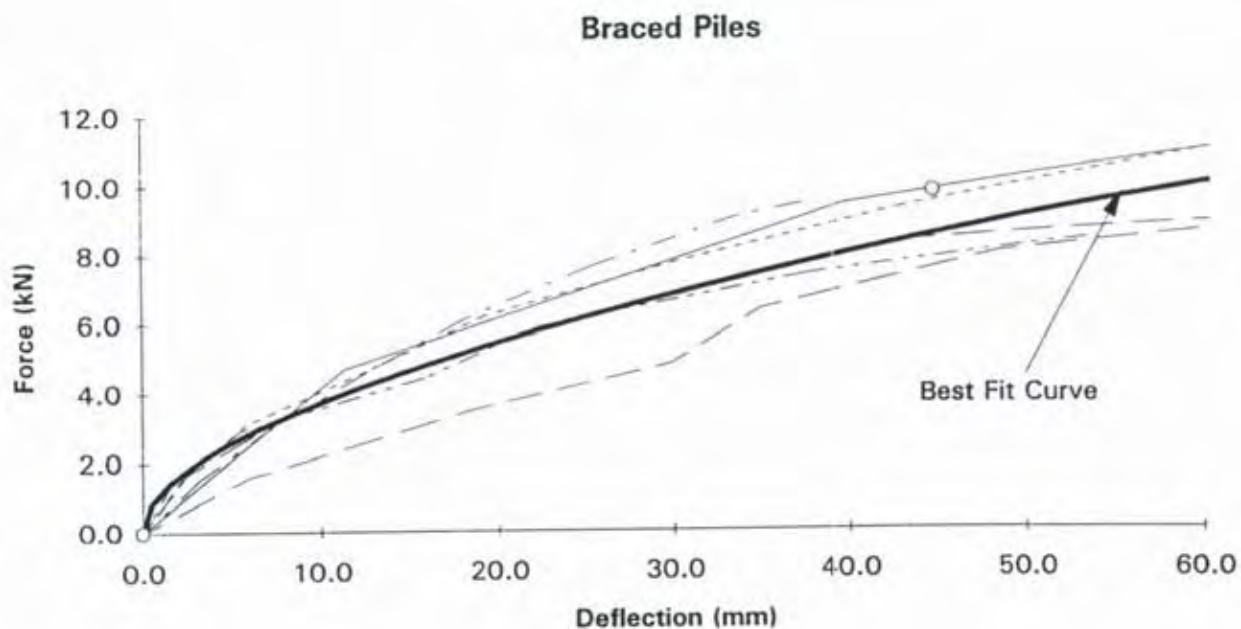


Figure C.7 Comparison of Best Fit Curve and Parent Curves for Braced Piles in Clay

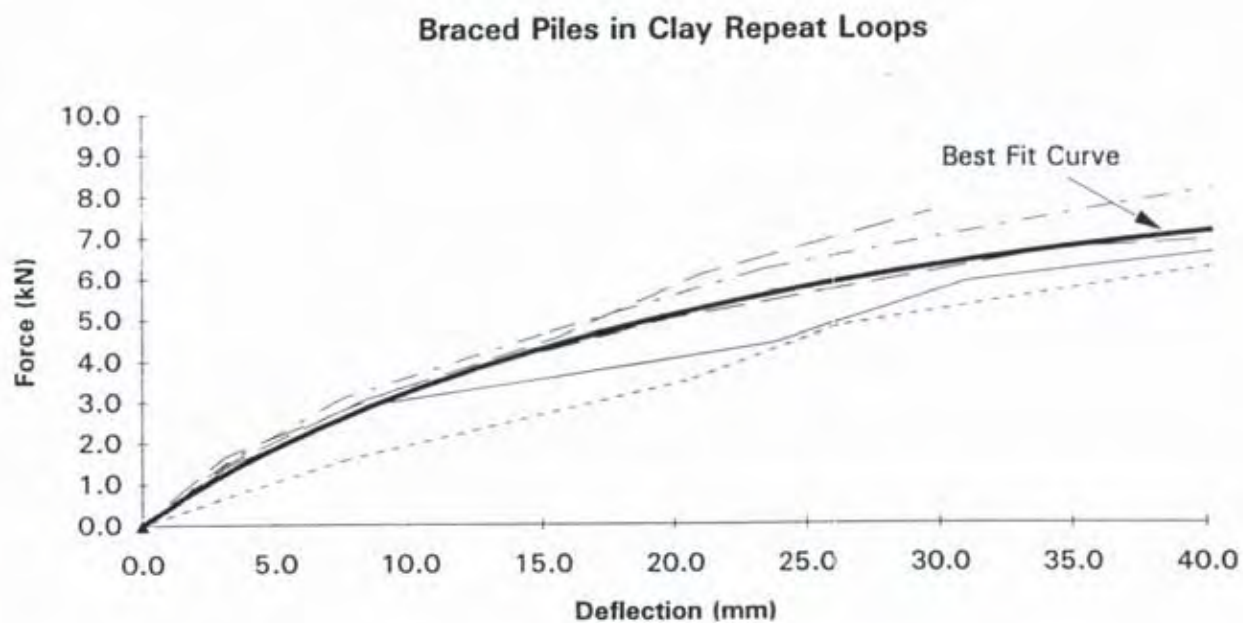


Figure C.8 Comparison of Best Fit Curve and Repeat Curves for Braced Piles in Clay

Shear Piles in Clay

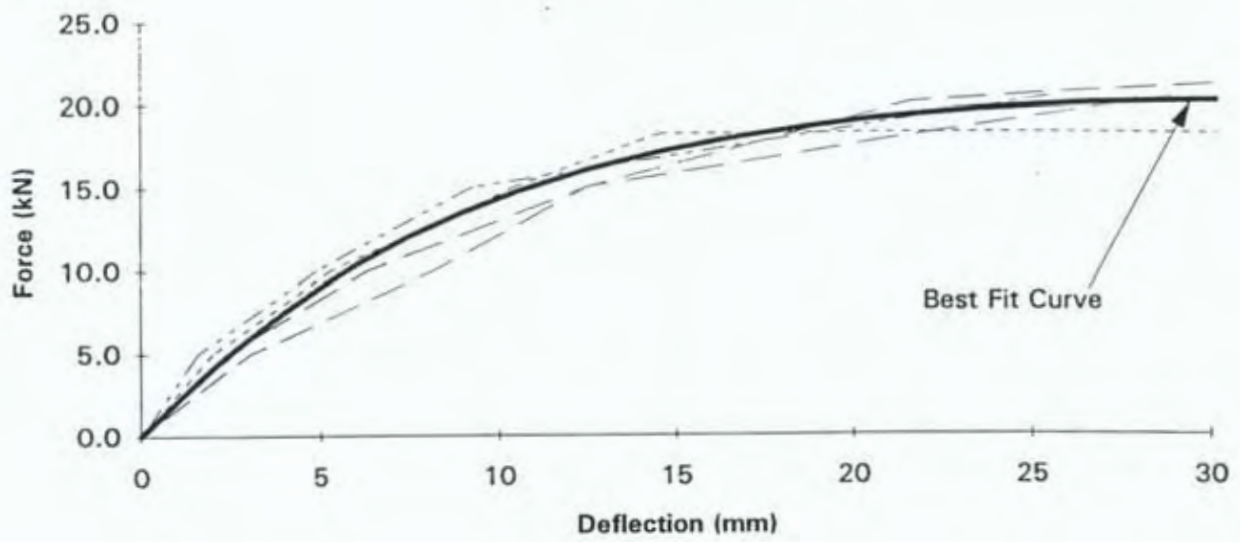


Figure C.9 Comparison of Best Fit Curve and Parent Curves for Shear Piles in Clay

Shear Piles in Peat

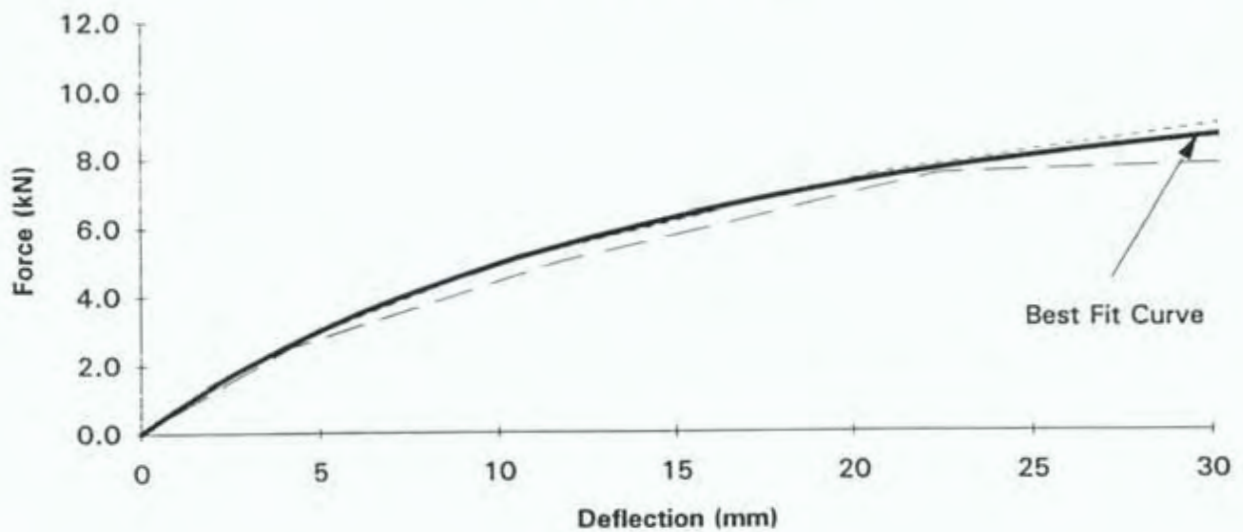


Figure C.10 Comparison of Best Fit Curve and Parent Curves for Shear Piles in Peat

Shear Piles in Sandy-silt

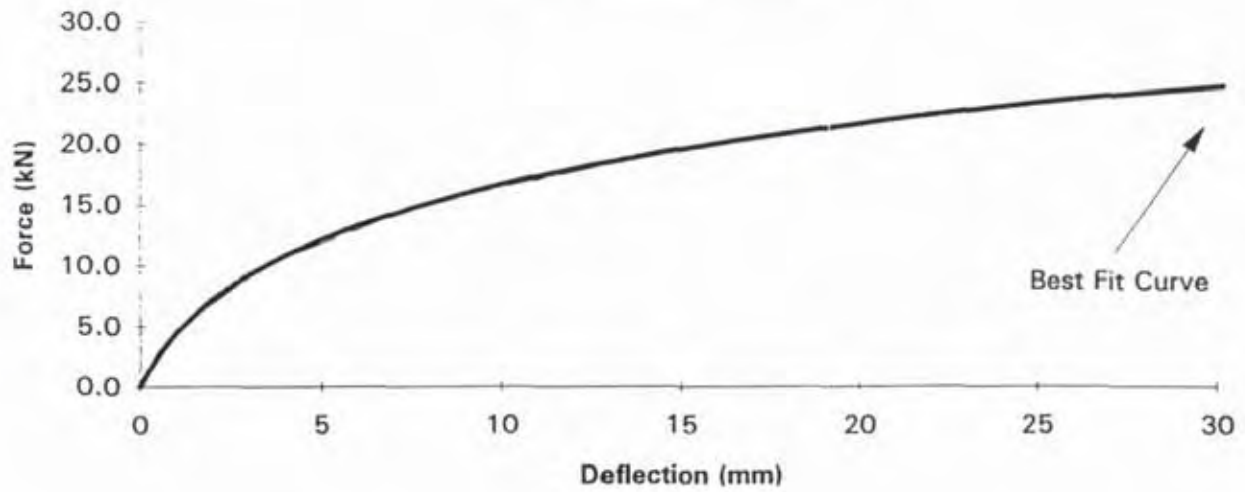


Figure C.11 Comparison of Best Fit Curve and Parent Curves for Shear Piles in Sandy-Silt

Shear Piles in Sand

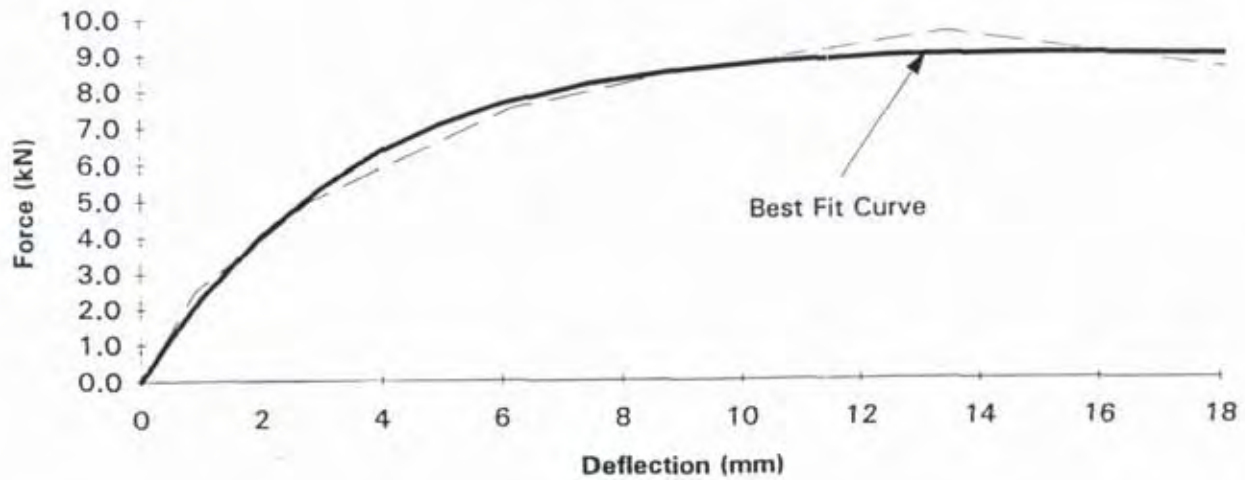


Figure C.12 Comparison of Best Fit Curve and Parent Curves for Shear Piles in Sand

Driven Piles in Peat

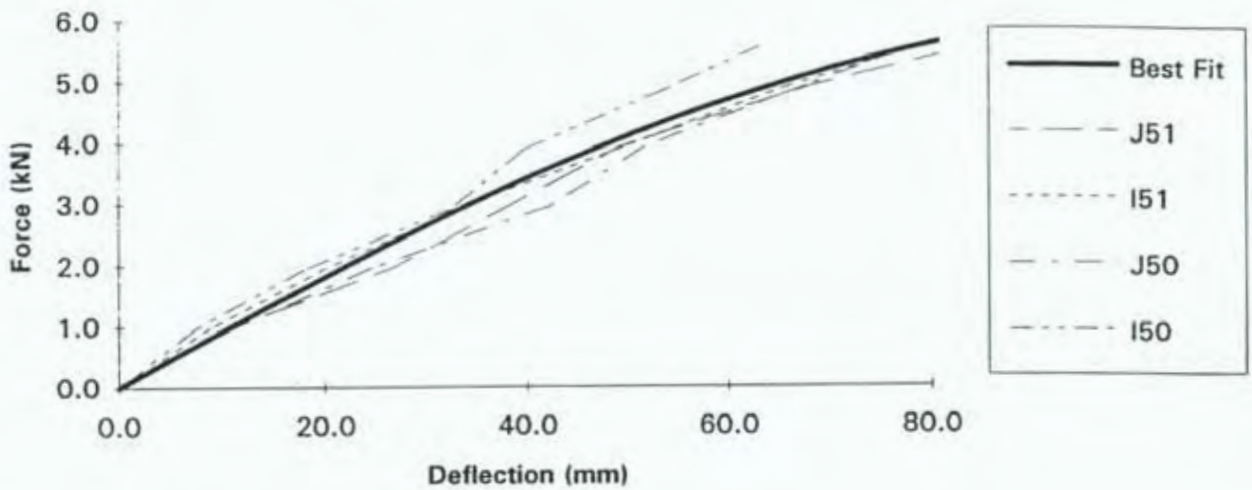


Figure C.13 Comparison of Best Fit Curve and Parent Curves for Driven Piles in Peat

Driven Piles in Peat Repeat Loops

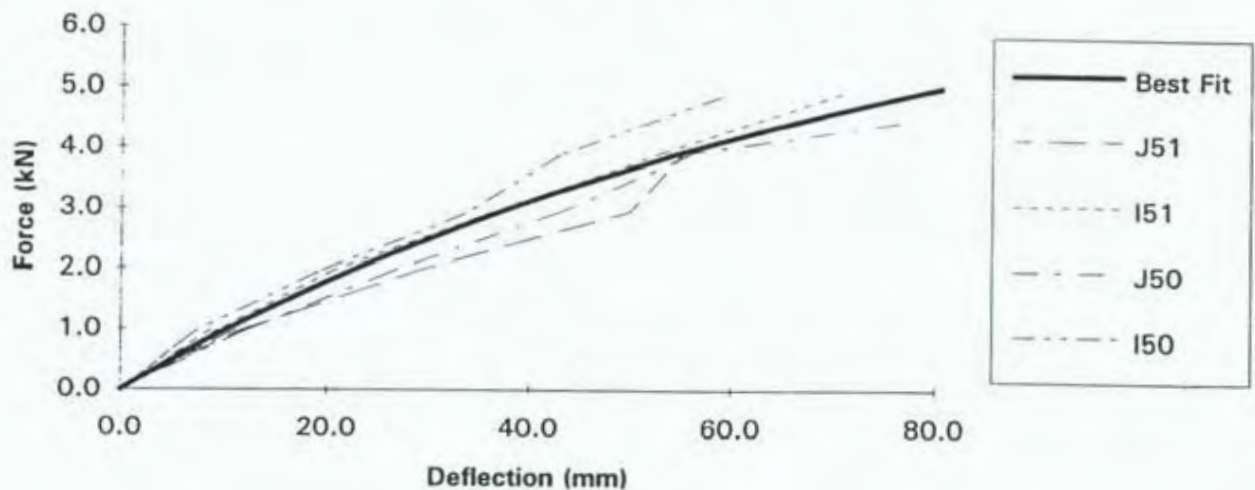


Figure C.14 Comparison of Best Fit Curve and Repeat Curves for Driven Piles in Peat

Appendix D Fitting PhylMas Loops to Experimental Data

D.1 Introduction

The process used to derived earthquake design loads from a given set of pinched hysteresis loops first required matching the loops using the PhylMas parameters. The test loops (from Appendix A) are reproduced in this Appendix, along with the PhylMas simulated loops. It can be seen that there is a good match.

Table D.1 gives a list of the parameters used by PhylMas to match the loops and has been provided to allow other researchers with access to PhylMas to duplicate the results and analyse the data for different earthquakes. Table D.1 also provides the cross reference number to the plots in Appendix A.

Table D.1 Parameters Used by PhylMas

Pile Type	P*	Soil	R _K	R _U	R _X	K	Cy	Ry	Jp	X _Z
Anchor	36	Clay	0.36	0.70	0.46	0.8	8	0.26	2	0.1
Anchor	86	Peat	0.36	0.80	0.42	0.20	3.5	0.3	4	0.32
Braced	50	Clay	0.36	1.1	0.34	0.48	8.0	0.26	4	0.1
Shear	63	Clay	0.12	1.7	0.08	1.8	28	0.60	3	-0.04
Shear	89	Peat	0.24	1.3	0.28	0.50	11	0.4	5	0.12
Shear	105	Sandy-silt	0.12	1.0	0.30	3.0	30	0.02	1	0.0
Shear	117	Sand	1.0	1.6	1.0	1.0	8.0	0.1	4	-0.18
Driven	77	Peat	0.36	0.50	0.46	0.27	1.0	0.26	4	0.10

Note: X_p and X_N always set to 0.0

Legend

P* = plot number used in Appendix A and H.

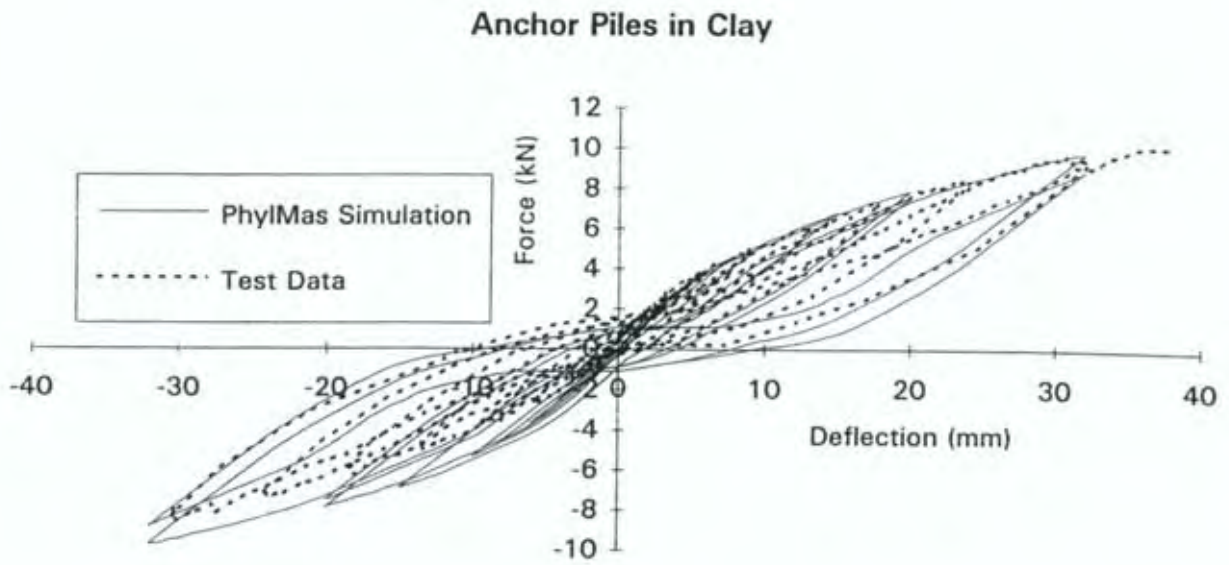


Figure D.1 PhylMas Fitting of Test Data for Anchor Piles in Clay

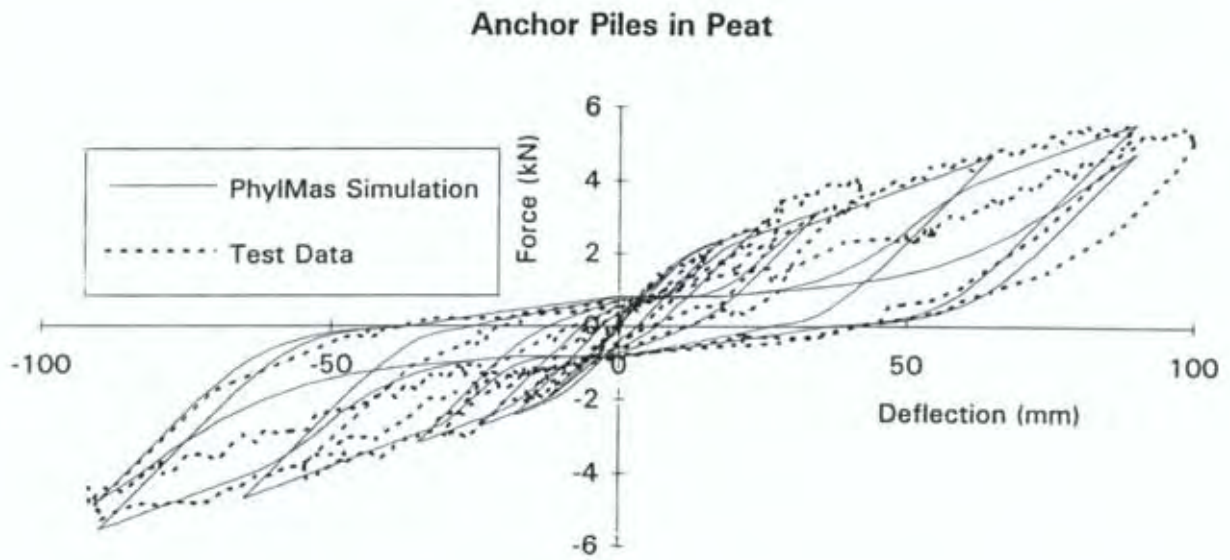


Figure D.2 PhylMas Fitting of Test Data for Anchor Piles in Peat

Anchor Piles in Sandy-silt and Sand

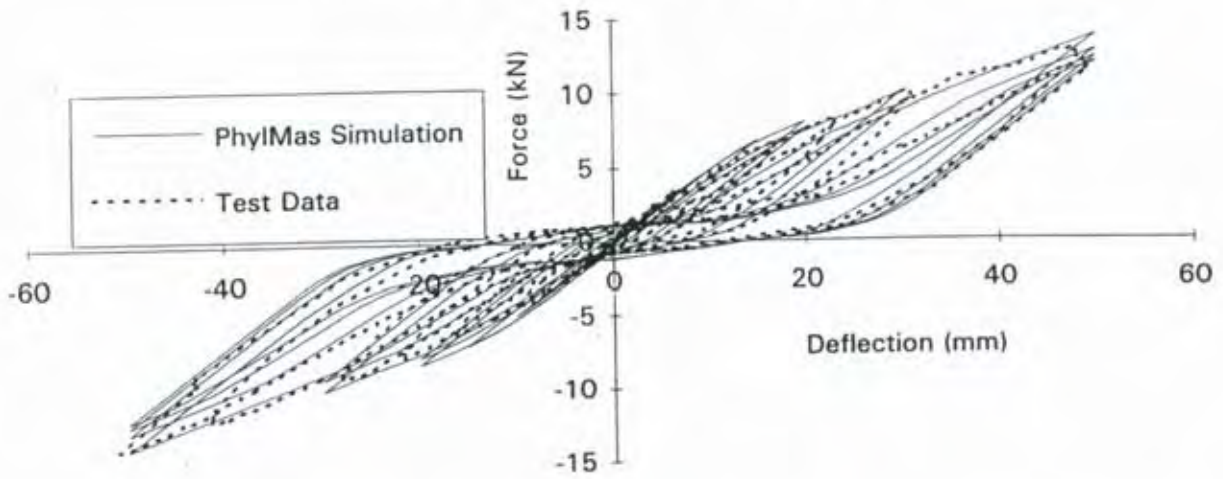


Figure D.3 PhylMas Fitting of Test Data for Anchor Piles in Sandy-silt and Sand

Braced Piles In Clay

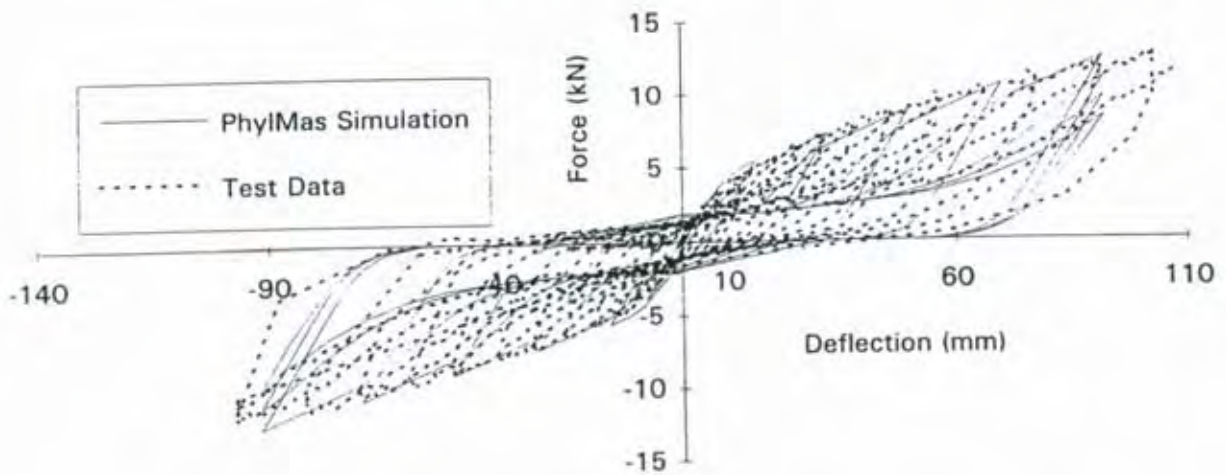


Figure D.4 PhylMas Fitting of Test Data for Braced Piles in Clay

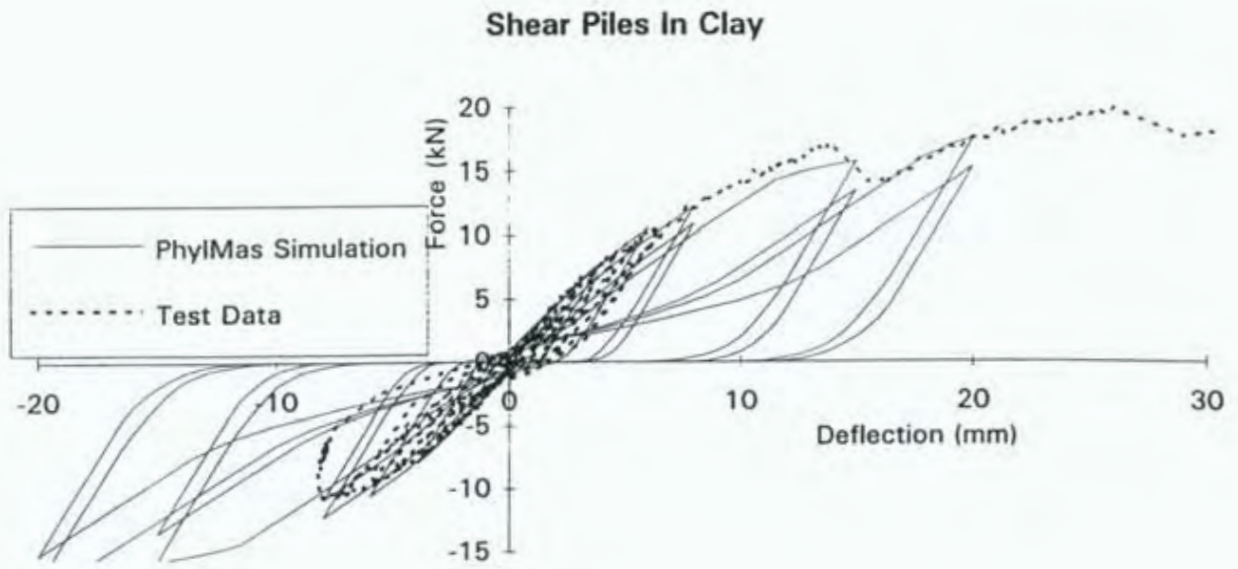


Figure D.5 PhylMas Fitting of Test Data for Shear Piles in Clay

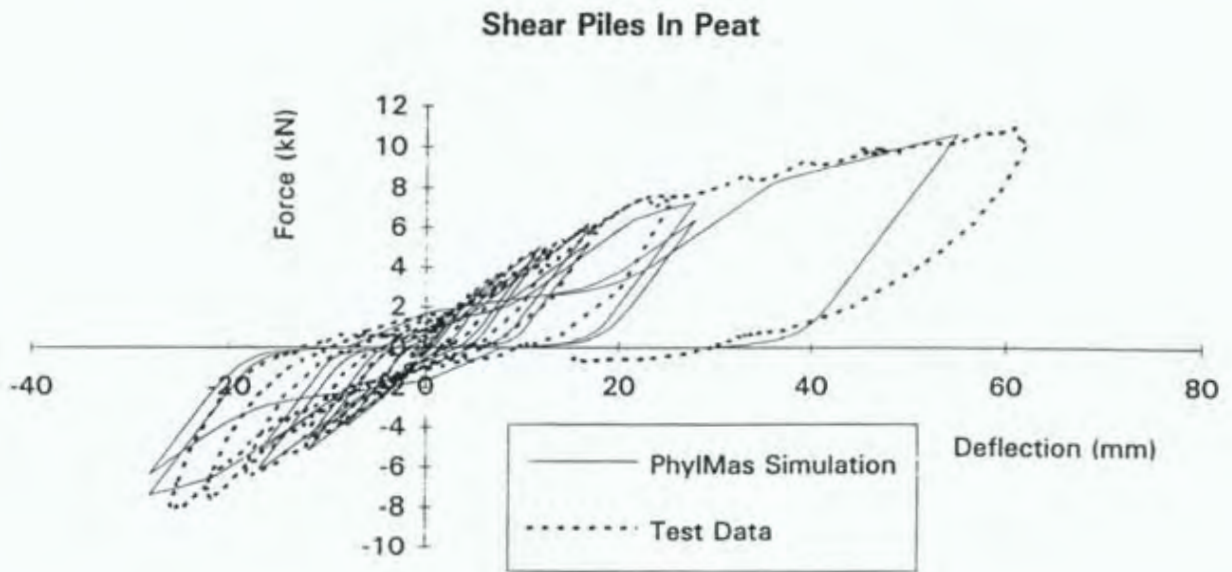


Figure D.6 Relationship Between Design Loads and Deflection for Shear Piles in Peat

Shear Piles In Sandy-silt

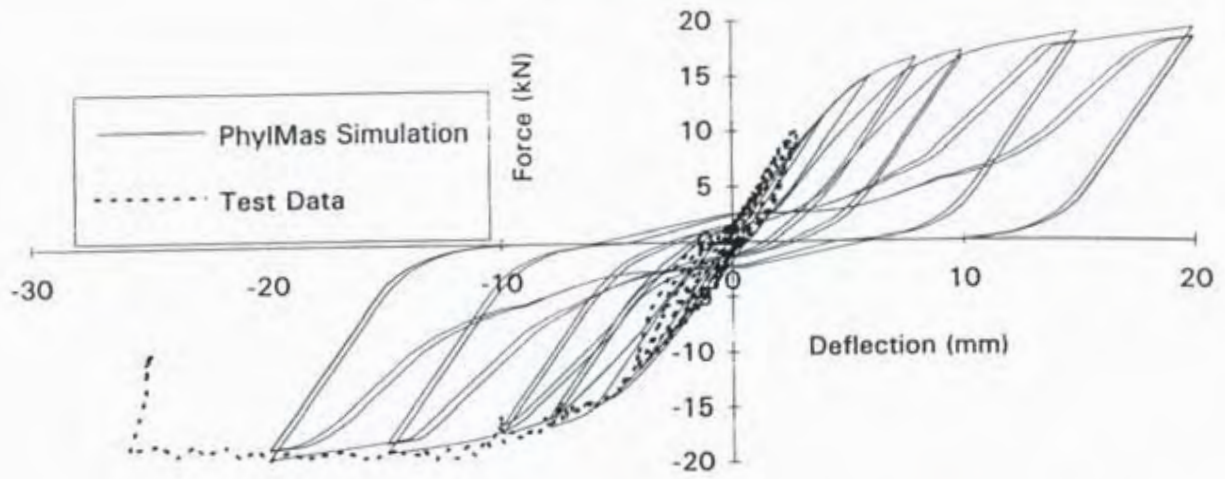


Figure D.7 PhylMas Fitting of Test Data for Shear Piles in Sandy-silt

Shear Piles In Sand

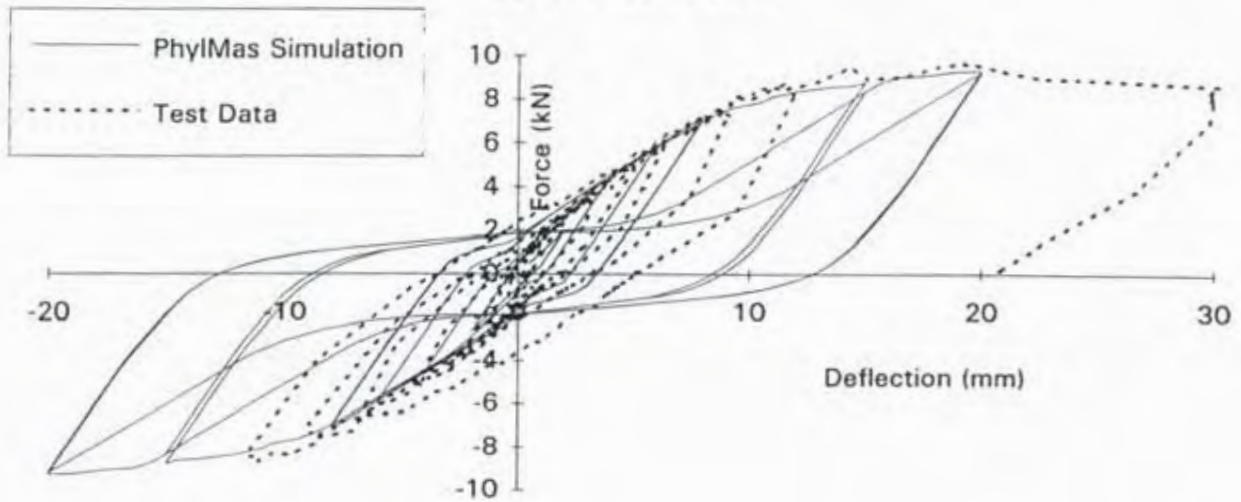


Figure D.8 PhylMas Fitting of Test Data for Shear Piles in Sand

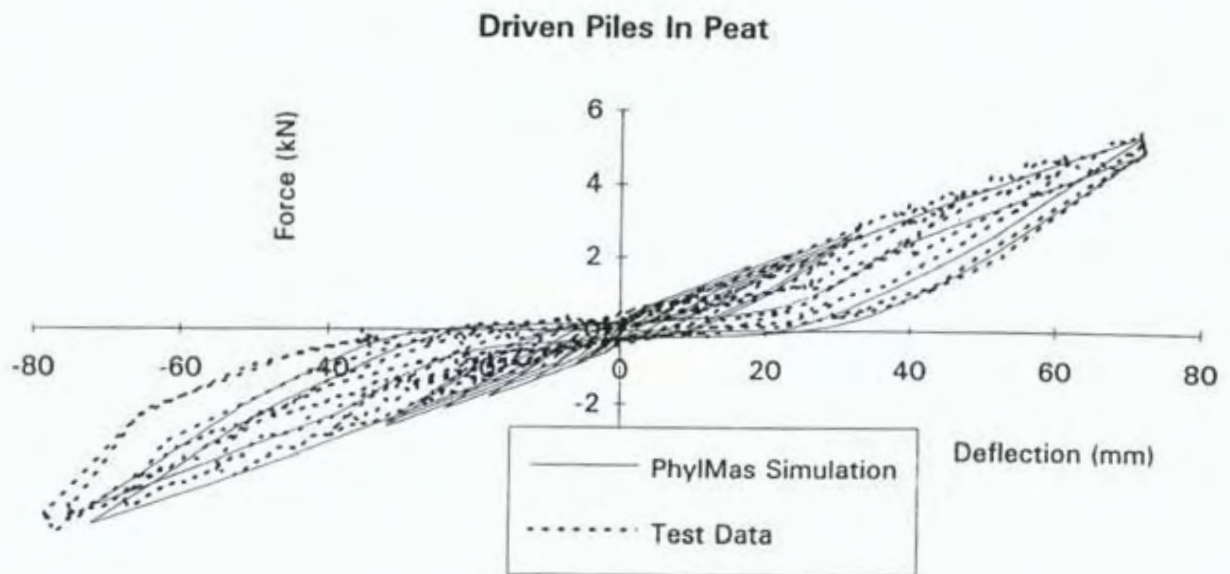


Figure D.9 PhylMas Fitting of Test Data for Driven Piles in Peat

Appendix E Earthquake and Wind Pile Design Loads

E.1 Introduction

The methodology used to determine earthquake and wind design loads is described in Section 6.3 and 6.4 respectively.

The displacement response spectra found for each pile type from PhylMas was fed into a spreadsheet programme. This was used to calculate the earthquake design force for each displacement from steps 3 and 4 of Section 6.3.6, and the relationship between design force and displacement is plotted in this Appendix. The earthquake design force of 70 BU stipulated by NZS 3604 (SANZ, 1990) is also plotted for comparison.

The parent curve best fit equations in Appendix C were used to derive the relationship between wind design force and deflection which is also plotted in this appendix. The wind design force of 160 BU is also plotted for comparison.

The forces in this Appendix are plotted in terms of Bracing Units (BU) where 20 BU = 1kN.

Anchor Piles in Clay

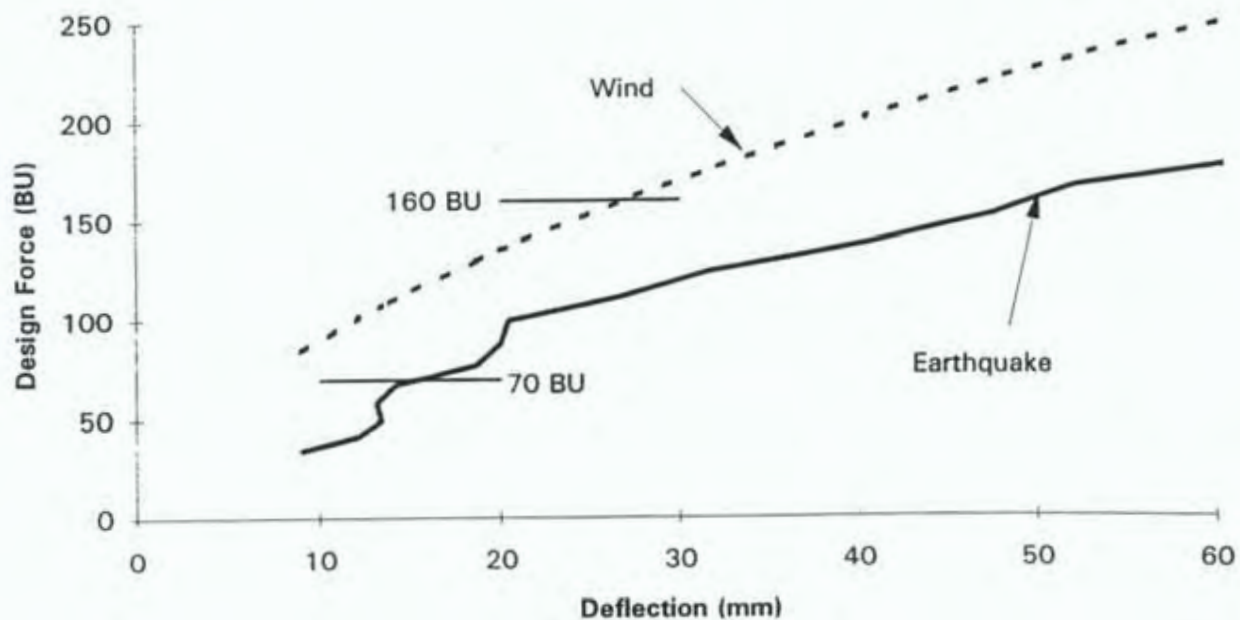


Figure E.1 Relationship Between Design Loads and Deflection for Anchor Piles in Clay

Anchor Piles in Peat

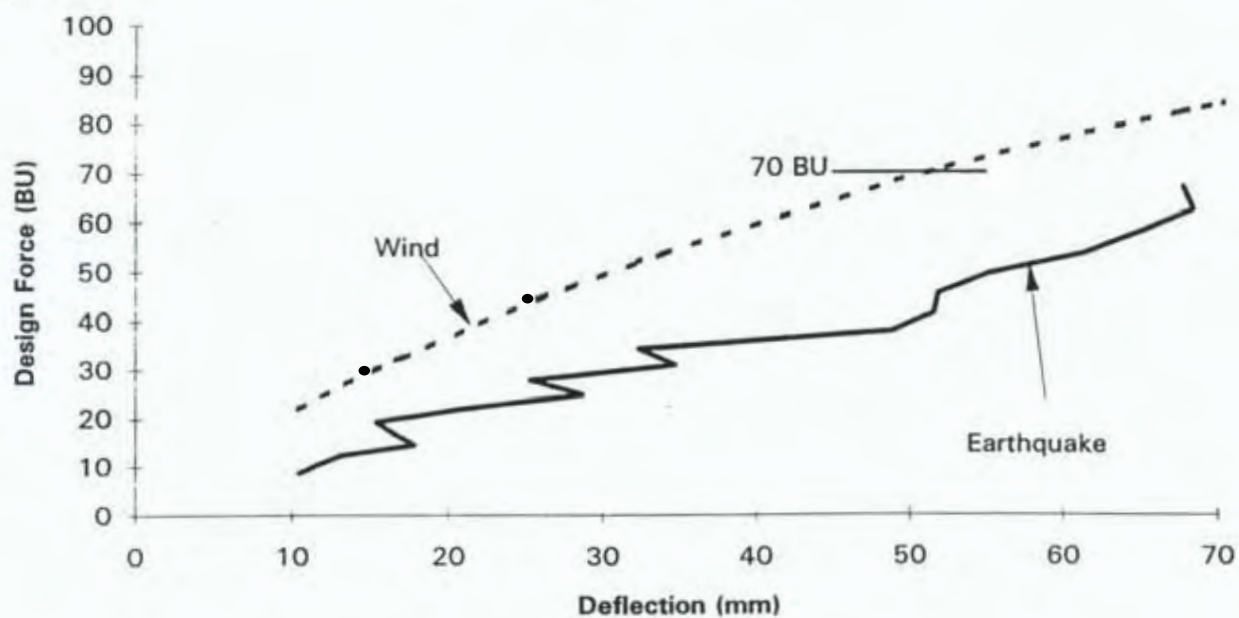


Figure E.2 Relationship Between Design Loads and Deflection for Anchor Piles in Peat

Anchor Piles in Sandy-silt and Sand

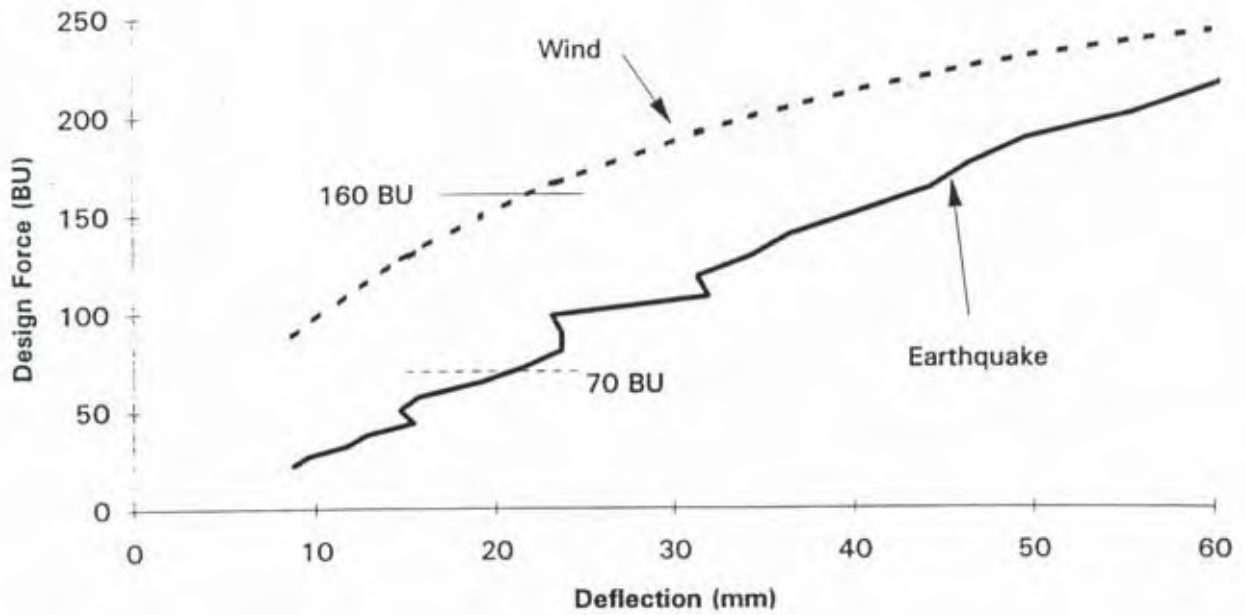


Figure E.3 Relationship Between Design Loads and Deflection for Anchor Piles in Sandy-silt and Sand

Braced Piles in Clay

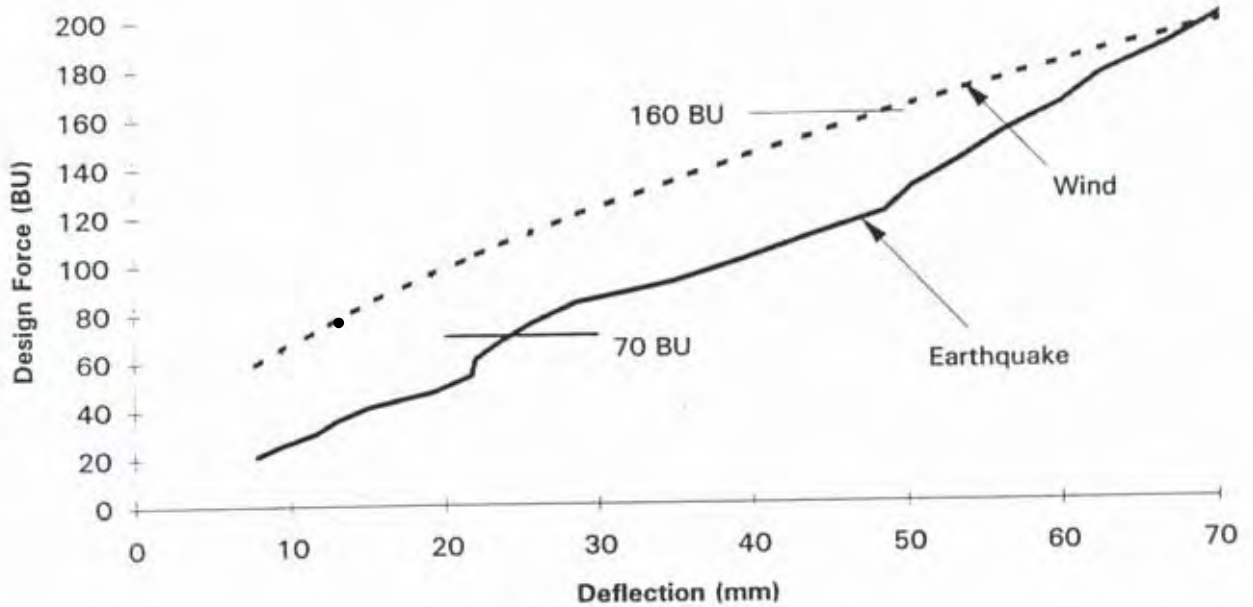


Figure E.4 Relationship Between Design Loads and Deflection for Braced Piles in Clay

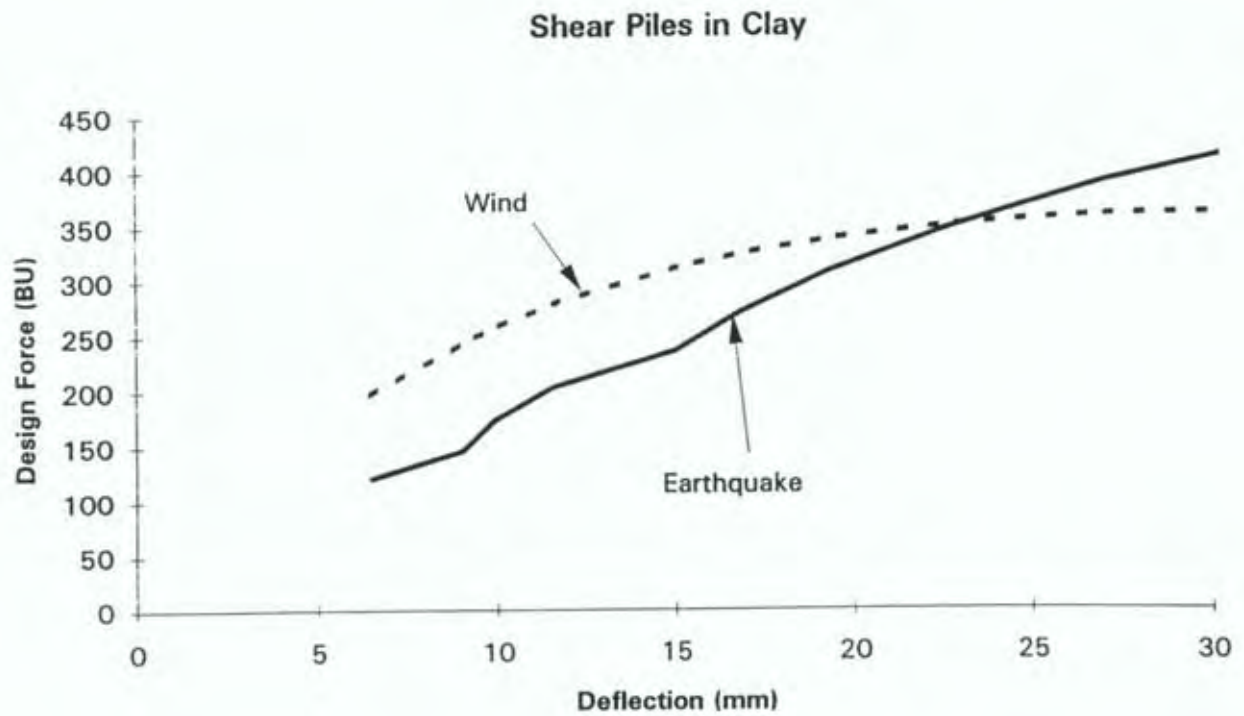


Figure E.5 Relationship Between Design Loads and Deflection for Shear Piles in Clay

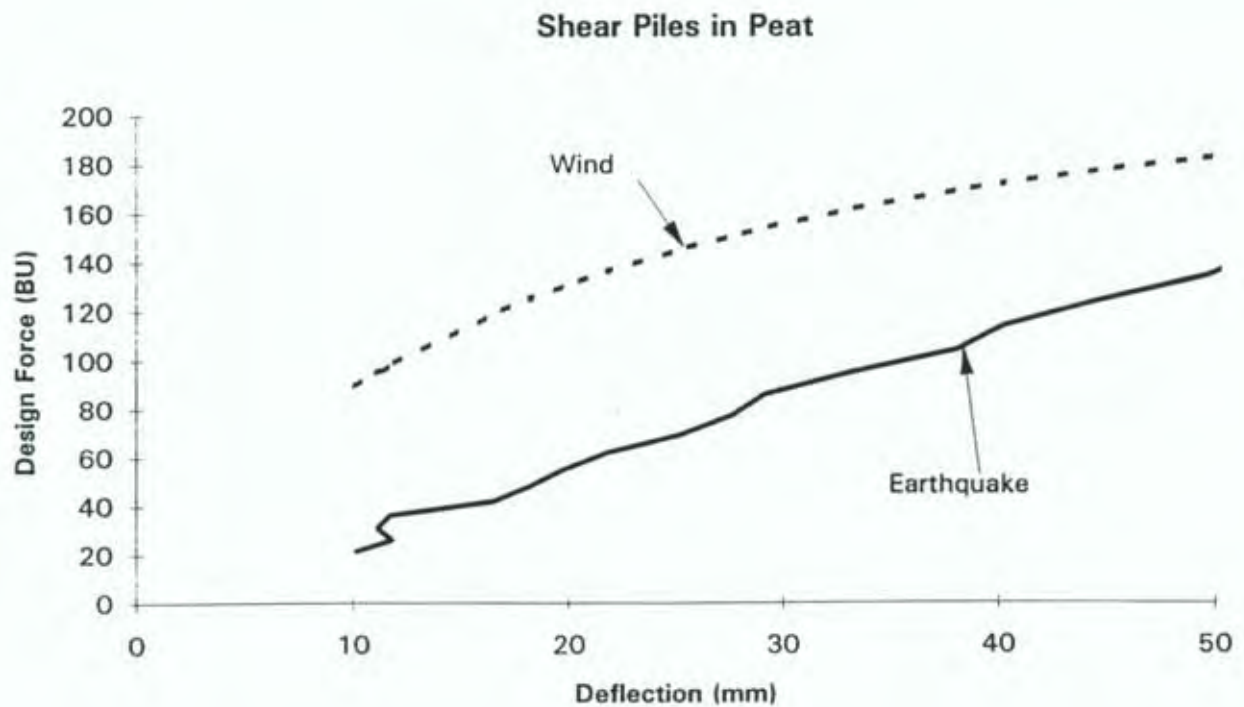


Figure E.6 Relationship Between Design Loads and Deflection for Shear Piles in Peat

Shear Piles in Sandy-silt

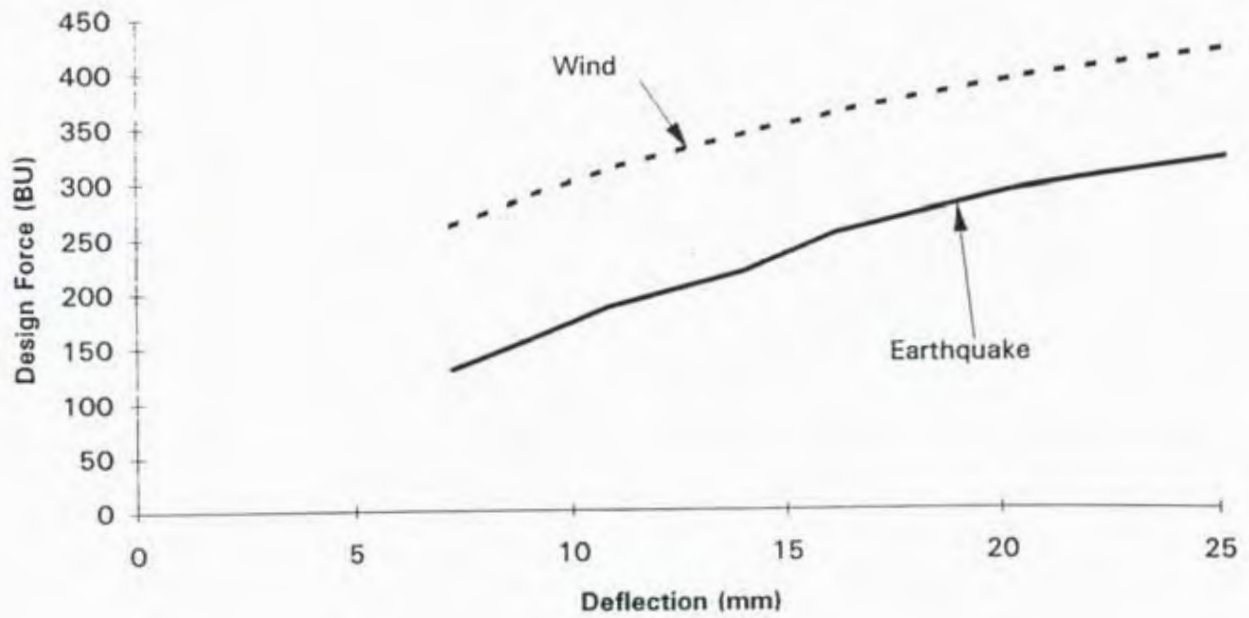


Figure E.7 Relationship Between Design Loads and Deflection for Shear Piles in Sandy-silt

Shear Piles in Sand

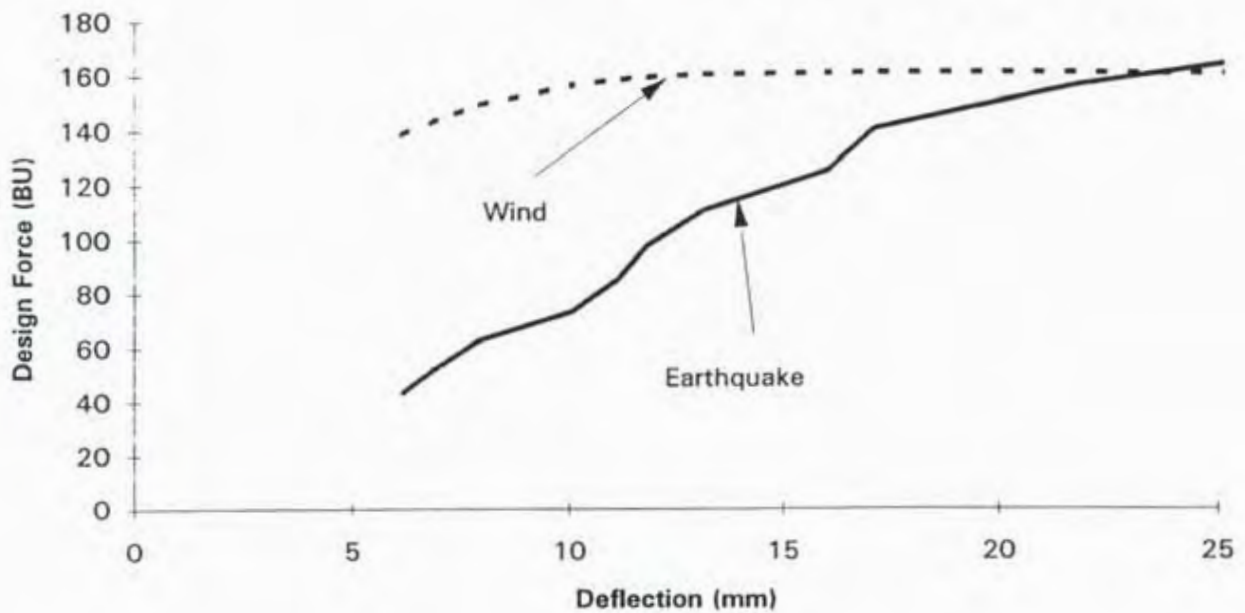


Figure E.8 Relationship Between Design Loads and Deflection for Anchor Piles in Sand

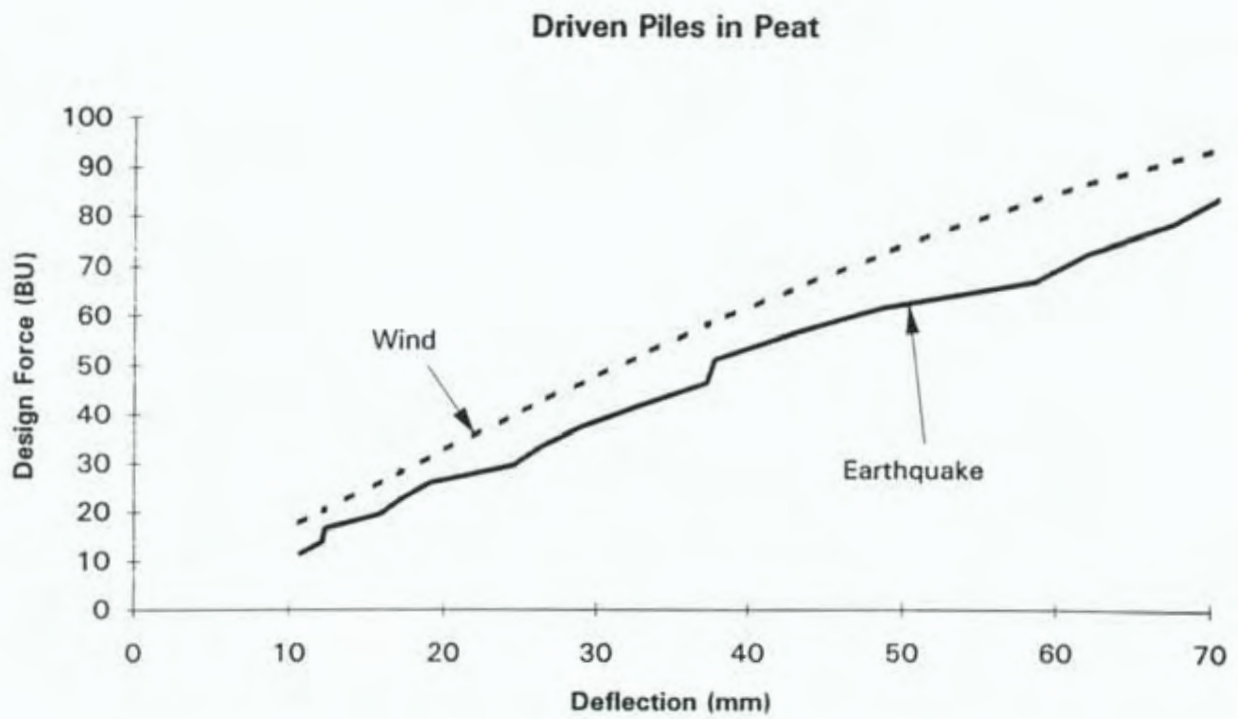


Figure E.9 Relationship Between Design Loads and Deflection for Driven Piles in Peat

Appendix F Soil Properties

F.1 Soil Logs

Soils logs are given in Tables F.13 - F.17. The soil in Groups 1 and 2 was a soft clay with some silt and an estimated friction angle of 25° . The peat was very soft and saturated, and contained some organic clay. The sandy-silt had a low cohesion strength, some organic content and an estimated friction angle of 30° . The sand was fine clean dune sand with no cohesion strength and was at less than optimum density.

F.2 Soil Strengths

Scala penetrometer soundings (using BTL's equipment) and shear vane soil tests (using Central Laboratories $\frac{3}{4}$ " diameter Hand Vane No VT-416) were performed at the locations shown in Figure 11.

Plots of scala penetrometer sounding versus depth are given at the back of this Appendix and averaged soundings over 300 mm depth increments are given in Table F.1 - F.5. Overall averages are given in Table F.6. Shear vane readings were taken near mid-depth of each 300 mm depth increment and are given in Table F.7 - F.11 and averaged values are given in Table F.12. The instrument was only capable of reading to a maximum of 234 kPa, and thus averaged results given in the table will be on the low side.

The dates of taking the soundings are provided in these tables, and may be useful if comparisons between the time of recording soundings and doing the lateral load test are required. The test dates are given in Appendix H.

Table F.1 Average Scala Penetrometer Penetration (mm/blow) - Group 1

Test No.	Date	Pile	Depth Range (mm)			
			0 - 300	300 - 400	600 - 900	900 - 1200
P1	8/11/93	A1	60	90	160*	35
P2	4/12/93	A1	70	60	30	30
P3	8/11/93	A4	75	18	18	20
P4	4/12/93	A4	40	15	24	-
P5	8/11/93	D1	50	16	38	25
P6	8/11/93	D1	60	43	58	24
P8	9/11/93	E2	60	34	31	-
P9	8/11/93	G2	42	31	30	22
P10	8/11/93	G1	46	38	29	-
P11	8/11/93	G1	45	31	46	27
P12	22/12/93	G1	38	78	65	-
P13	22/12/93	G2	49	40	20	-
P15	14/12/93	J1	74	37	28	-
P16	14/12/93	J2	75	36	28	-
P17	14/12/93	J3	76	64	36	34
P18	14/12/93	J4	98	46	31	31
P19	18/11/93	J4	93	54	30	26
P20	8/11/93	J3	60	83	54	30
P21	8/11/93	J4	35	47	33	31
P22	22/12/93	E2	44	32	38	-
P23	22/12/93	E2	39	35	-	-
P24	8/12/94	J1	46	31	18	20
P25	8/2/94	J4	35	46	30	32
Averages			57	44	34	28

⁶

Legend

* Ignored in average given

Table F.2 Average Scala Penetrometer Penetration (mm/blow) - Group 2

Test No.	Date	Pile	Depth Range (mm)			
			0 - 300	300 - 600	600 - 900	900 - 1200
P40	8/2/94	V10	57	44	33	20
P41	8/2/94	Y10	26	33	36	-
P42	8/2/94	V13	23	33	43	22
P43	9/2/94	W13	50	35	47	24
P44	9/2/94	W13	15	21	33	-
P45	9/2/94	V13	52	37	34	-
P46	9/2/94	V13	56	45	40	-
P47	10/2/94	U13	30	33	-	-
P42	10/2/94	T13	27	36	-	-
P49	10/2/94	U10	30	26	45	-
P50	10/2/94	U10	28	34	-	-
P51	10/2/94	W10	45	23	45	-
Averages			37	33	40	22

Table F.3 Average Scala Penetrometer Penetration (mm/blow) Group 3

Test No.	Date	Pile	Depth Range (mm)			
			0 - 300	300 - 600	600 - 900	900 - 1200
P60	9/11/93	-	150	105	73	62
P61	9/11/93	-	120	130	95	40
P64	8/2/94	J50	120	175	66	39
P65	8/2/94	G51	200	400*	200	80
P66	8/2/94	H50	200	105	75	100
P67	8/2/94	H51	107	137	58	42
Averages			150	130	95	61

Legend

* Ignored in average given

Table F.4 Average Scala Penetrometer Penetration (mm/blow) Group 4

Test No.	Date	Pile	Depth Range (mm)			
			0 - 300	300 - 600	600 - 900	900 - 1200
P70	8/2/94	M5	21	28	36	21
P71	8/2/94	M4	41	31	26	23
P72	8/2/94	M2	44	39	40	23
P73	8/2/94	M1	41	40	29	19
Averages			37	35	33	22

Table F.5 Average Scala Penetrometer Penetration (mm/blow) Group 5

Test No.	Date	Pile	Depth Range (mm)			
			0 - 300	300 - 600	600 - 900	900 - 1200
P80	9/11/93	P1	28	26	23	17
P82	9/11/93	P2	58	38	42	27
P83	9/11/93	P1	26	33	28	18
Averages			37	32	31	21

Table F.6 - Average Scala Penetrometer Penetration (mm/blow)

Group No.	Soil Type	Depth Range (mm)			
		0 - 300	300 - 400	600 - 900	900 - 1200
1	Clay	57	44	34	28
2	Clay	37	33	40	22
3	Peat	150	130	95	61
4	Sandy-silt	37	35	33	22
5	Sand	37	32	31	21

Table F.7 Shear Vane Test Results Group 1 (Shear Strength (kPa))

Test	Pile	Date	Depth (mm)			
			150	450	750	1050
V11	J4	8-2-94	78	221	196	210
V13	J4	4-3-94	165	210	200	205
V12	J2	8-2-94	173	200	231	234+
V12a	J1	4-3-94	207	234+	234+	234+
V14	J2	4-3-94	197	231	200	193
V15	H2	4-3-94	210	234+	234+	234+
V16	G2	4-3-94	205	189	234+	234+
V17	F2	4-3-94	234+	234+	220	234+
V18	G1	4-3-94	234+	234+	234+	234+
V19	F1	4-3-94	234+	234+	234+	234+
Average			194	222	222	225

Table F.8 Shear Vane Test Results Group 2 (Shear Strength (kPa))

Test	Pile	Date	Depth (mm)			
			150	450	750	1050
V21	Y10	8-2-94	234+	234+	234+	234+
V22	Y13	4-3-94	183	193	180	234+
V23	X13	4-3-94	141	234+	155	176
V24	W13	4-3-94	158	221	210	193
V25	U13	4-3-94	172	138	82	112
V26	U13	4-3-94	124	234+	234+	234+
V27	T13	4-3-94	183	234+	200	234+
V28	V13	4-3-94	172	196	186	172
Average			171	211	185	197

Table F.9 Shear Vane Test Results Group 3 (Shear Strength (kPa))

Test	Pile	Date	Depth (mm)			
			150	450	750	1050
V31	G51	8-2-94	71	34	74	33
V32	H50	8-2-94	48	22	31	24
V33	I51	8-2-94	59	24	24	51
V34	F50	8-2-94	55	38	41	48
Average			58	30	43	39

Table F.10 Shear Vane Test Result Group 4 (Shear Strength (kPa))

Test	Pile	Date	Depth (mm)			
			150	450	750	1050
V41	M1	8-2-94	131	135	138	138
V42	M2	8-2-94	120	135	138	124
V43	M3	8-2-94	124	124	140	145
V44	M4	8-2-94	225	200	151	138
V45	M5	8-2-94	207	131	172	172
Average			161	145	148	143

Table F.11 Shear Vane Test Results Group 5 (Shear Strength (kPa))

Test	Pile	Date	Depth (mm)			
			150	450	750	1050
V51	P1	8-2-94	207	162	162	172
V52	P2	8-2-94	144	162	145	160
Average			176	162	154	166

Table F.12 - Average Shear Vane Test Results (Shear Strength kPa)

Group No.	Soil Type	Depth (mm)			
		150	450	750	1050
1	Clay	194	222	222	225
2	Clay	171	211	185	197
3	Peat	58	30	43	39
4	Sandy-silt	161	145	148	143
5	Sand	176	162	154	166

Table F.13 Soil Log, Location J4, Group 1

Depth (mm)	Description
0-130	Light brown, (dry) organic topsoil, breaks up when rolled
130-500	Light brown, firm silty-clay, moulds when rolled, dry
500-600	Firm clay, yellow with mottled orange weathering, moulds under pressure
600-1000	Silty-clay, dark brown, moulds when rolled
1000+	Firm clay, yellow with mottled orange weathering moulds under pressure

Table F.14 Soil Log, Location V10, Group 2

Depth (mm)	Description
0-15-	Light brown (dry) organic topsoil, breaks up when rolled
150-500	Light brown silty-clay, moulds when rolled, dry
500-1200	Firm yellow clay which moulds under pressure, orange weathering

Table F.15 Soil Log, Location H50, Group 3

Depth (mm)	Description
0-150	Dark peat bound together with grass roots
150-1070	Organic peat - smears and moulds easily, moisture content increasing from 350 to 500%
1070+	Dark peat stained organic silt

Table F.16 Soil Log, Group 4

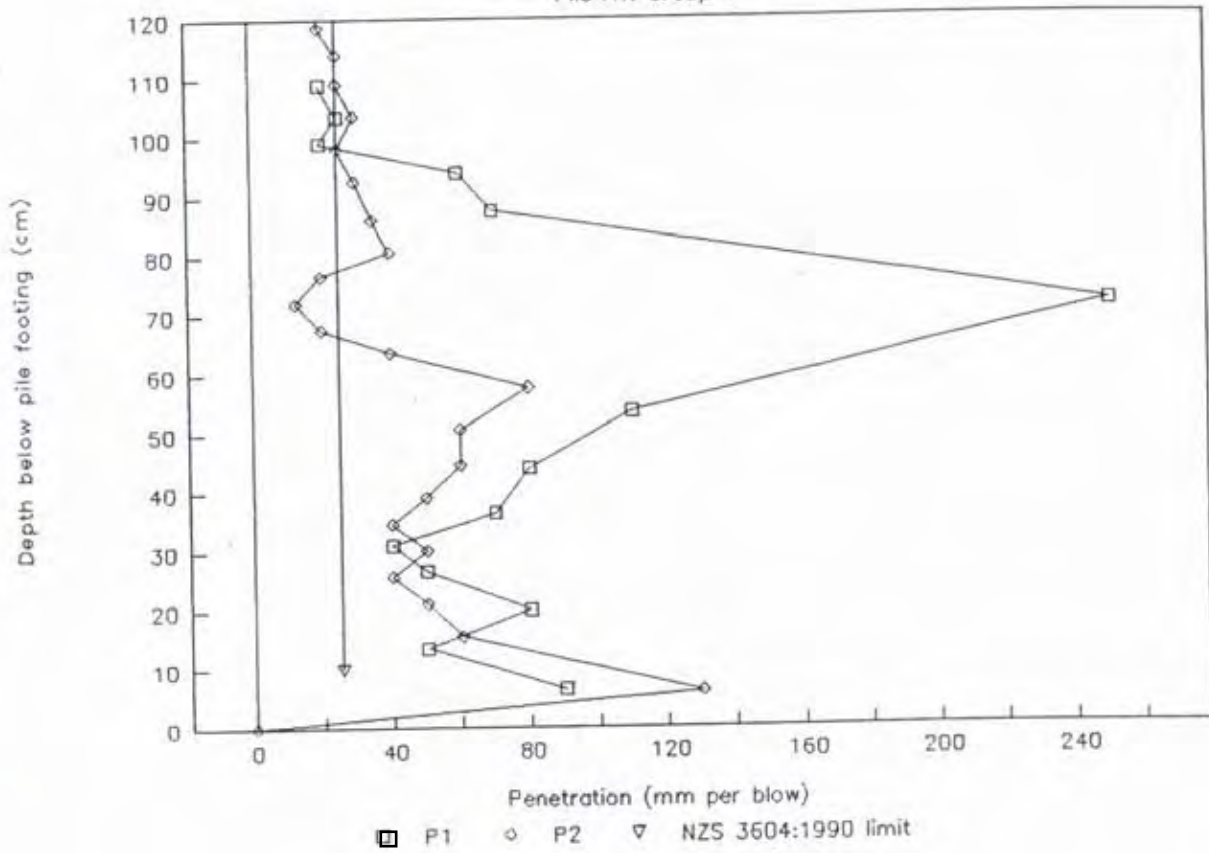
Depth (mm)	Description
0-550	Organic sandy-silt, uniform light brown with evidence of grass roots, moisture content 17%
550-900	Grey sand with mottled brown patches, moisture content 7%
900+	Grey sand with moisture content 10%

**Table 17
Soil Log, Group 5**

Depth (mm)	Description
0-1300	Light grey fine dune sand with moisture content increasing from 5% at 550 mm depth to 5% at 900 mm depth and 29% at 1200 mm depth

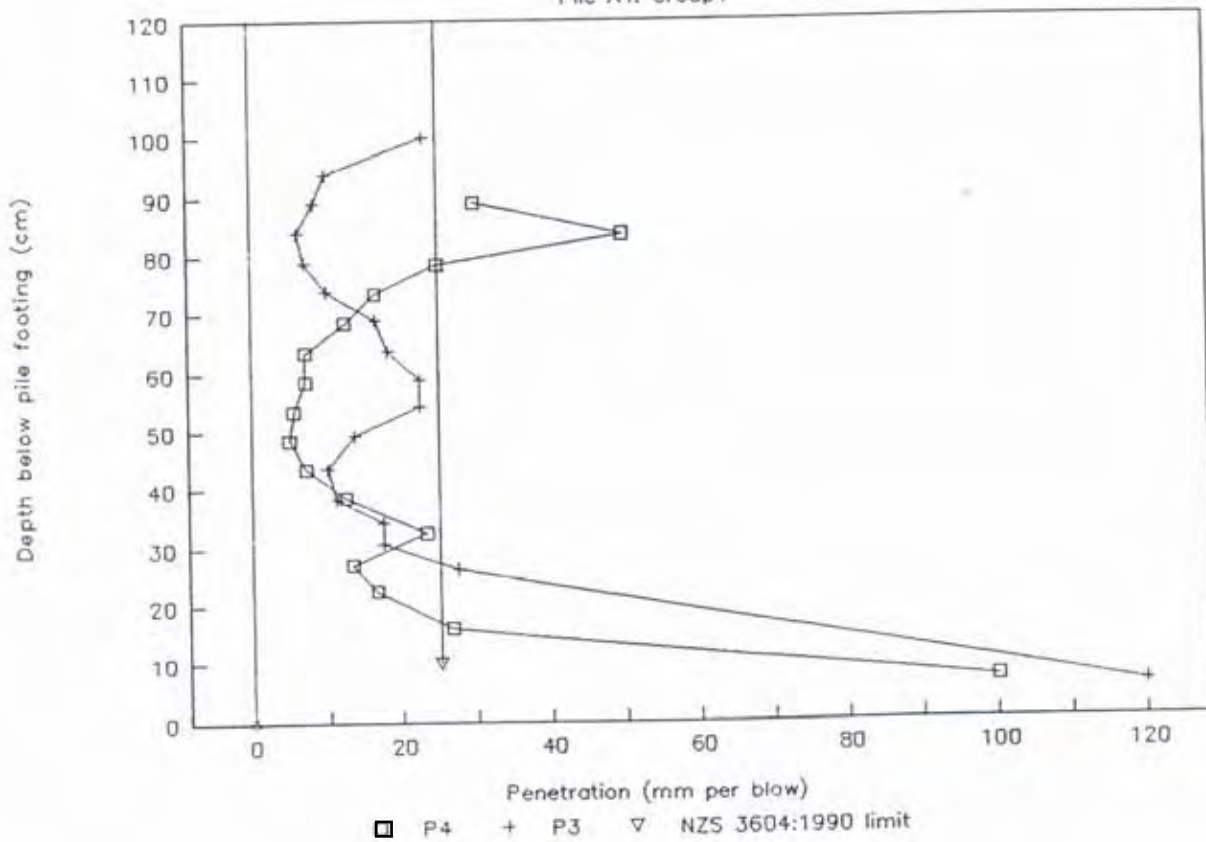
Scala Penetrometer Soundings

File A1: Group 1



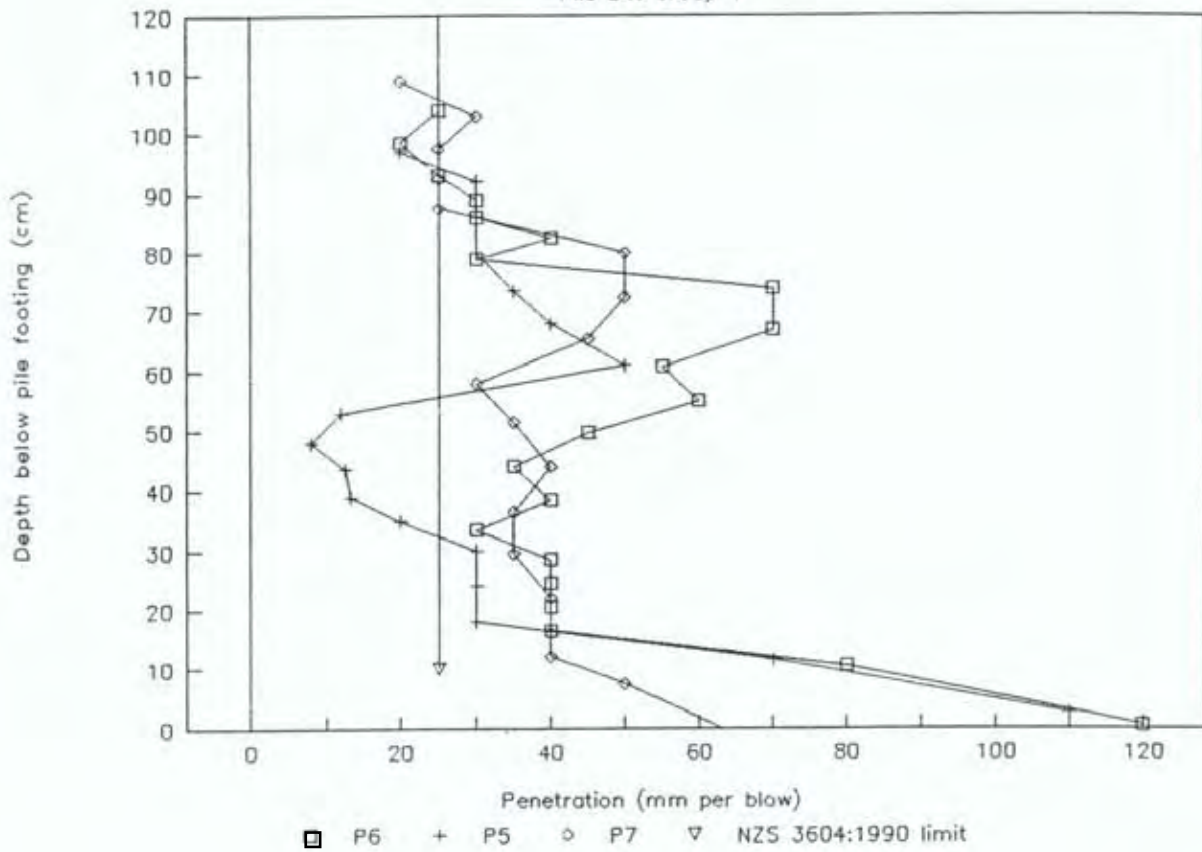
Scala Penetrometer Soundings

File A4: Group 1



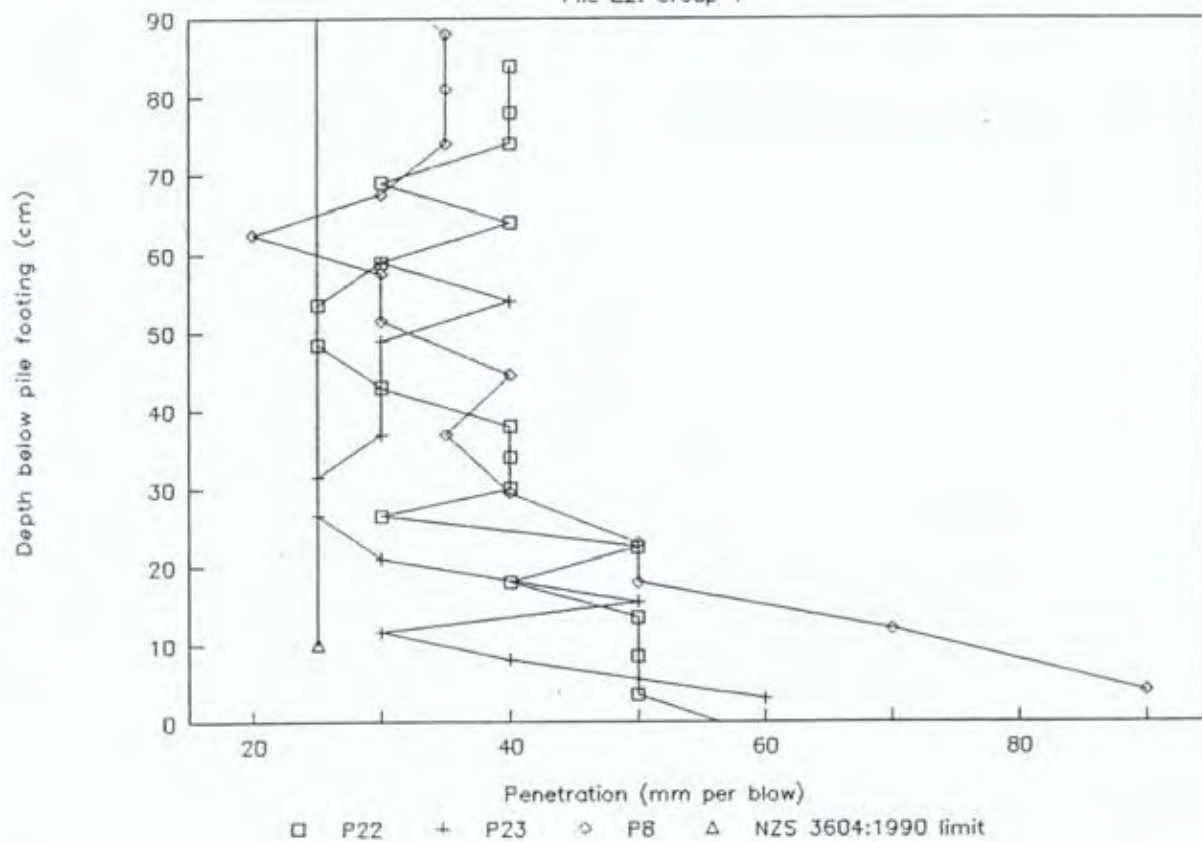
Scala Penetrometer Soundings

File D1: Group 1



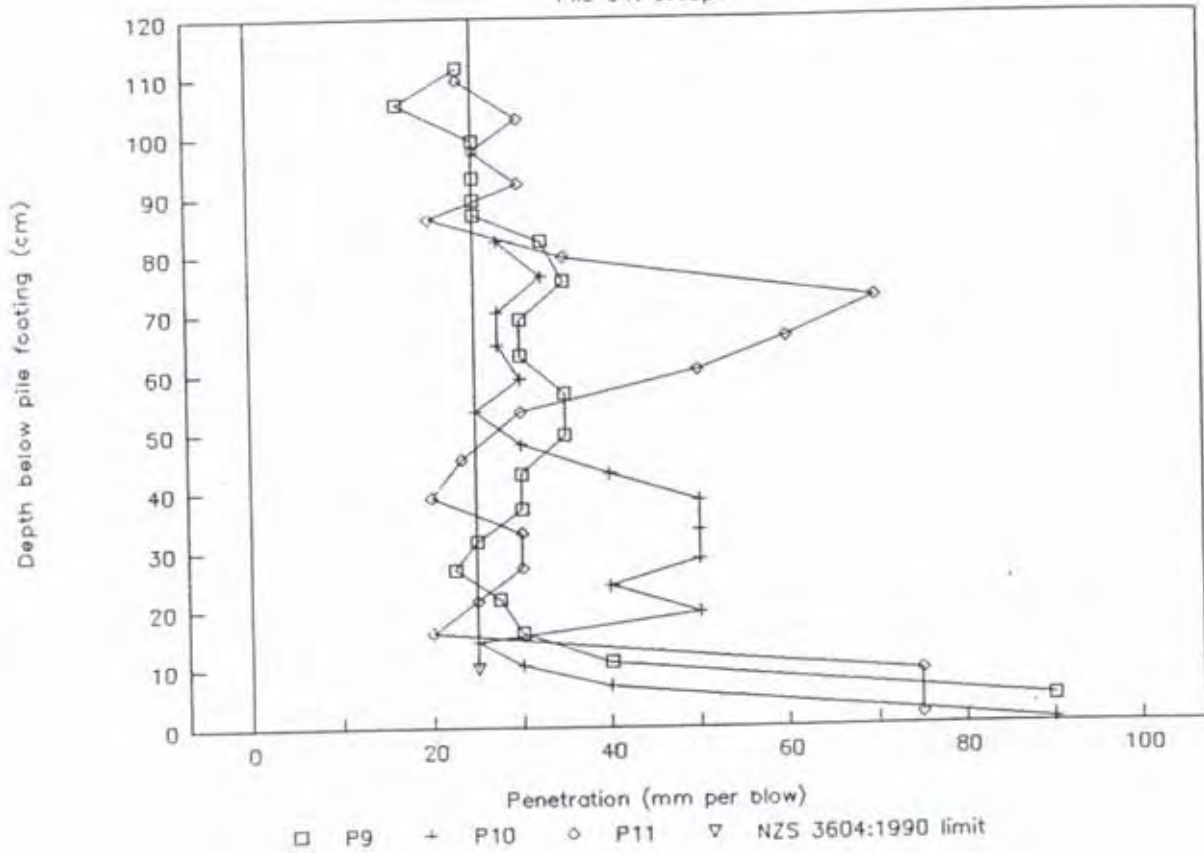
Scala Penetrometer Soundings

File E2: Group 1



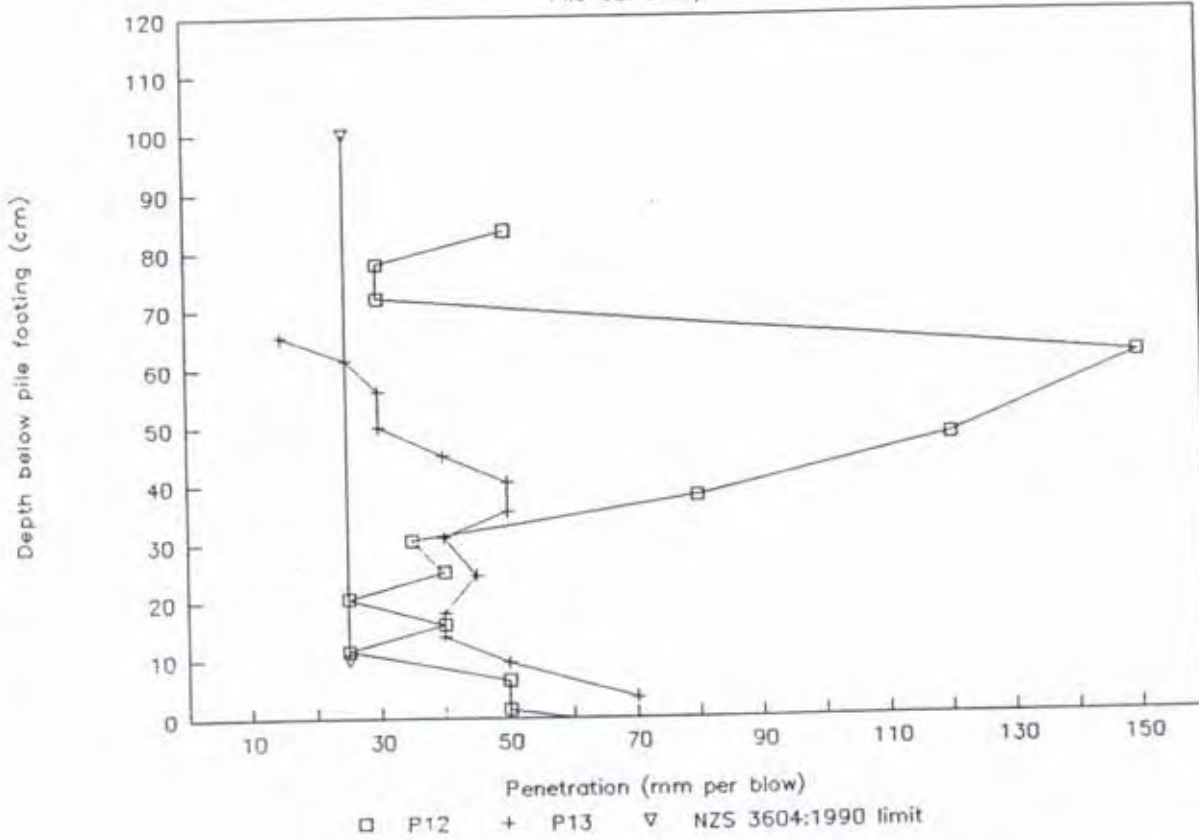
Scala Penetrometer Soundings

File G1: Group 1



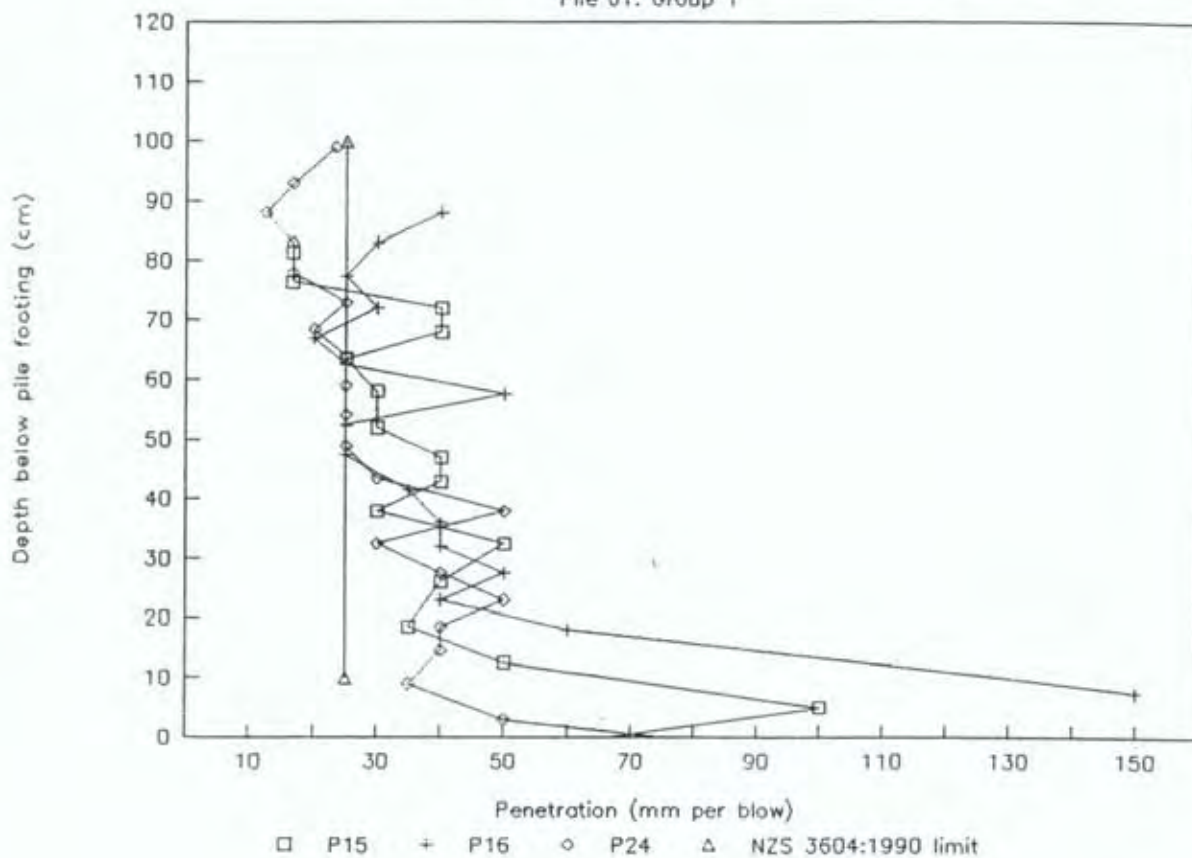
Scala Penetrometer Soundings

File G2: Group 1



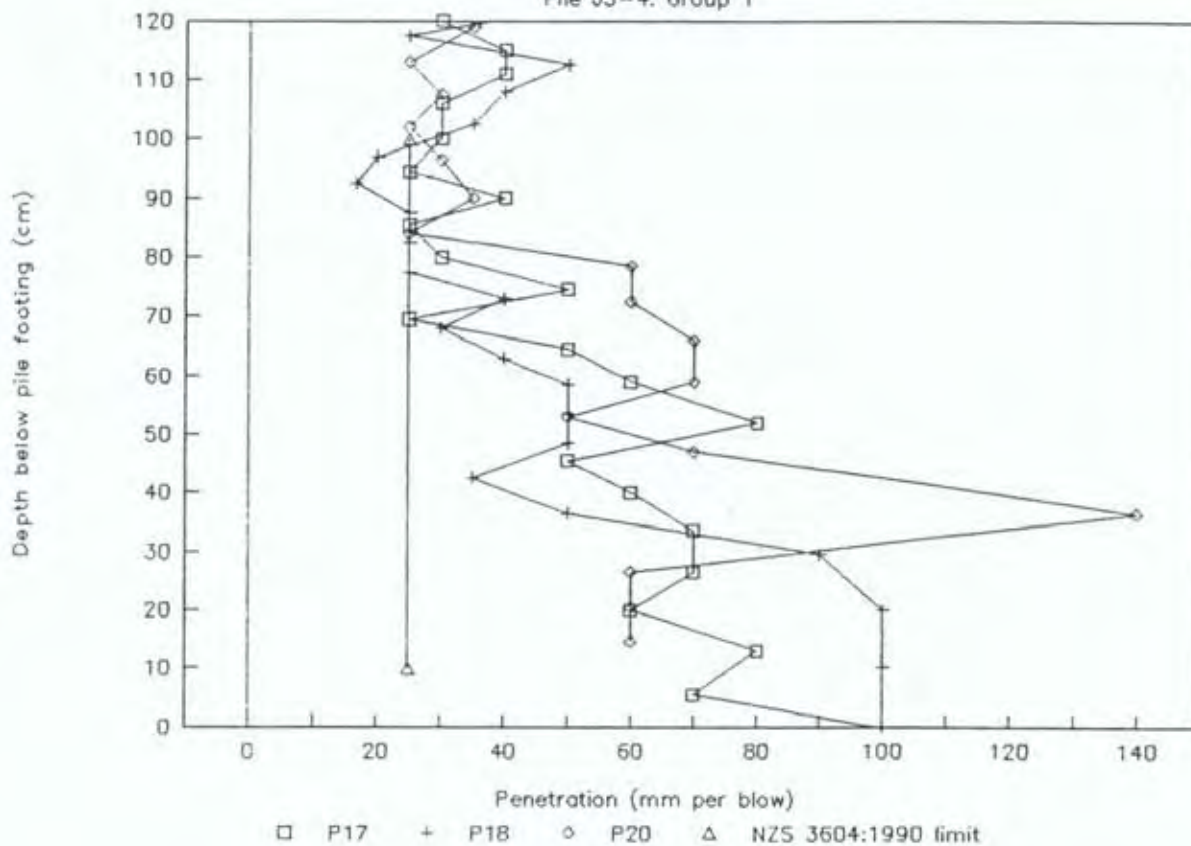
Scala Penetrometer Soundings

File J1: Group 1



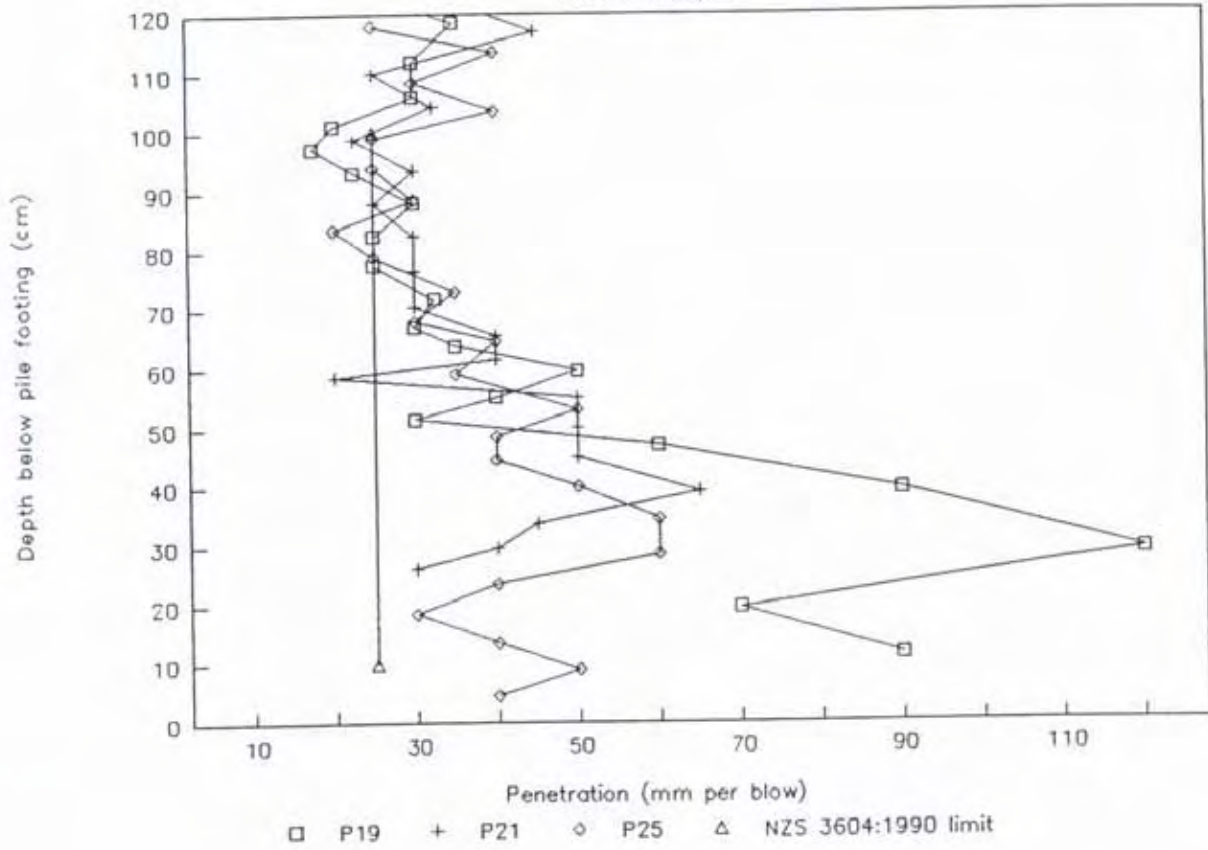
Scala Penetrometer Soundings

File J3-4: Group 1

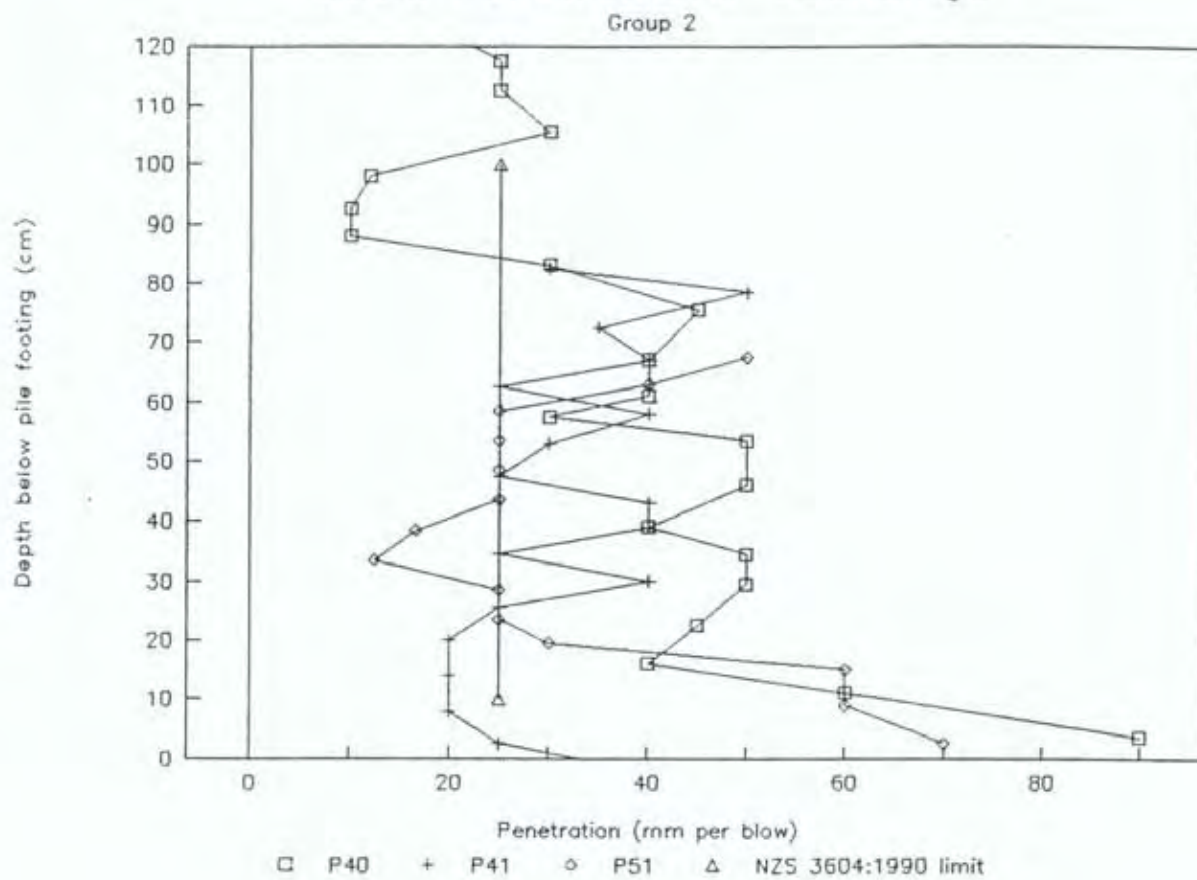


Scala Penetrometer Soundings

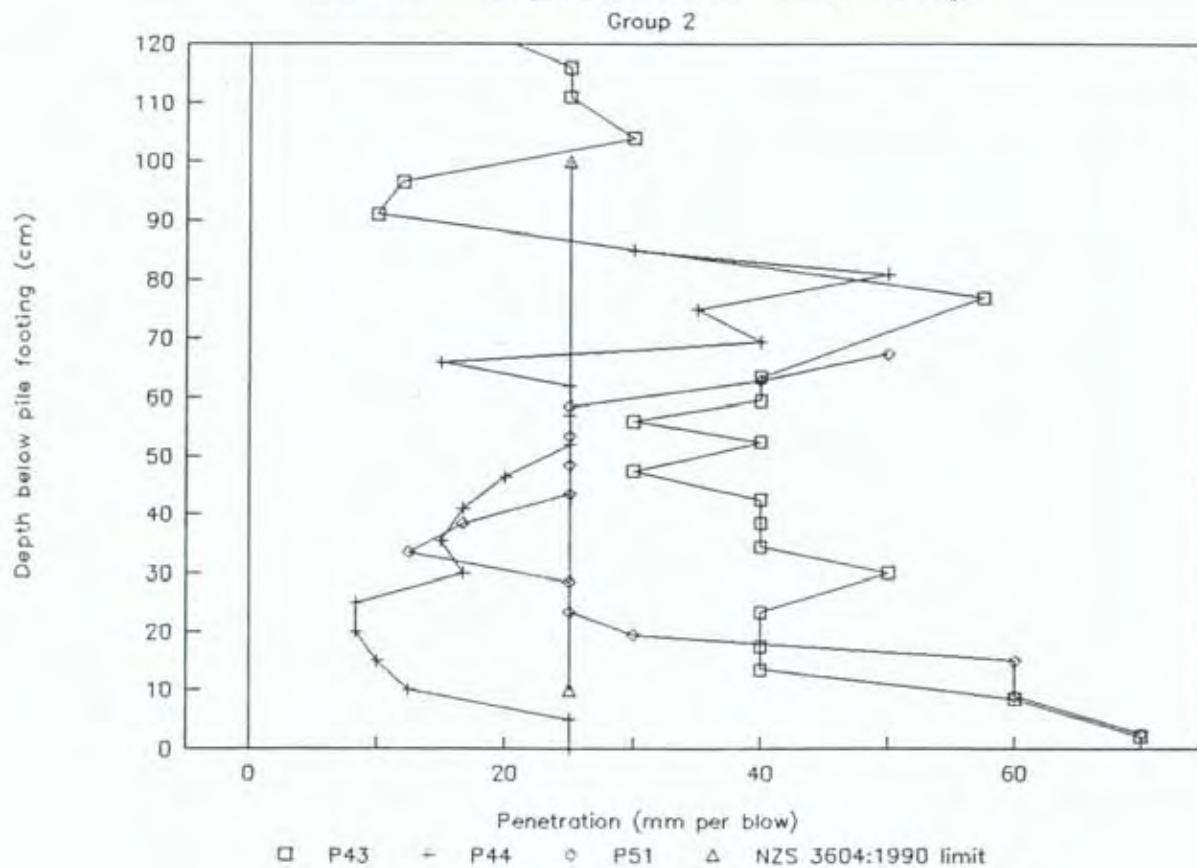
Pile J4: Group 1



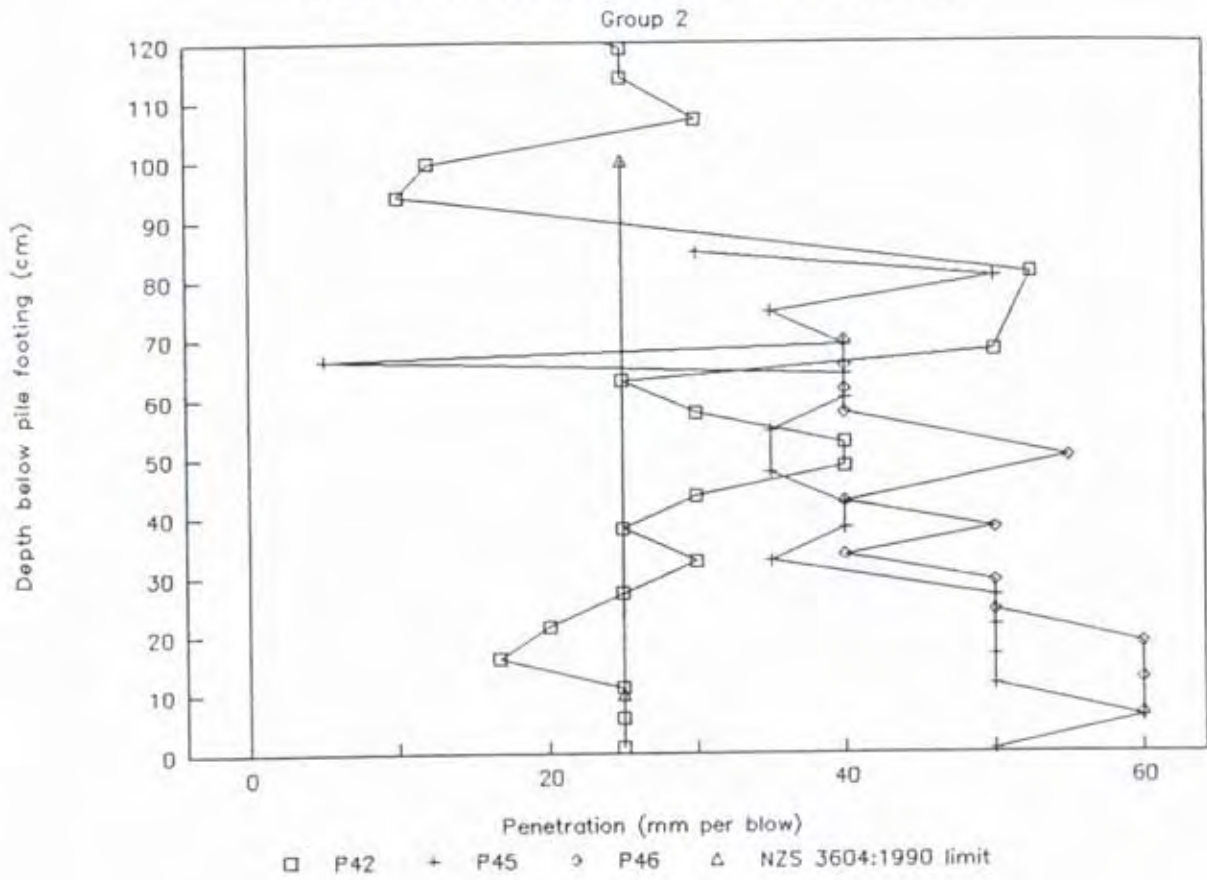
Scala Penetrometer Soundings



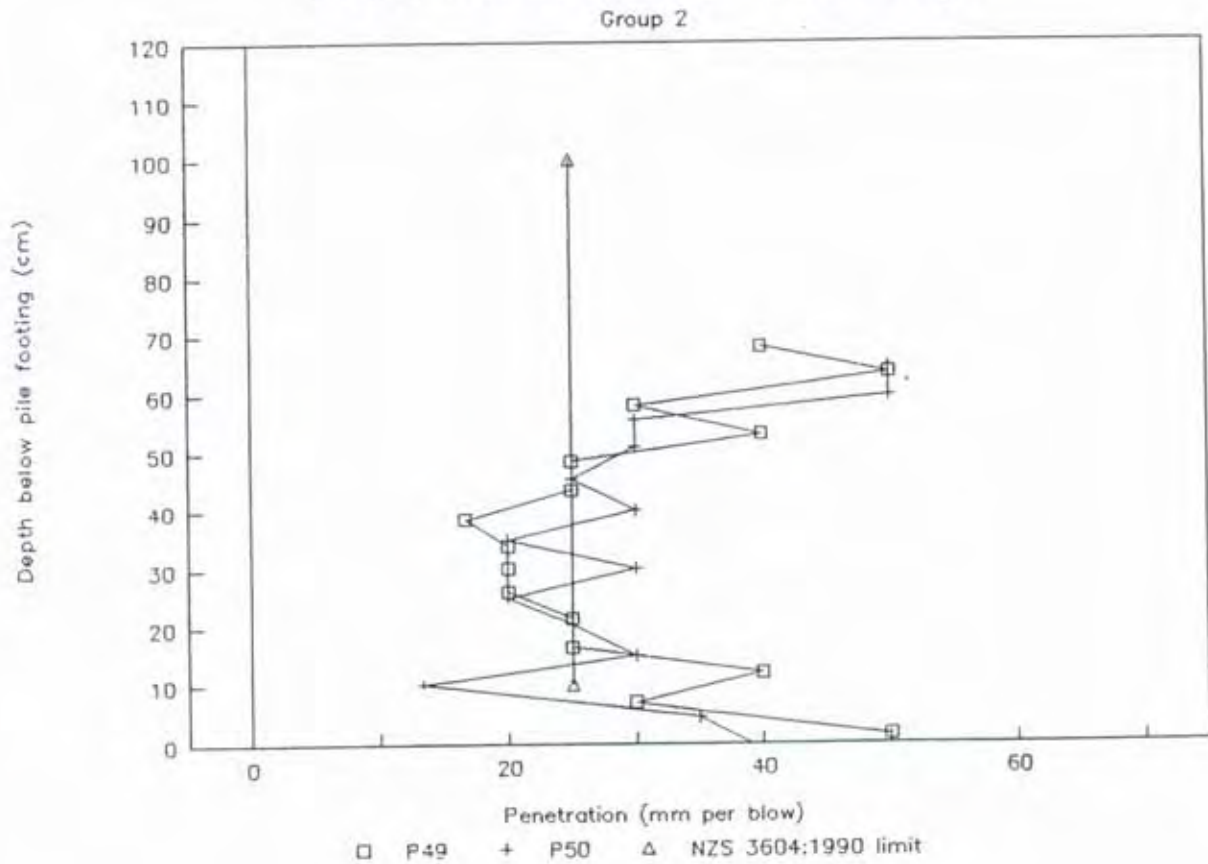
Scala Penetrometer Soundings



Scala Penetrometer Soundings

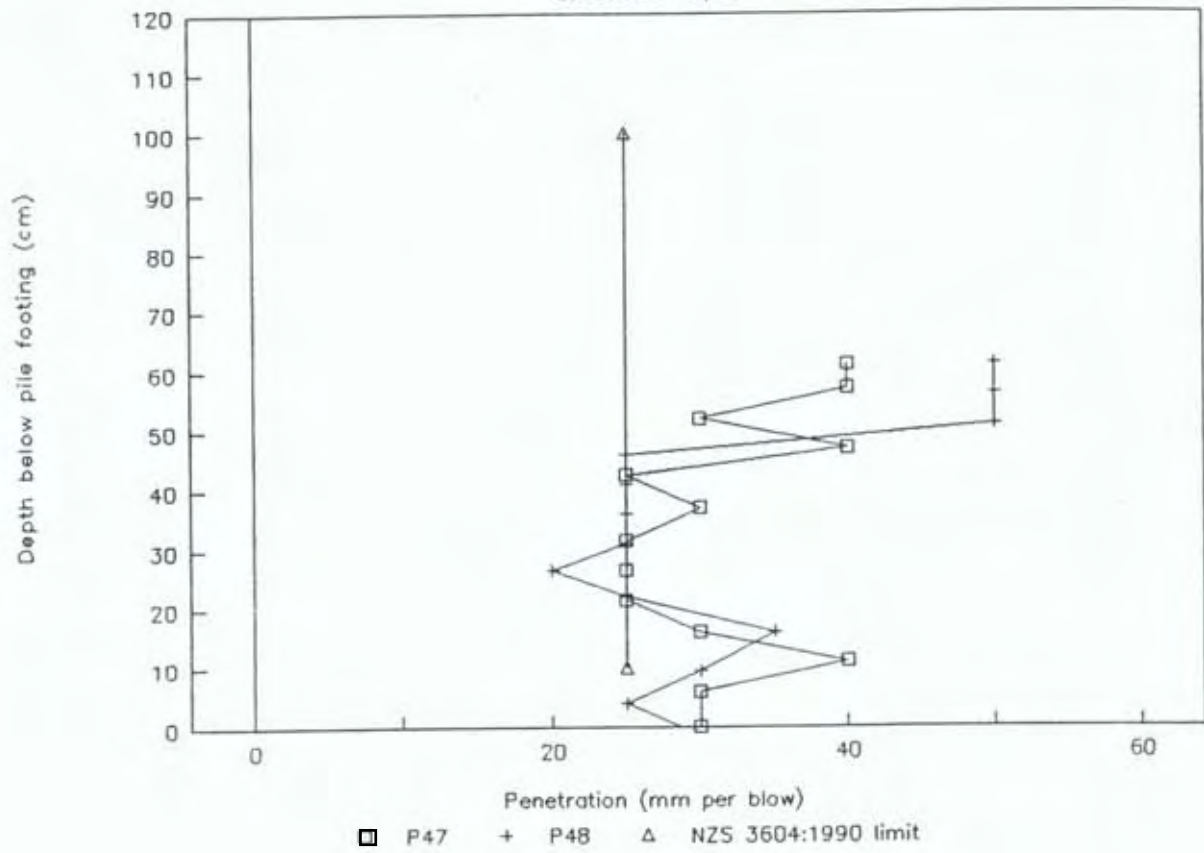


Scala Penetrometer Soundings



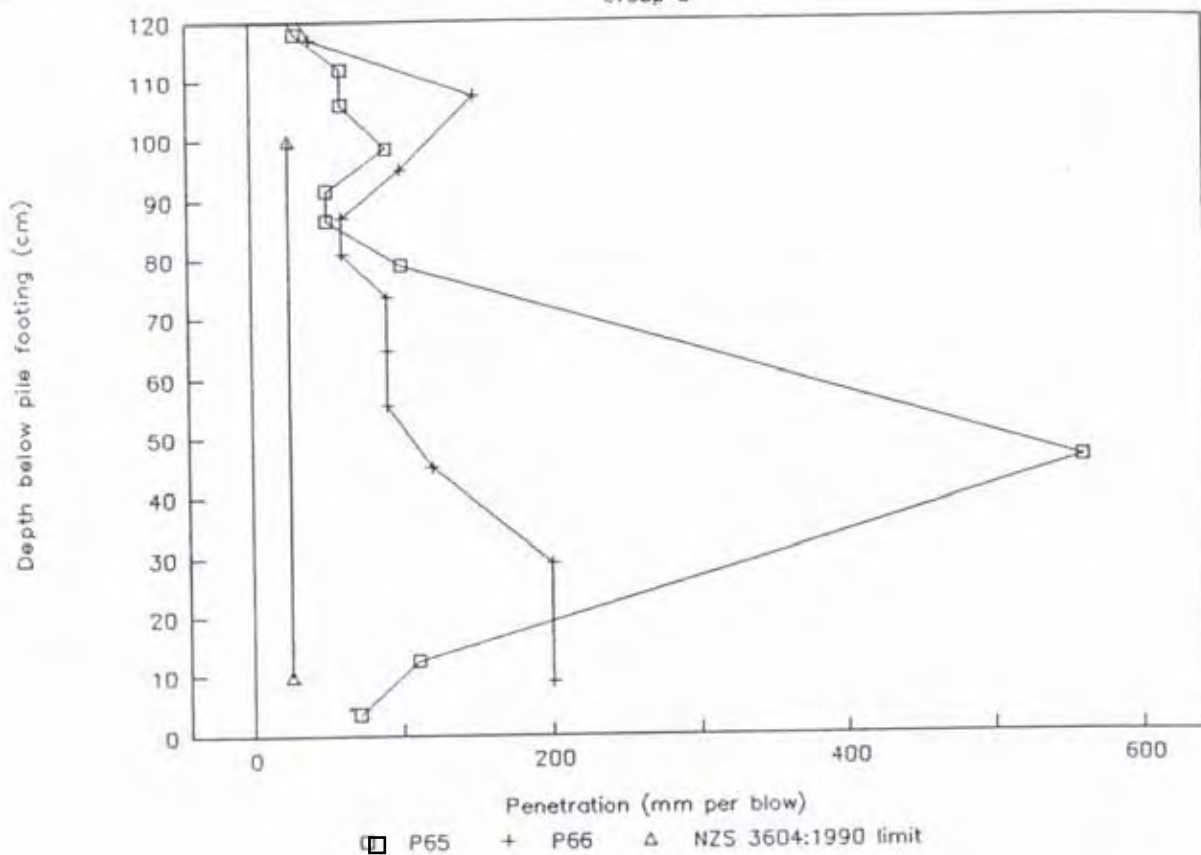
Scala Penetrometer Soundings

Location: Group 2



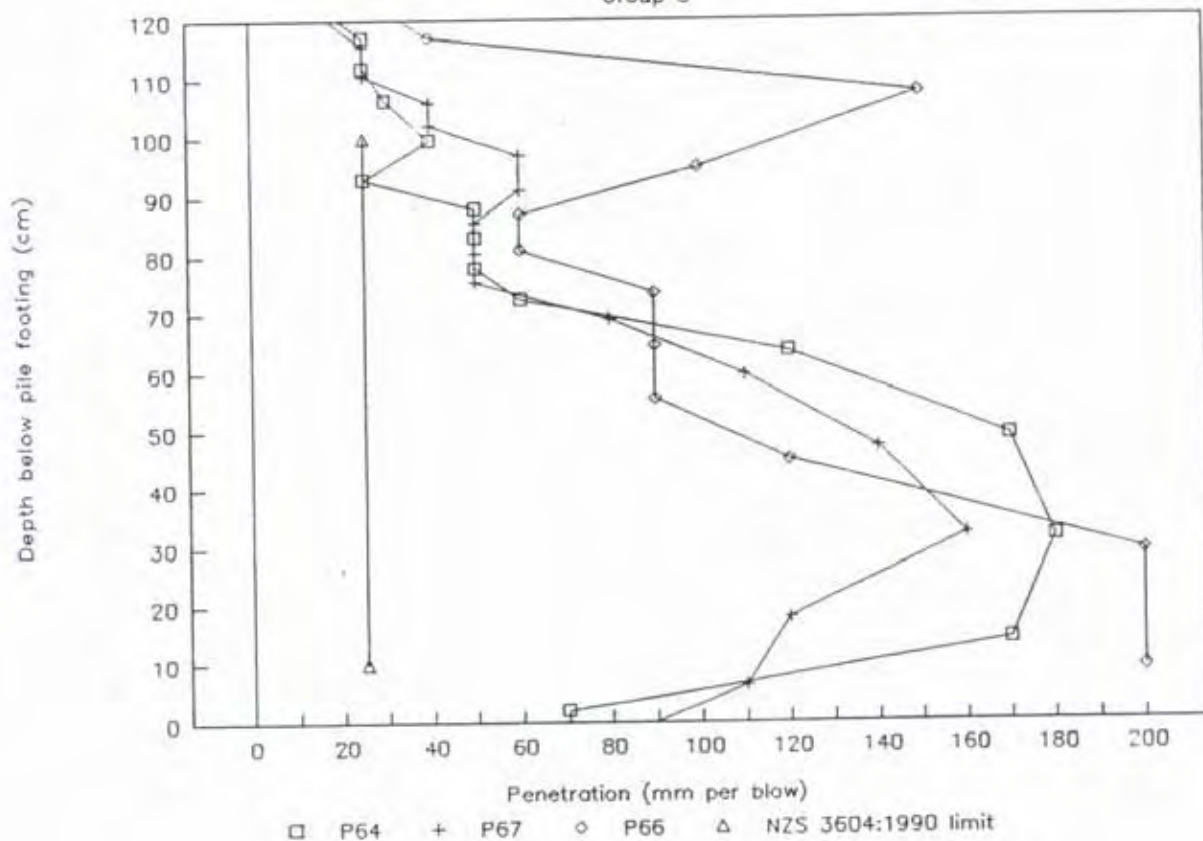
Scala Penetrometer Soundings

Group 3



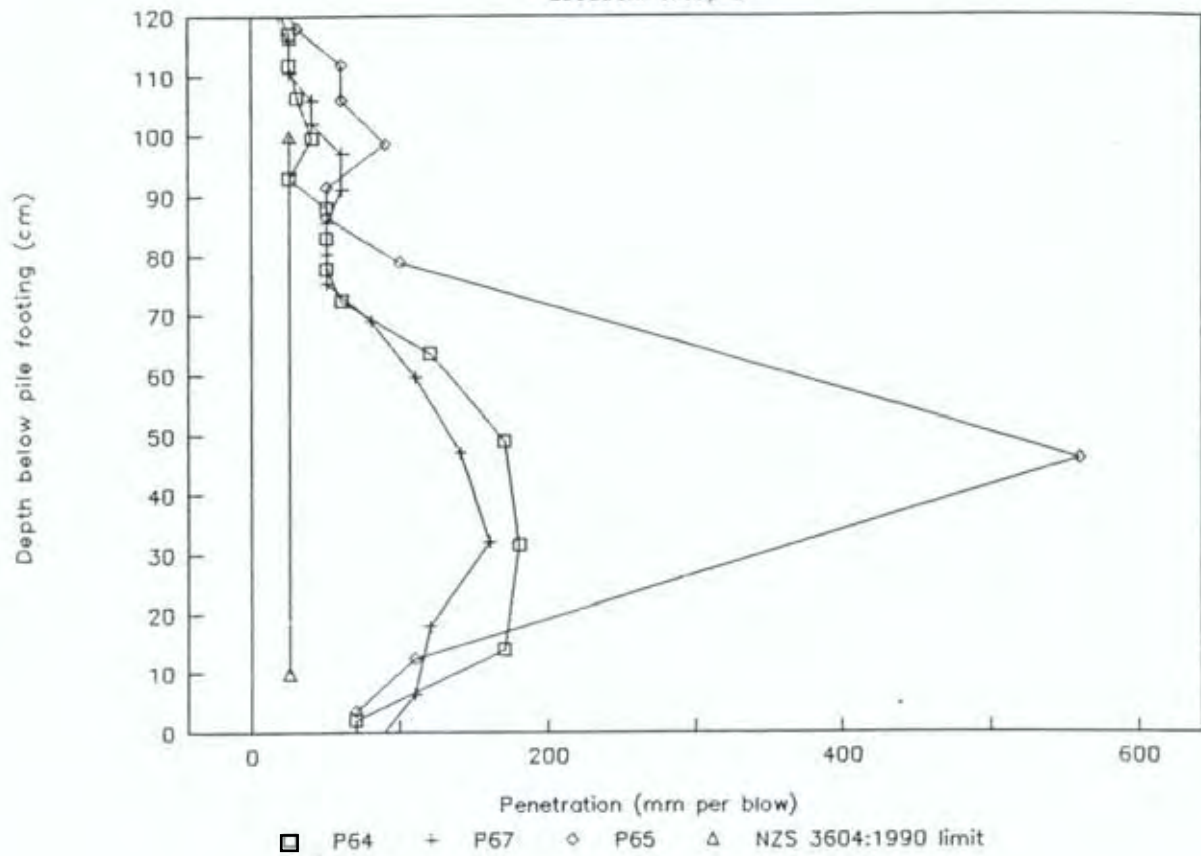
Scala Penetrometer Soundings

Group 3



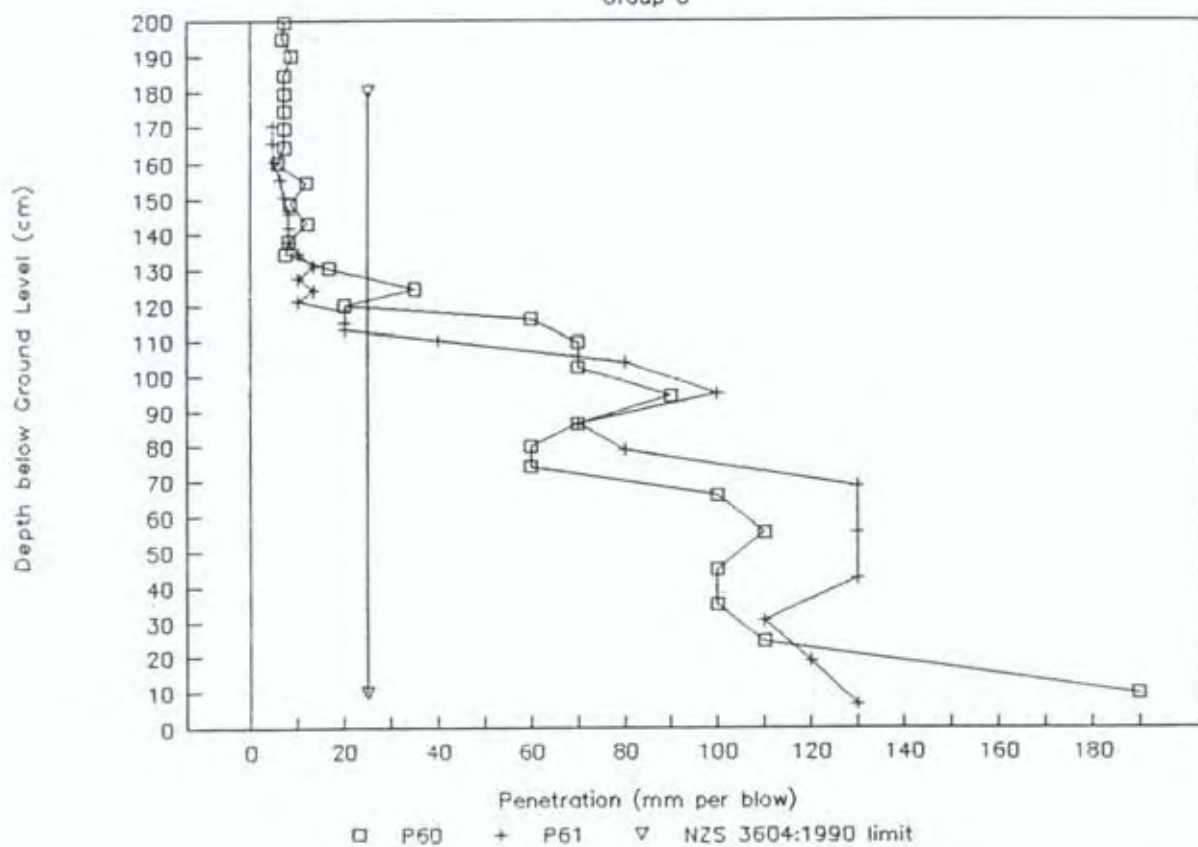
Scala Penetrometer Soundings

Location: Group 3

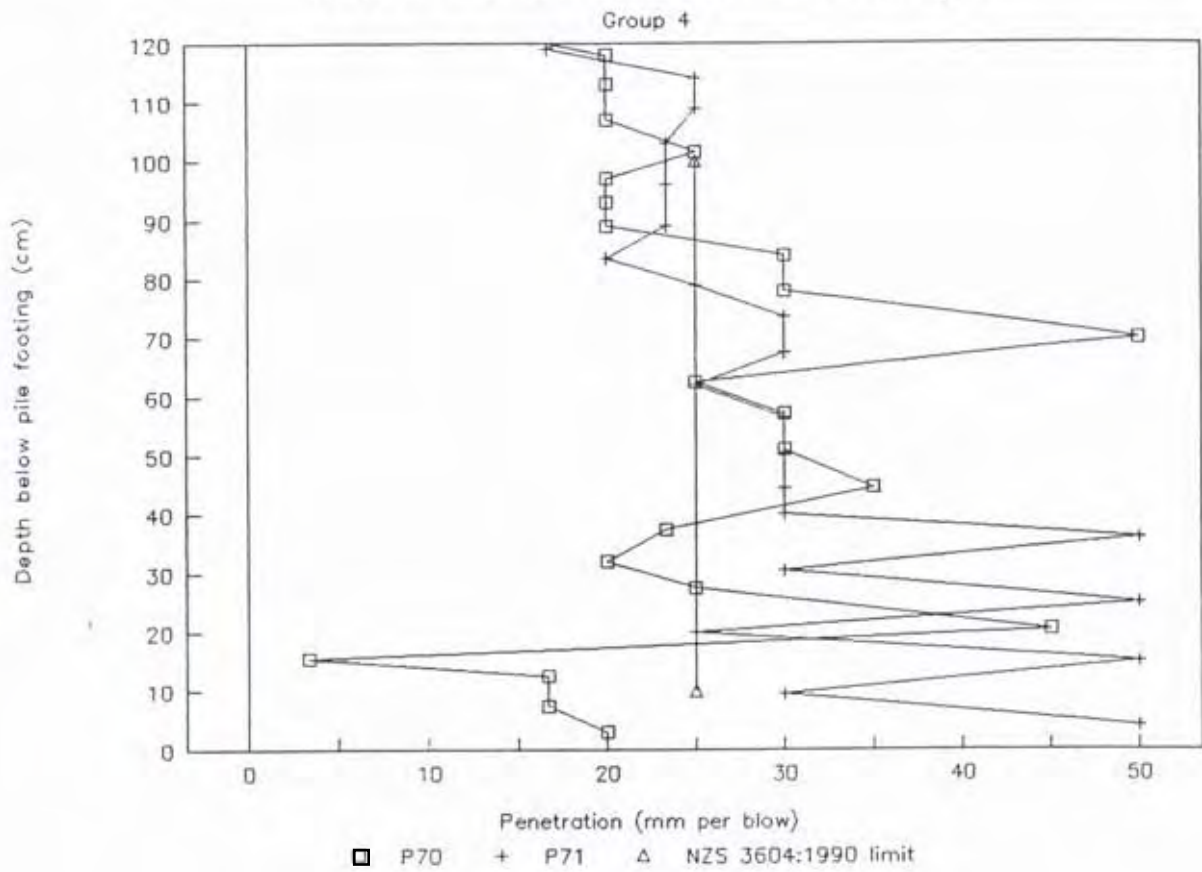


Scala Penetrometer Soundings

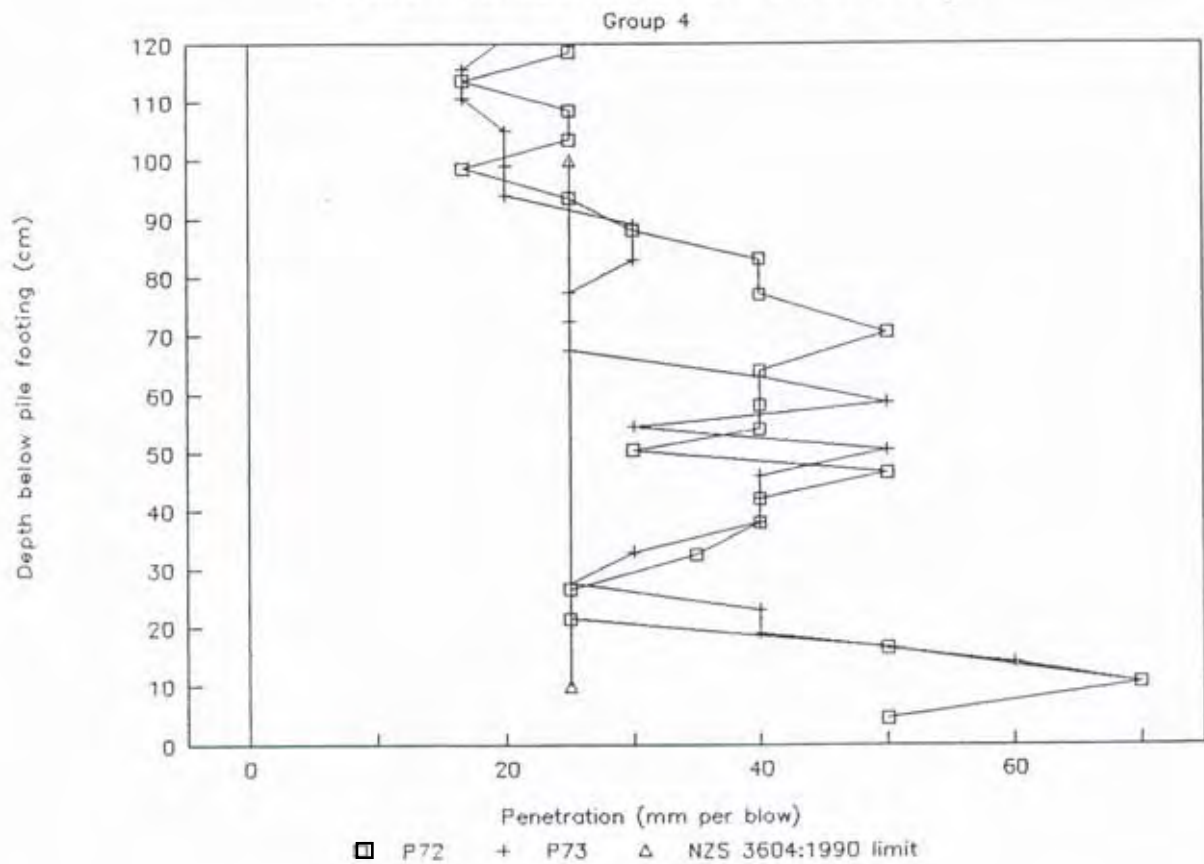
Group 3



Scala Penetrometer Soundings

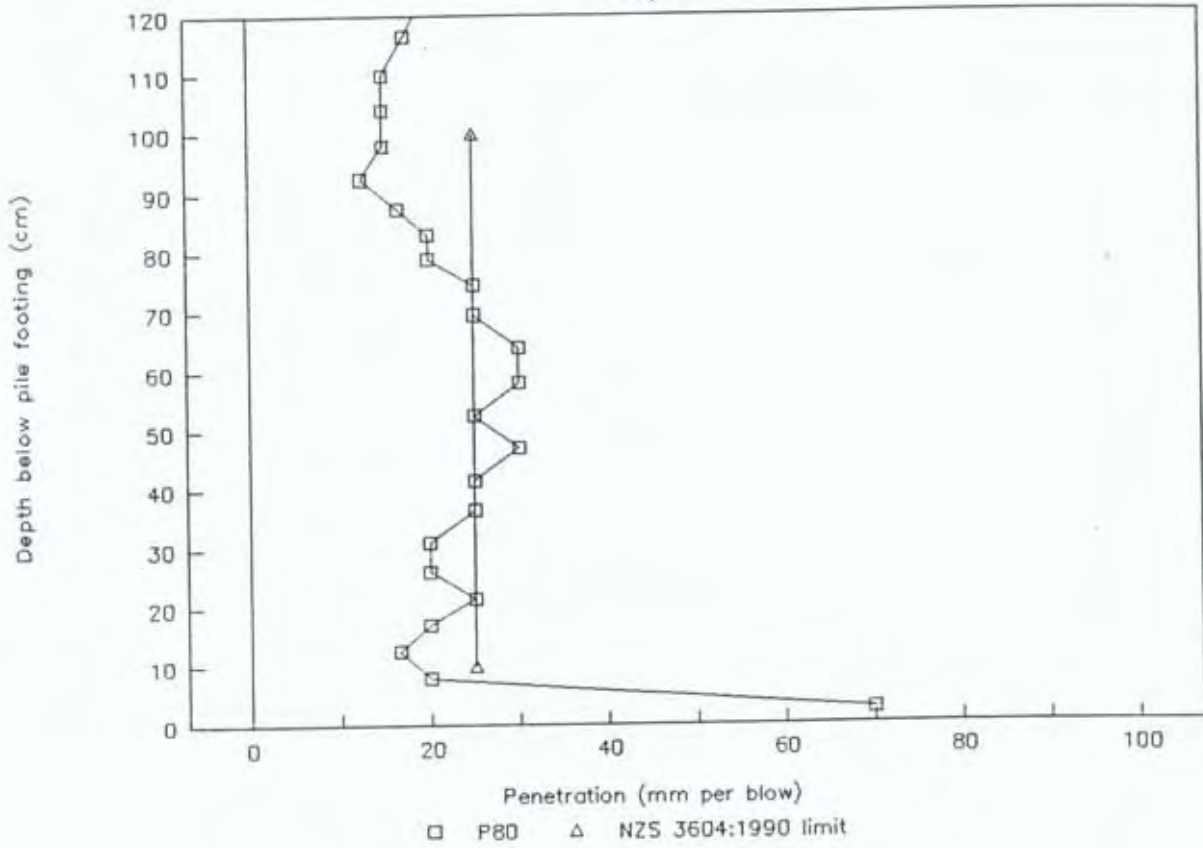


Scala Penetrometer Soundings



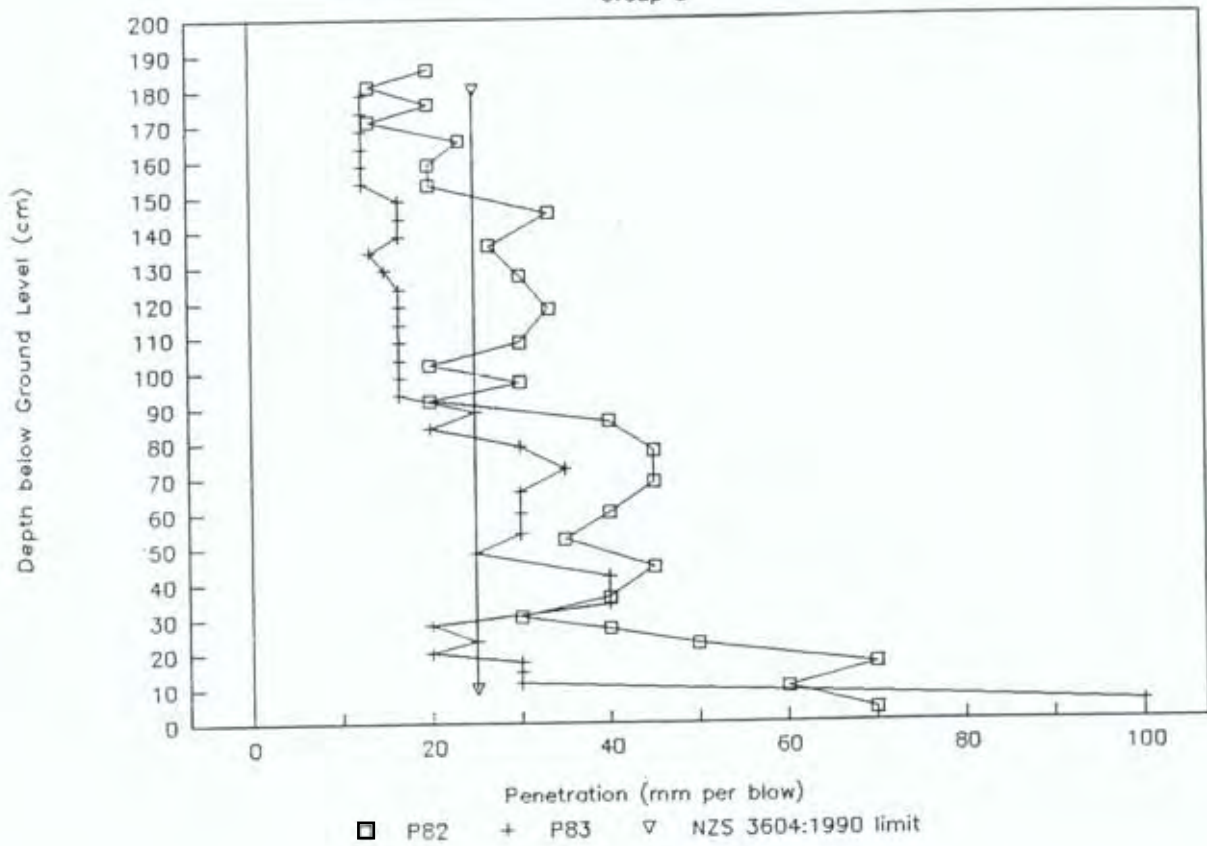
Scala Penetrometer Soundings

Group 5



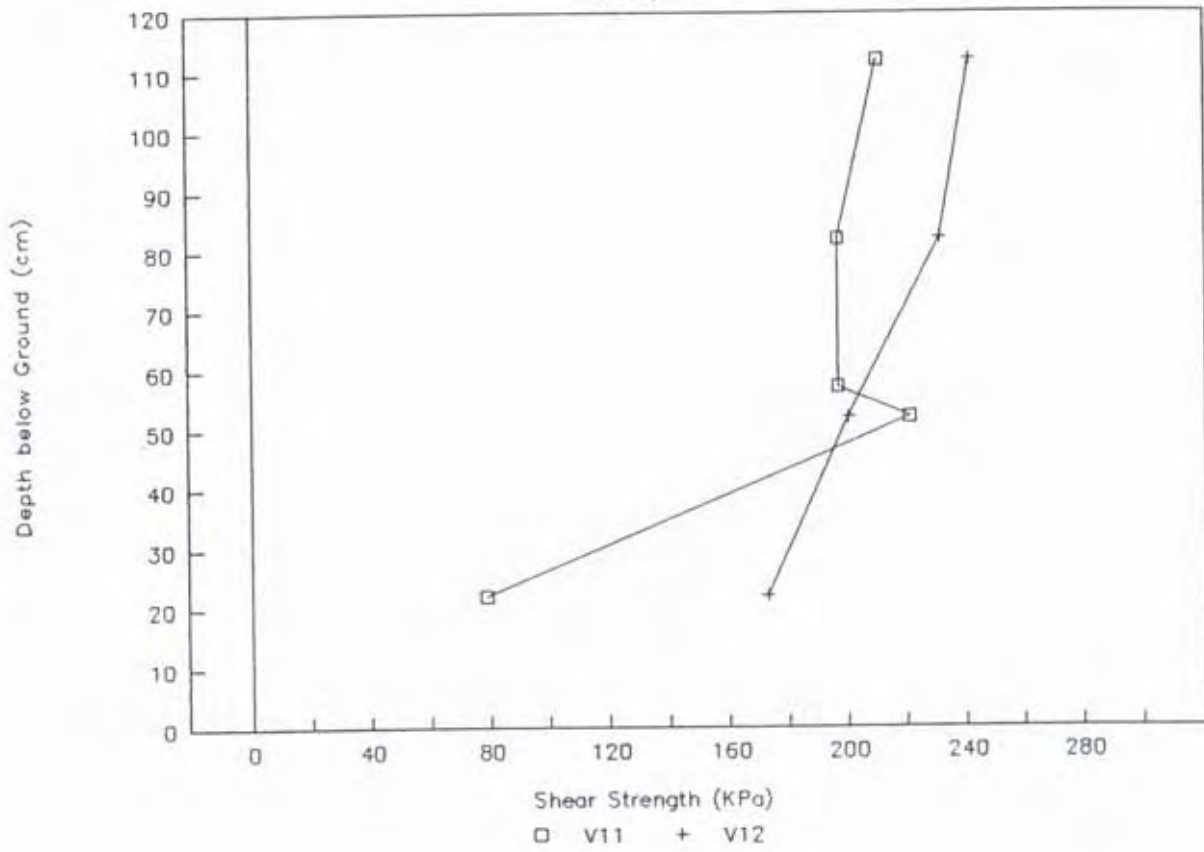
Scala Penetrometer Soundings

Group 5



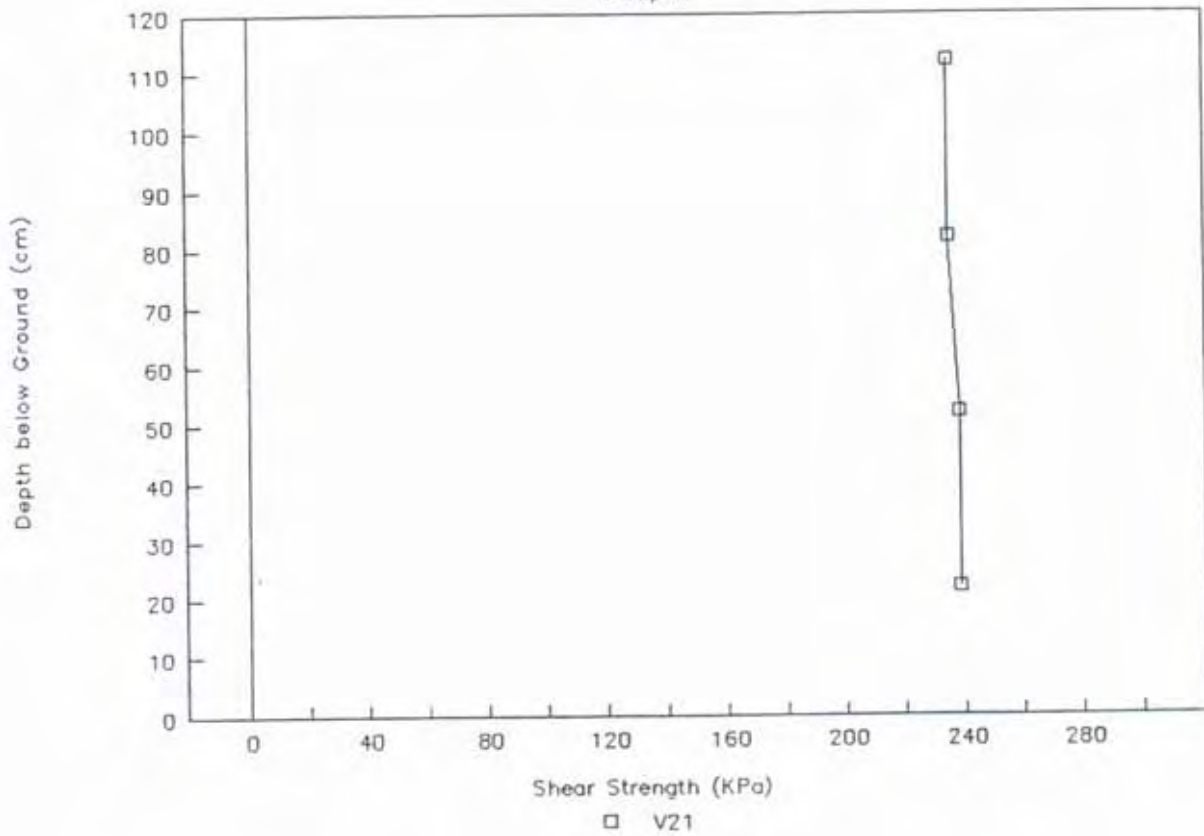
Shear Vane Tests

Group 1



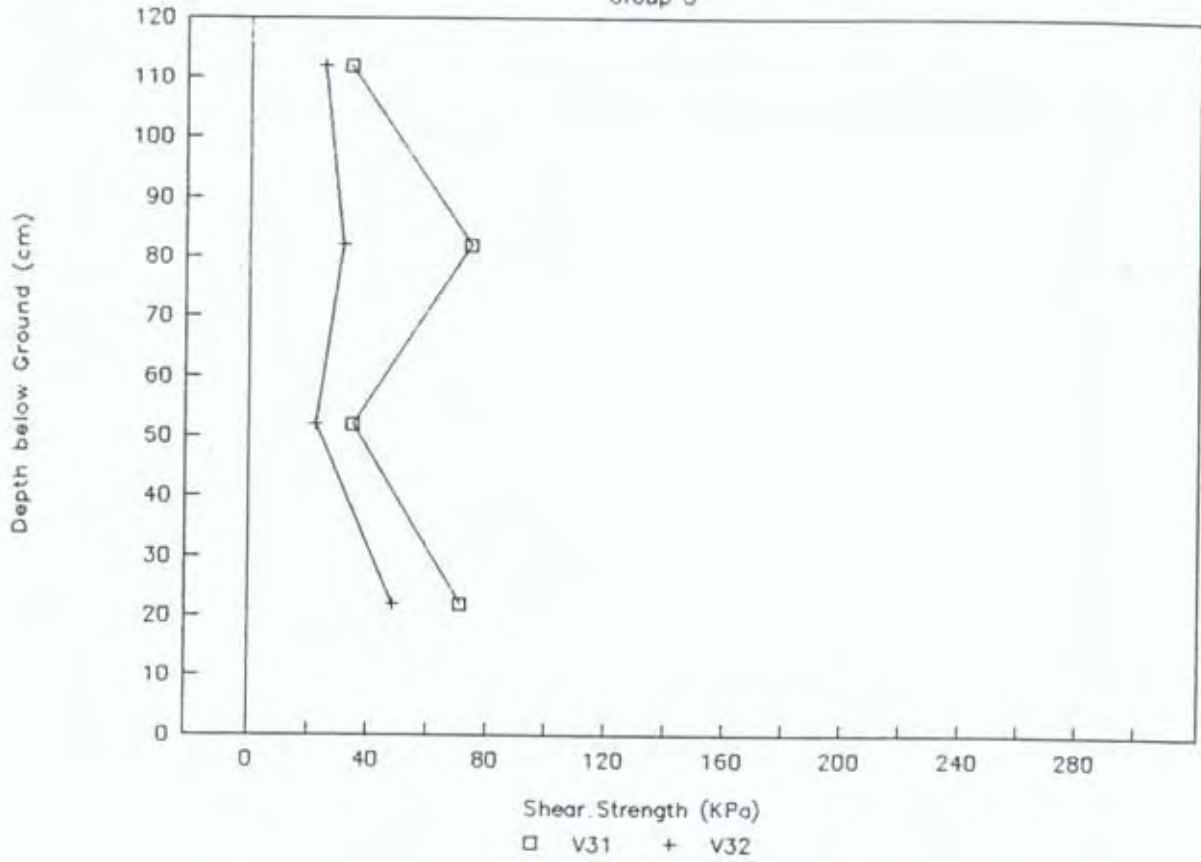
Shear Vane Tests

Group 2



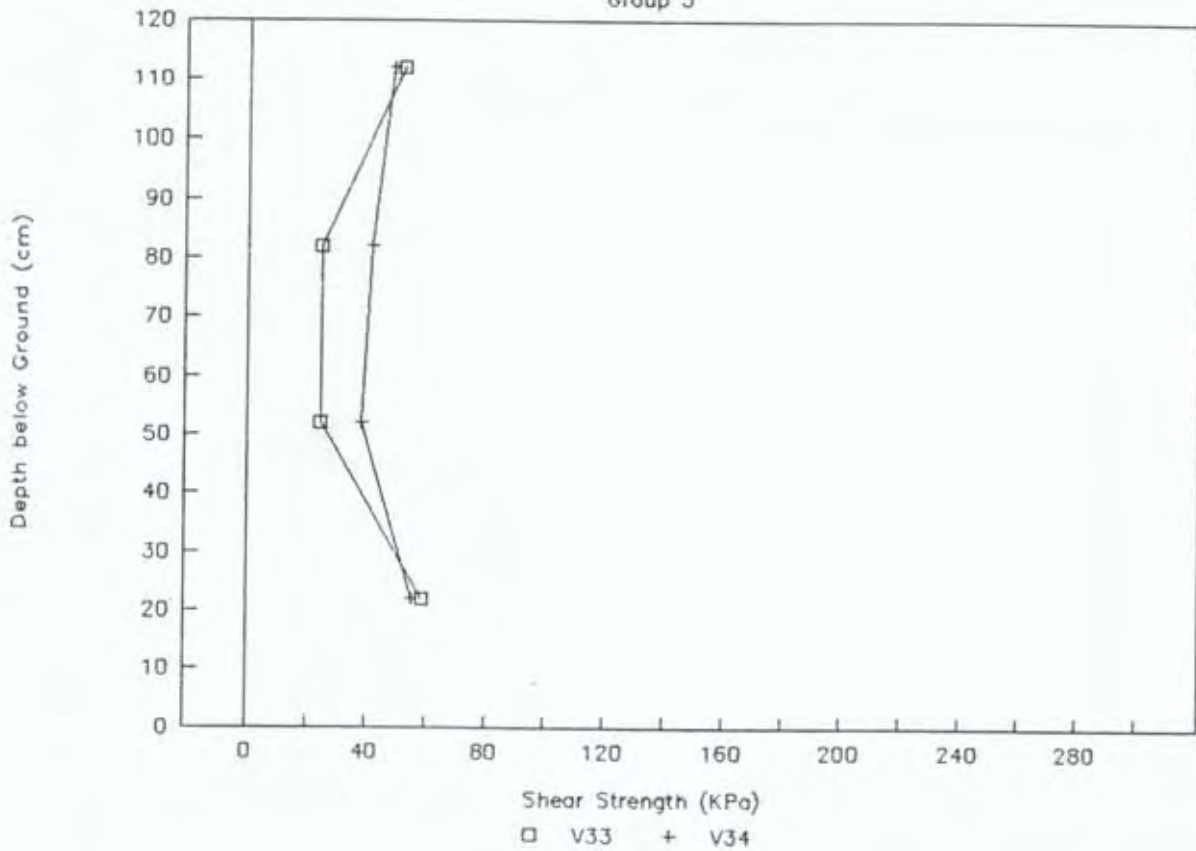
Shear Vane Tests

Group 3



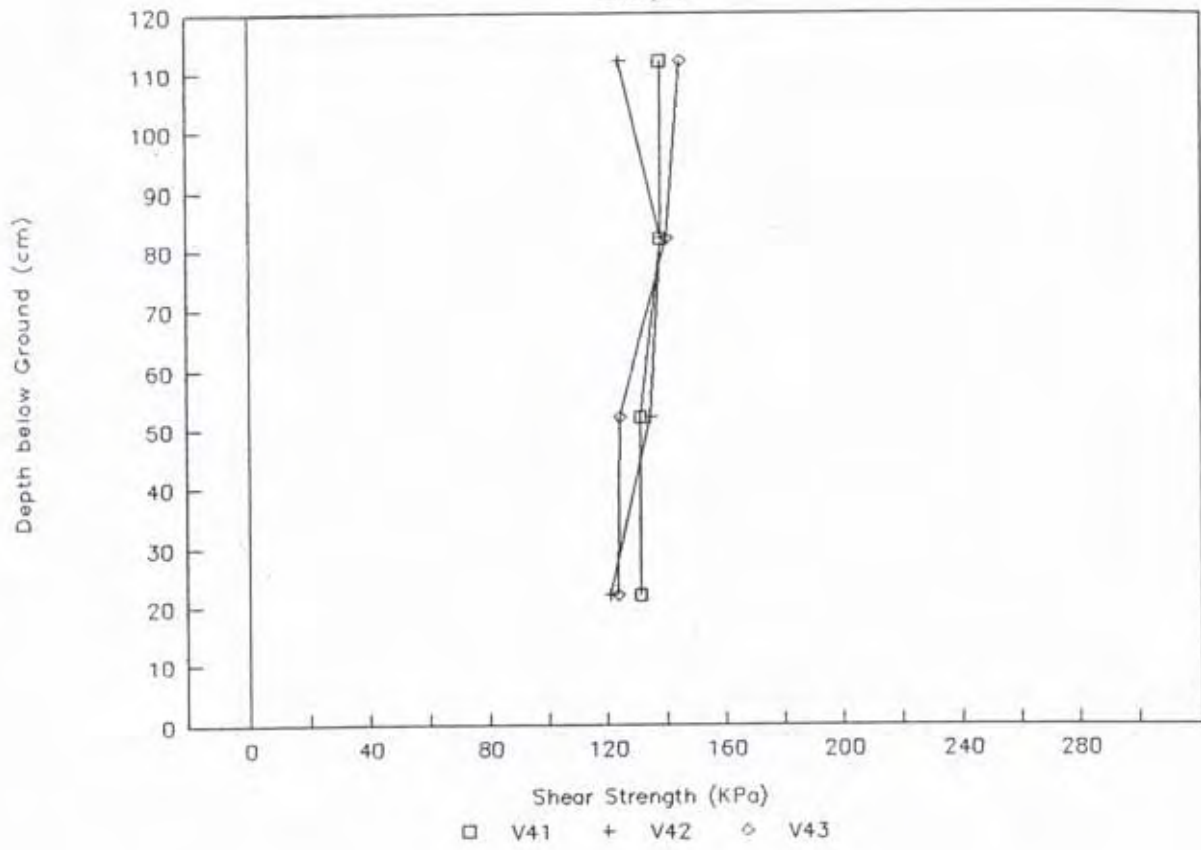
Shear Vane Tests

Group 3



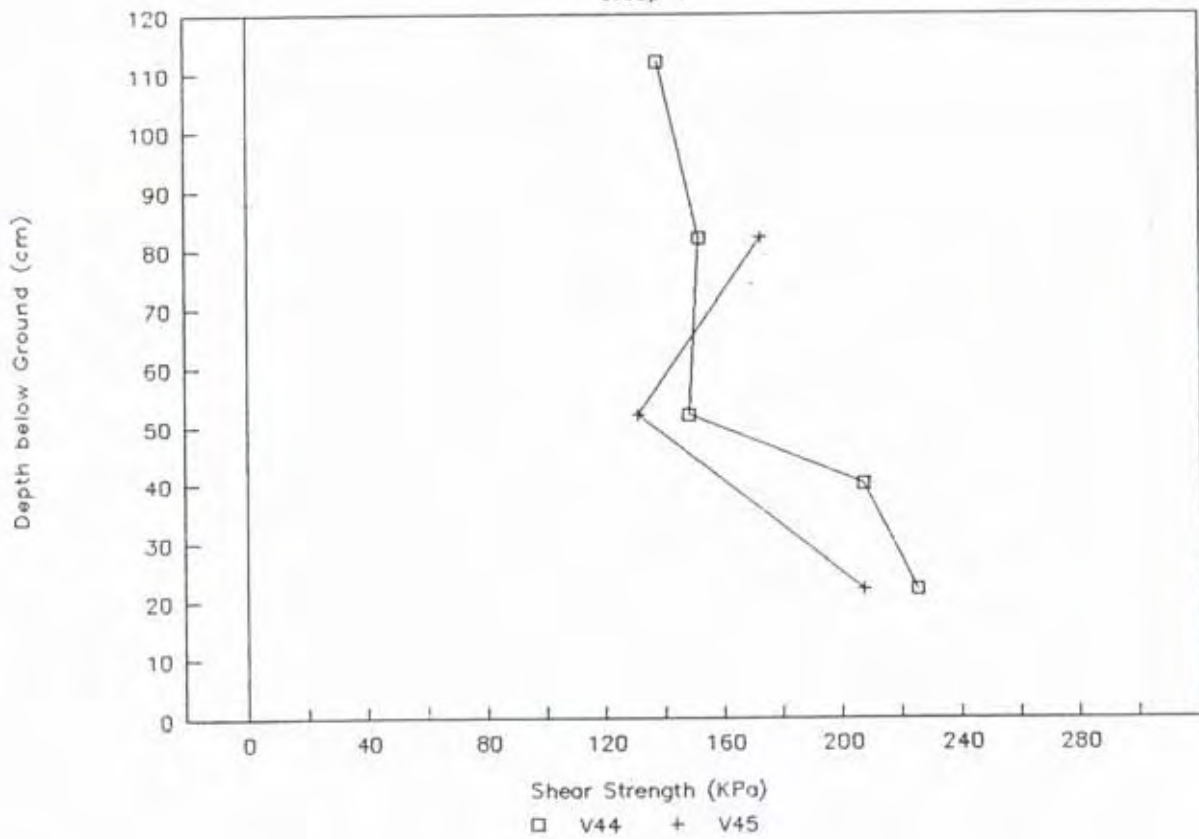
Shear Vane Tests

Group 4



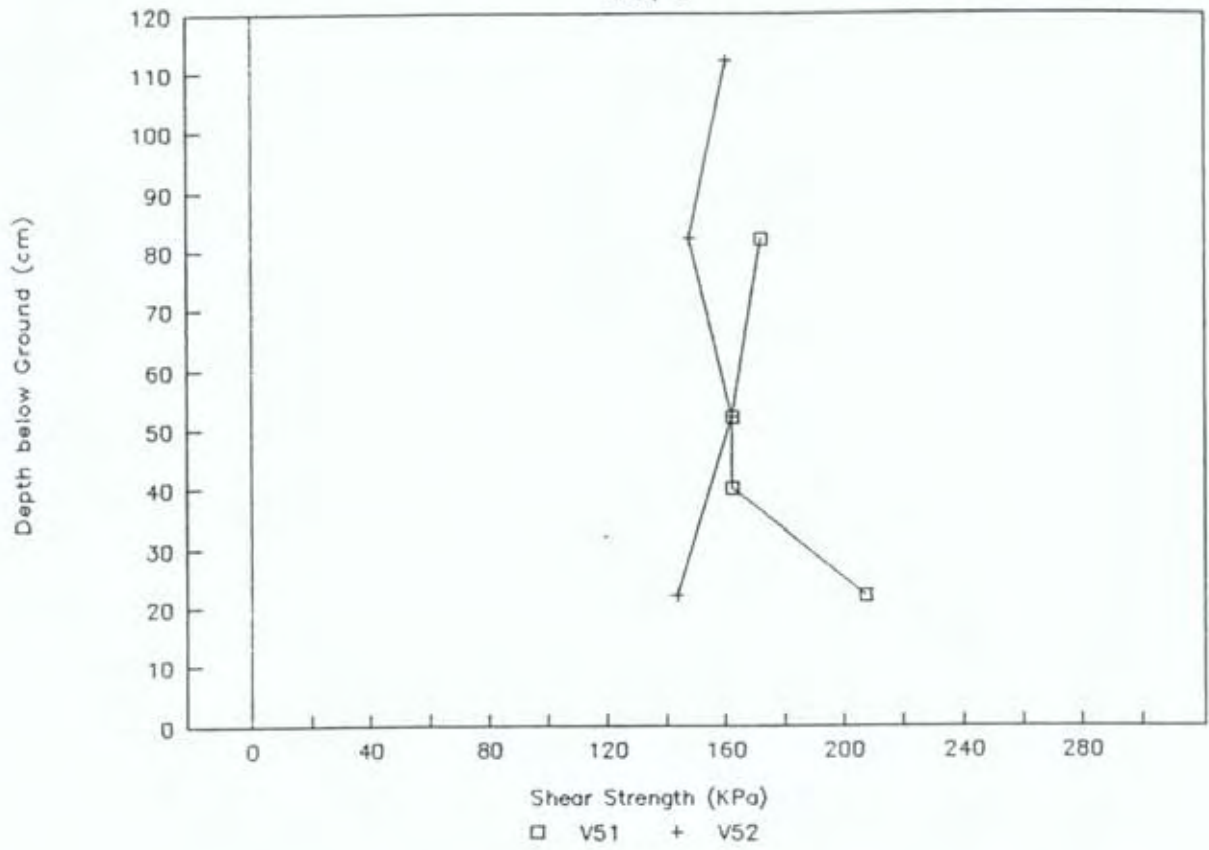
Shear Vane Tests

Group 4



Shear Vane Tests

Group 5



Appendix G Proprietary Products Used

Three proprietary sheathings were used in the experimental programme described in this report and are referred to as Type PLB, PY or TX. These products are defined below:

Type TX was a nominal 7.5 mm thick pink smooth-faced fibre-cement Harditex sheet with a measured thickness of 7.9 mm and density of 11.3 kg/sq. m.

Type TL connectors were PB2100 Timberlink 12 kN pile connectors as described in BRANZ Appraisal Certificate No. 187 1990. Twelve 35 x 3.55 mm diameter dome-head nails were used in each plate into the pile and an additional 4 nails were used in each plate flange and 4 in the plate tongue to fasten the connector to the bearer.

Note: Results obtained in this study relate only to the samples tested, and not to any other item of the same or similar description. BRANZ does not necessarily test all brands or types available within the class of items tested and exclusion of any brand or type is not to be taken as any reflection on it.

This work was carried out for specific research purposes, and BRANZ may not have assessed all aspects of the products named which would be relevant in any specific use. For this reason, BRANZ disclaims all liability for any loss or other deficit, following use of the named products, which is claimed to be reliance on the results published here.

Further, the listing of any trade or brand names above does not represent endorsement of any named product nor imply that it is better or worse than any other available product of its type. A laboratory test may not be exactly representative of the performance of the item in general use.



BRANZ MISSION

To be the leading resource for the development of the building and construction industry.

HEAD OFFICE AND RESEARCH CENTRE

Moonshine Road, Judgeford
Postal Address - Private Bag 50908, Porirua
Telephone - (04) 235-7600, FAX - (04) 235-6070

REGIONAL ADVISORY OFFICES

AUCKLAND

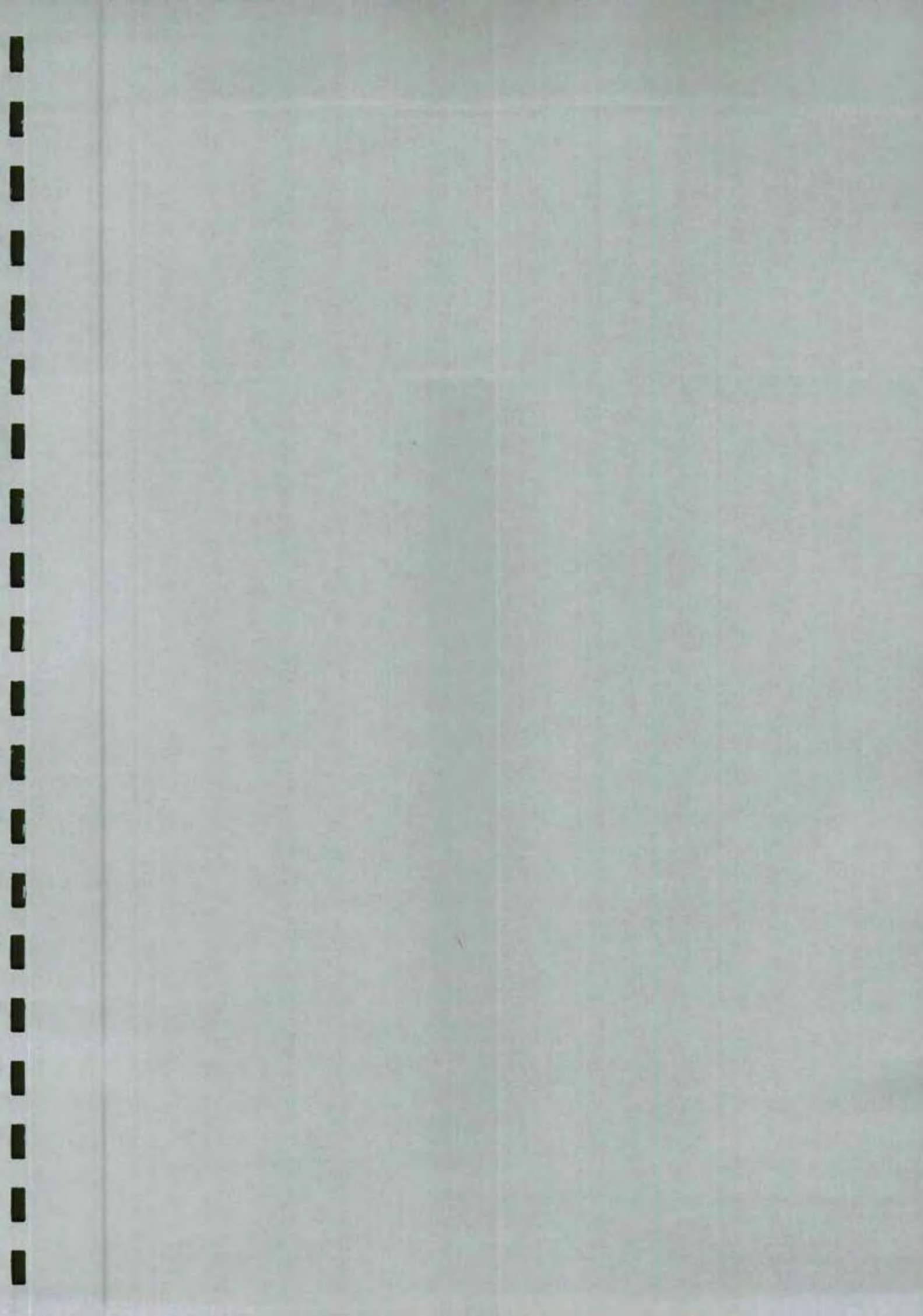
Telephone - (09) 526 4880
FAX - (09) 526 4881
419 Church Street, Penrose
PO Box 112-069, Penrose

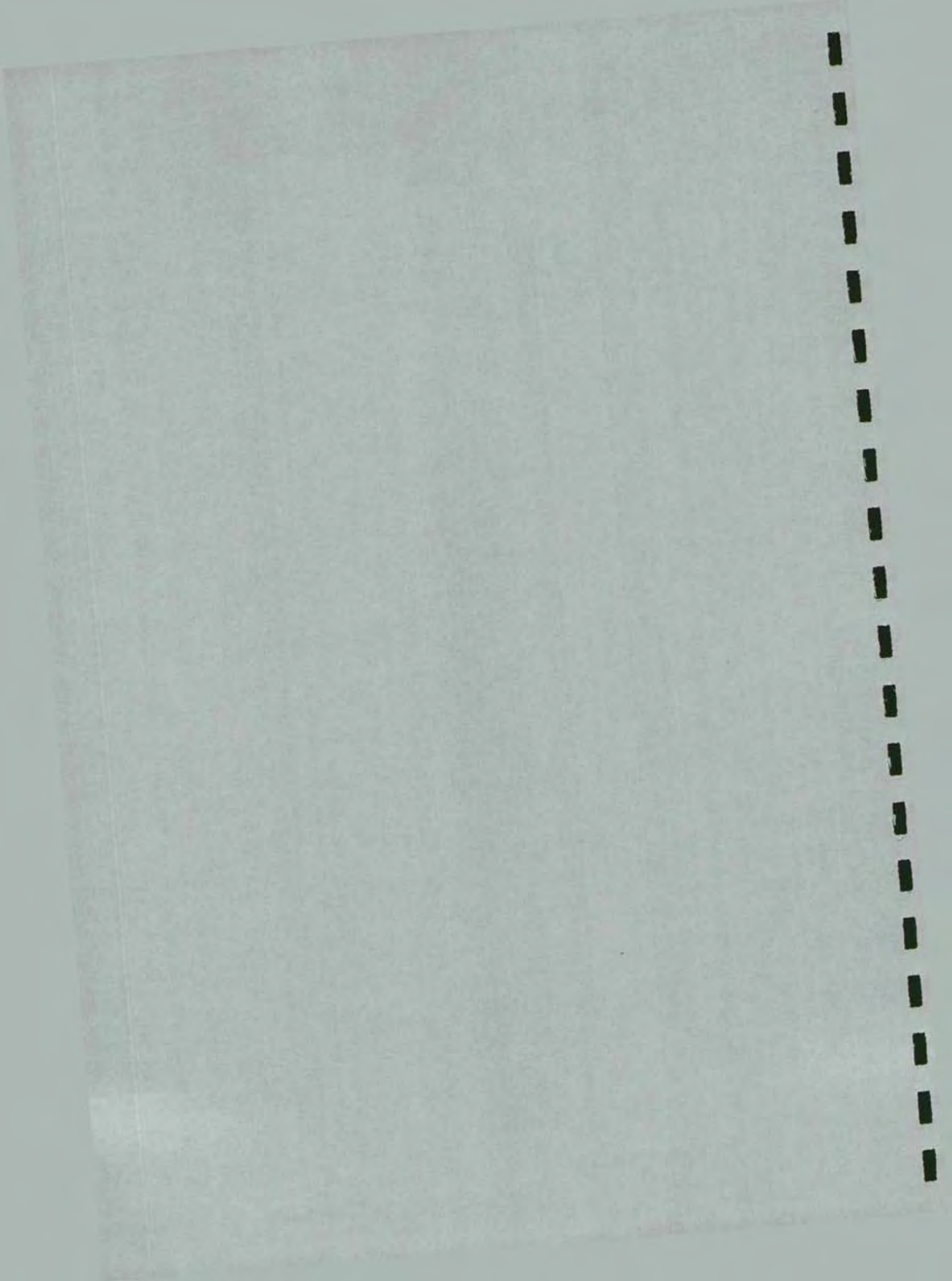
WELLINGTON

Telephone - (04) 235-7600
FAX - (04) 235-6070
Moonshine Road, Judgeford

CHRISTCHURCH

Telephone - (03) 366-3435
FAX (03) 366-8552
GRE Building
79-83 Hereford Street
PO Box 496





STUDY REPORT

No.58 (1996)

Appendix H

Appendix H Test Hysteresis Loops

H.1 Introduction

This Appendix contains all the load versus deflection hysteresis plots measured as part of the research project for BRANZ Study Report 58. For space reasons it is presented as a separate volume to Study Report 58 as the interest in the data will be largely limited to researchers wishing to re-analyse the data.

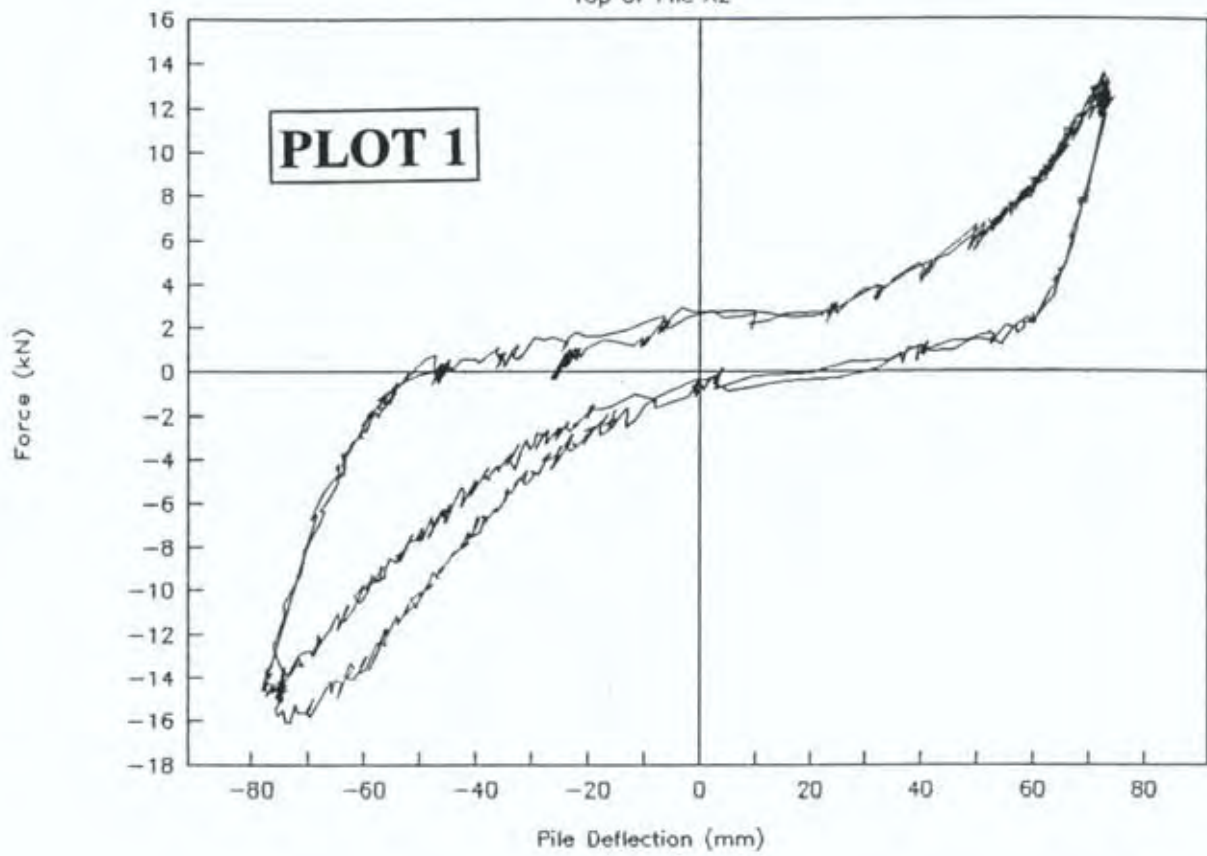
Table H.1 relates the plot numbers to the type of pile tested, pile location and soil type. Locations of applied load and measured deflections are fully described in Section 4 of the main study report. The actual location on the pile where the measurements were taken (eg top, bottom, bearer, etc.) are given in the plot titles.

Table H.1 Relationship Between Plot Number and Test Details

From Plot Number	To Plot Number	Pile Type	Soil Type	Group Number	Pile Labels	Test Date
1	2	Braced	Clay	1	A1-A2	1/12/93
4	5	Braced	Clay	1	A4-A5	1/12/93
6	7 & 11	Braced	Clay	1	D1-E1	9/12/93
8	10 & 12	Braced	Clay	1	I1-J1	9/12/93
13	20	Anchor	Clay	1	J3-J4	10/12/93
21	27	Braced	Clay	1	J1-J2	14/12/93
28	29	Braced	Clay	1	G1-G2	15/12/93
30	34	Braced	Clay	1	G3-G4	15/12/93
35	38	Anchor	Clay	2	V13-W13	4/2/94
39	42	Anchor	Clay	2	V10-W10	4/2/94
43	49	Braced	Clay	2	X13-Y13	7/2/94
50	56	Braced	Clay	2	X10-Y10	9/2/94
57	62	Shear	Clay	2	T13-U13	9/2/94
63	68	Shear	Clay	2	T10-U10	10/2/94
69	75	Shear	Clay	1	E2-H2	20/12/94
76	79	Driven	Peat	3	I50-J50	14/2/94
80	93	Driven	Peat	3	I51-J51	14/2/94
84	85	Anchor	Peat	3	H51	14/2/94
86	87	Anchor	Peat	3	H50	14/2/94
88	91	Shear	Peat	3	F50-G50	15/2/94
92	95	Shear	Peat	3	F51-G51	15/2/94
96	99	Anchor	Sandy-silt	4	M1-M2	15/2/94
100	103	Anchor	Sandy-silt	4	M3-M4	15/2/94
104	109	Shear	Sandy-silt	4	M5-M6	15/2/94
110	113	Anchor	Sand	5	P1-P2	16/2/94
114	117	Shear	Sand	5	P3-P4	16/2/94

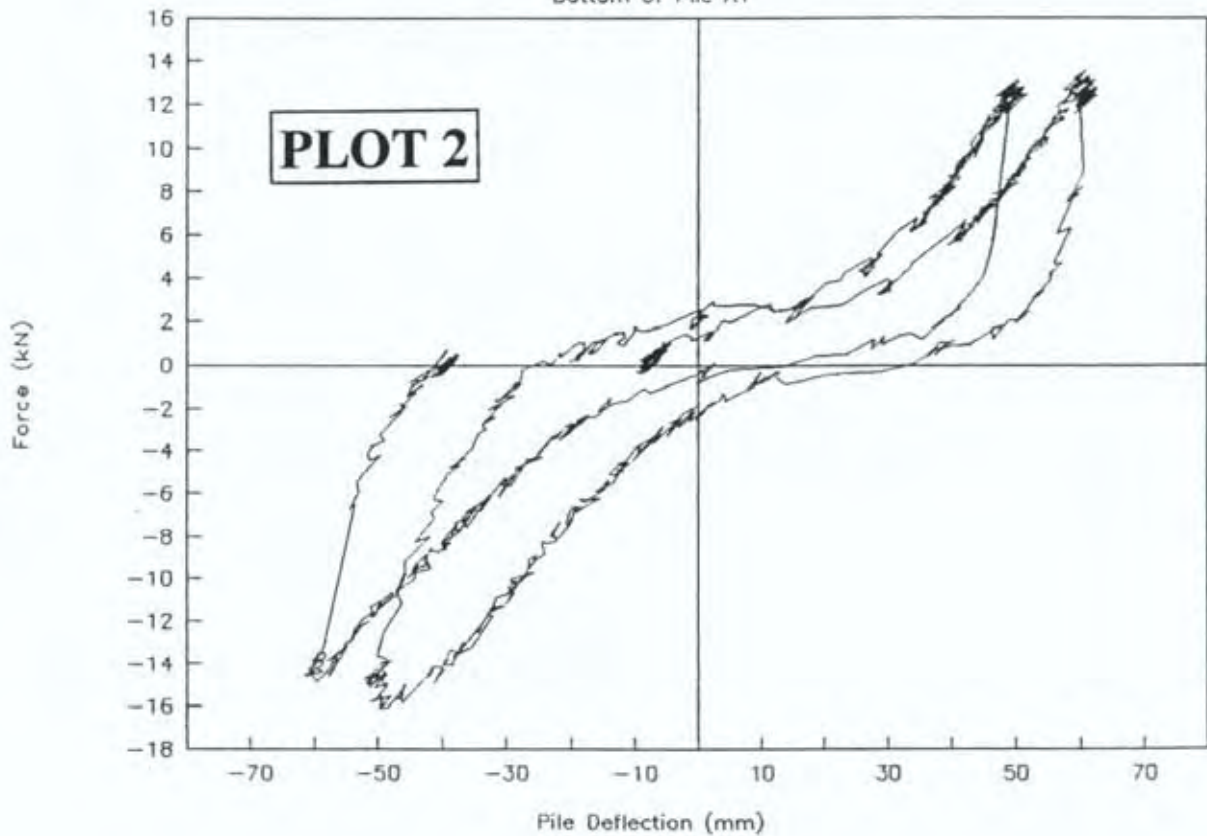
Braced Piles A1-A2 Group 1

Top of Pile A2



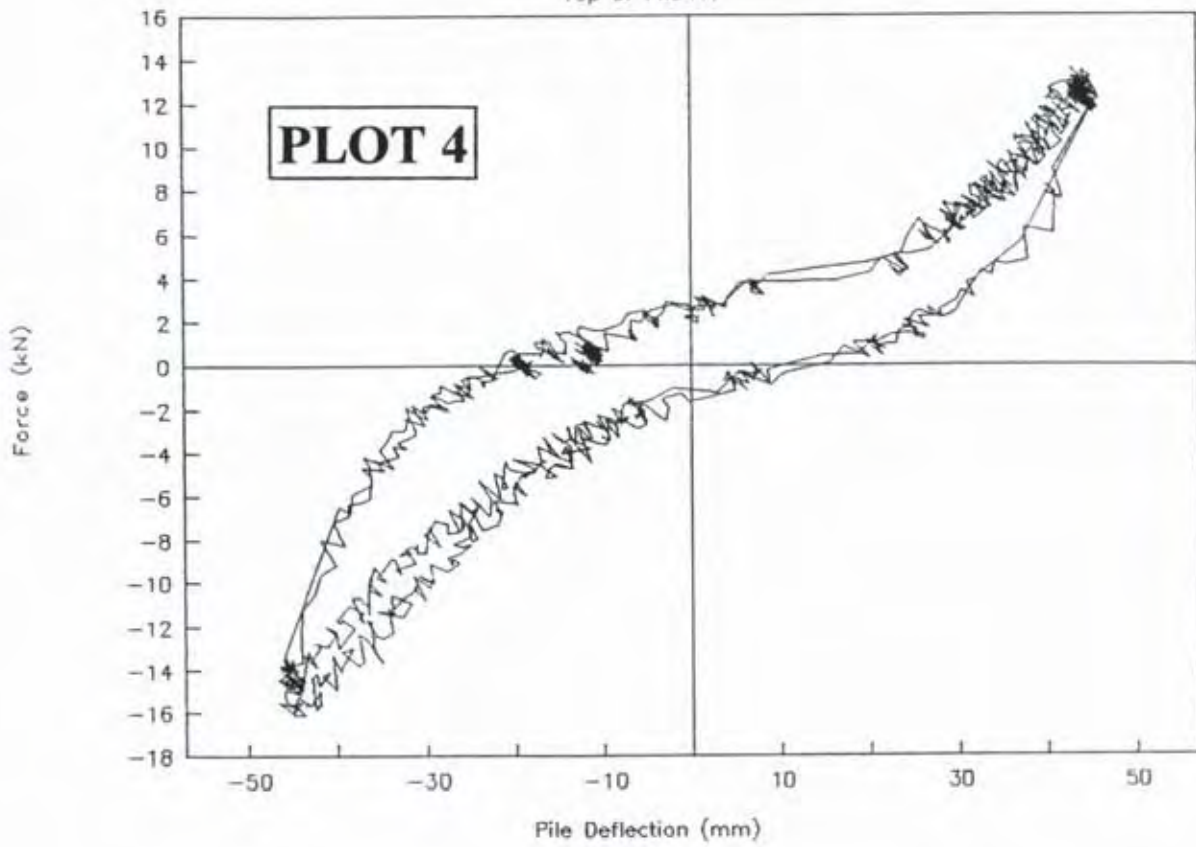
Braced Piles A1-A2 Group 1

Bottom of Pile A1



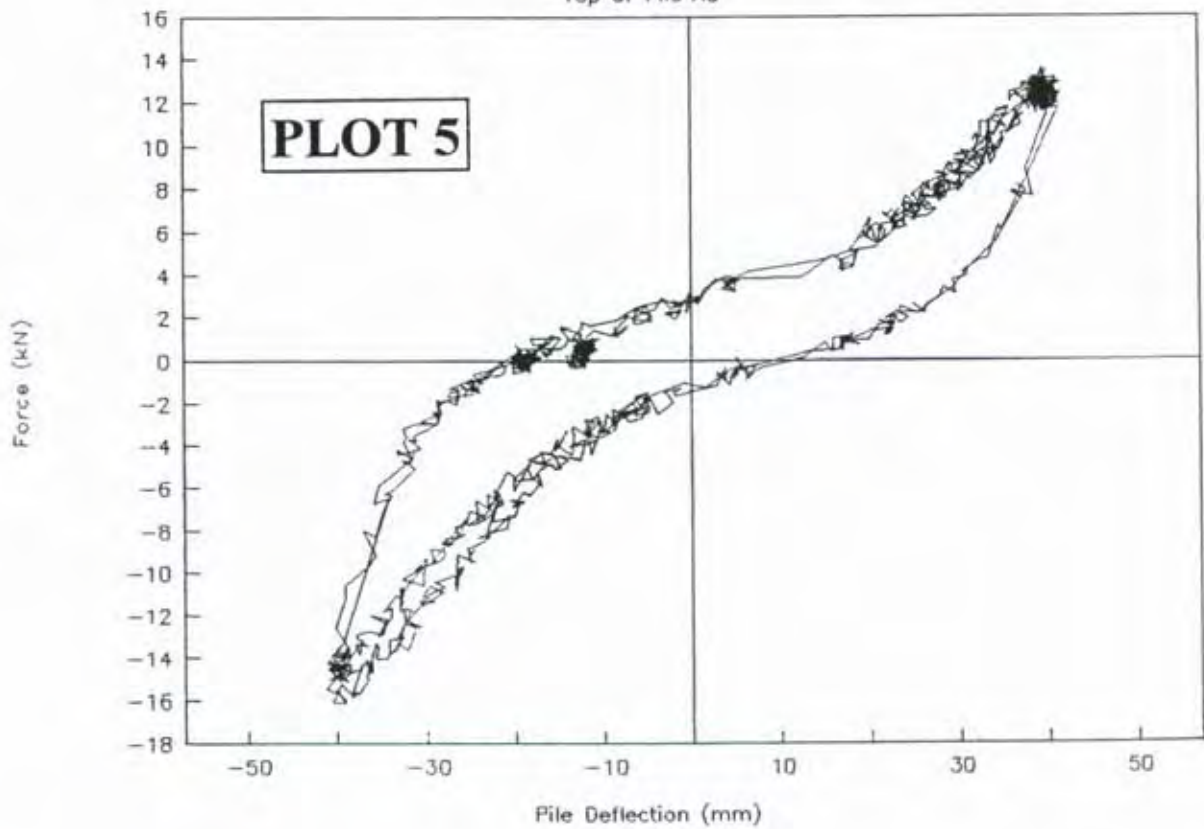
Braced Piles A4-A5

Top of Pile A4



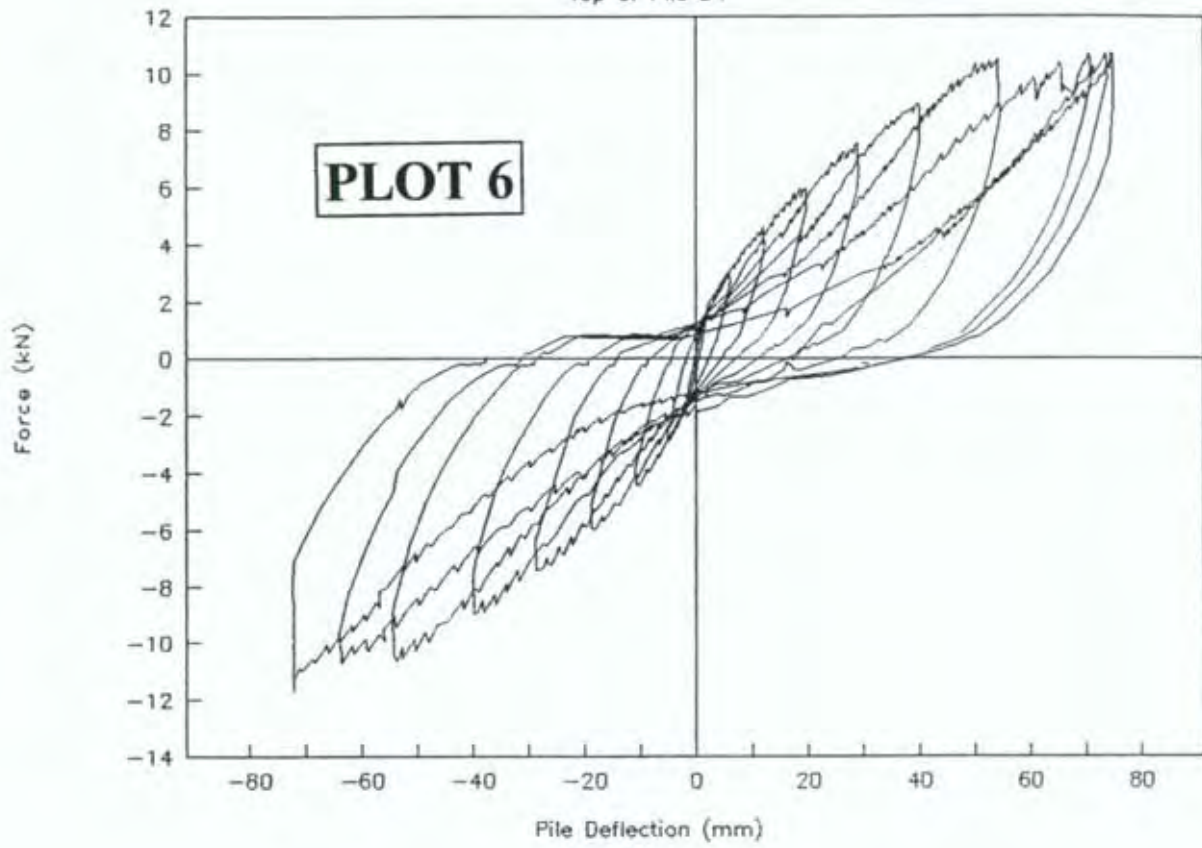
Braced Piles A4-A5

Top of Pile A5



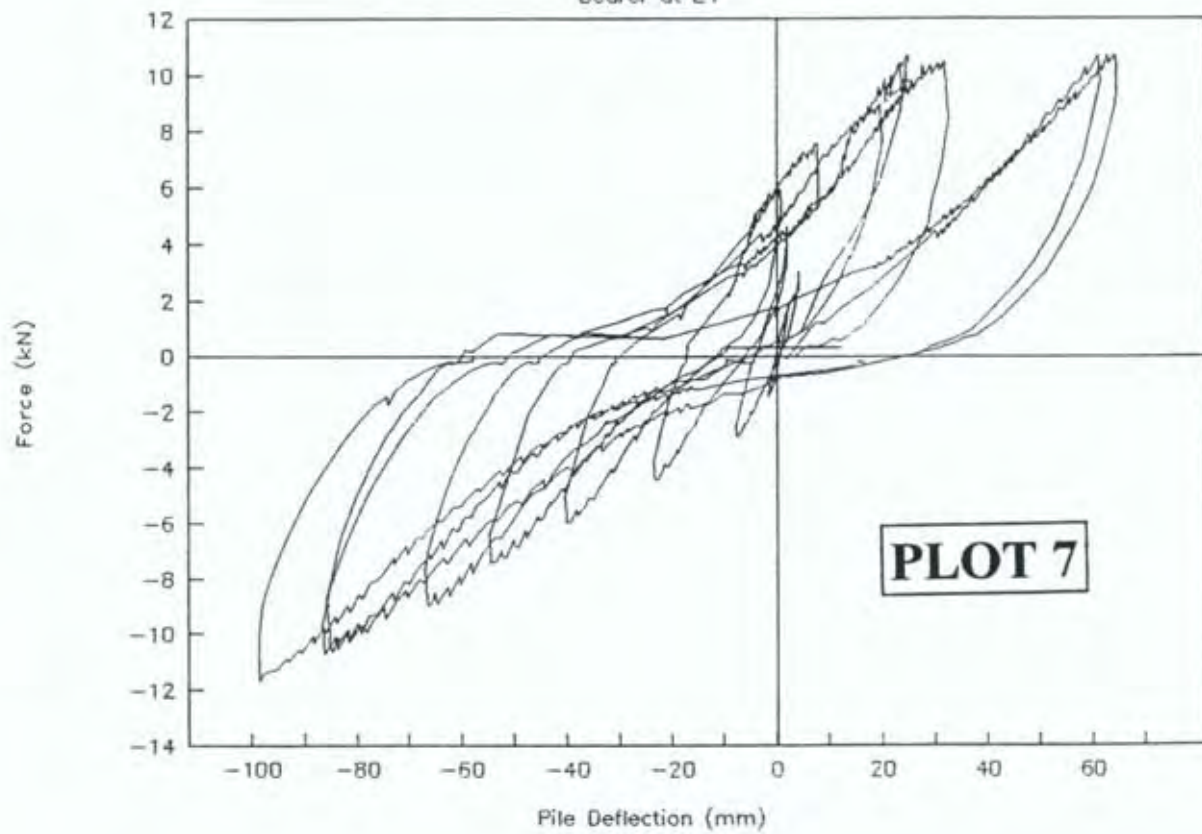
Braced Piles D1-E1

Top of Pile D1



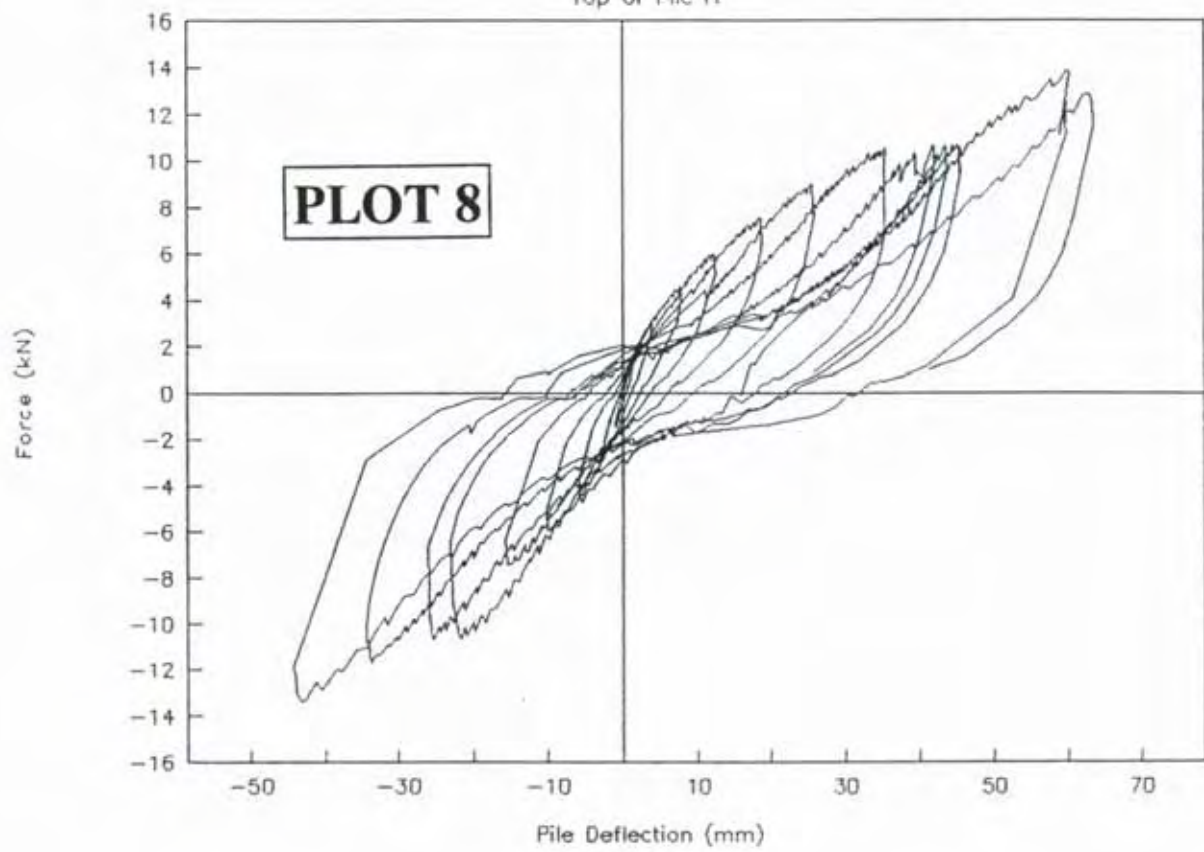
Braced Piles D1-E1

Bearer at E1



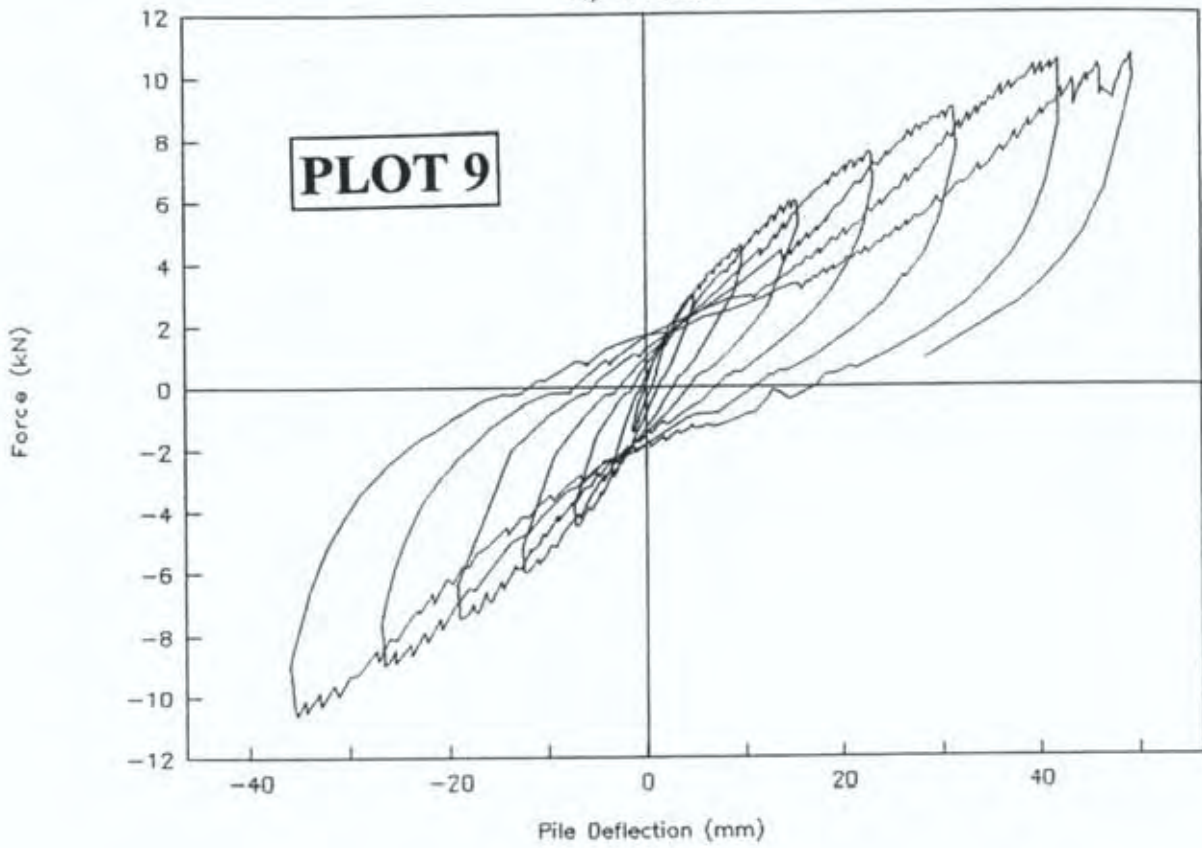
Braced Pile Test I1-J1

Top of Pile I1



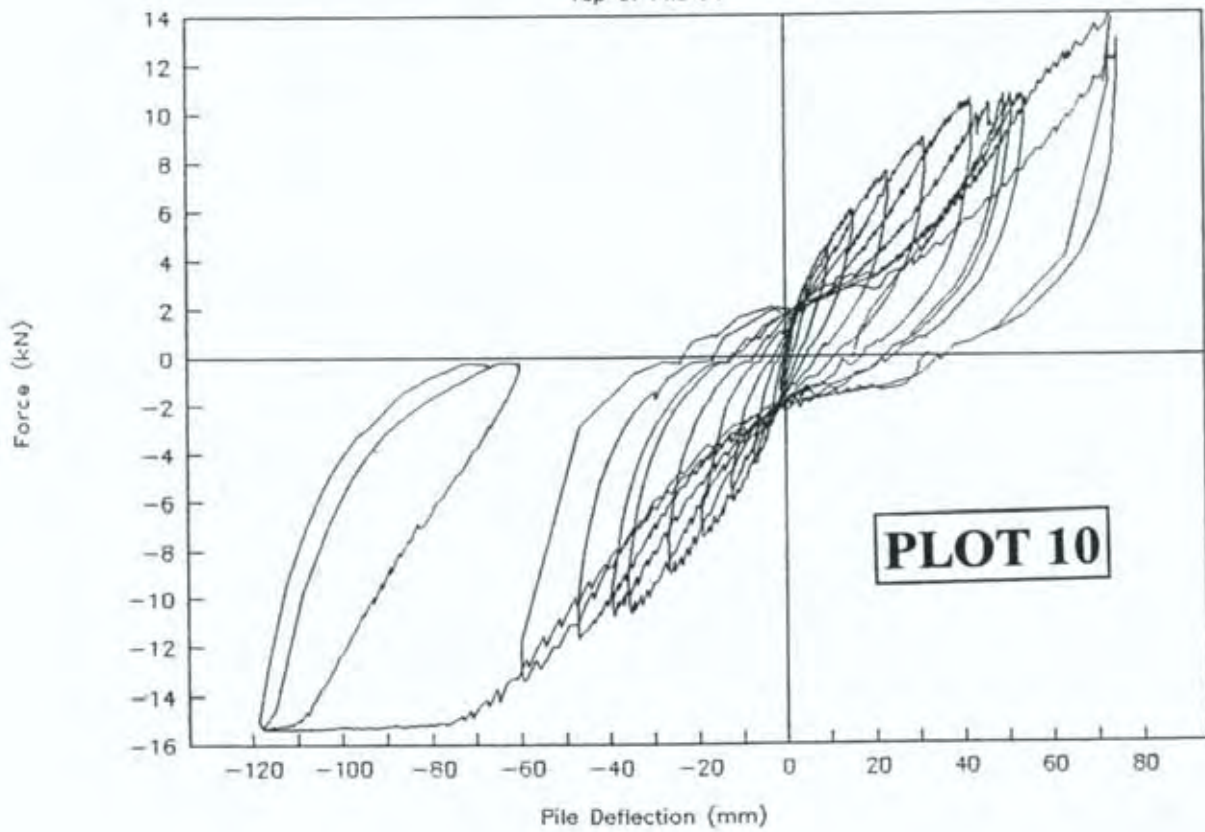
Braced Piles I1-J1

Top of Pile J1



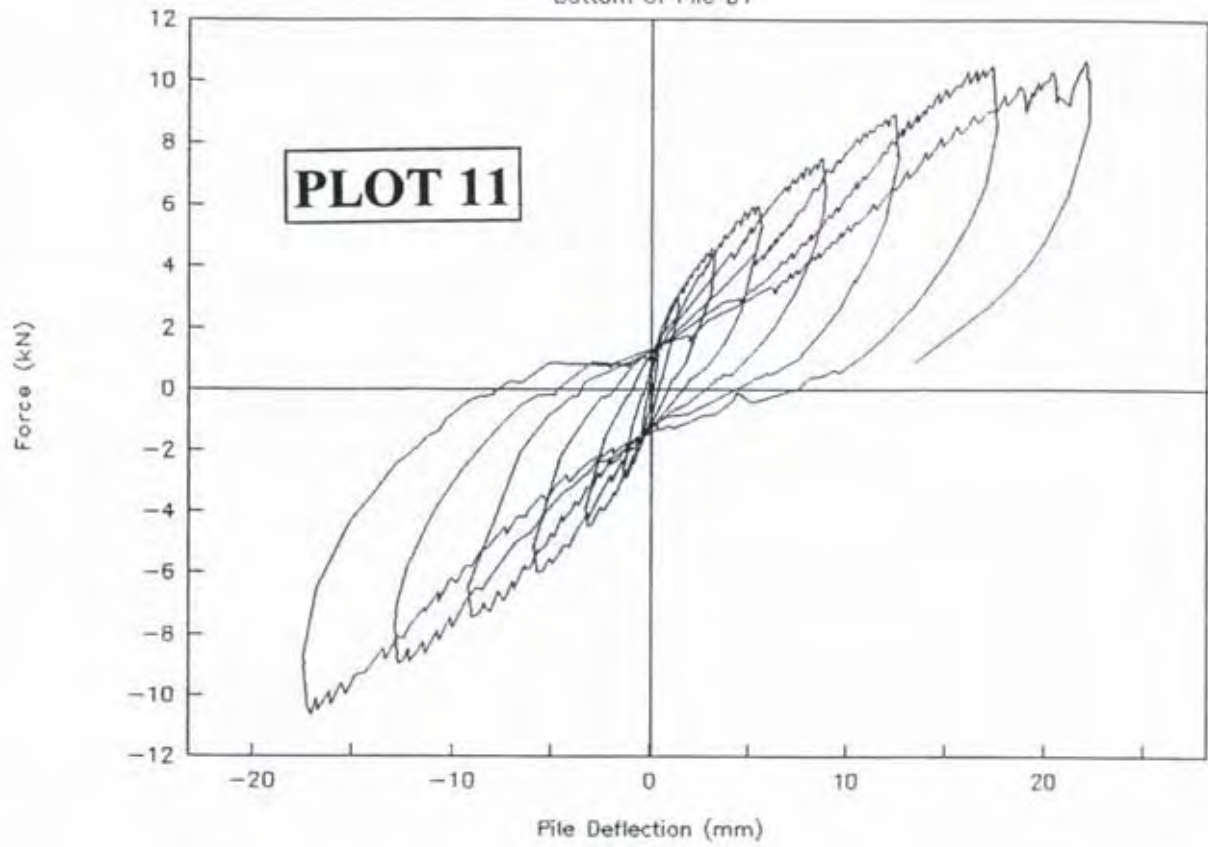
Braced Piles I1-J1

Top of Pile J1



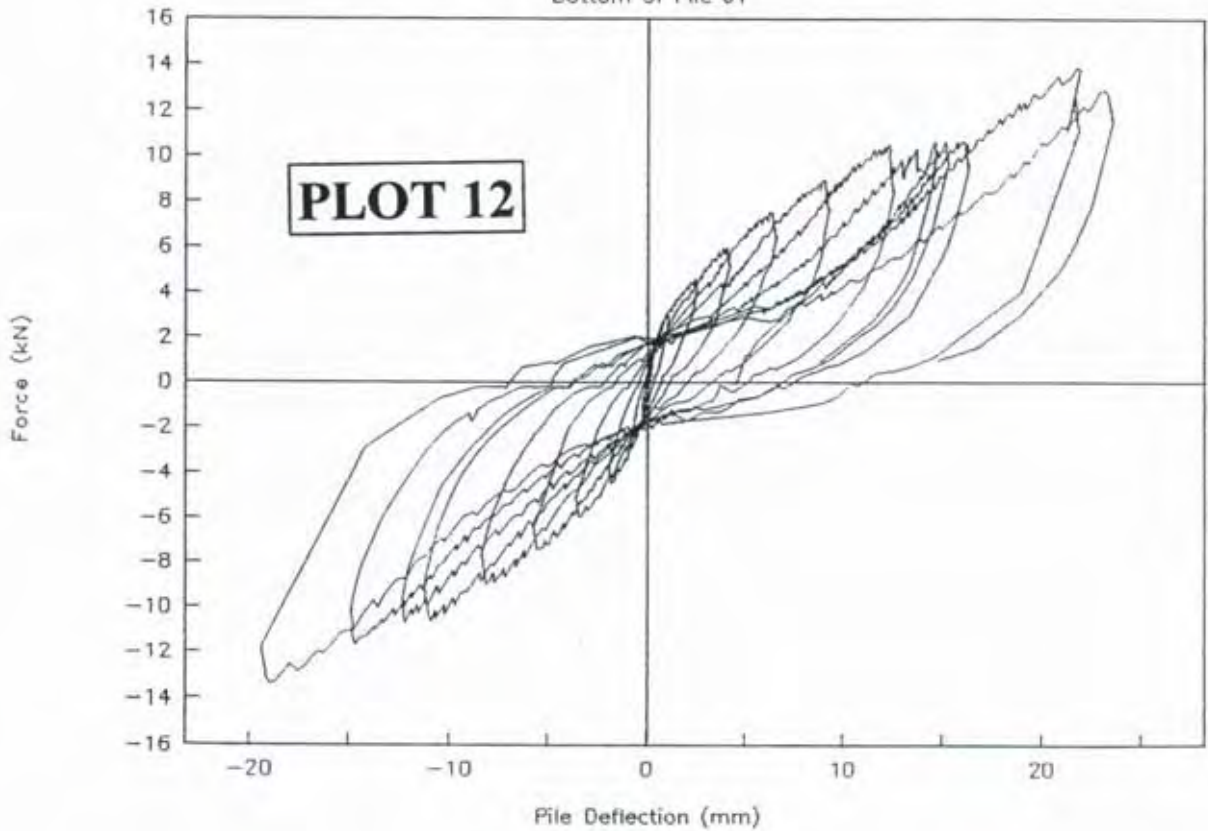
Braced Piles D1-E1

Bottom of Pile D1



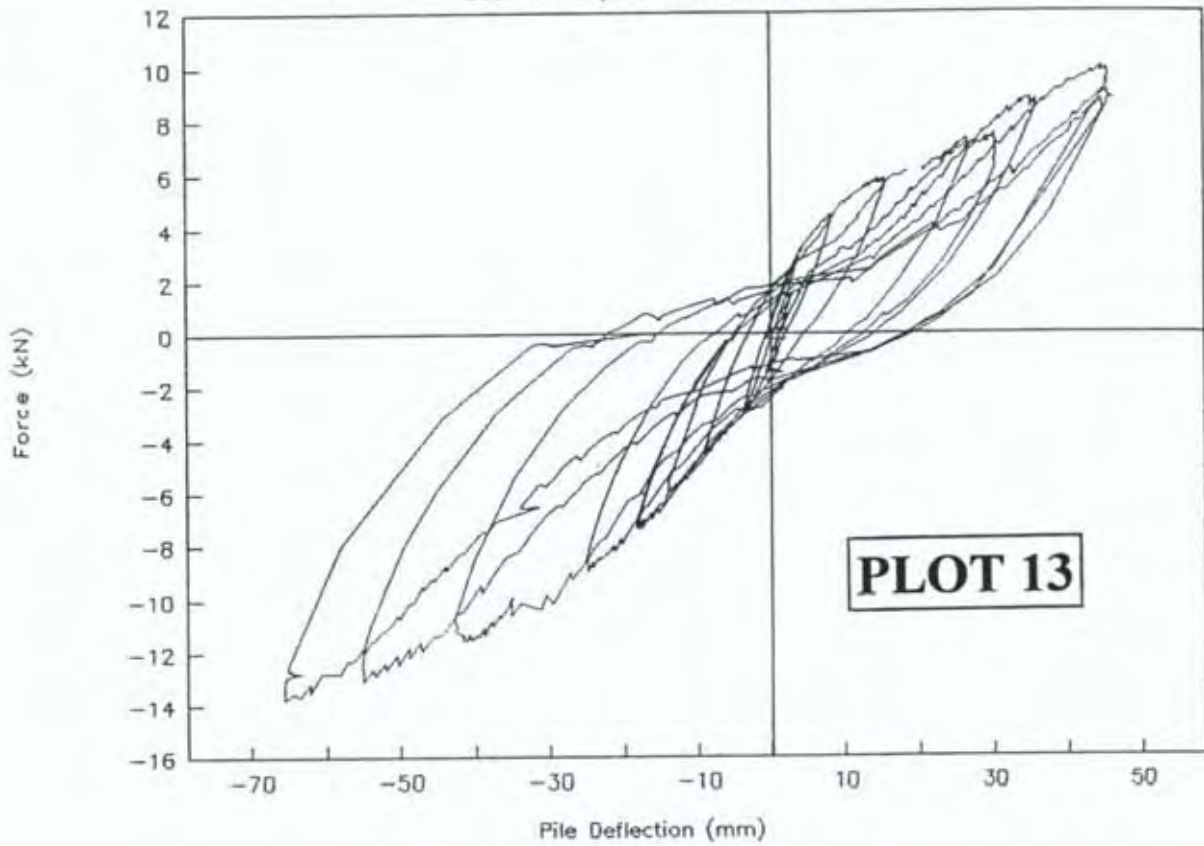
Braced Piles I1-J1

Bottom of Pile J1



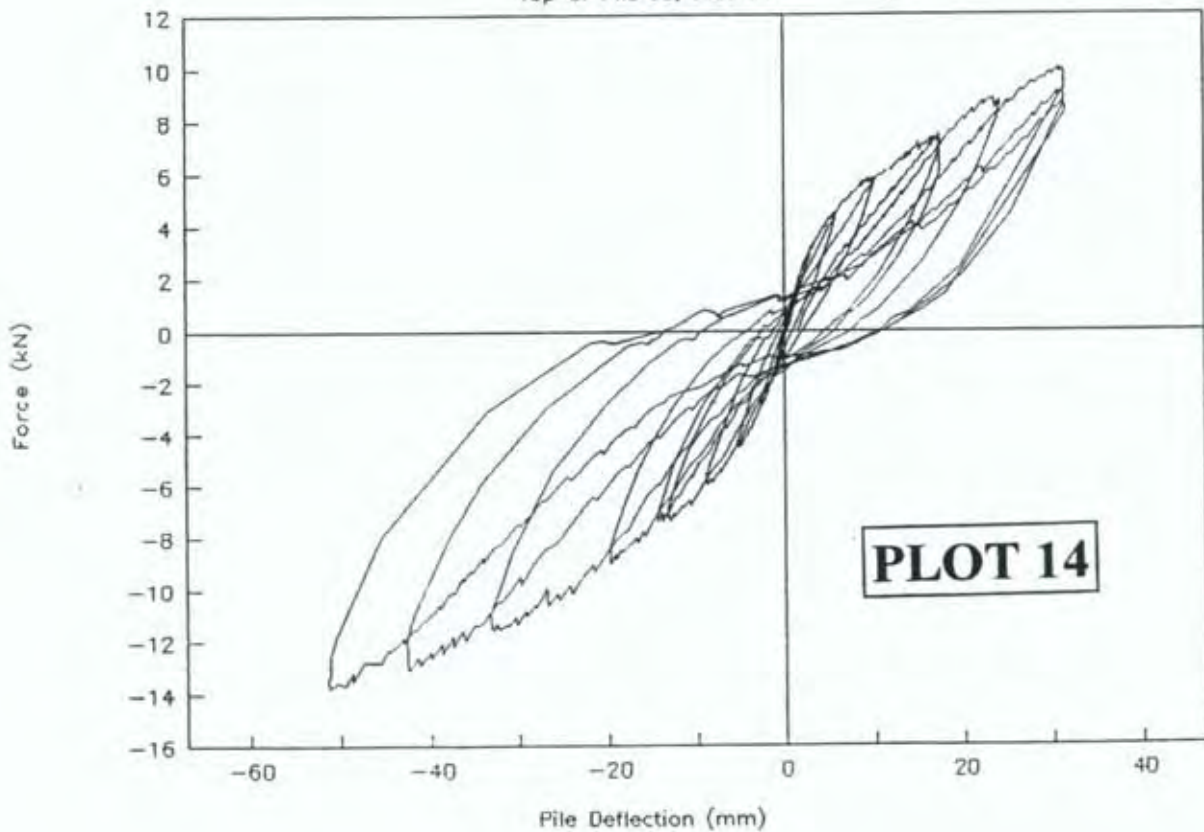
Anchor Pile Test J3-J4

Bearer at top of Pile J3, Plot 13



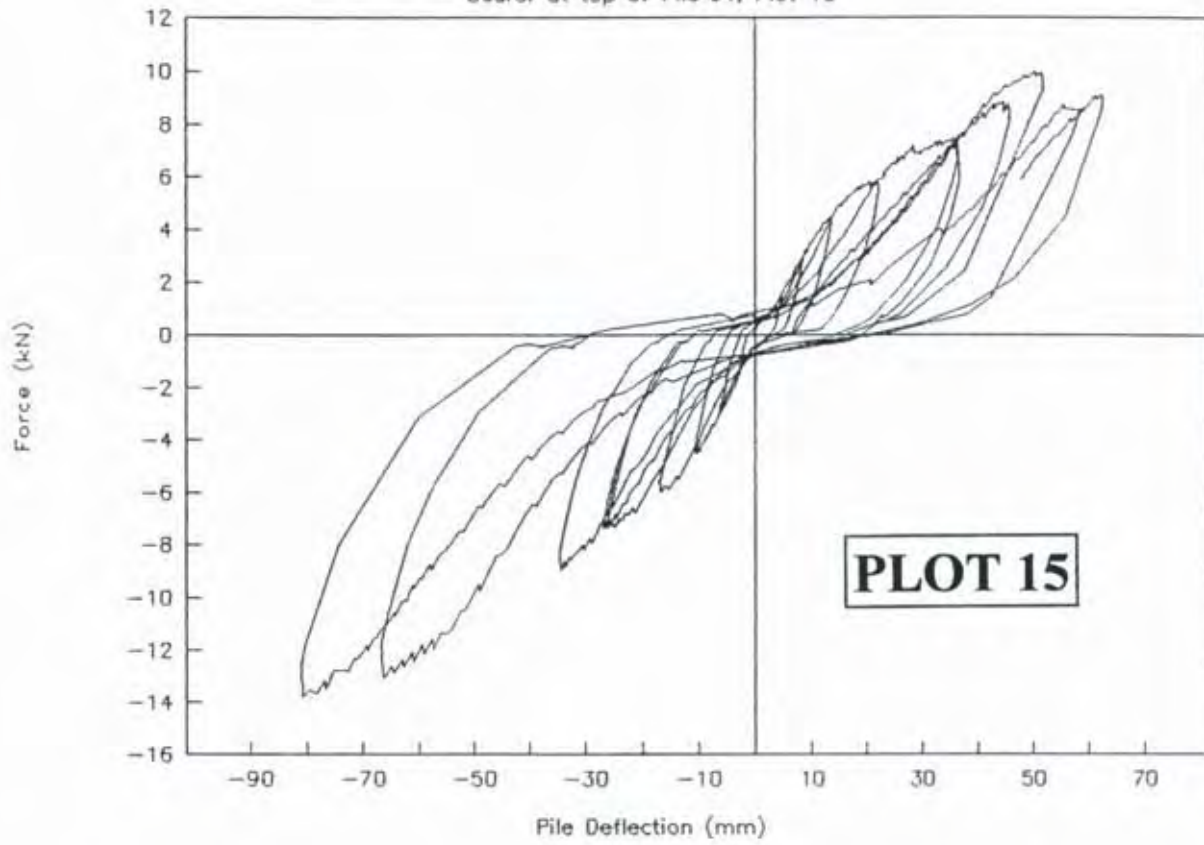
Anchor Pile Test J3-J4

Top of Pile J3, Plot 14



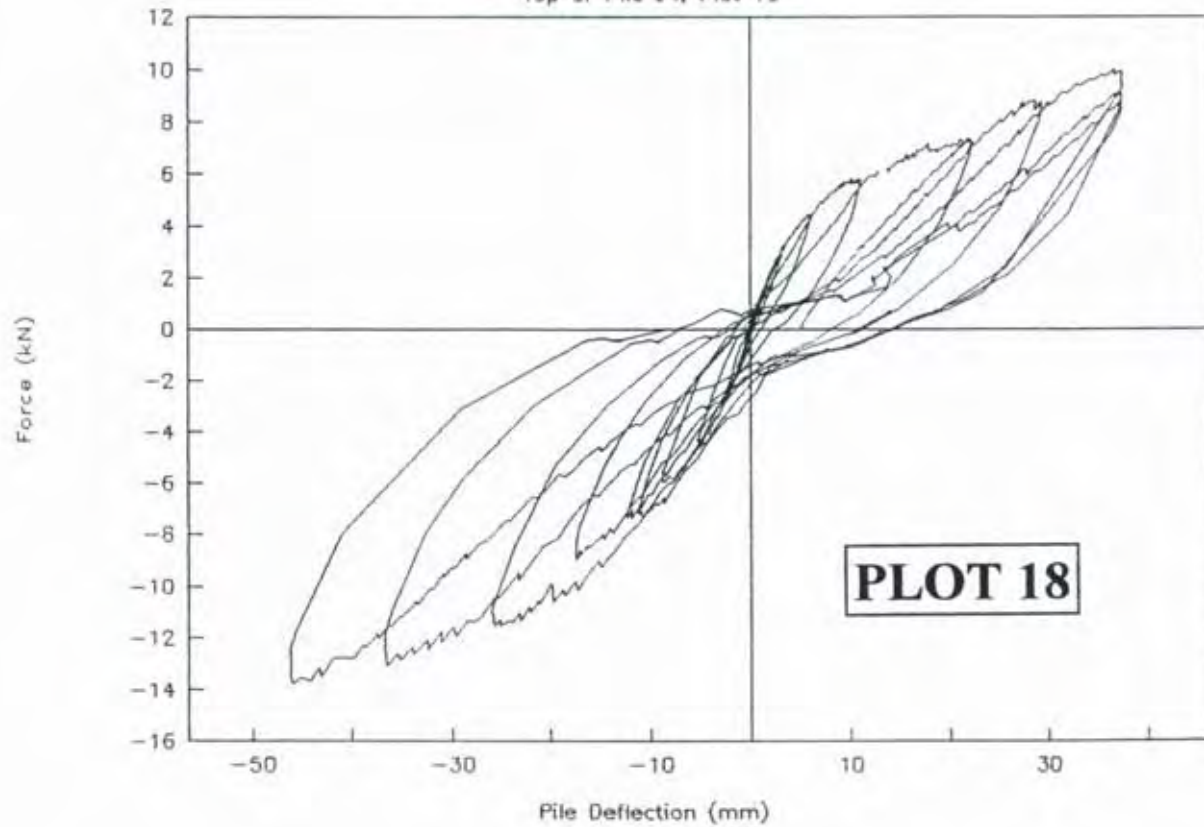
Anchor Pile Test J3-J4

Bearer at top of Pile J4, Plot 15



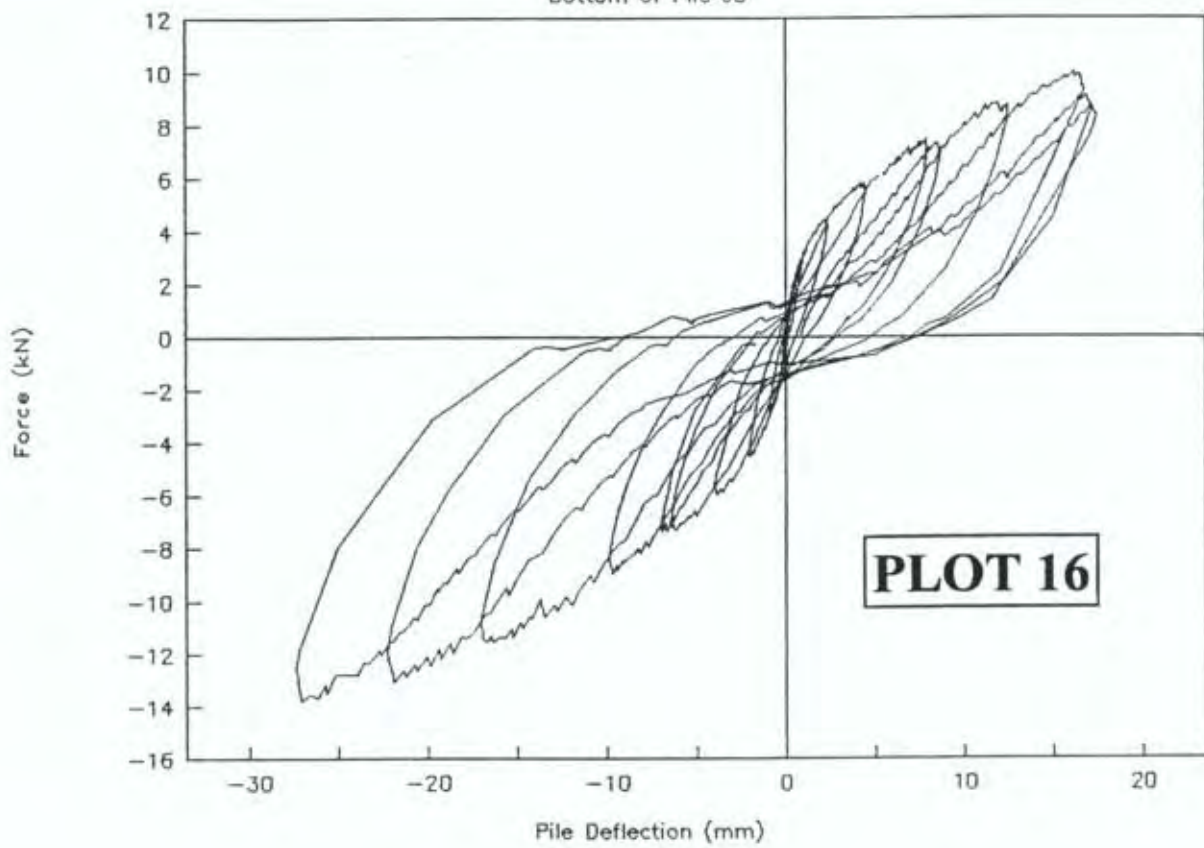
Anchor Pile Test J3-J4

Top of Pile J4, Plot 18



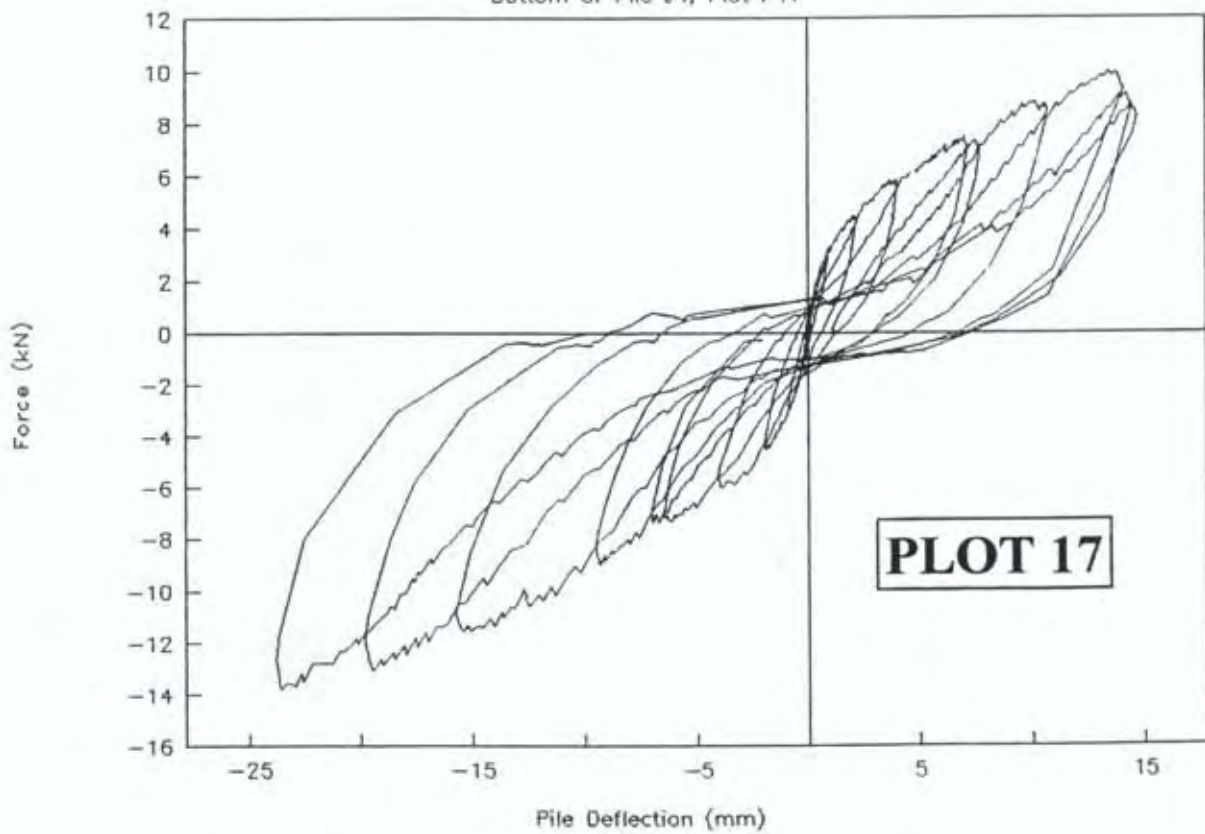
Anchor Pile Test J3-J4

Bottom of Pile J3



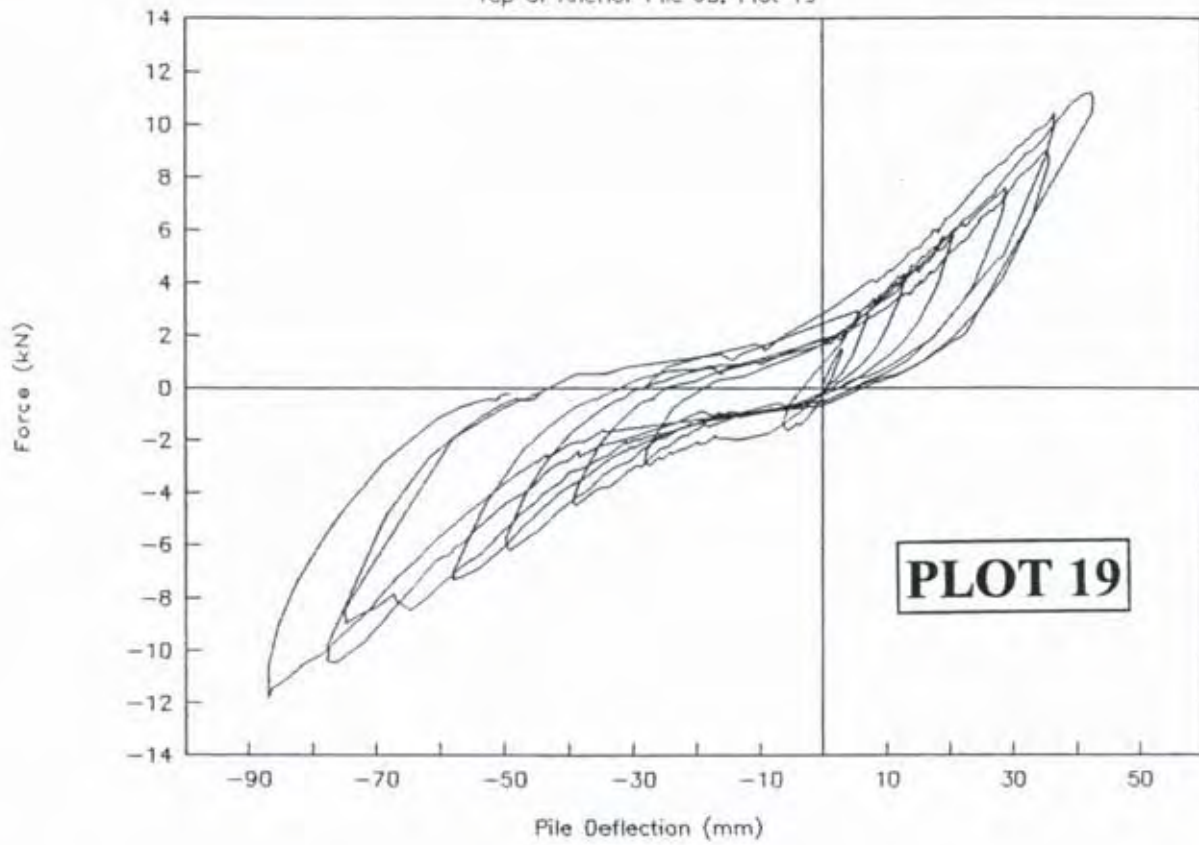
Anchor Pile Test J3-J4

Bottom of Pile J4, Plot P17



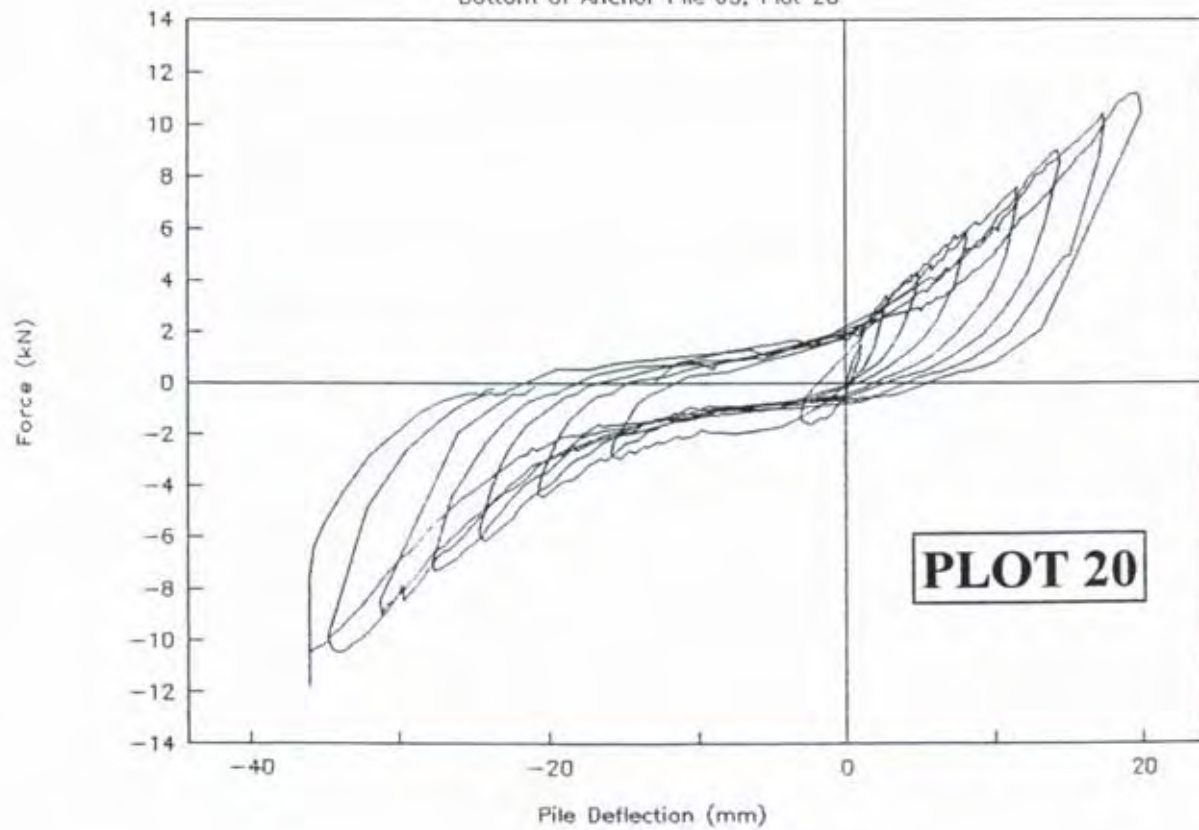
Anchor Pile J3

Top of Anchor Pile J3, Plot 19



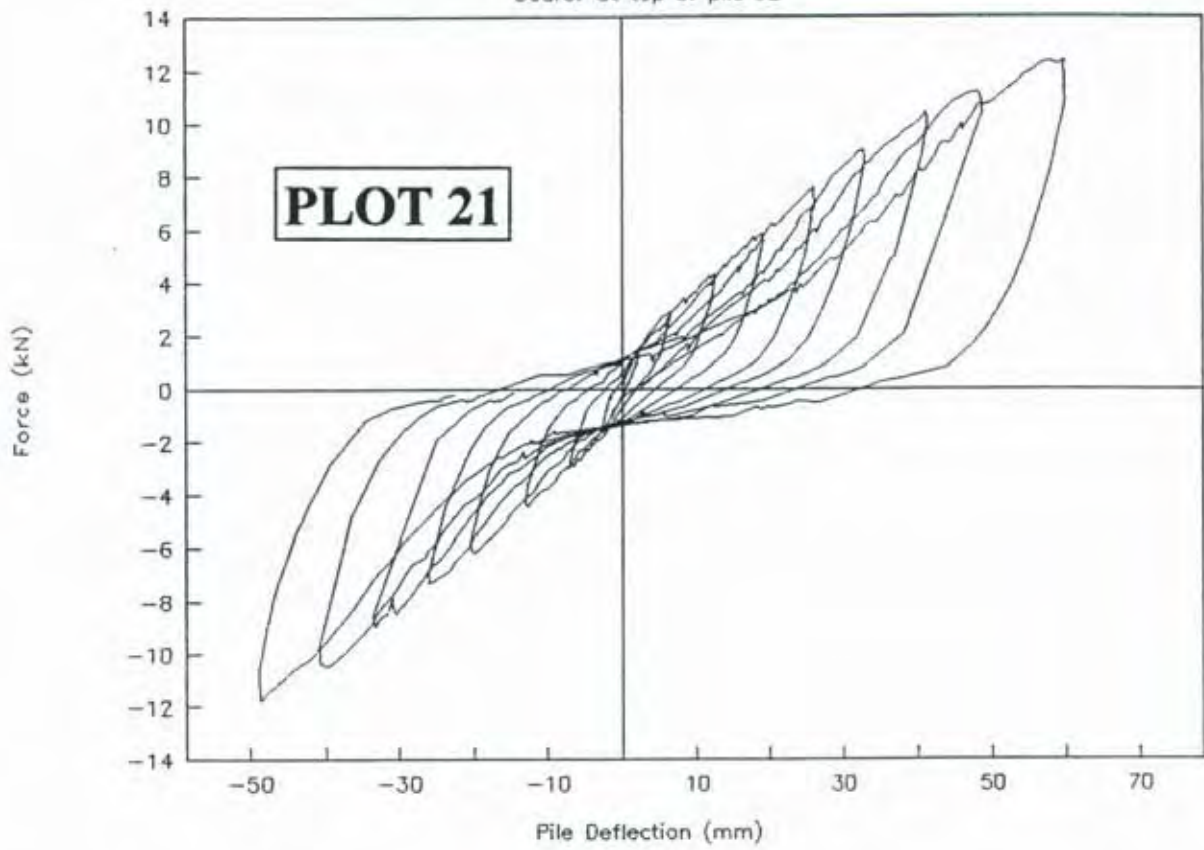
Anchor Pile J3

Bottom of Anchor Pile J3, Plot 20



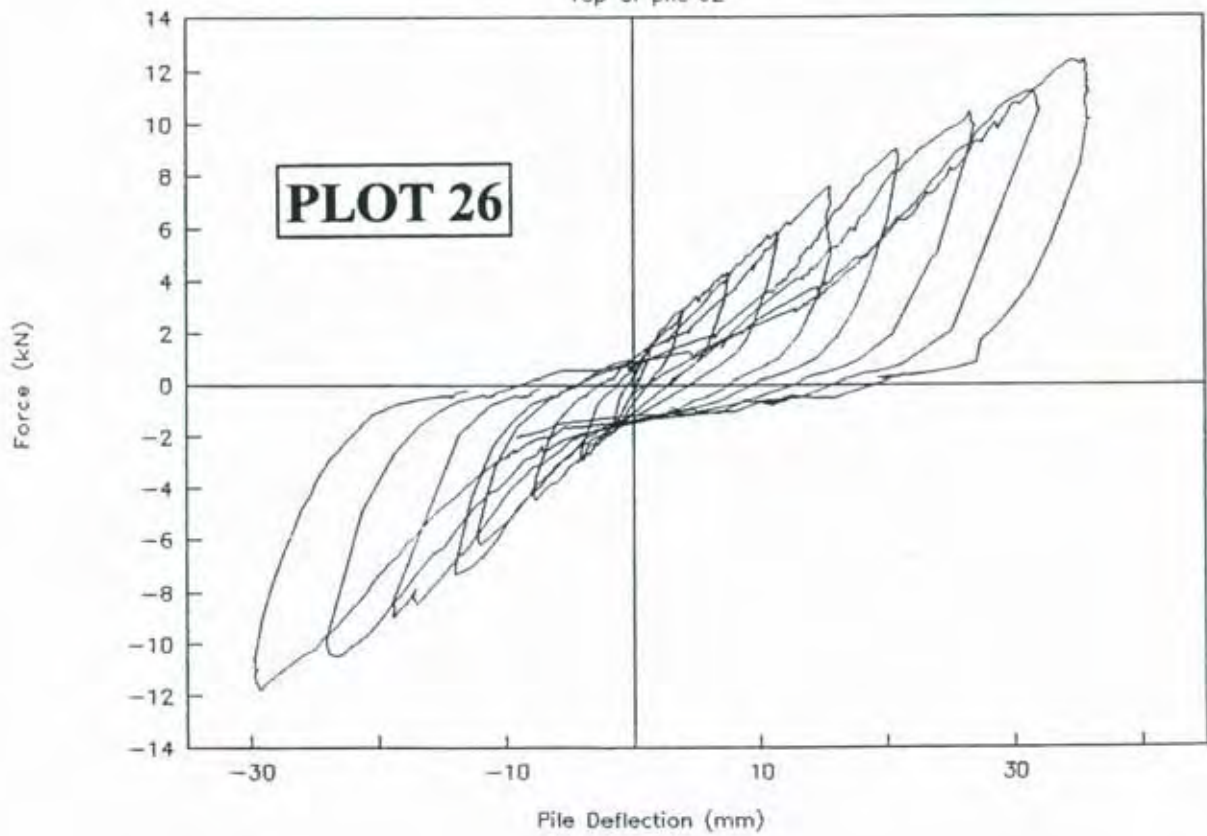
Braced Piles J1-J2

Bearer at top of pile J2



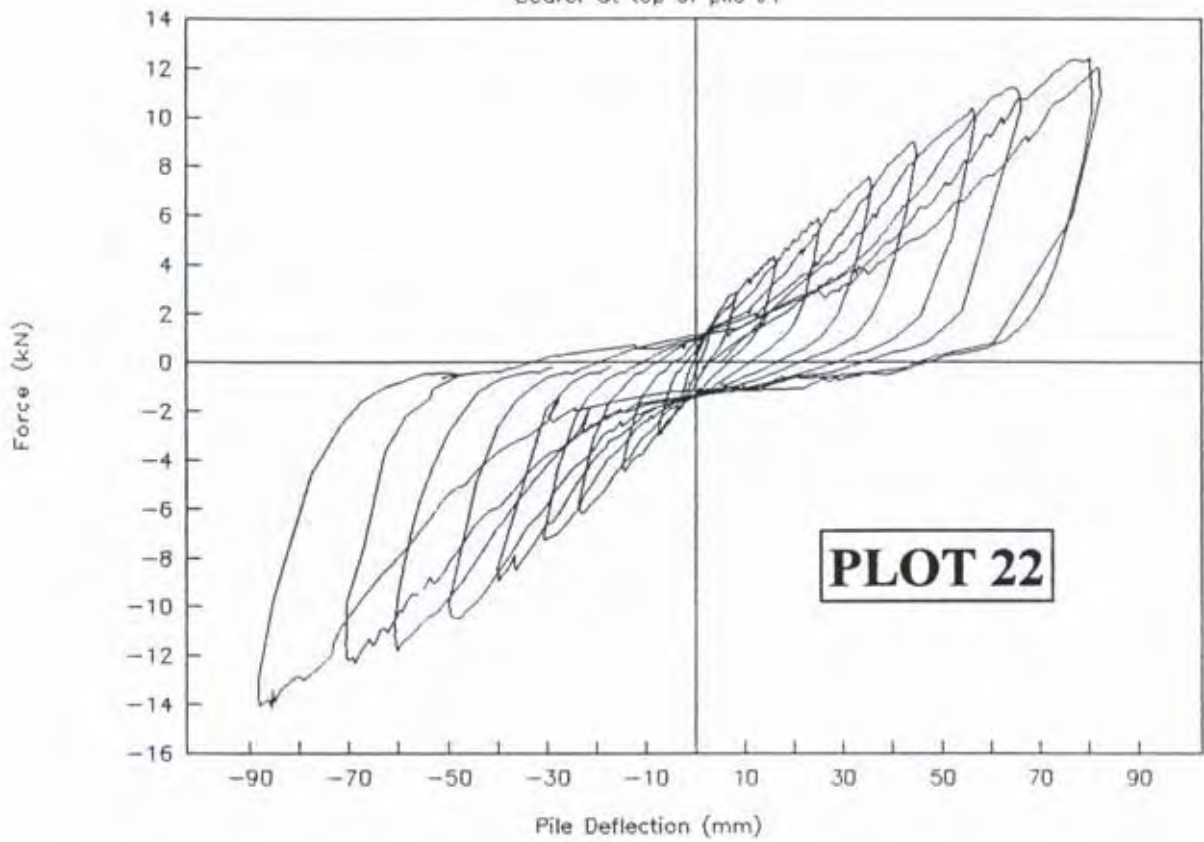
Braced Piles J1-J2

Top of pile J2



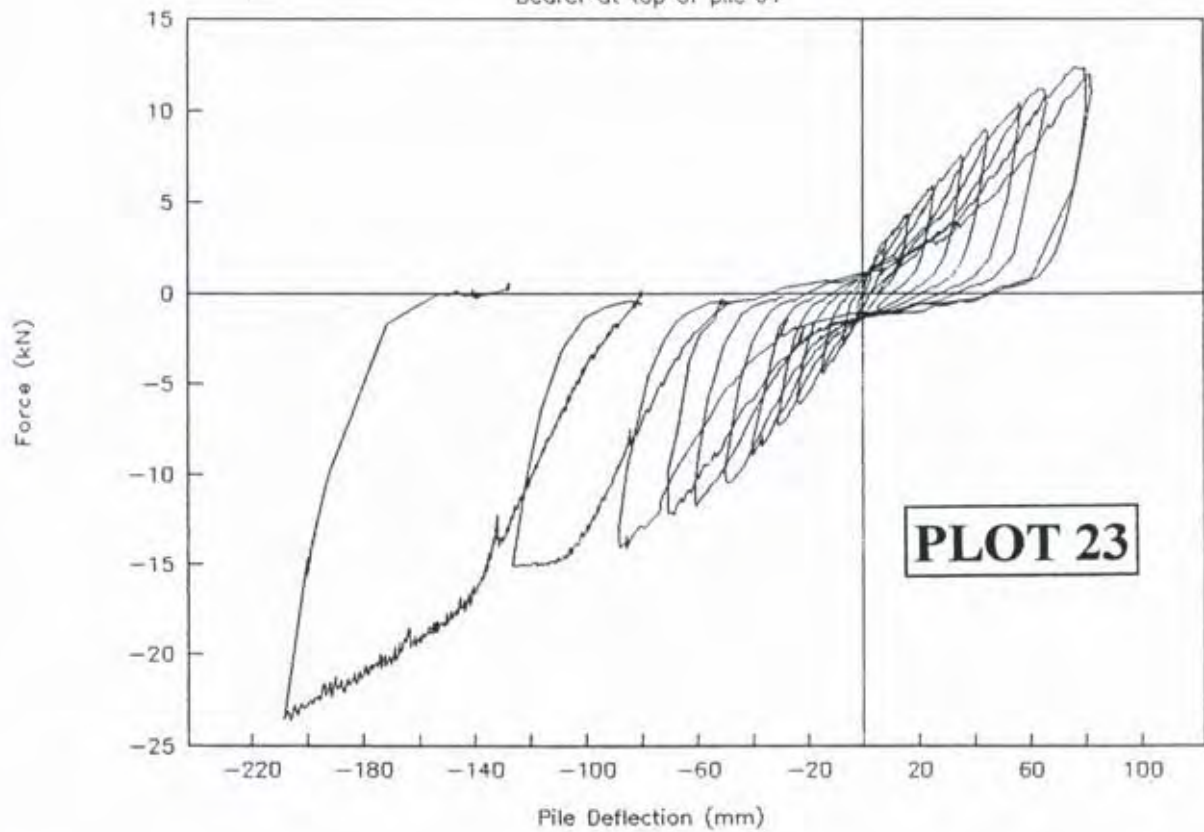
Braced Piles J1-J2

Bearer at top of pile J1



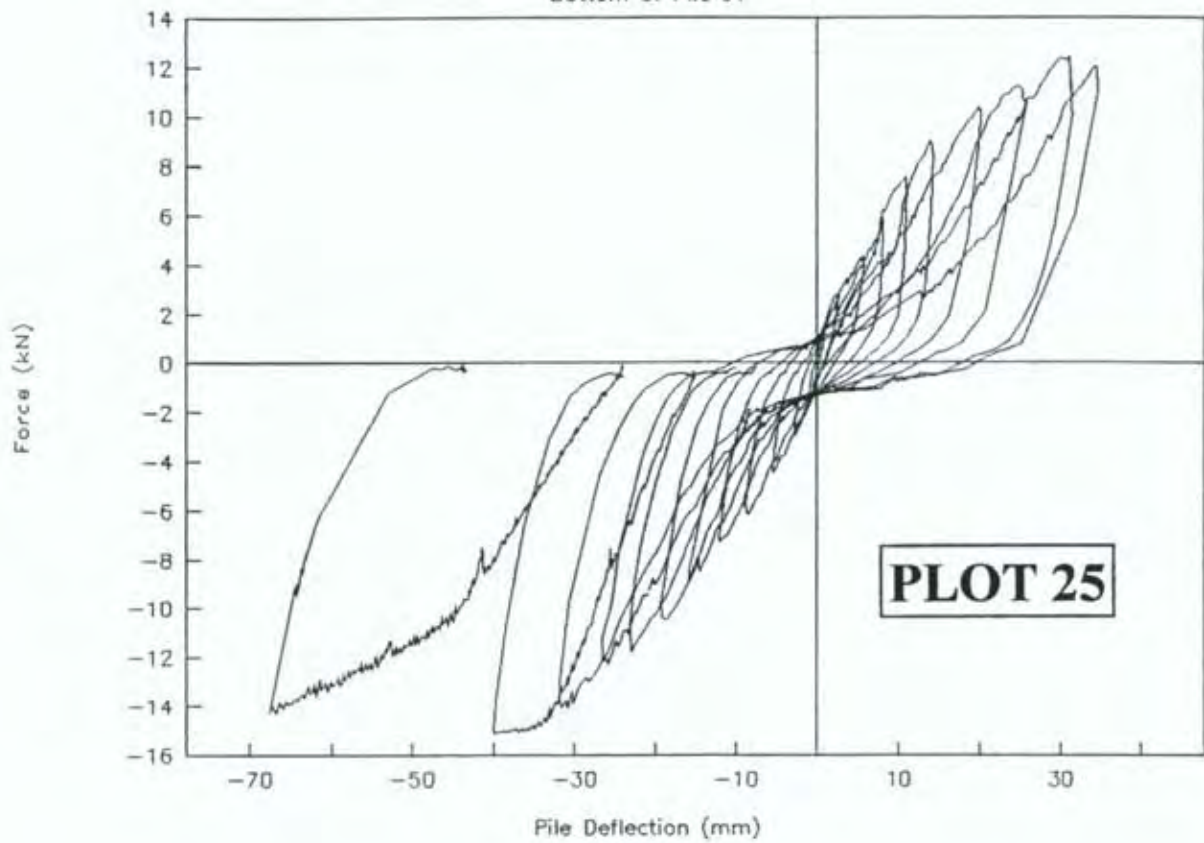
Braced Piles J1-J2

Bearer at top of pile J1



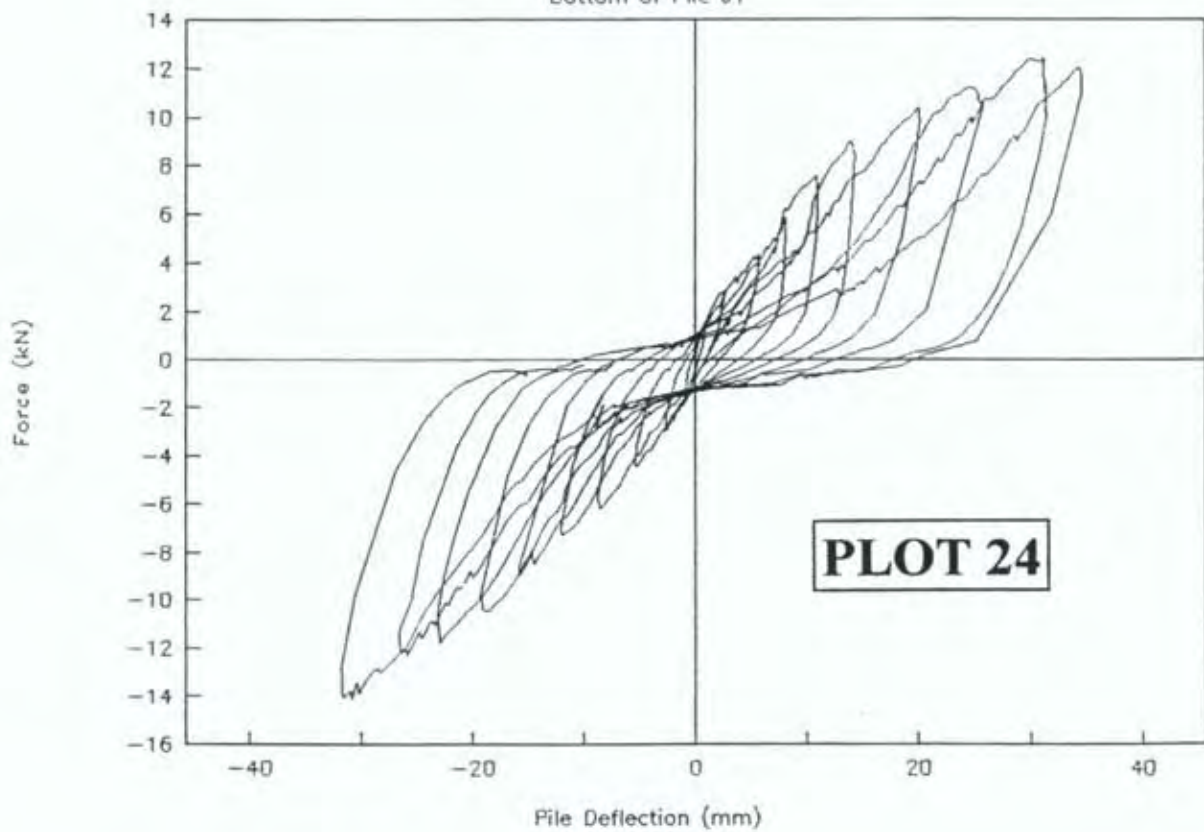
Braced Piles J1-J2

Bottom of Pile J1



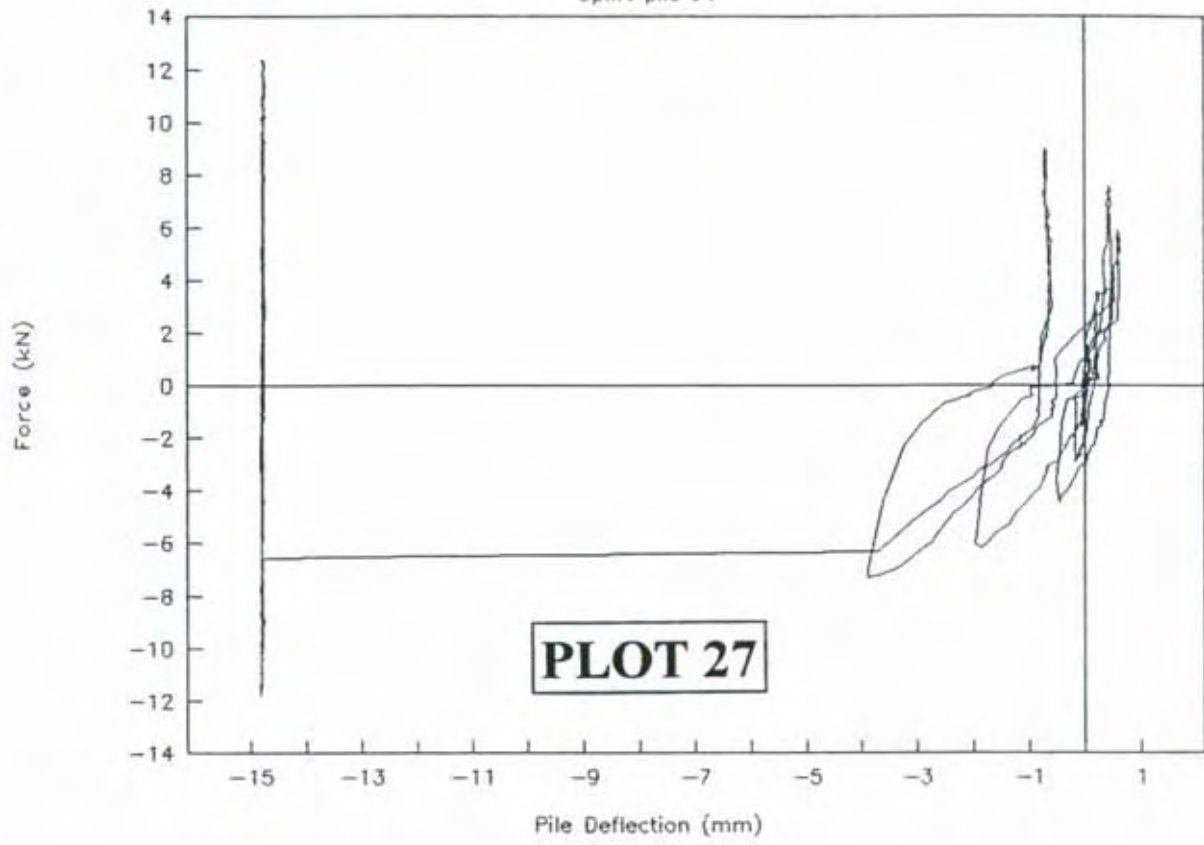
Braced Piles J1-J2

Bottom of Pile J1



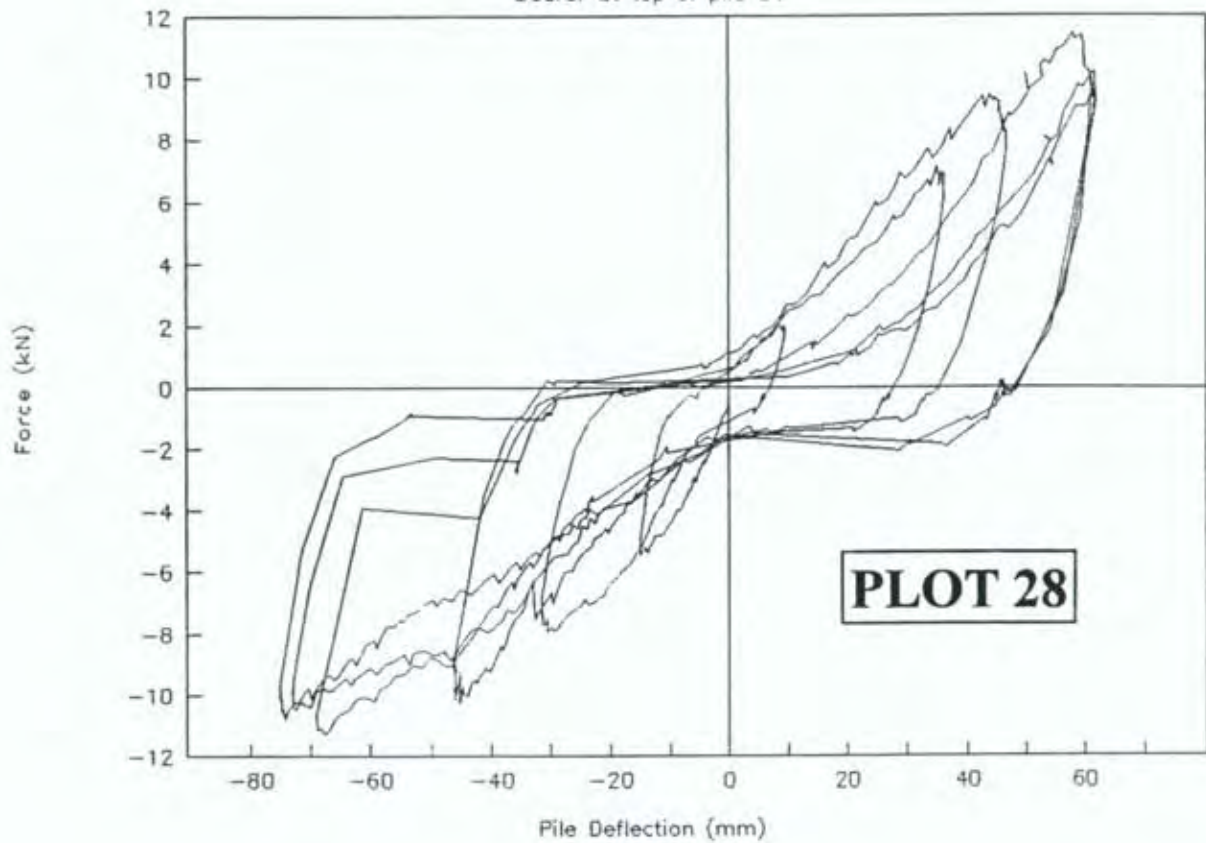
Braced Piles J1-J2

Uplift pile J1



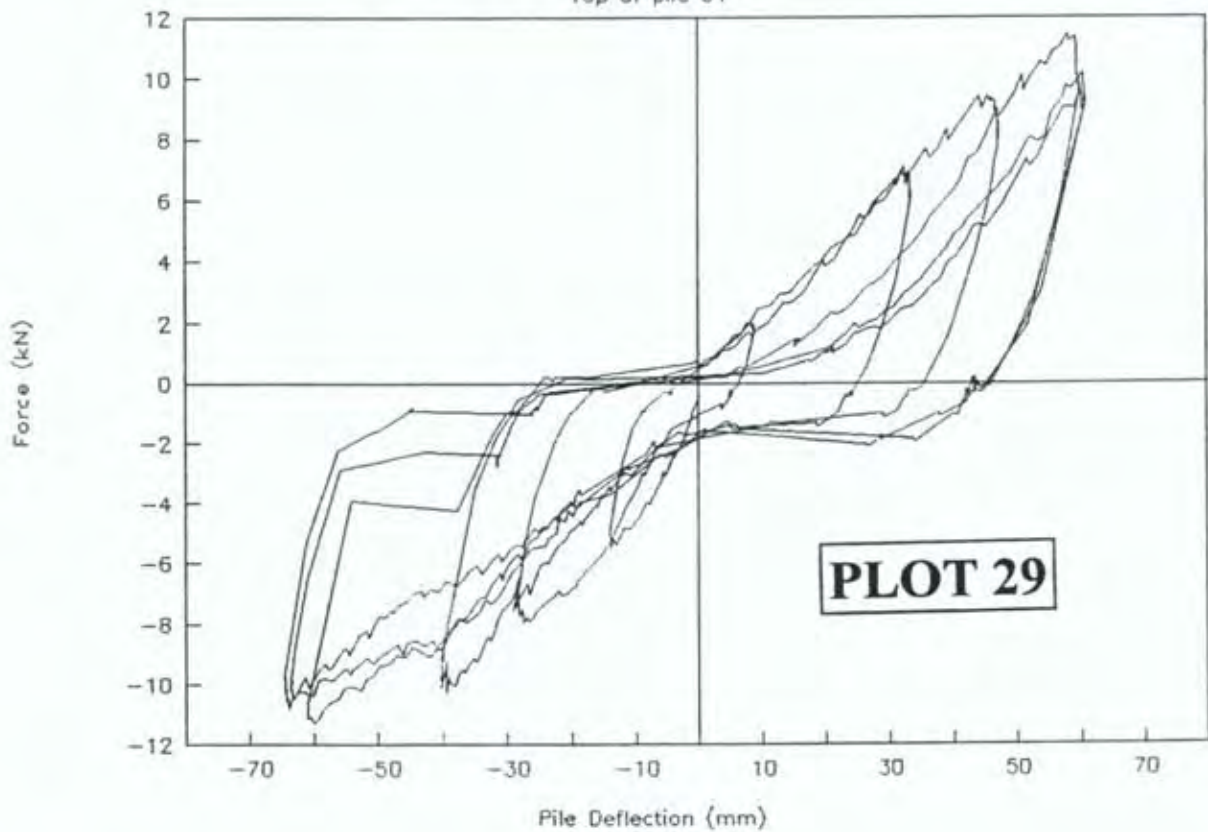
Braced Pile Test G1-G2

Bearer at top of pile G1



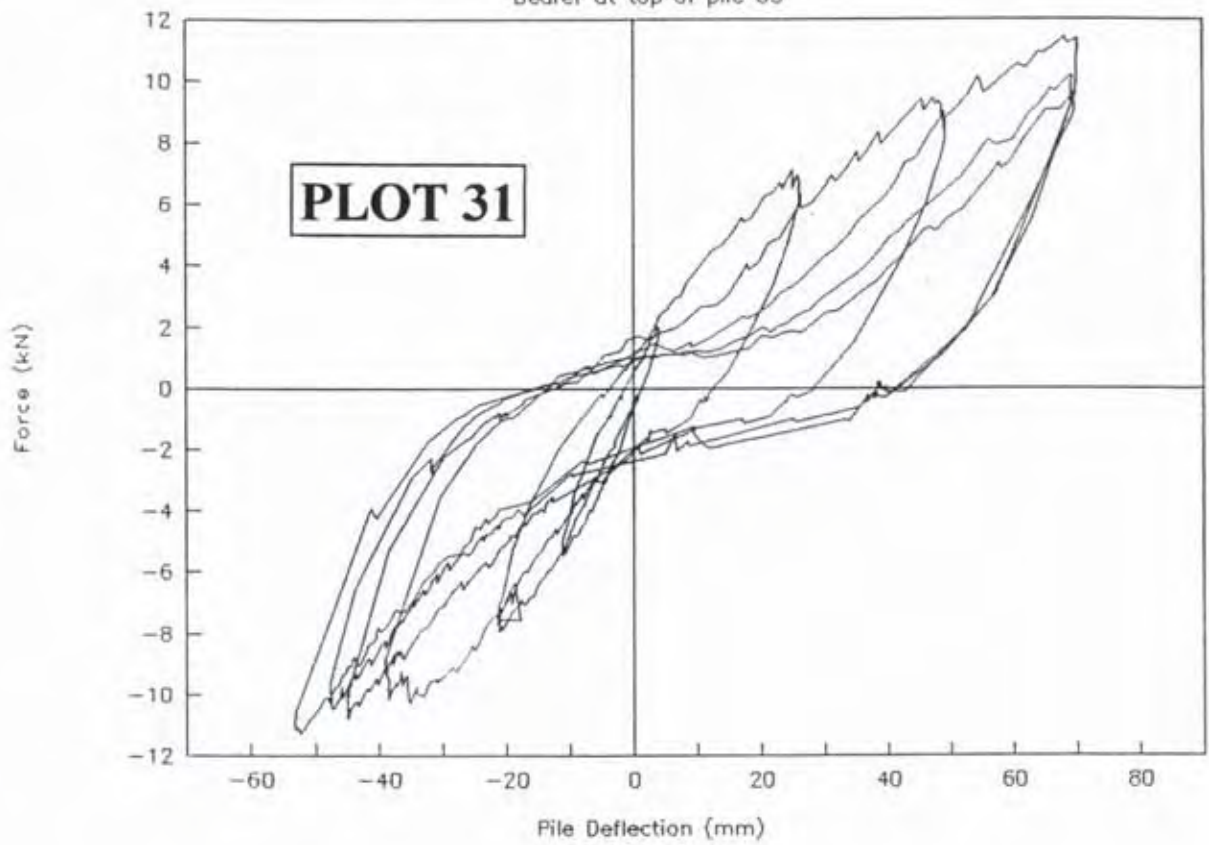
Braced Pile Test G1-G2

Top of pile G1



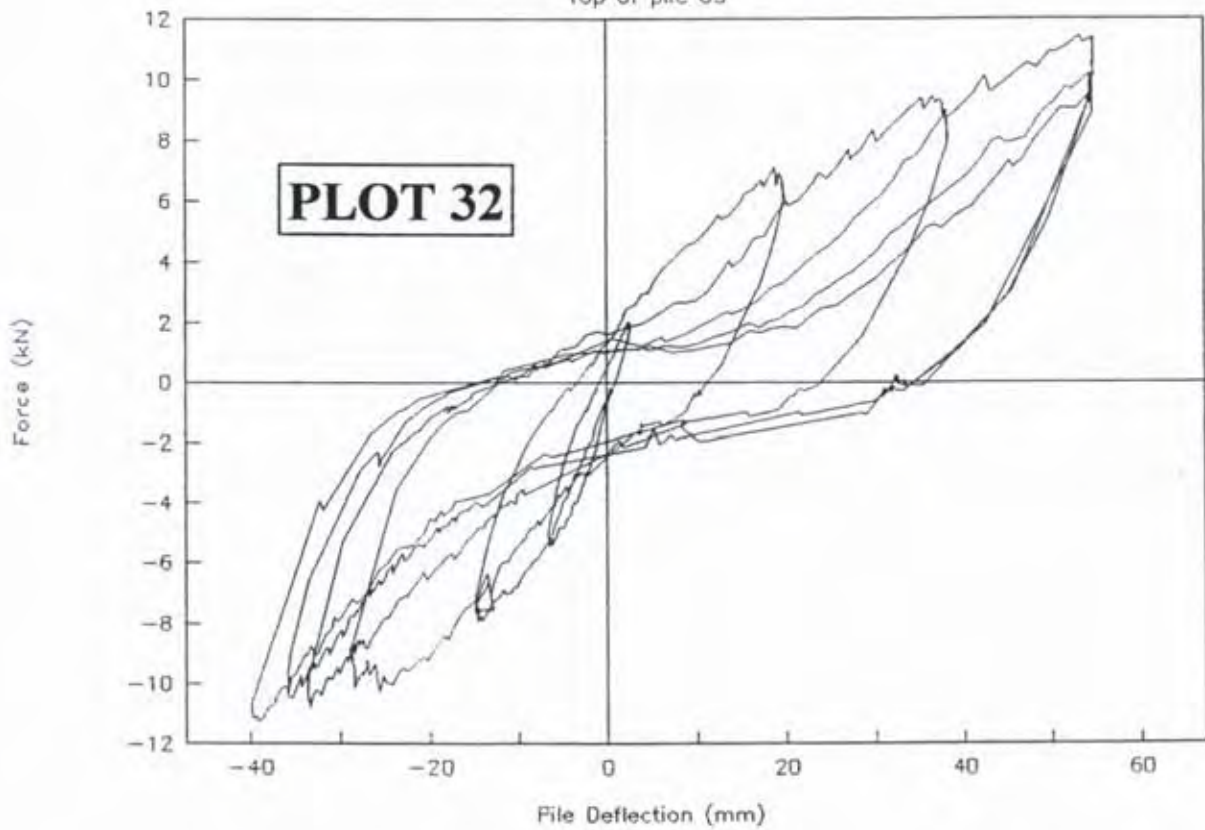
Braced Pile Test G3-G4

Bearer at top of pile G3



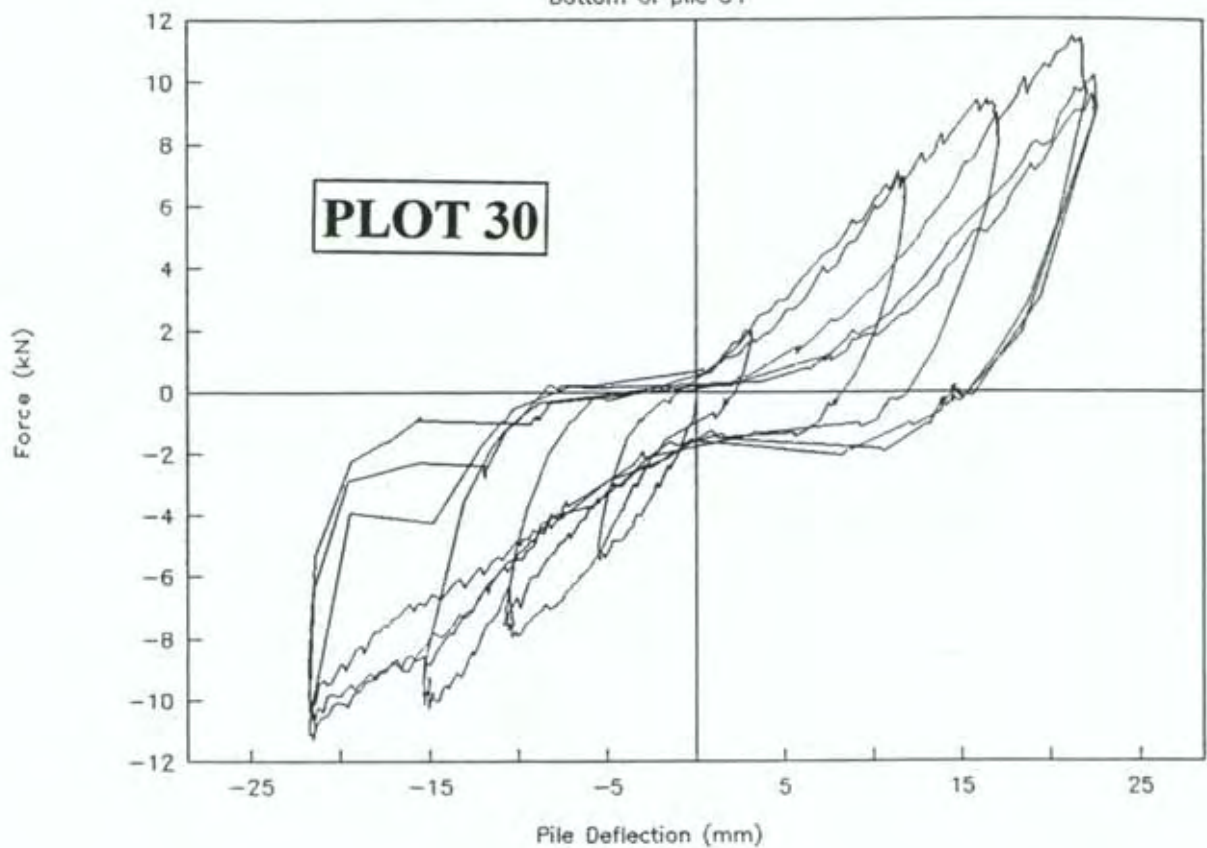
Braced Pile Test G3-G4

Top of pile G3



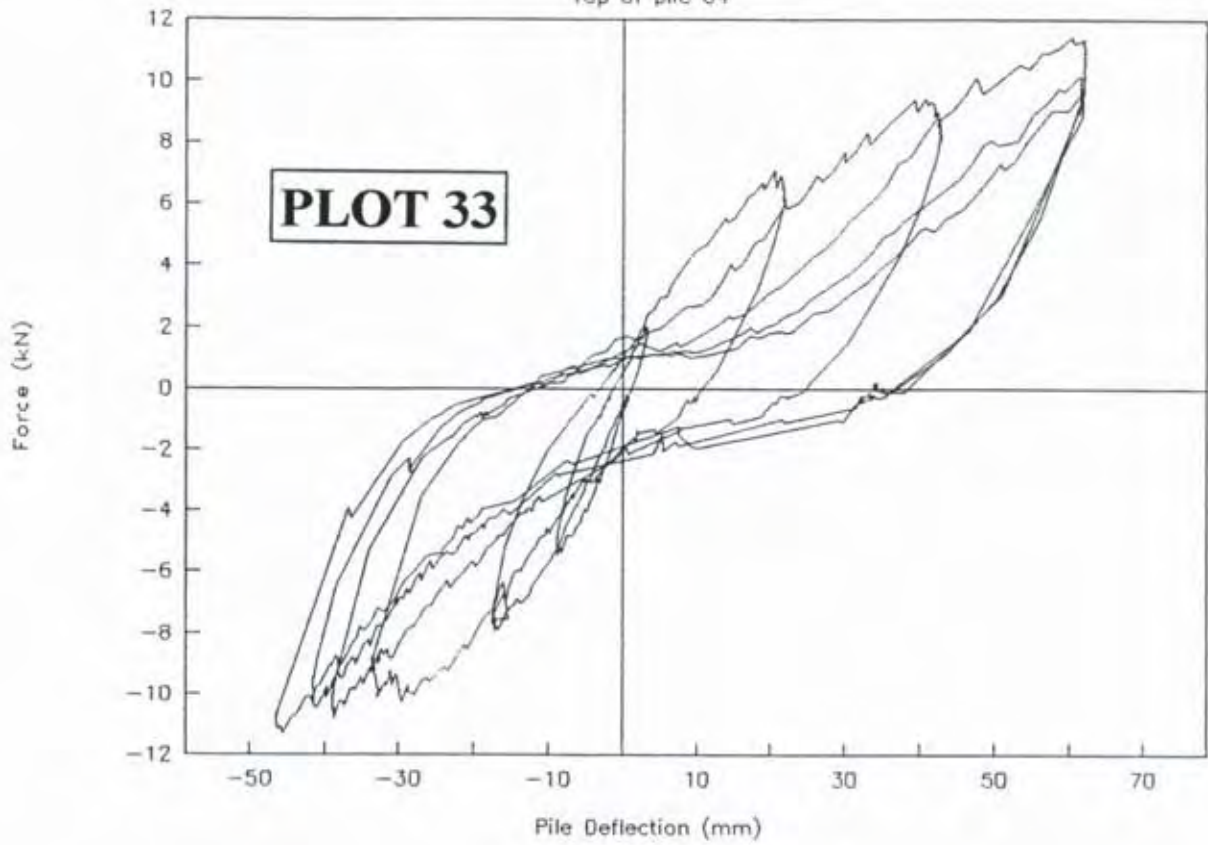
Braced Pile Test G1-G2

Bottom of pile G1



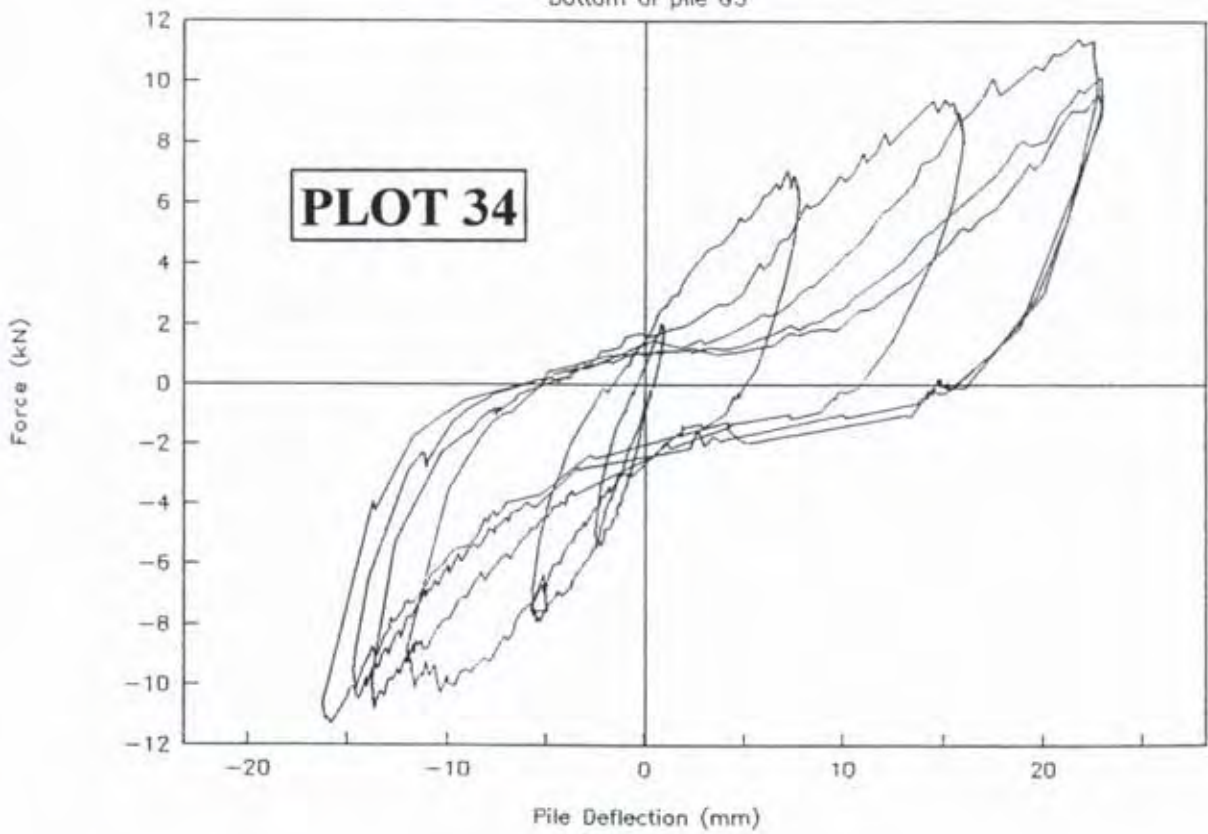
Braced Pile Test G3-G4

Top of pile G4



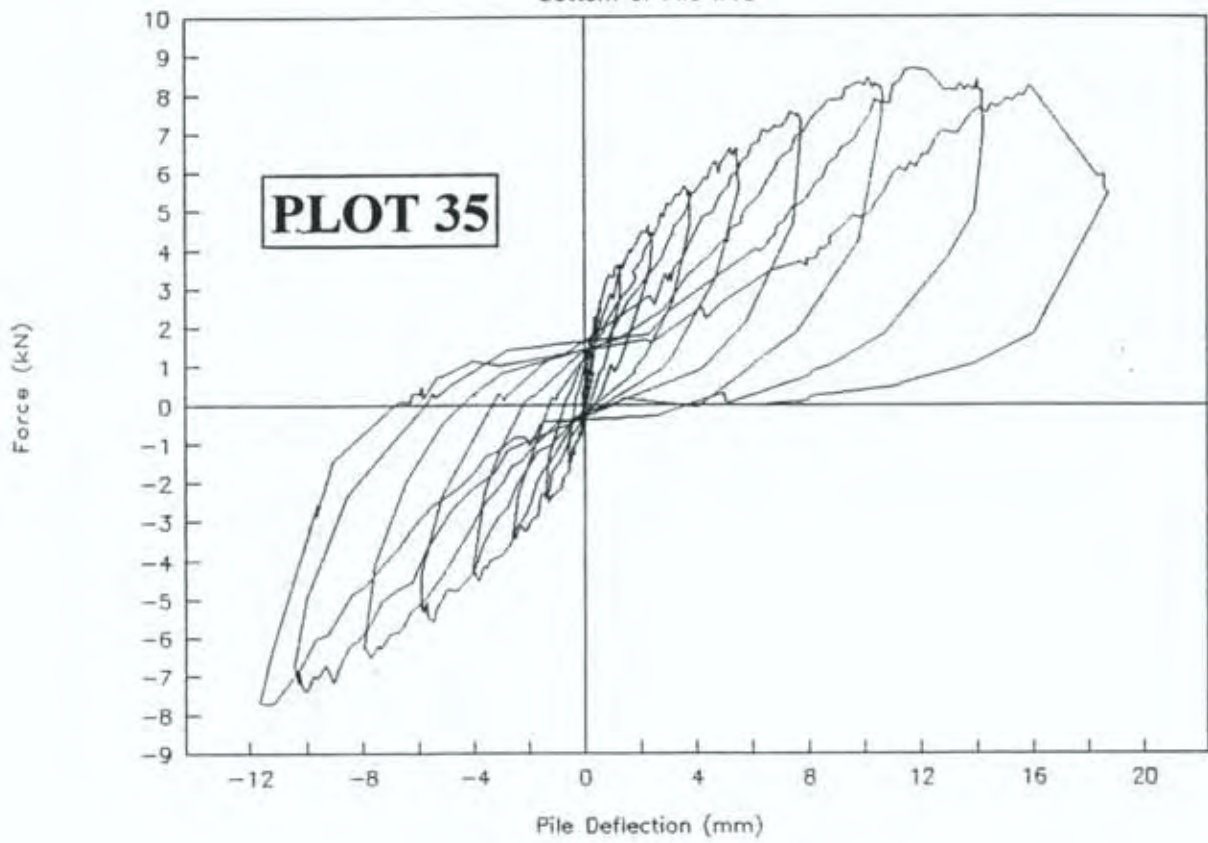
Braced Pile Test G3-G4

Bottom of pile G3



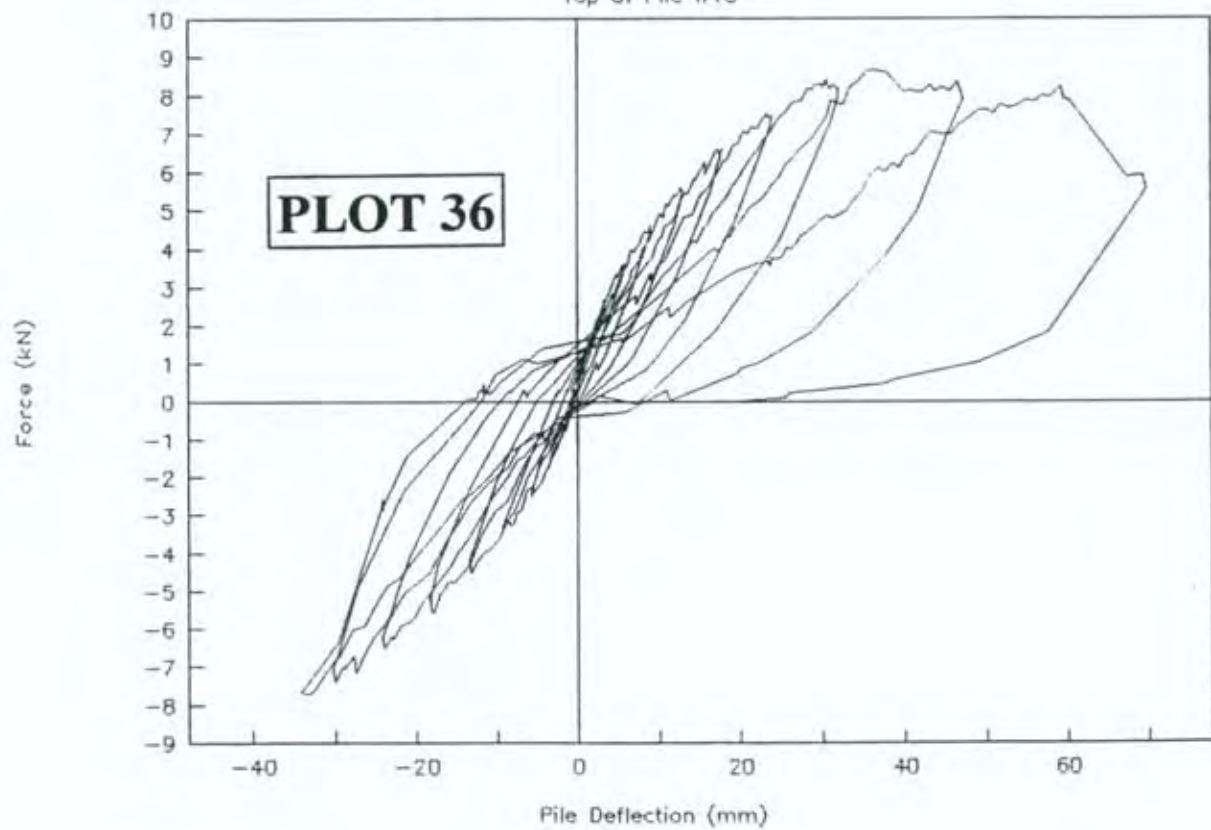
Anchor Piles V13-W13 GROUP 2

Bottom of Pile W13



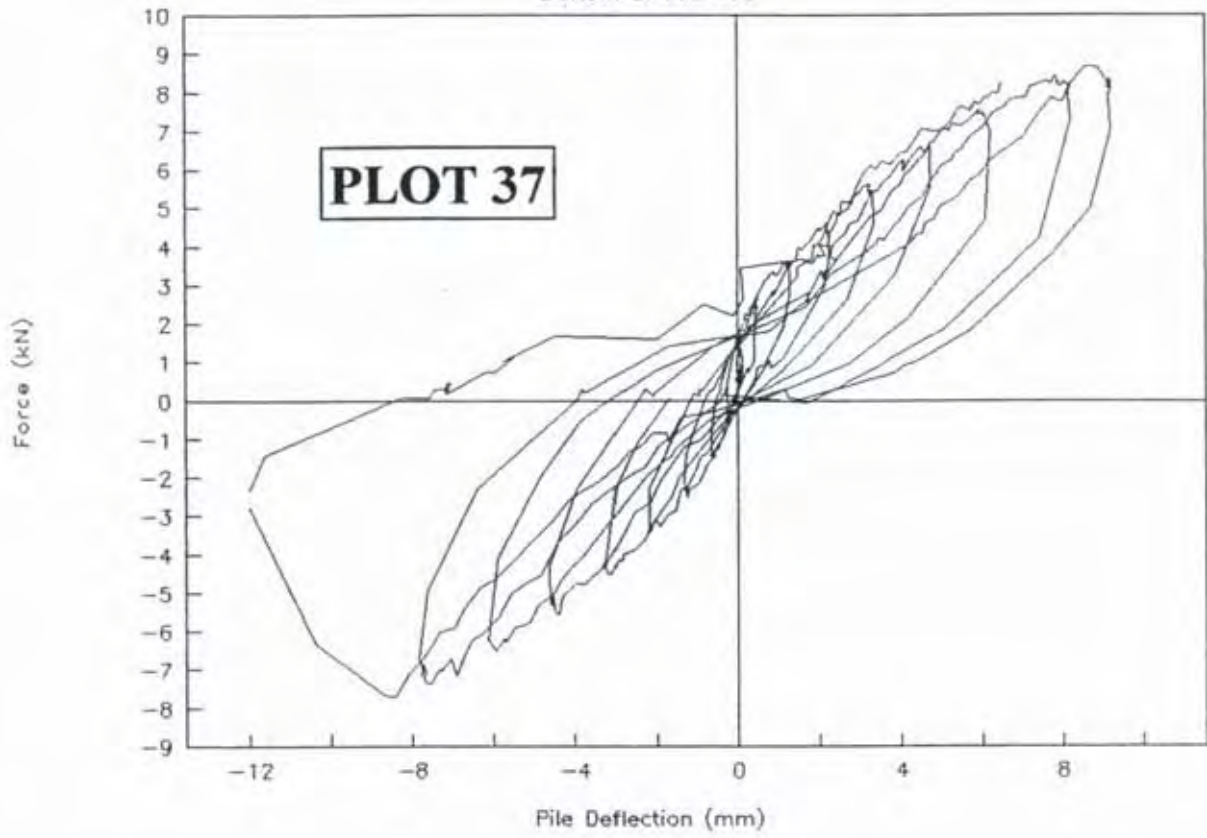
Anchor Pile V13-W13 GROUP 2

Top of Pile W13



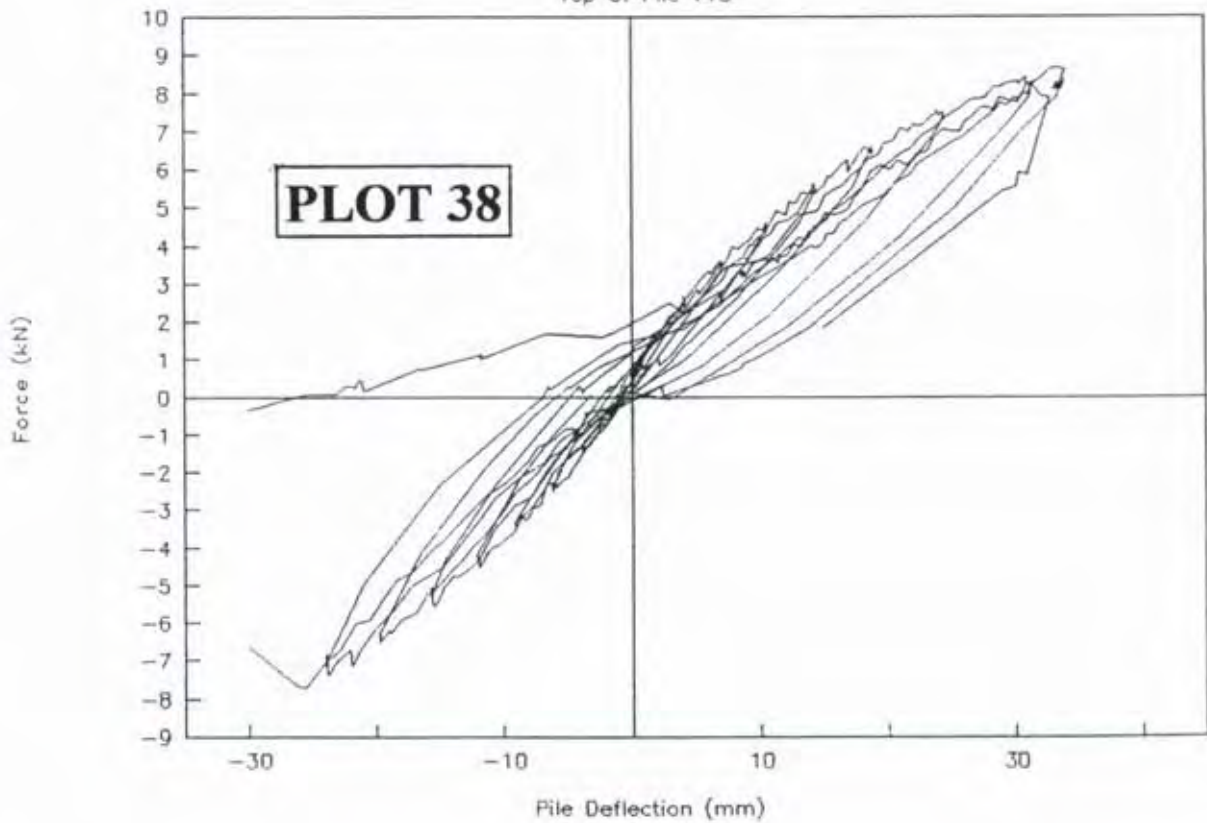
Anchor Pile V13-W13 GROUP 2

Bottom of Pile V13



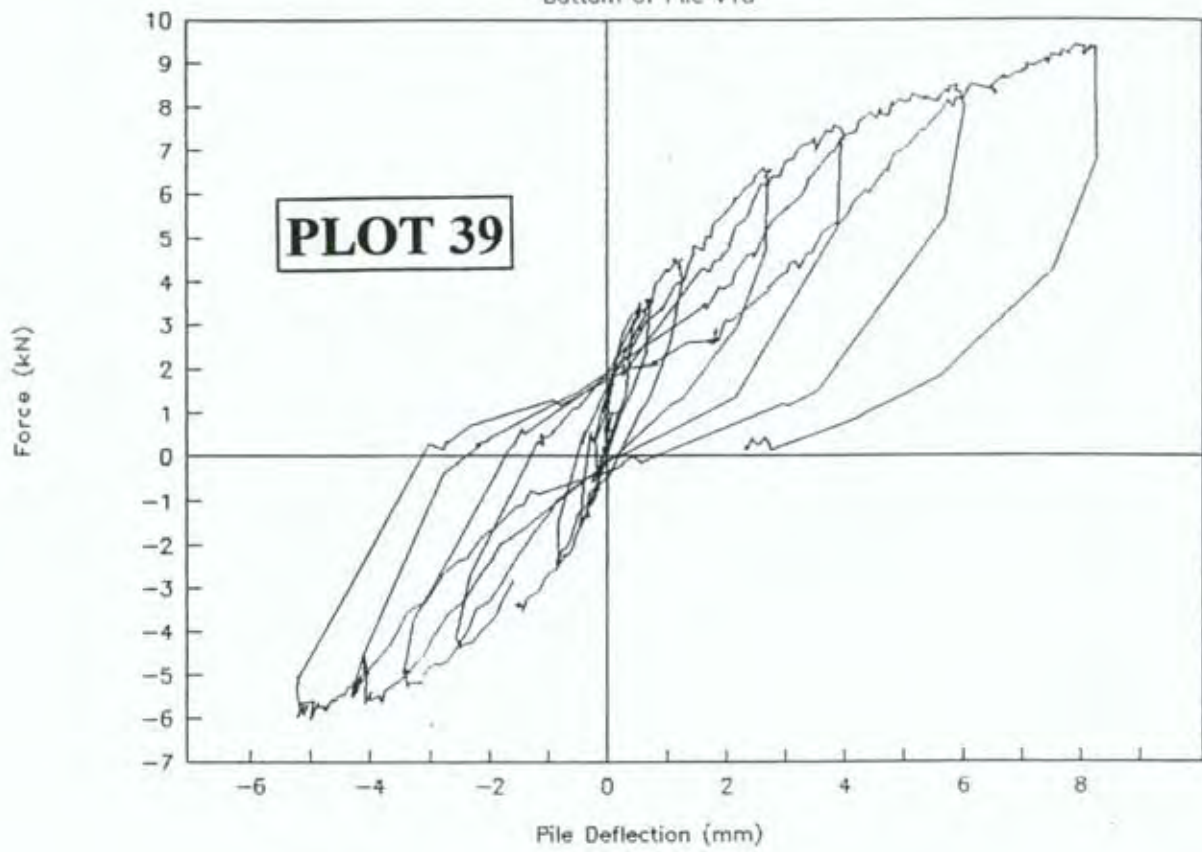
Anchor Pile V13-W13 GROUP 2

Top of Pile V13



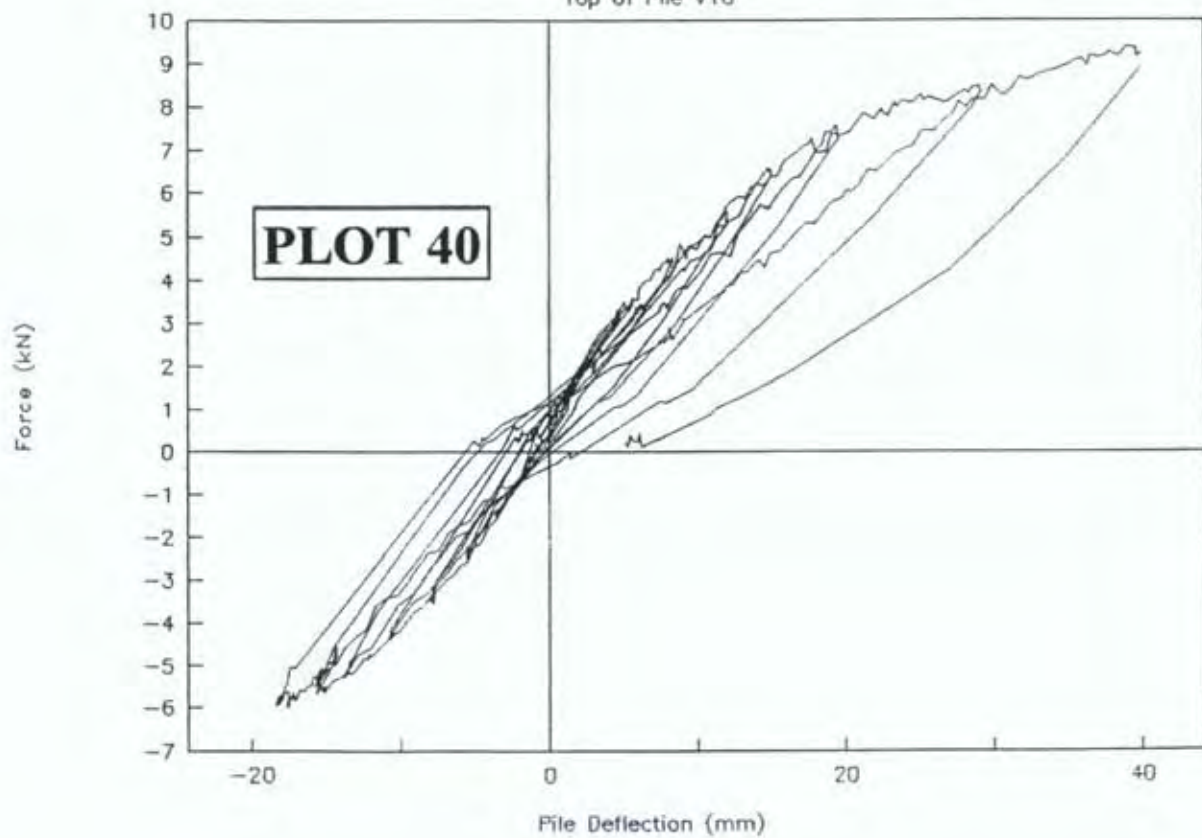
Anchor Pile V10-W10 GROUP 2

Bottom of Pile V10



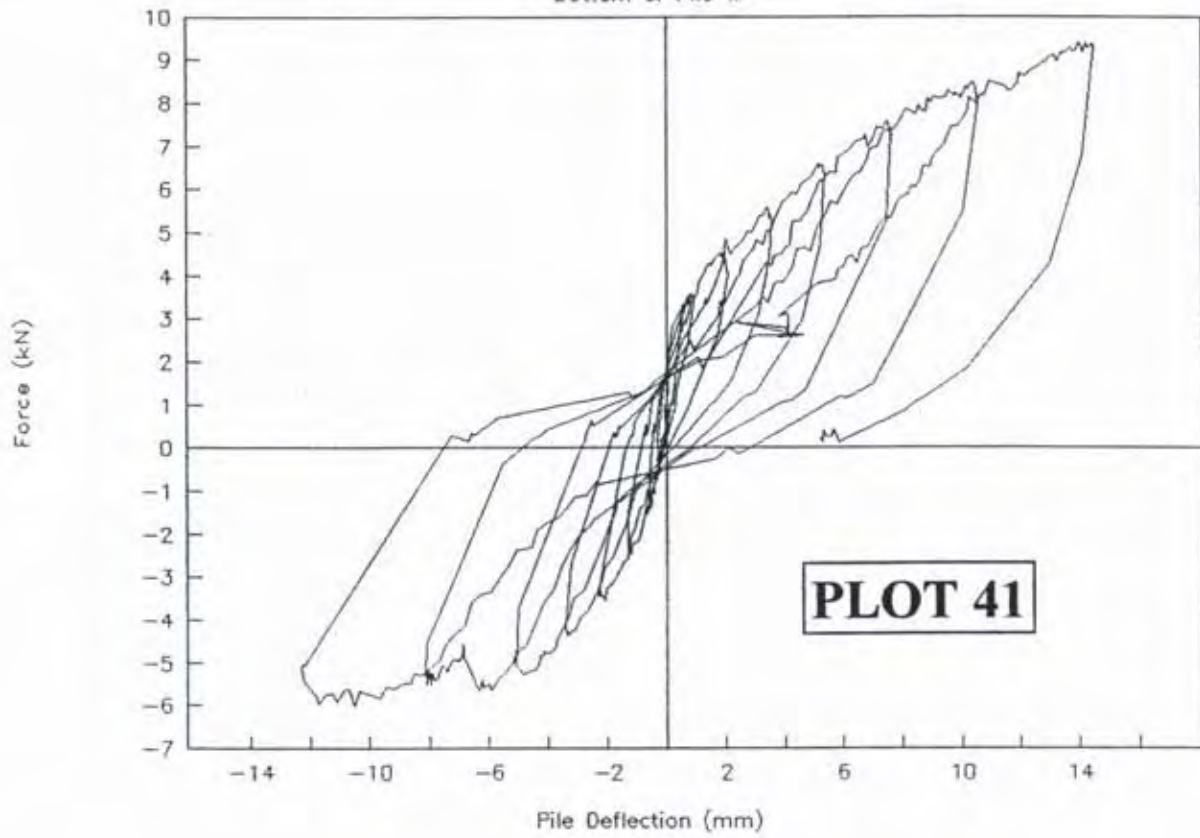
Anchor Pile Tests V10-W10 GROUP 2

Top of Pile V10



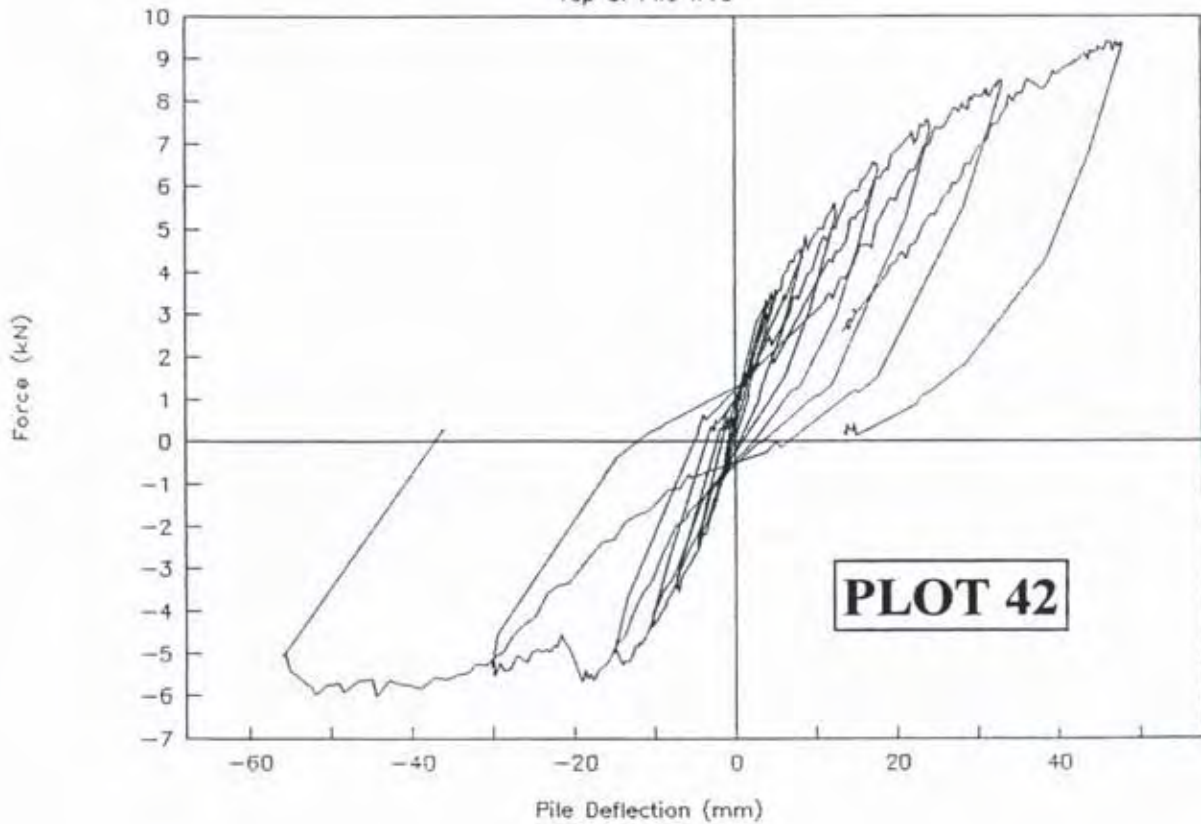
Anchor Pile Tests V10-W10 GROUP 2

Bottom of Pile W



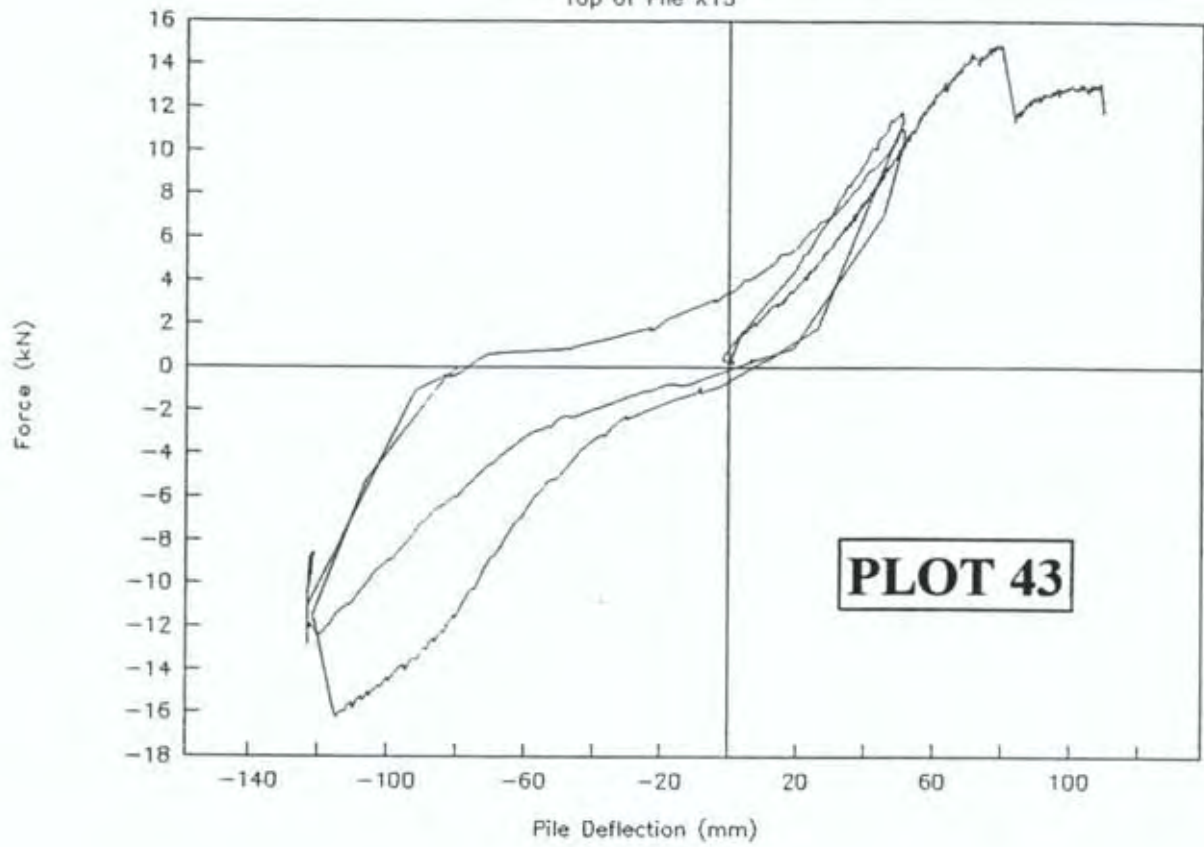
Anchor Pile Tests V10-W10 GROUP 2

Top of Pile W10



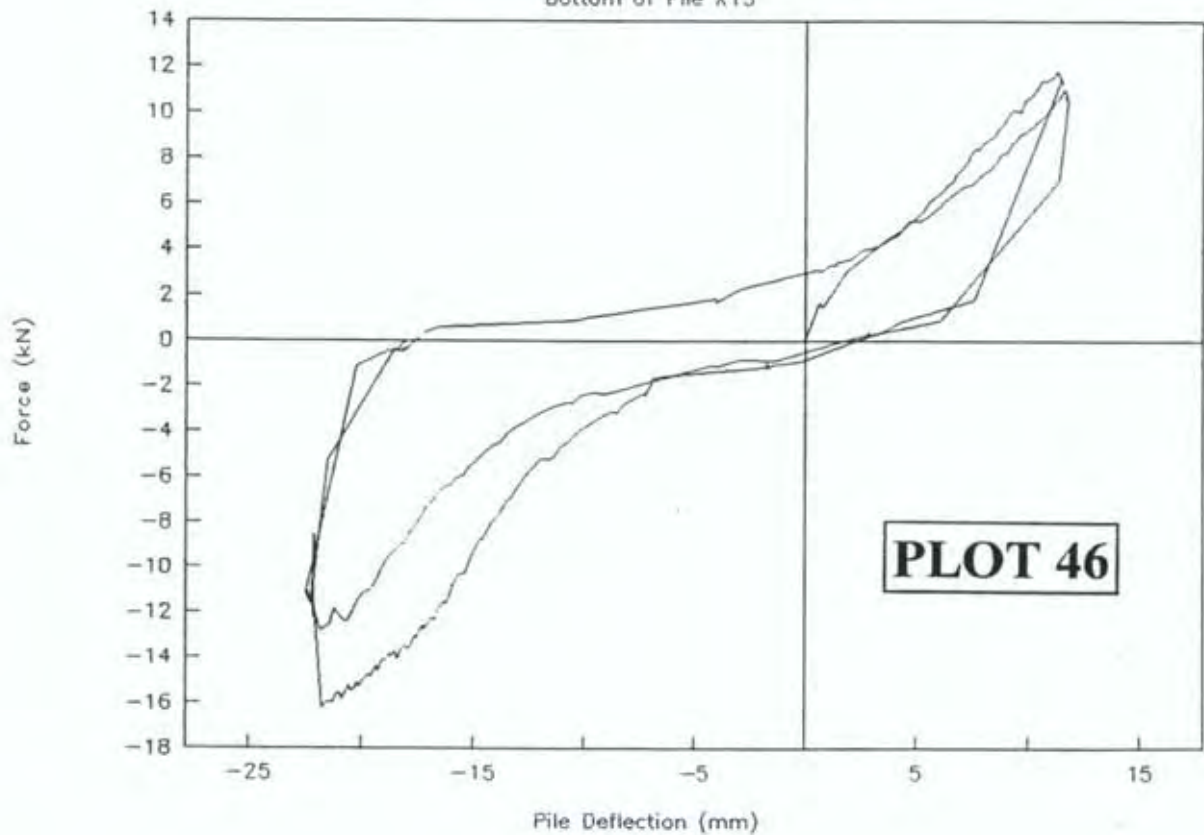
Braced Pile X13-Y13 GROUP 2

Top of Pile X13



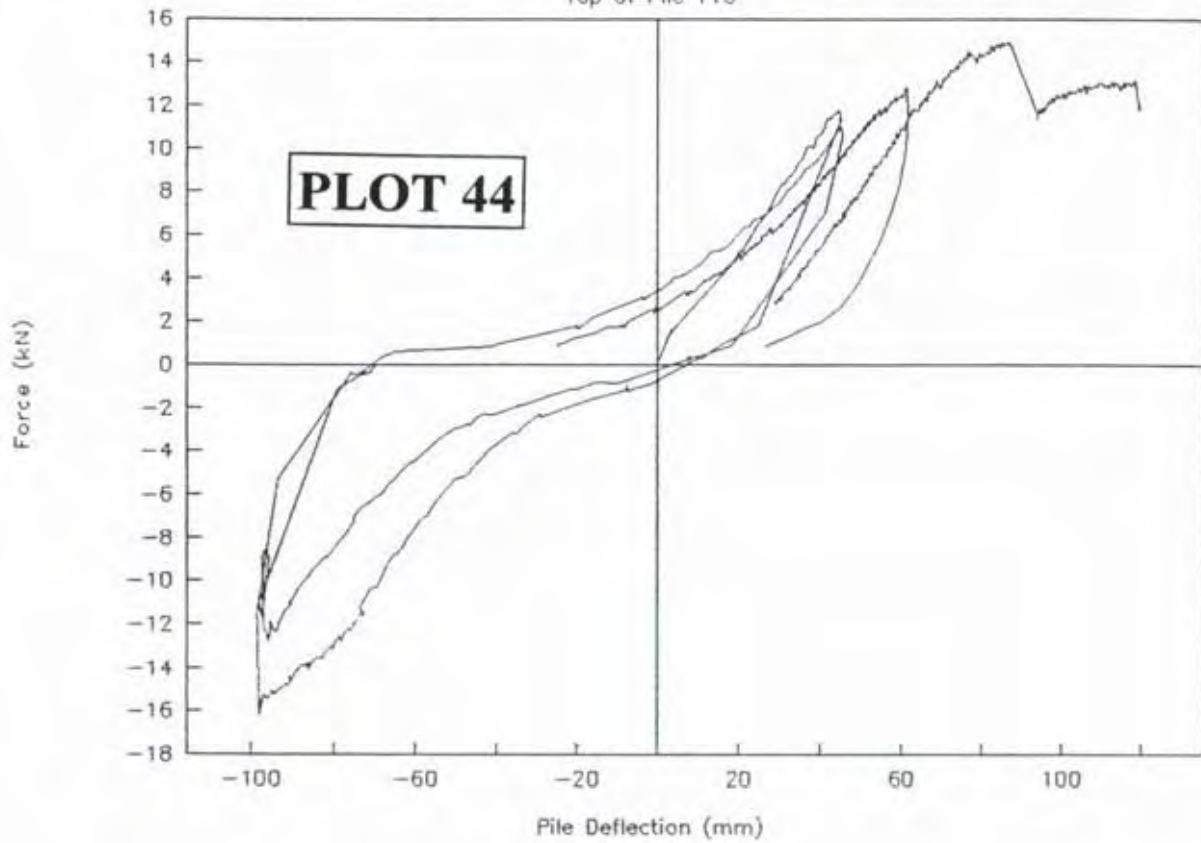
Braced Pile X13-Y13 GROUP 2

Bottom of Pile X13



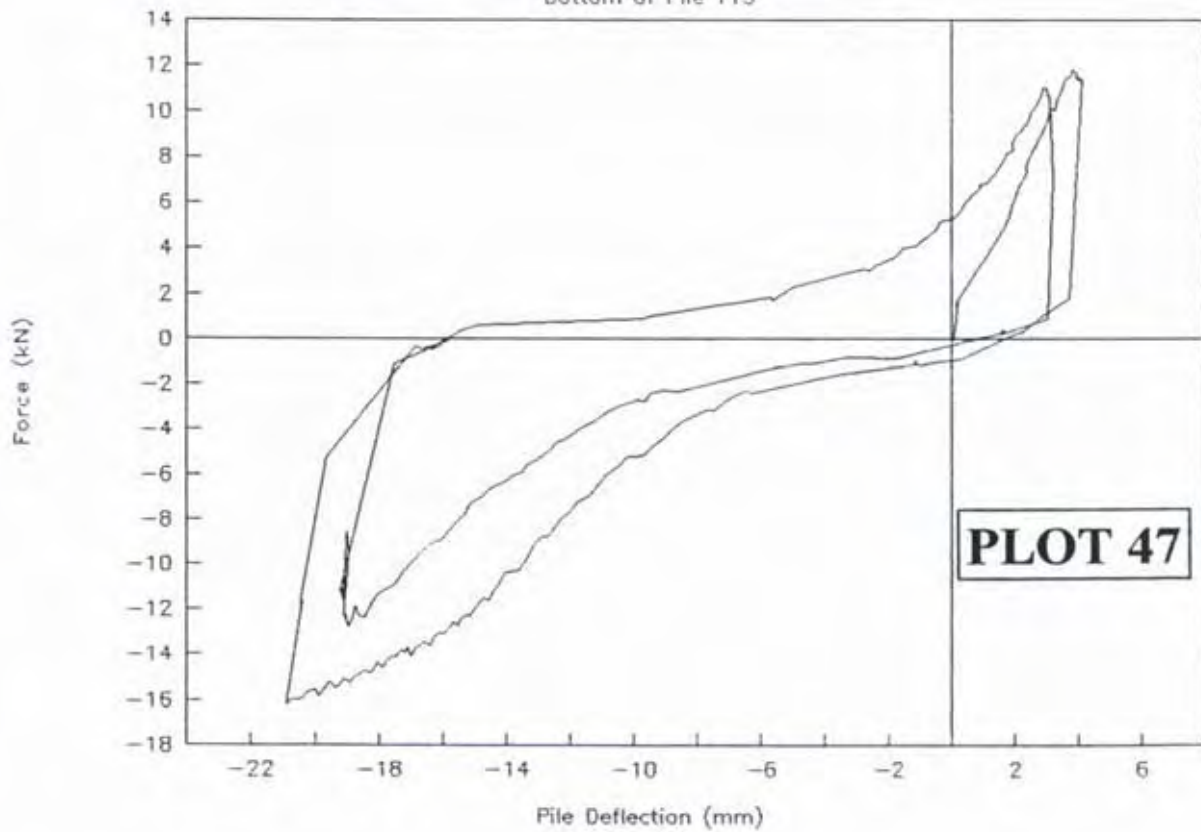
Braced Pile X13-Y13 GROUP 2

Top of Pile Y13



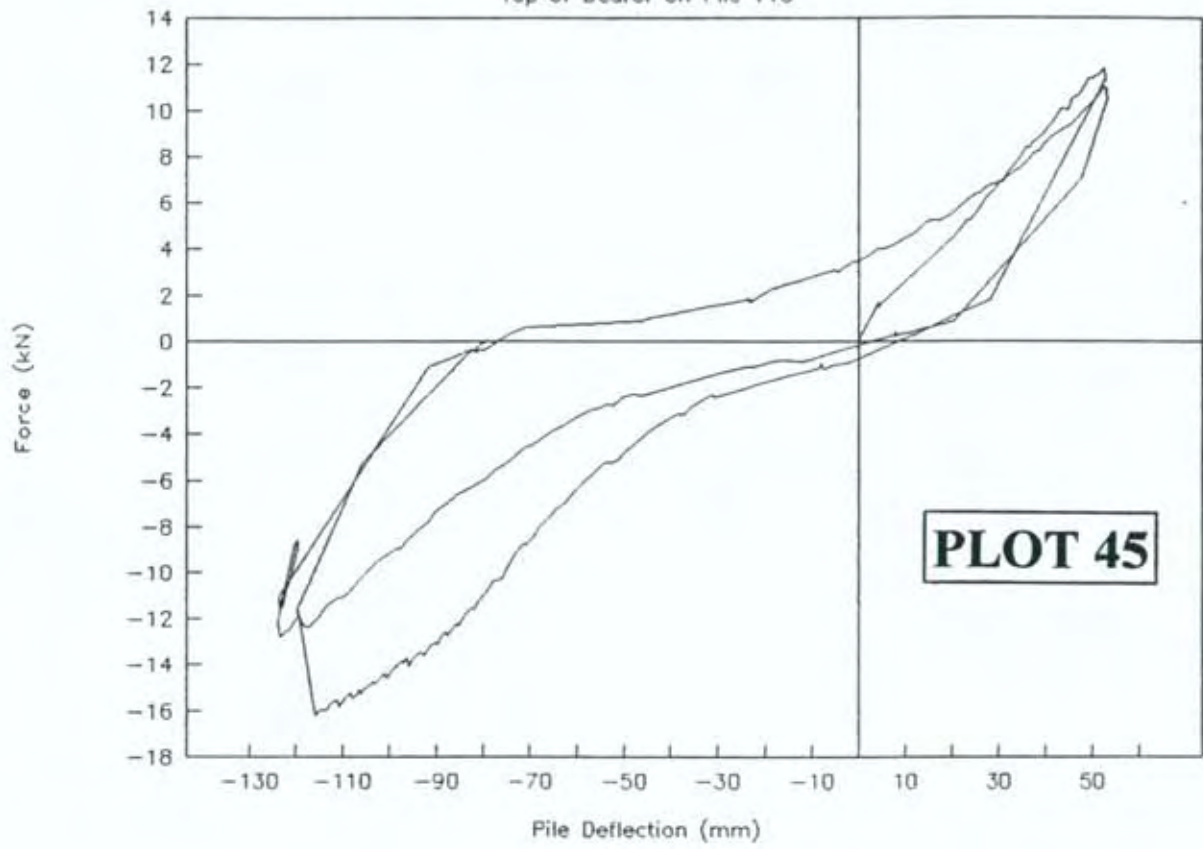
Braced Pile X13-Y13 GROUP 2

Bottom of Pile Y13



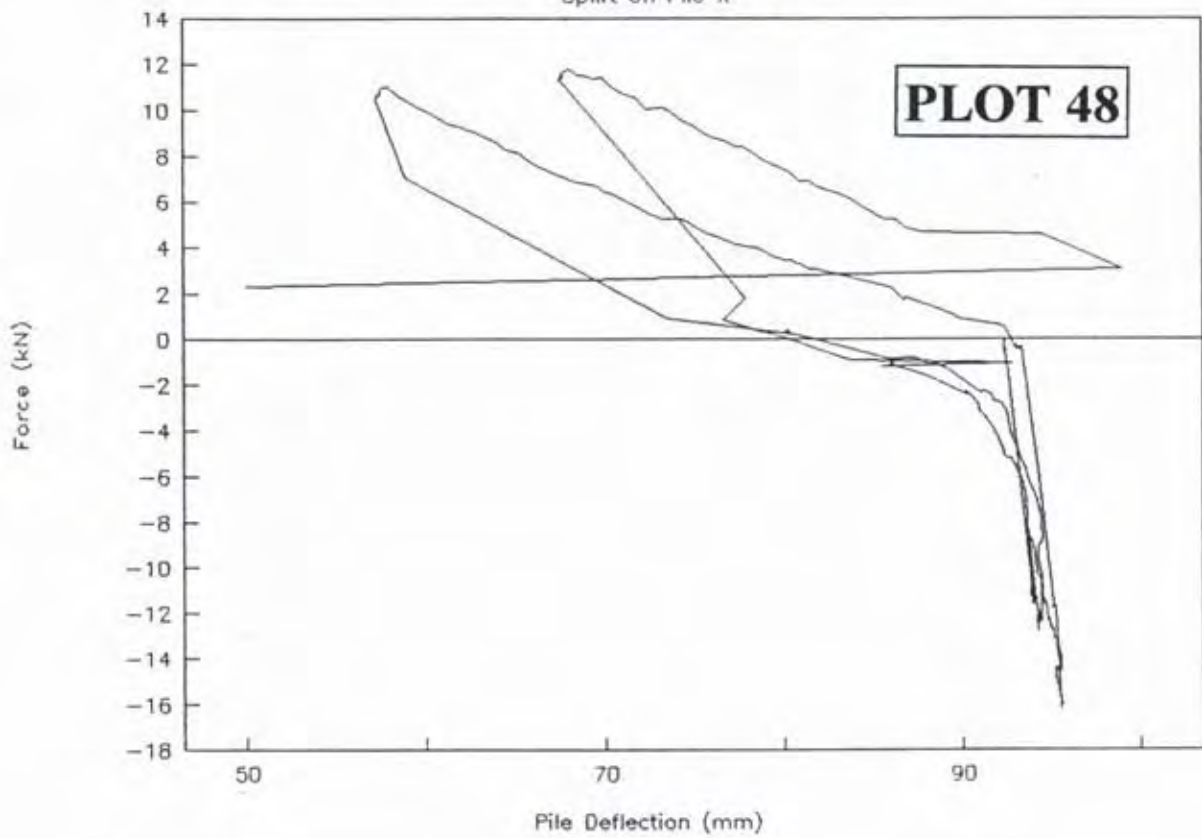
Braced Pile X13-Y13 GROUP 2

Top of Bearer on Pile Y13



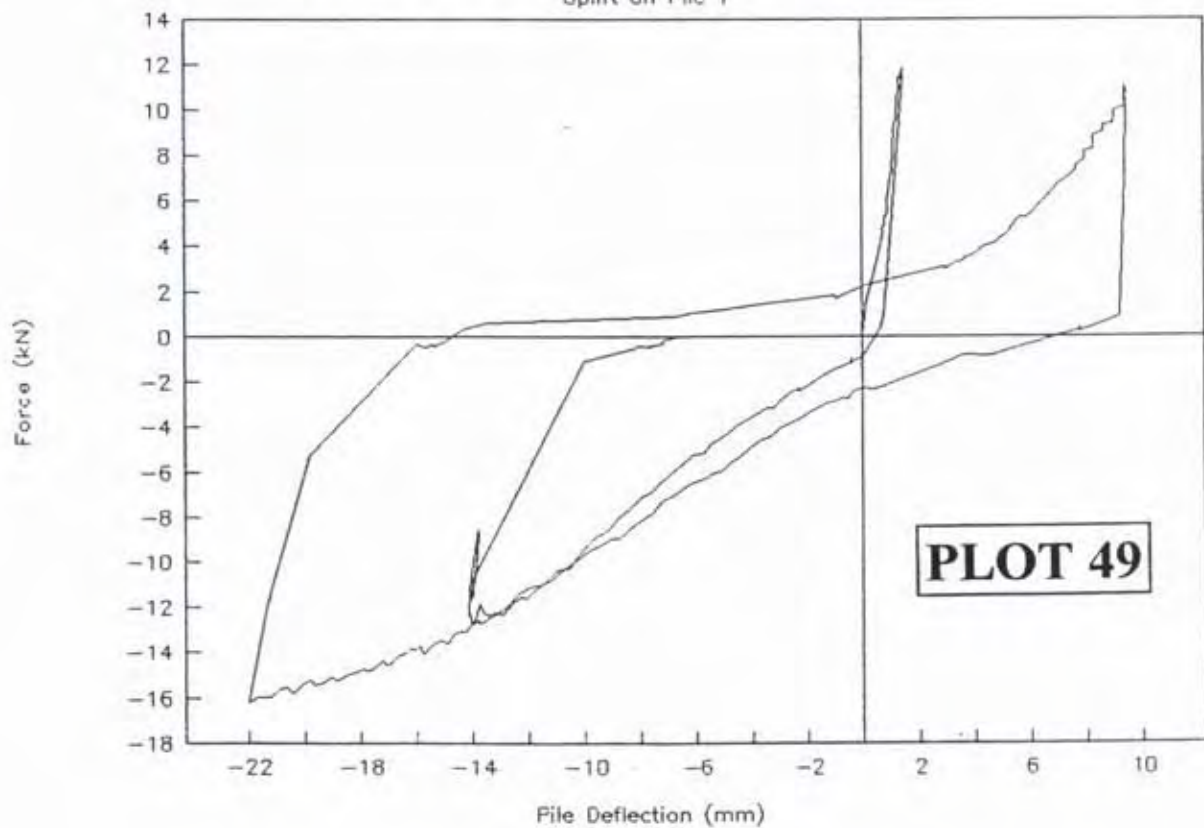
Braced Pile X13-Y13 GROUP 2

Uplift on Pile X



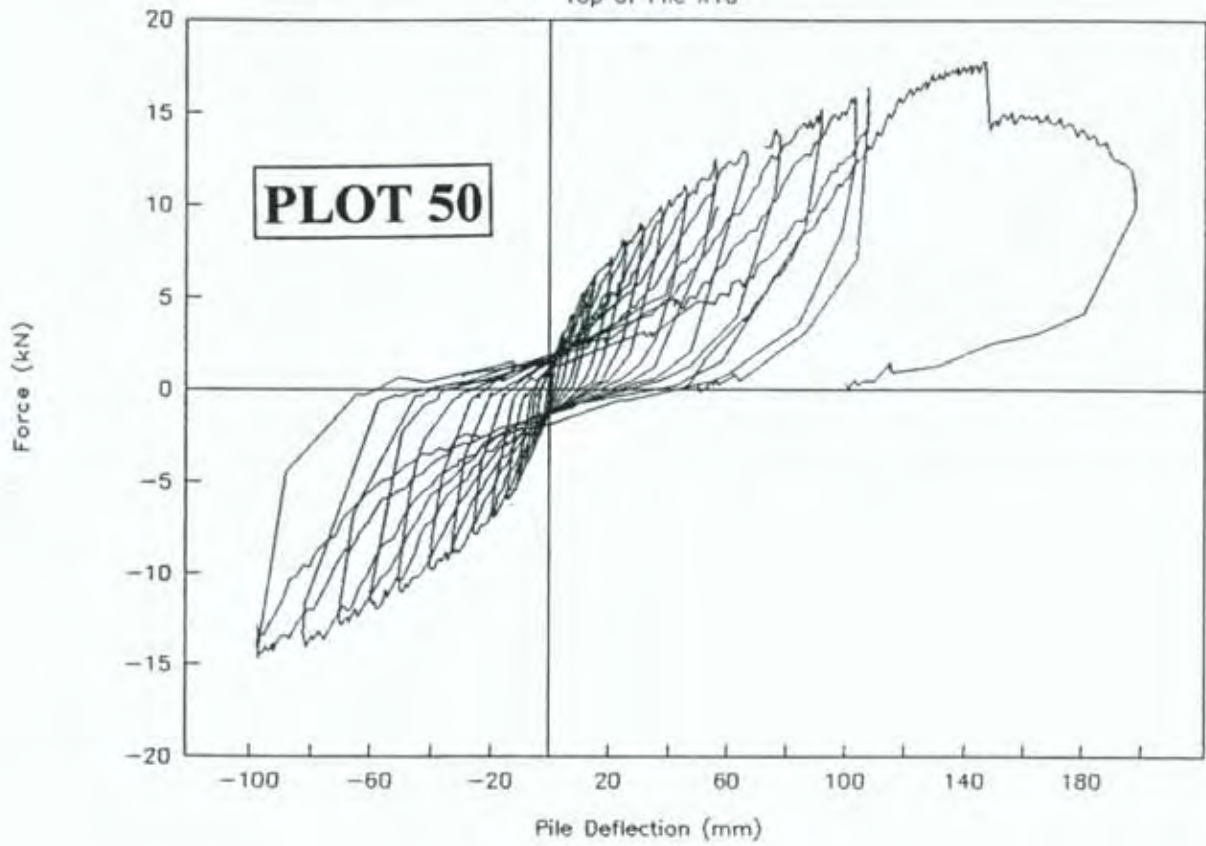
Braced Pile X13-Y13 GROUP 2

Uplift on Pile Y



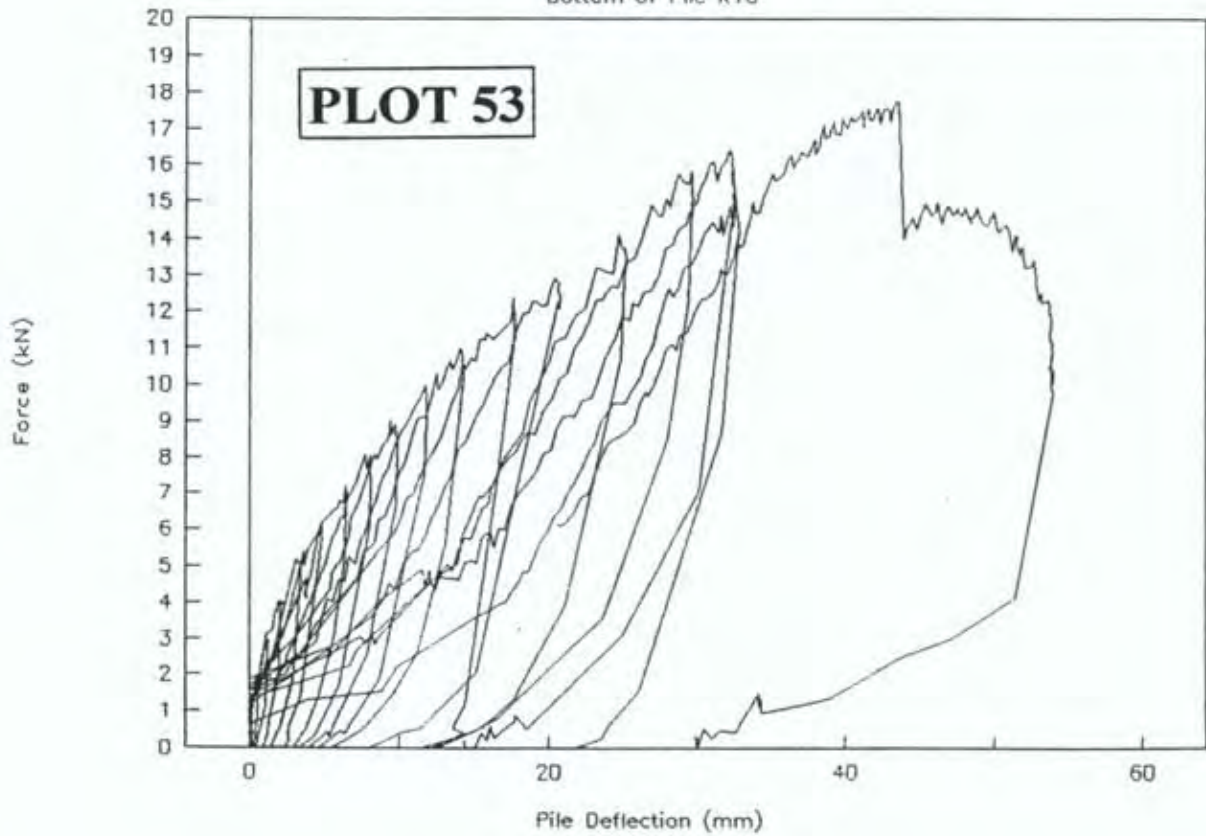
Braced Pile X10-Y10 GROUP 2

Top of Pile X10



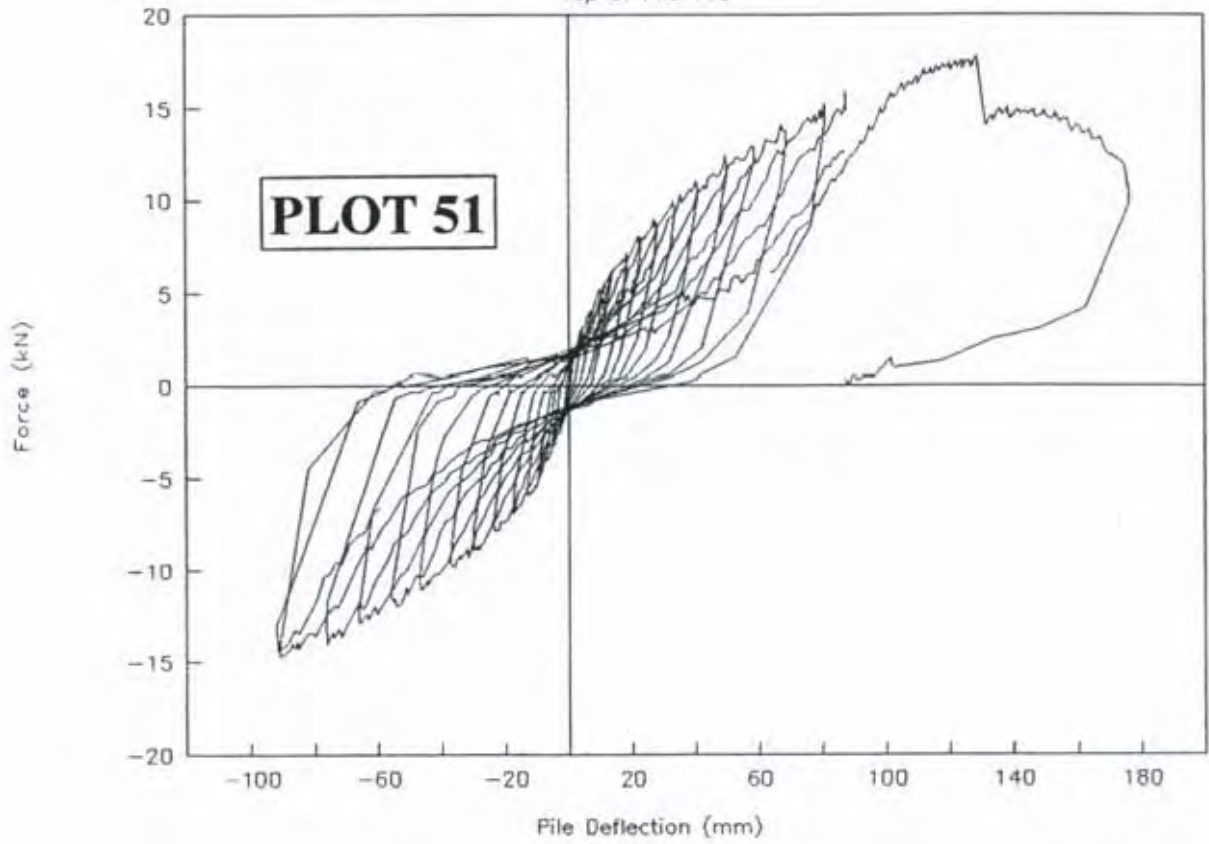
Braced Pile X10-Y10 GROUP 2

Bottom of Pile X10



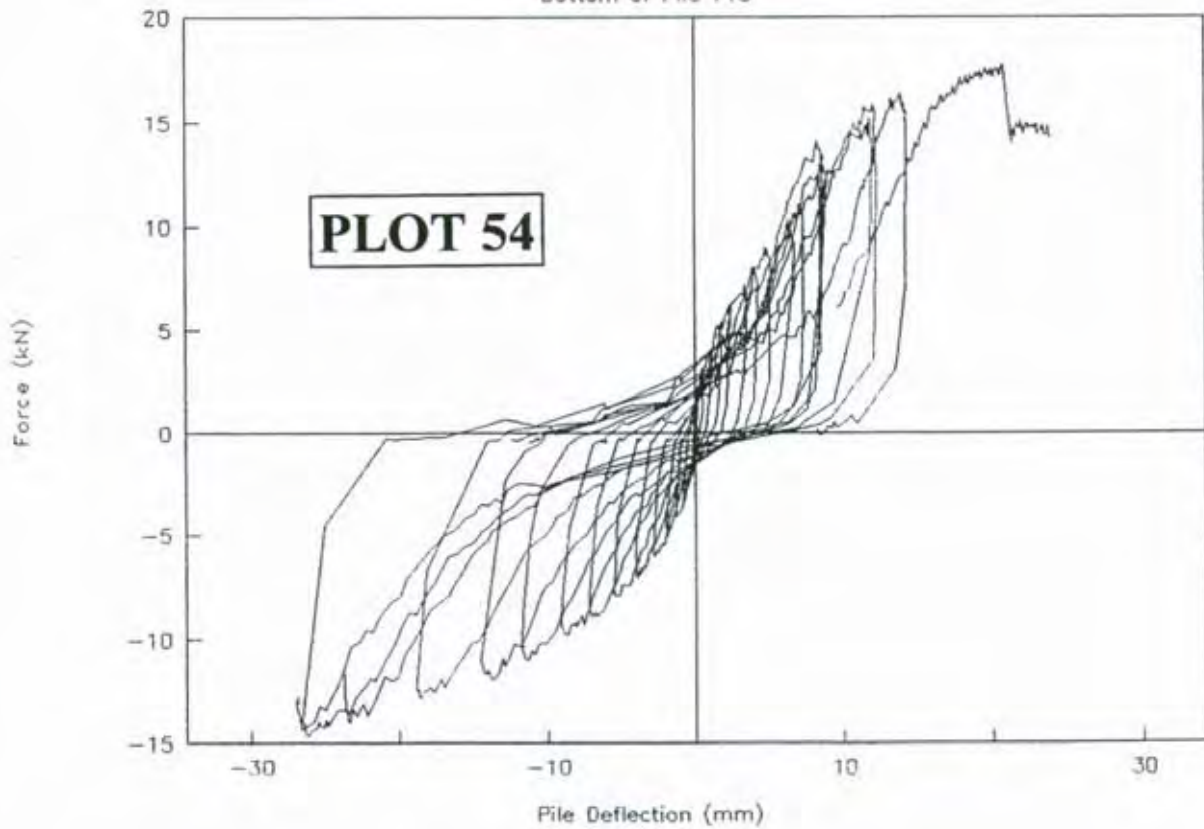
Braced Pile X10-Y10 GROUP 2

Top of Pile Y10



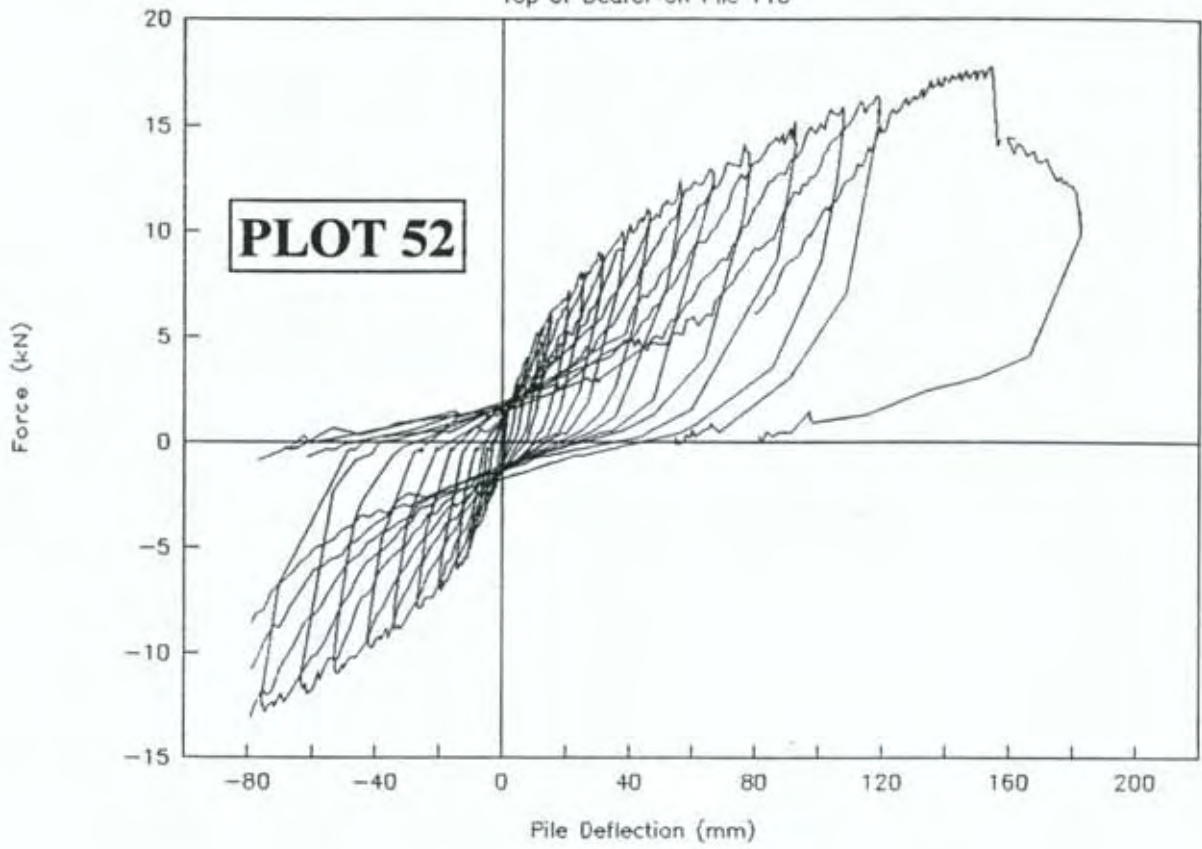
Braced Pile X10-Y10 GROUP 2

Bottom of Pile Y10



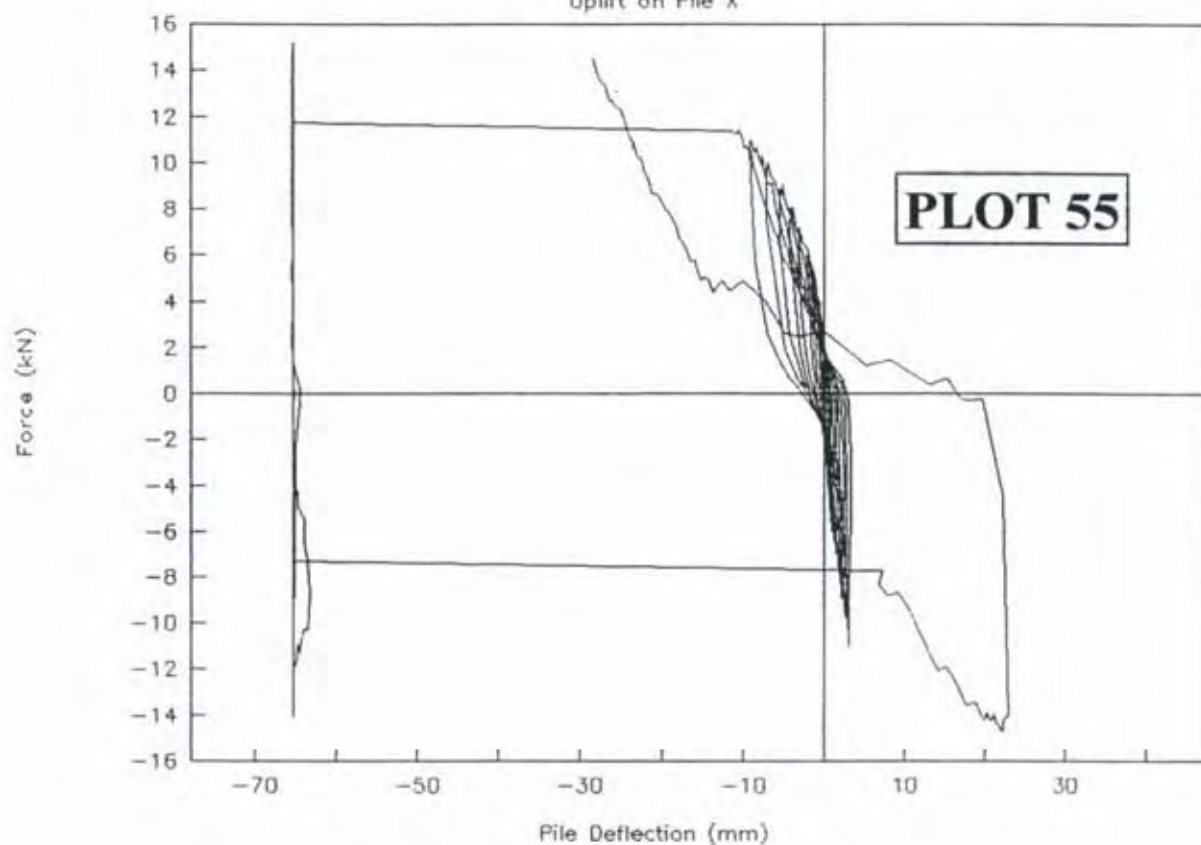
Braced Pile X10-Y10 GROUP 2

Top of Bearer on Pile Y10



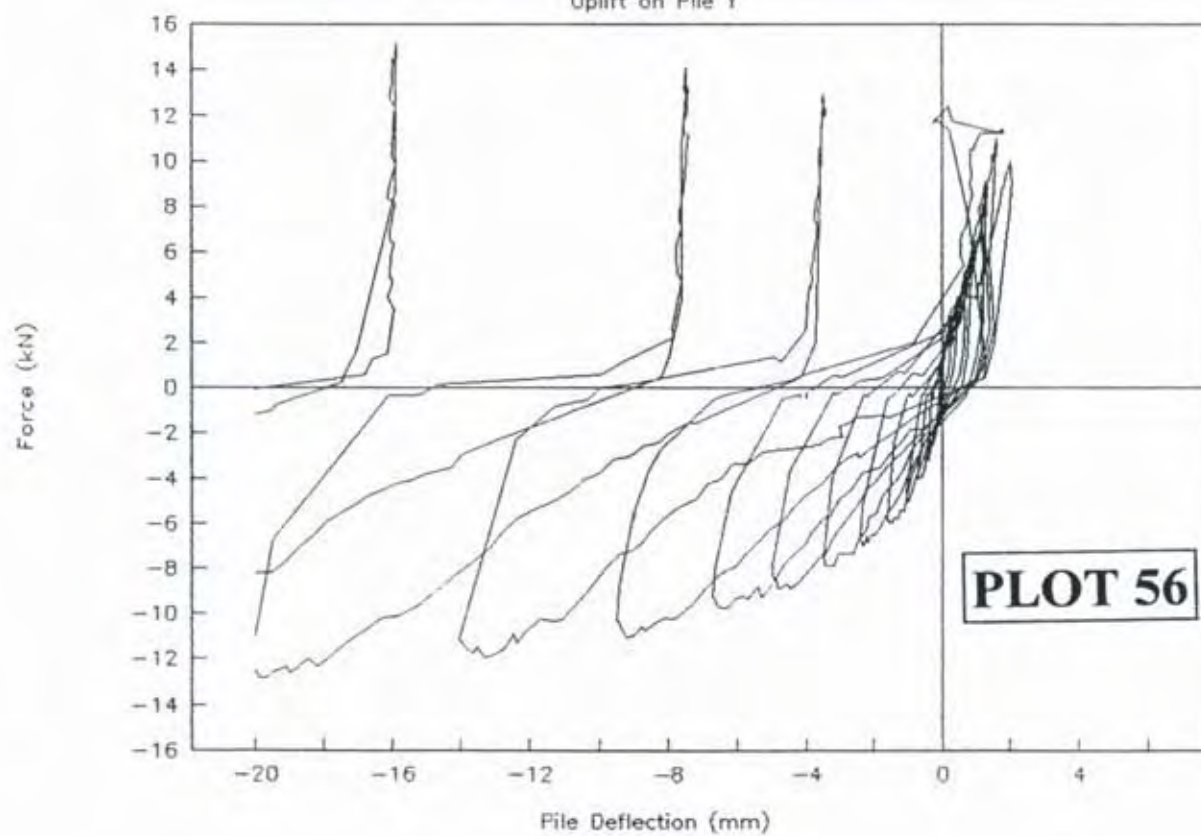
Braced Pile X10-Y10 GROUP 2

Uplift on Pile X



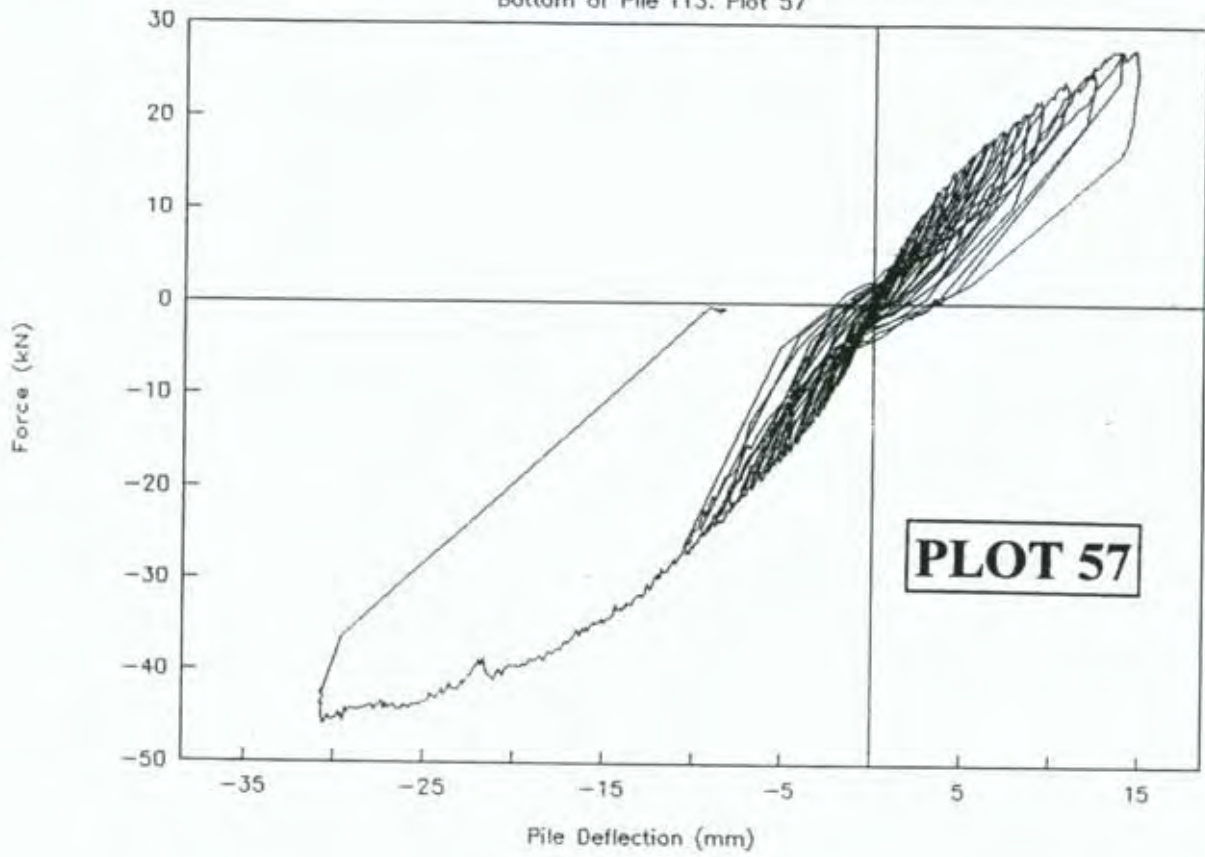
Braced Pile X10-Y10 GROUP 2

Uplift on Pile Y



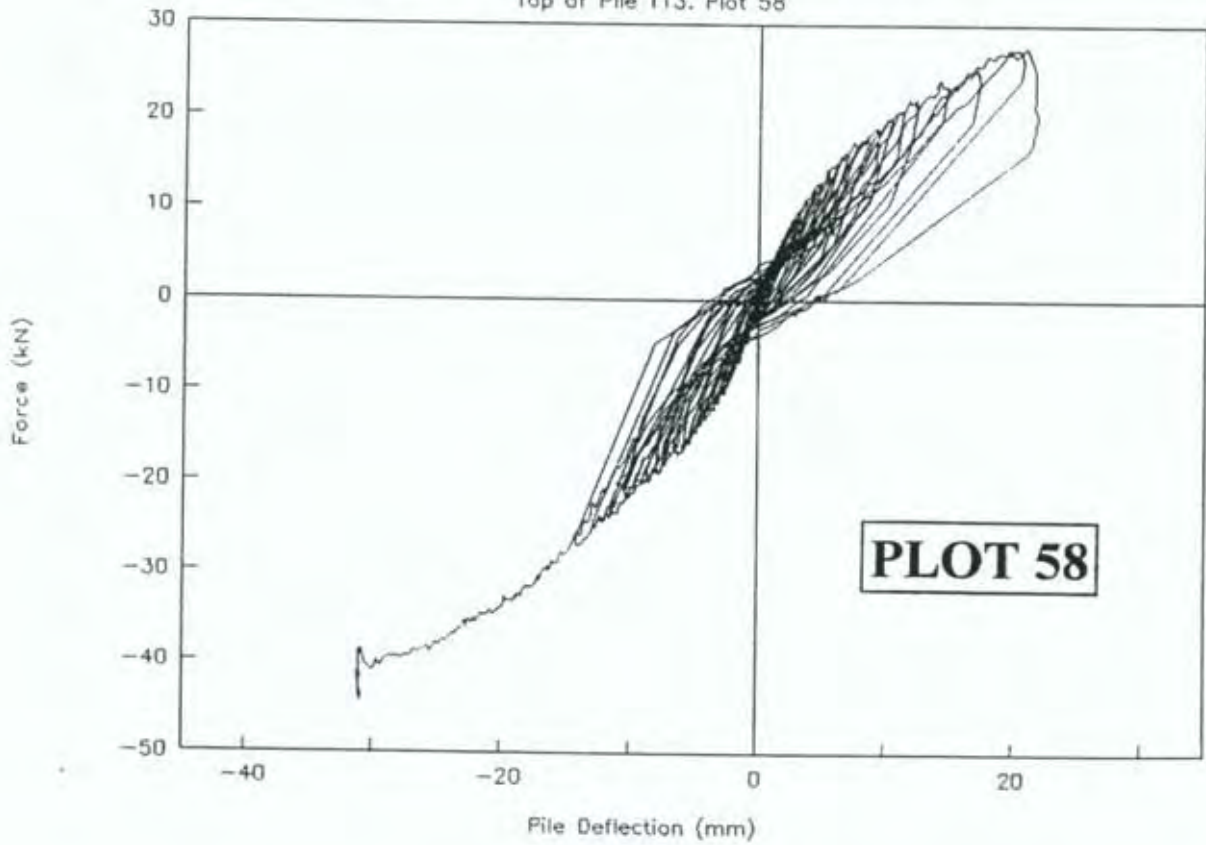
Shear Piles T13-U13 GROUP 2

Bottom of Pile T13. Plot 57



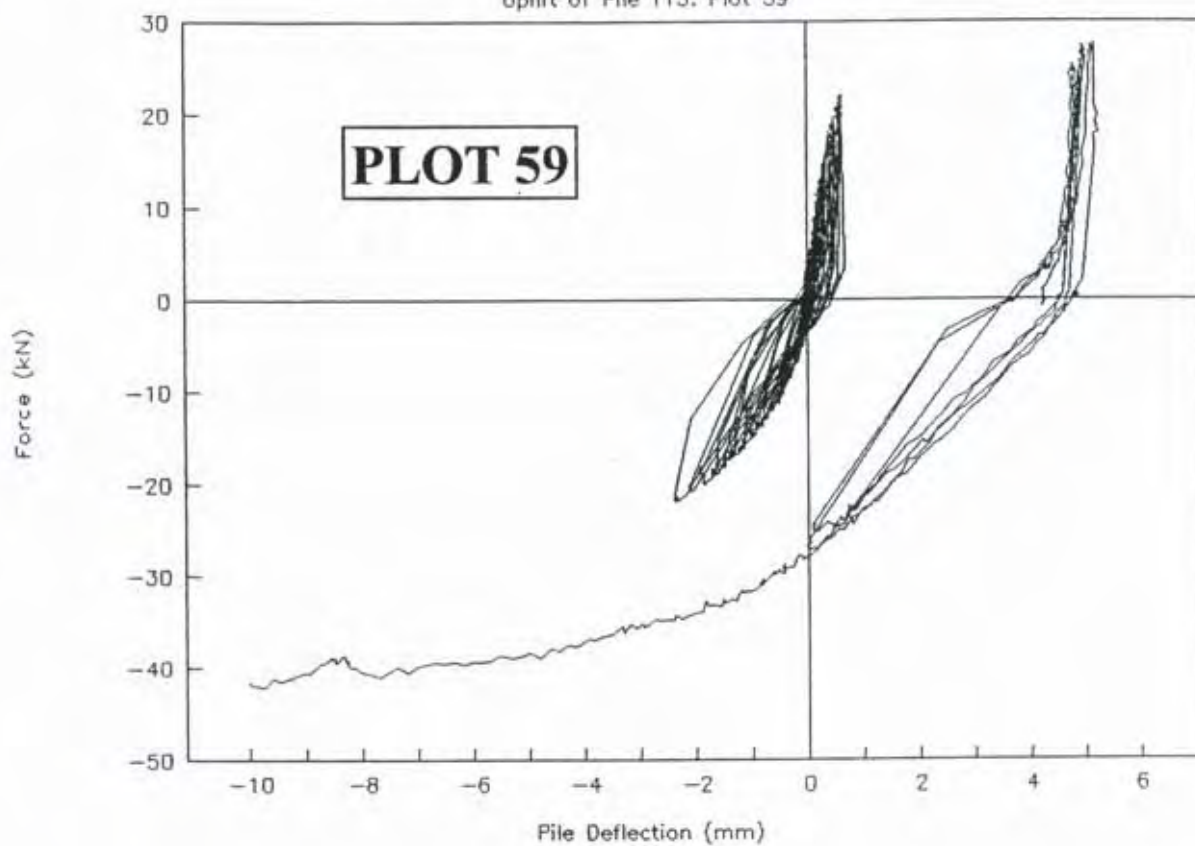
Shear Piles T13-U13 GROUP 2

Top of Pile T13. Plot 58



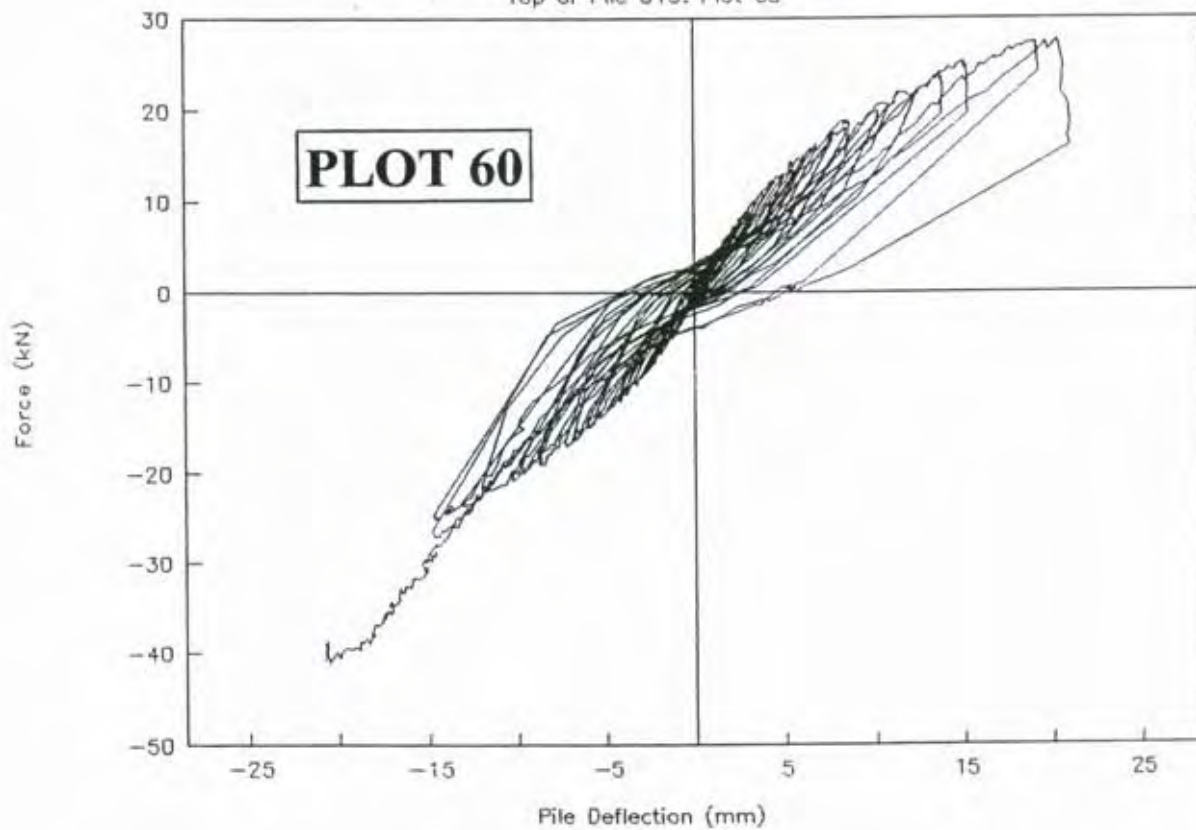
Shear Piles T13-U13 GROUP 2

Uplift of Pile T13. Plot 59



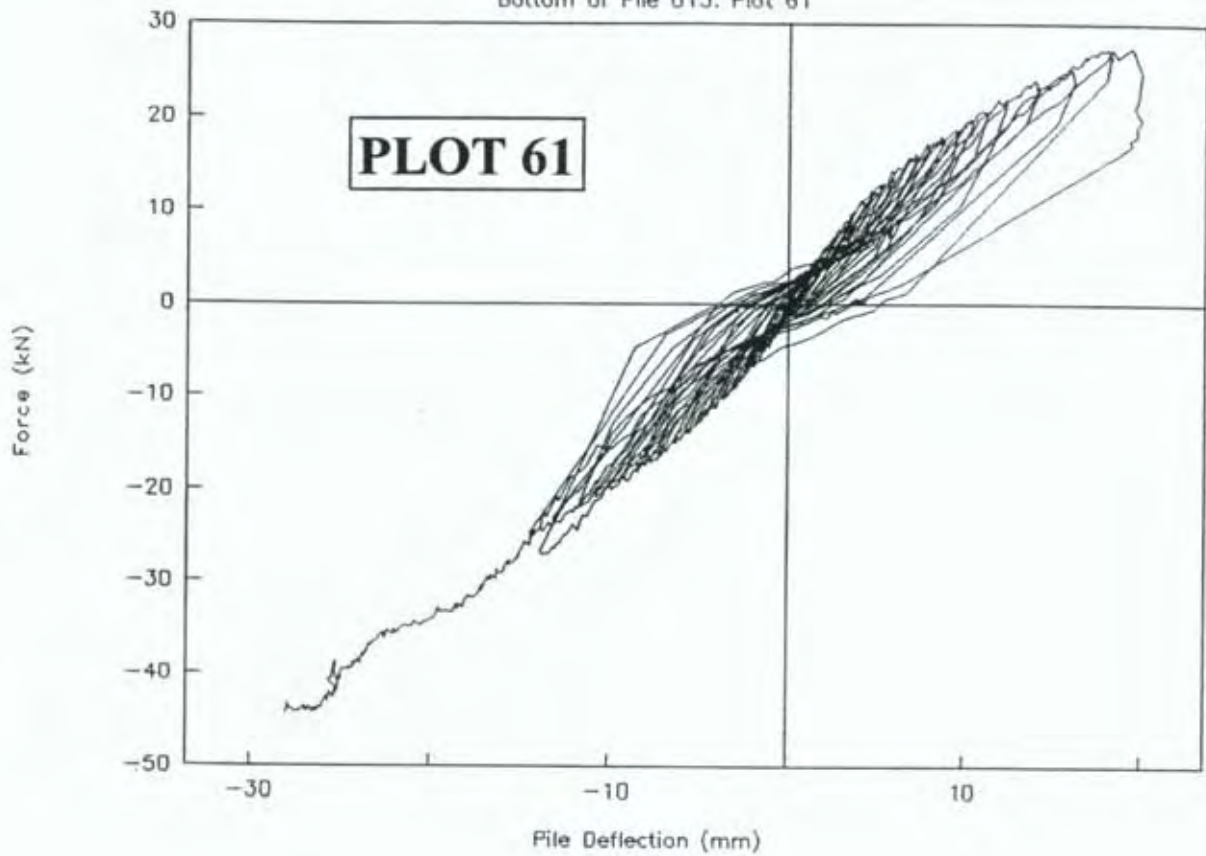
Shear Piles T13-U13 GROUP 2

Top of Pile U13. Plot 60



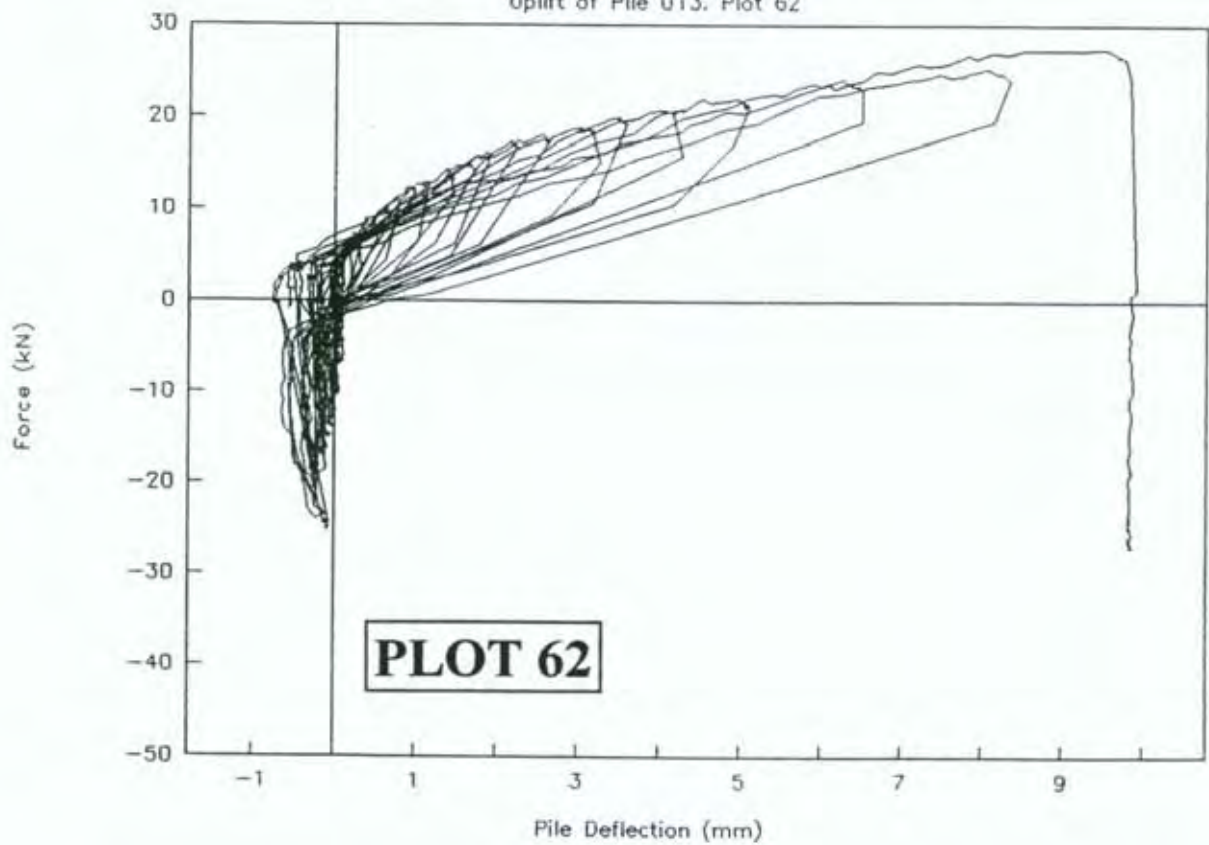
Shear Piles T13-U13 GROUP 2

Bottom of Pile U13. Plot 61



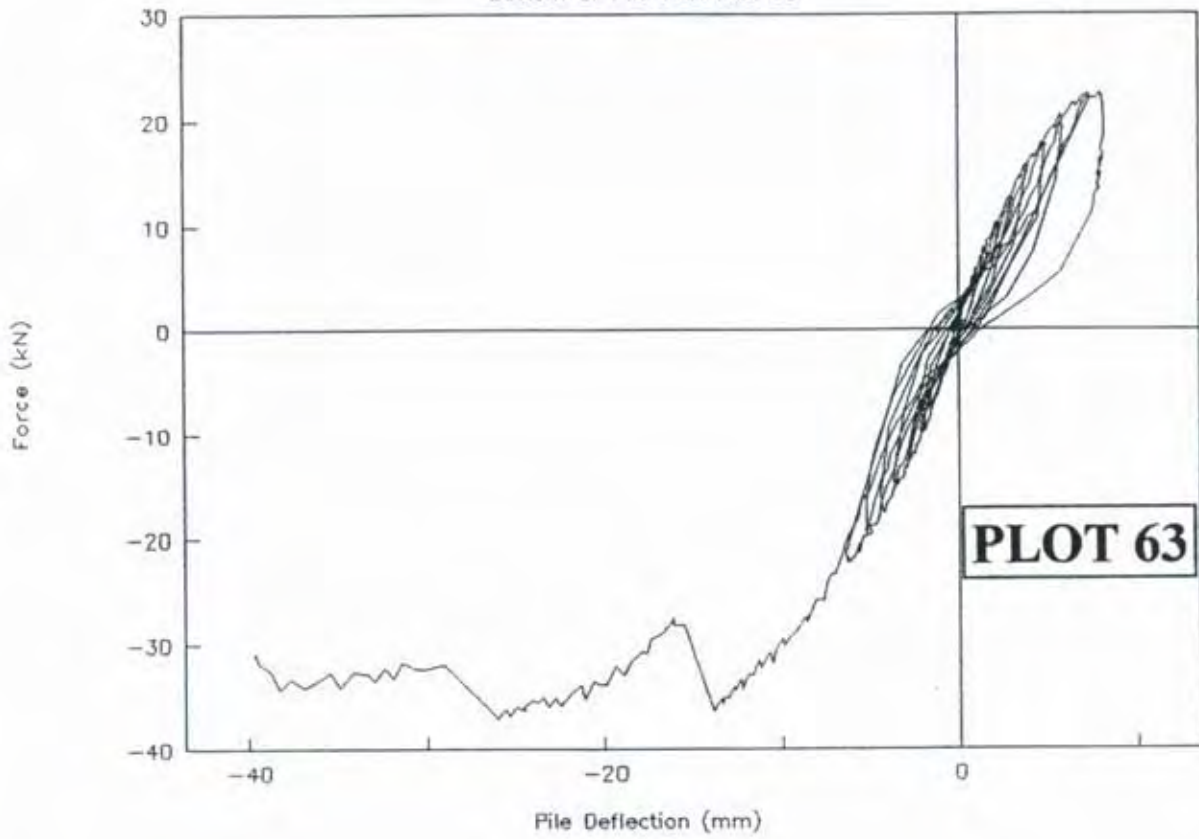
Shear Piles T13-U13 GROUP 2

Uplift of Pile U13. Plot 62



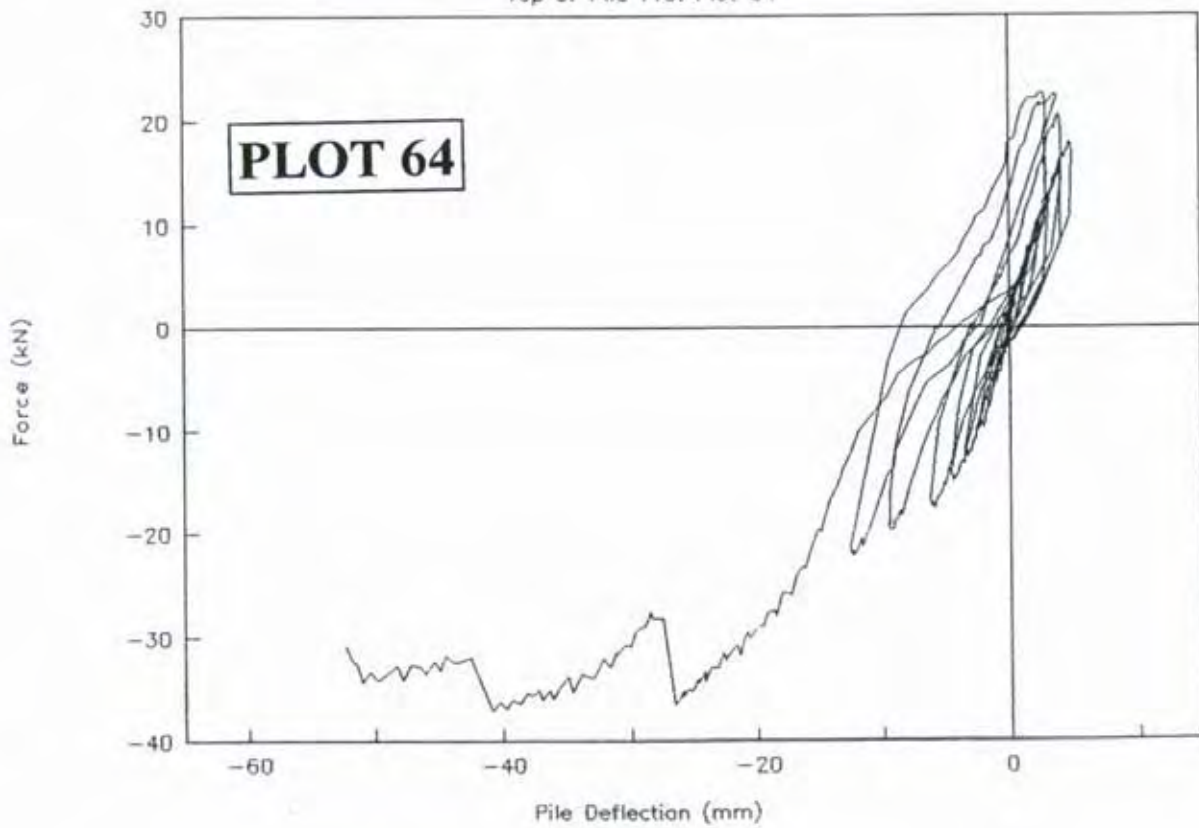
Shear Piles T10-U10 GROUP 2

Bottom of Pile T10. Plot 63



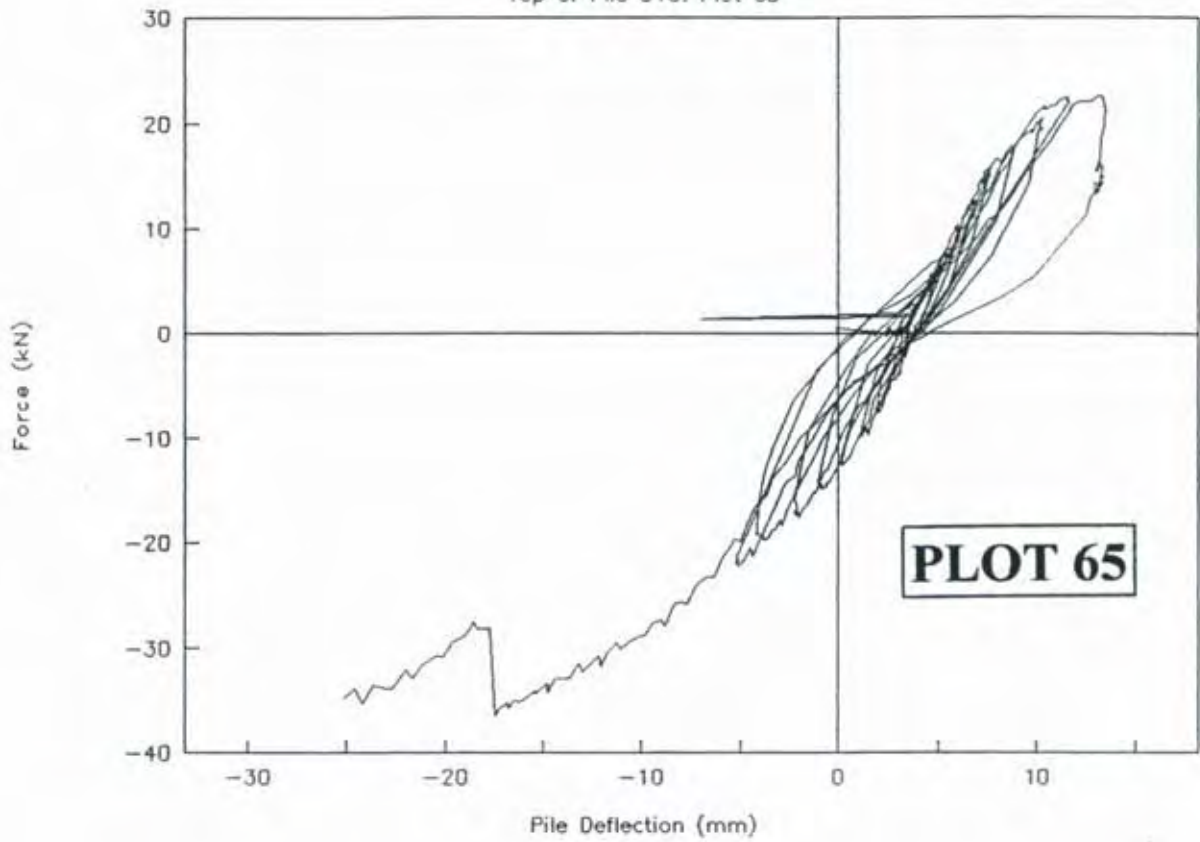
Shear Piles T10-U10 GROUP 2

Top of Pile T10. Plot 64



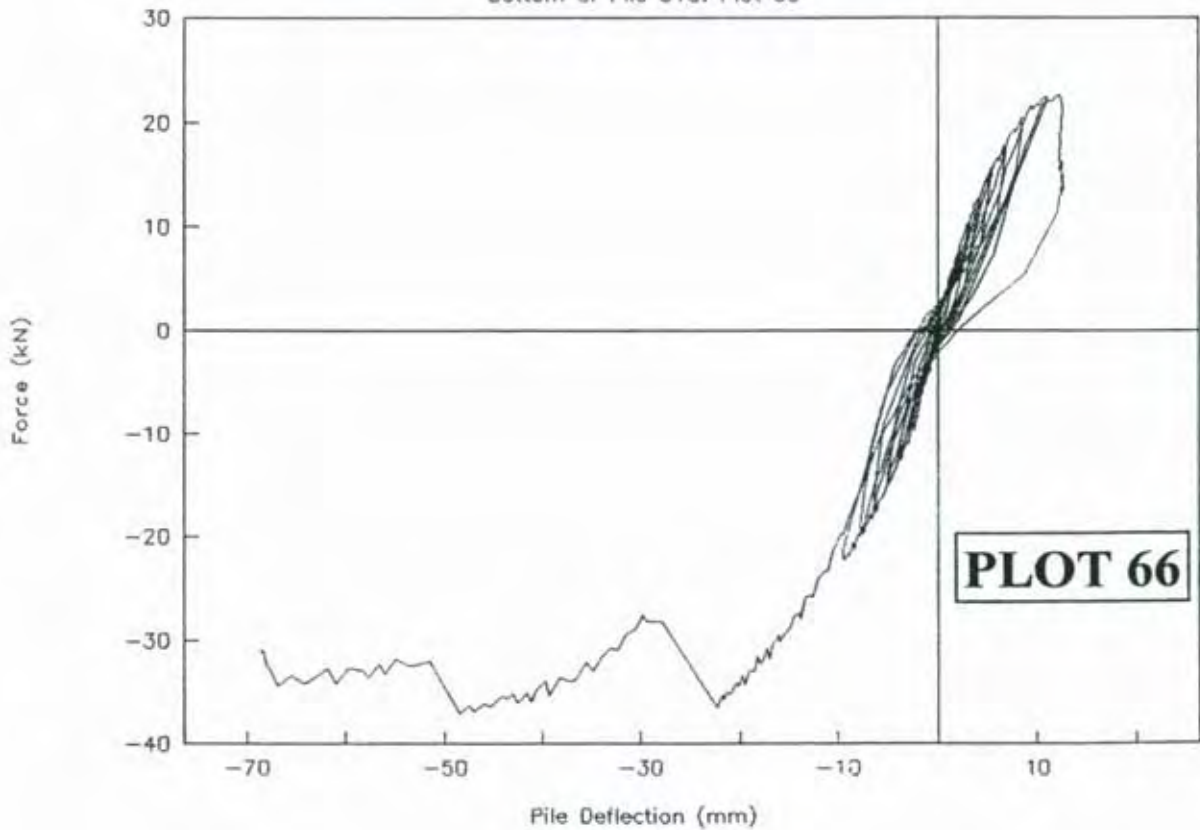
Shear Piles T10-U10 GROUP 2

Top of Pile U10. Plot 65



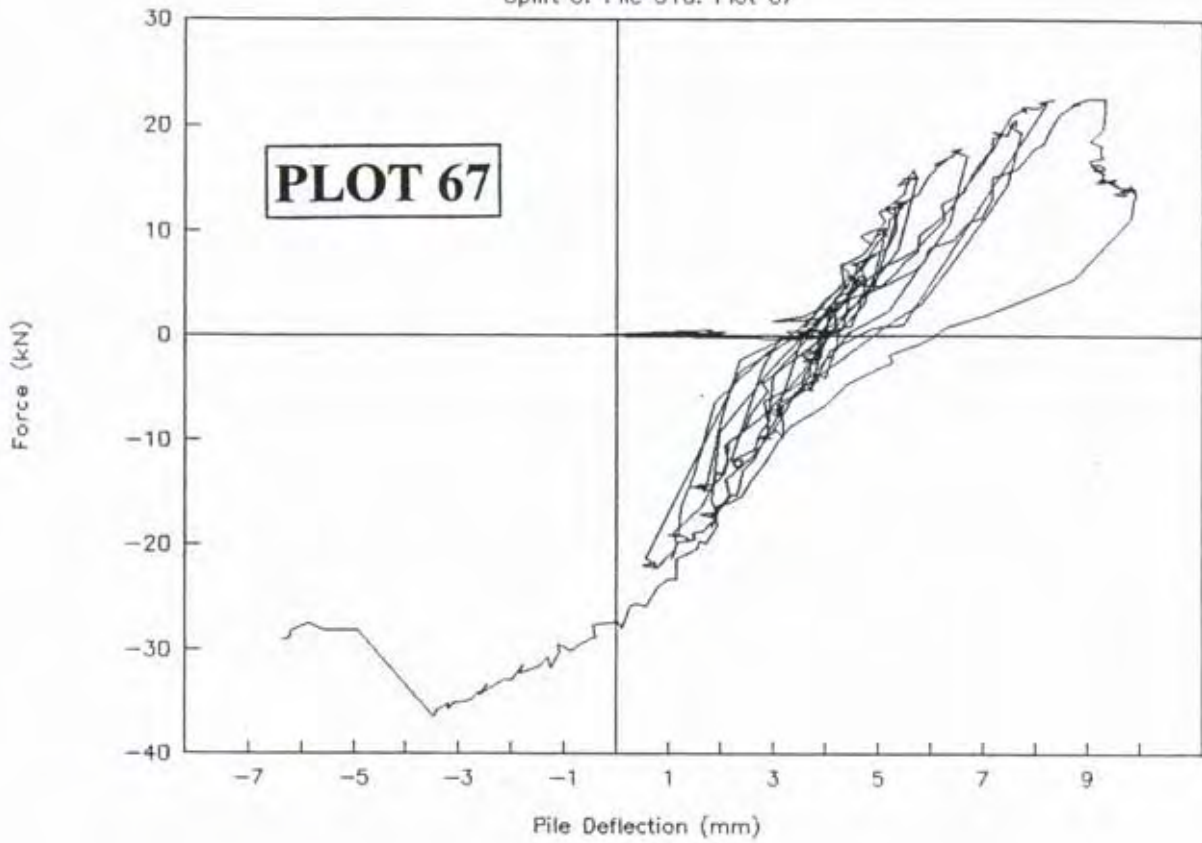
Shear Piles T10-U10 GROUP 2

Bottom of Pile U10. Plot 66



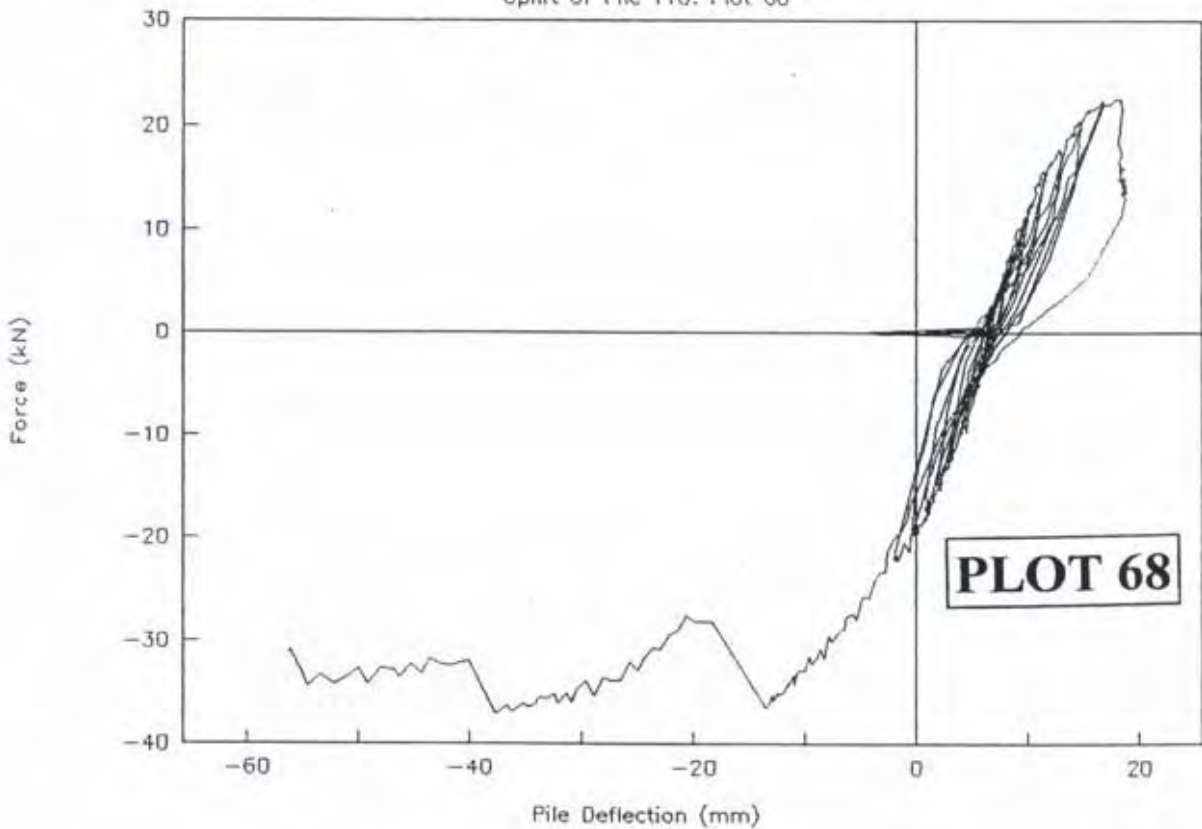
Shear Piles T10-U10 GROUP 2

Uplift of Pile U10. Plot 67



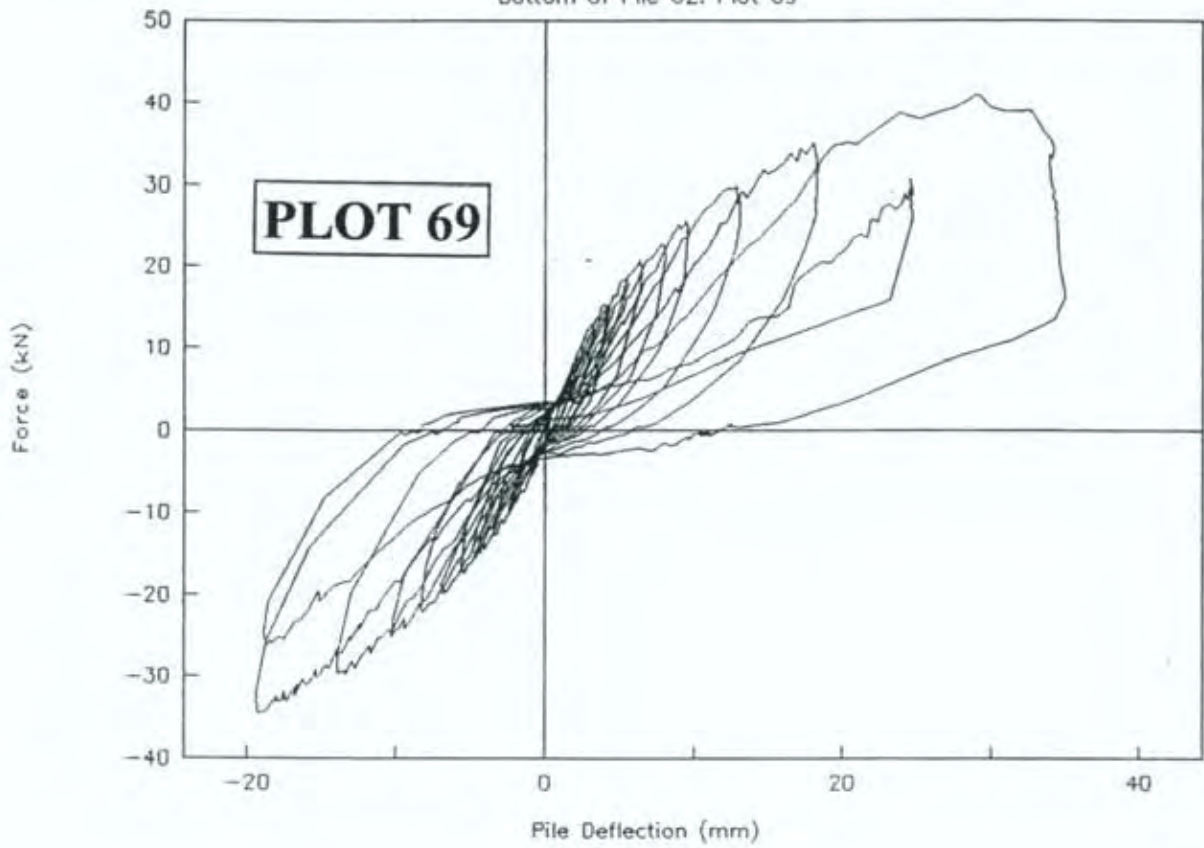
Shear Piles T10-U10 GROUP 2

Uplift of Pile T10. Plot 68



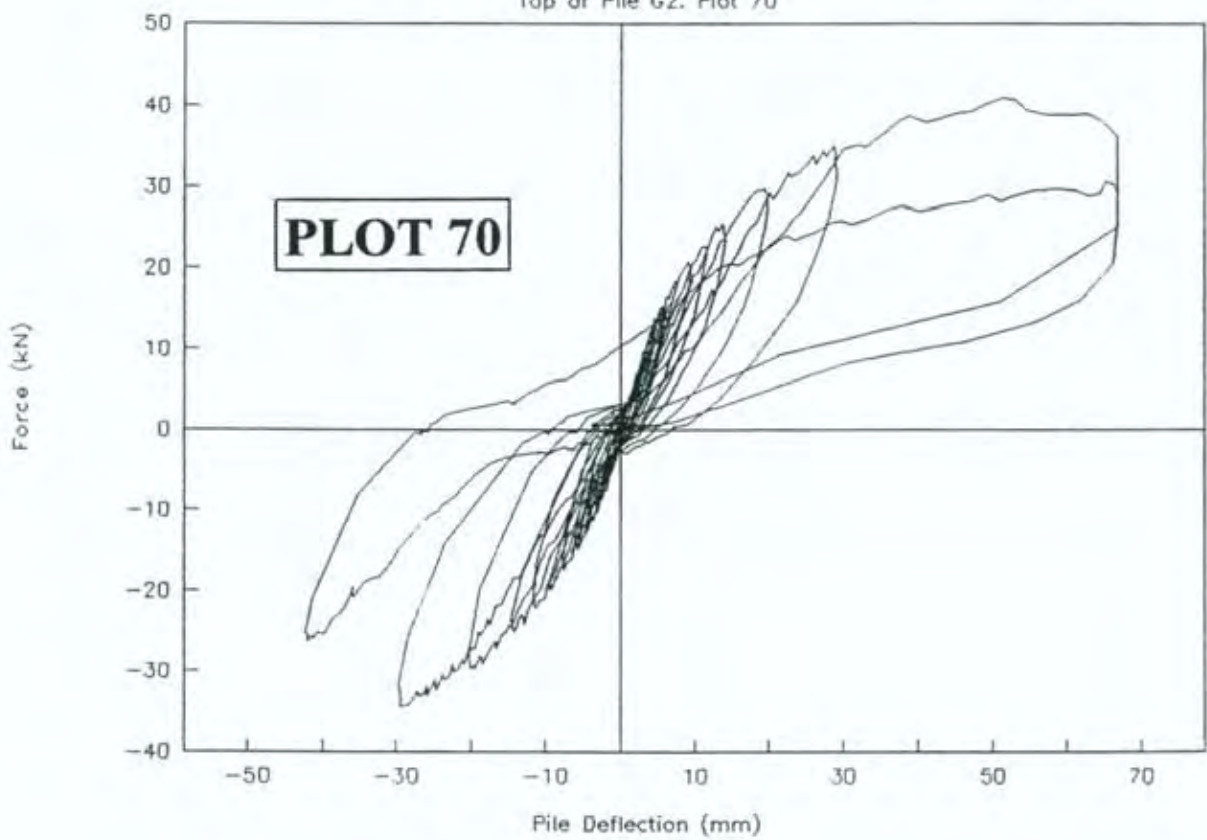
Shear Piles E2-H2 GROUP 1

Bottom of Pile G2. Plot 69



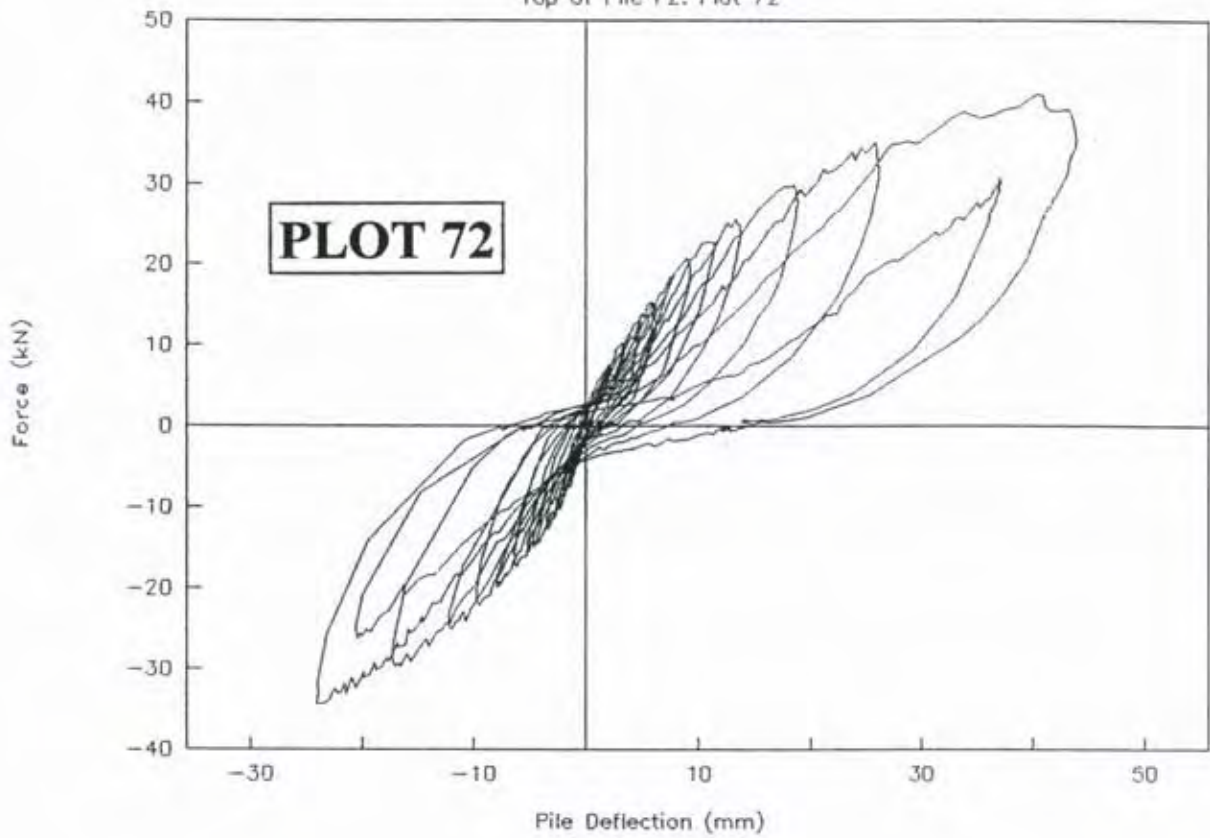
Shear Piles E2-H2 GROUP 1

Top of Pile G2. Plot 70



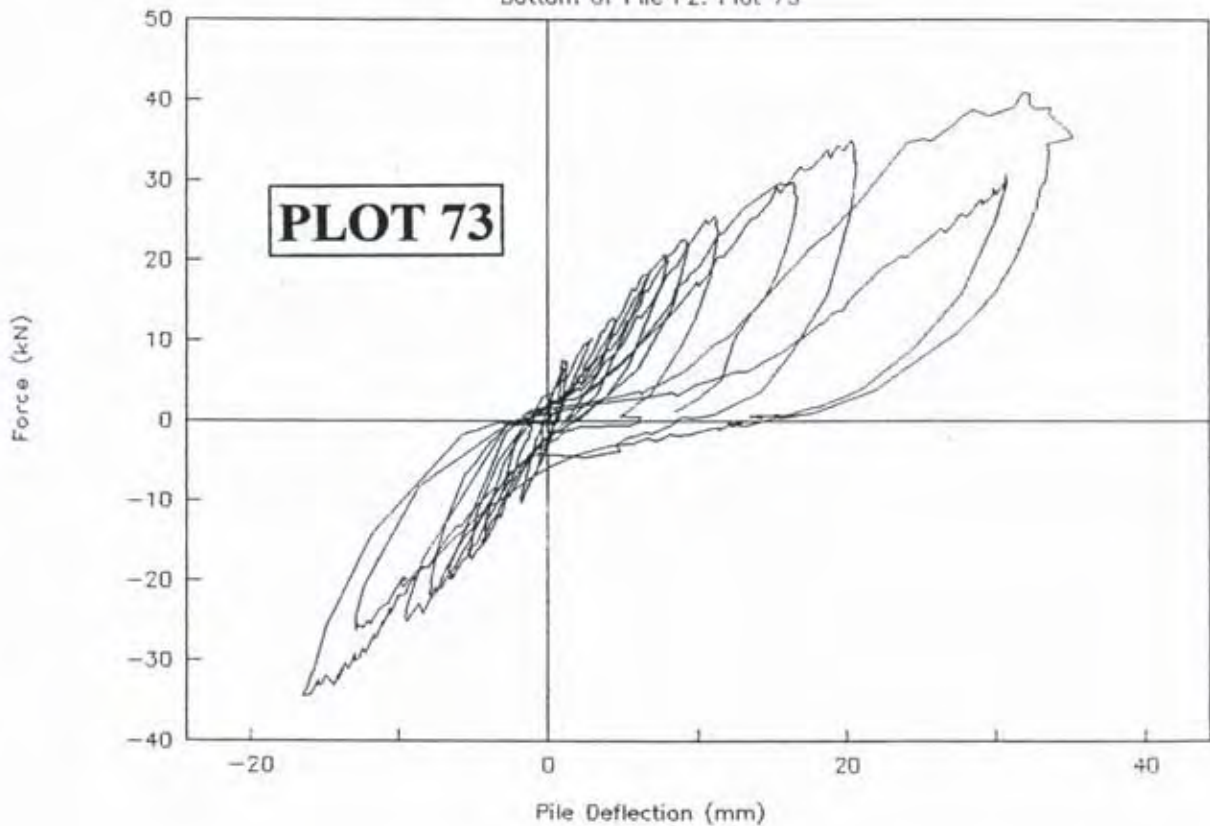
Shear Piles E2-H2 GROUP 1

Top of Pile F2. Plot 72



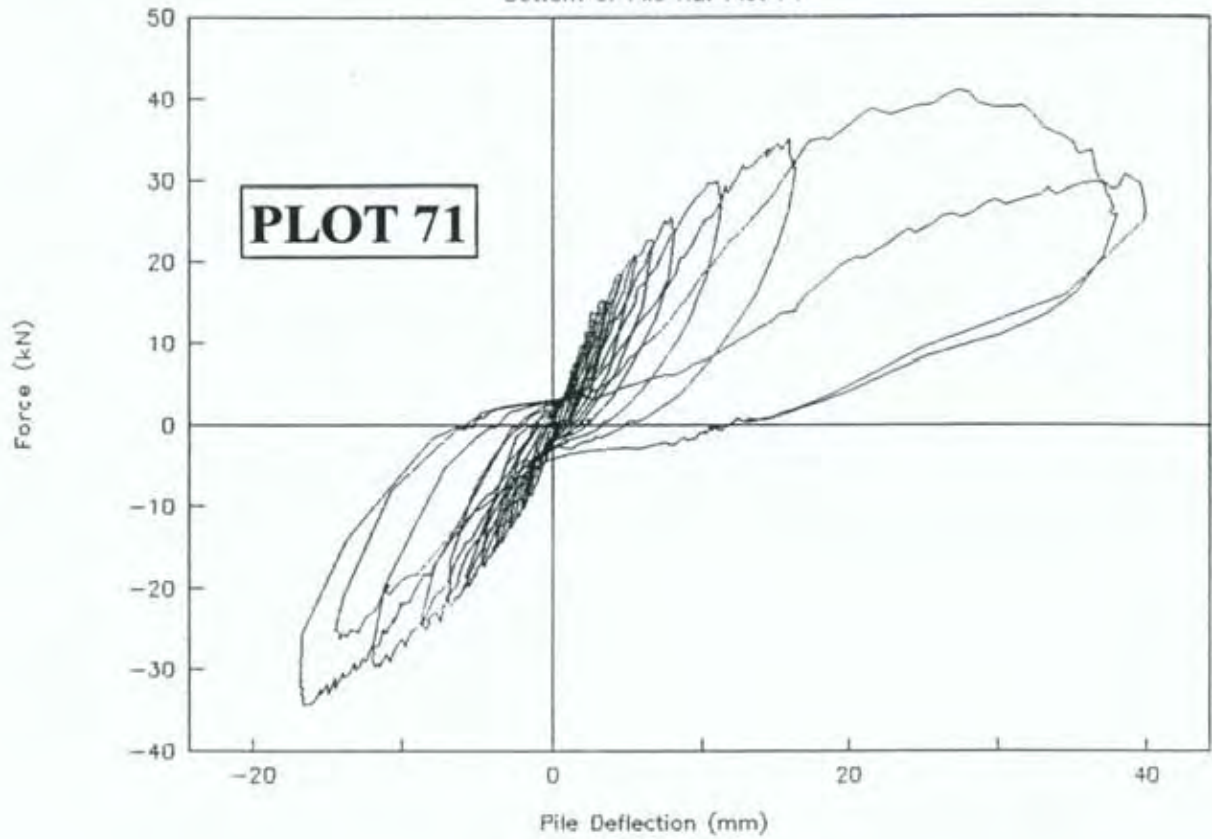
Shear Piles E2-H2 GROUP 1

Bottom of Pile F2. Plot 73



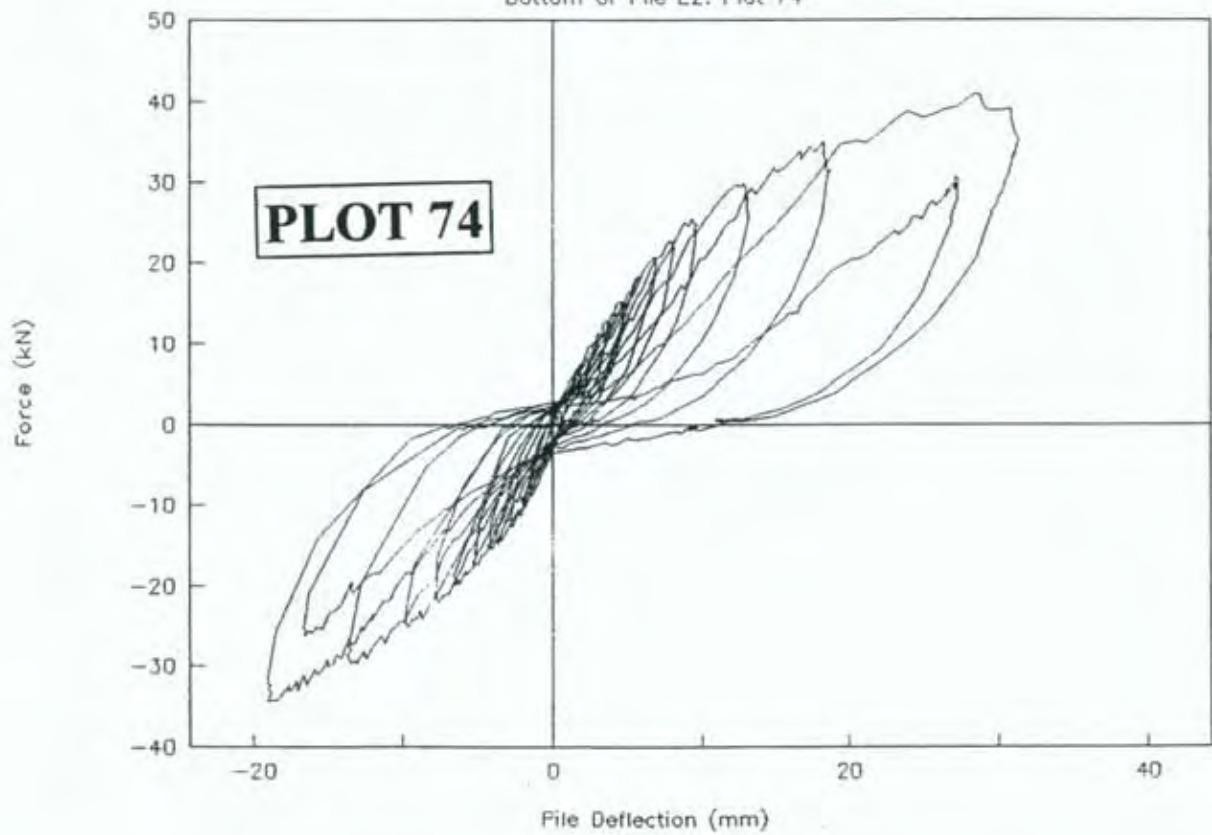
Shear Piles E2-H2 GROUP 1

Bottom of Pile H2. Plot 71



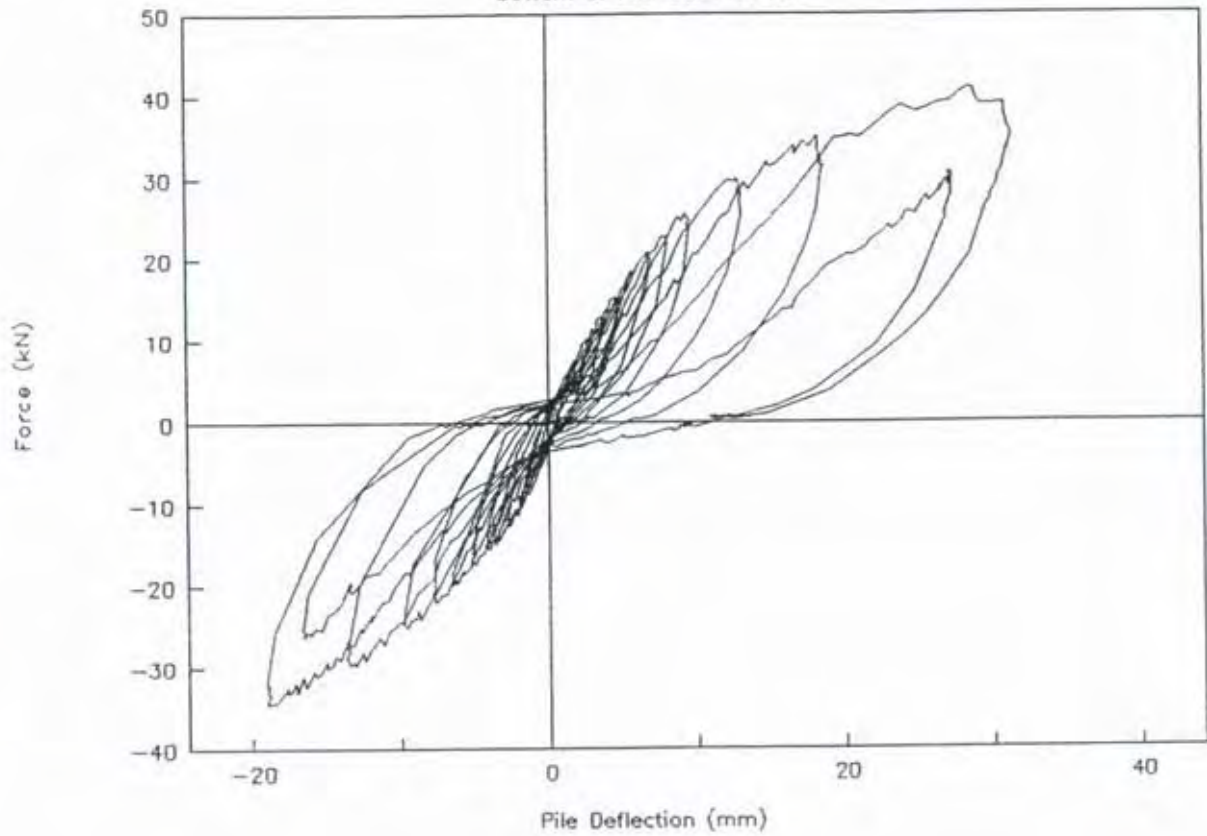
Shear Piles E2-H2 GROUP 1

Bottom of Pile E2. Plot 74



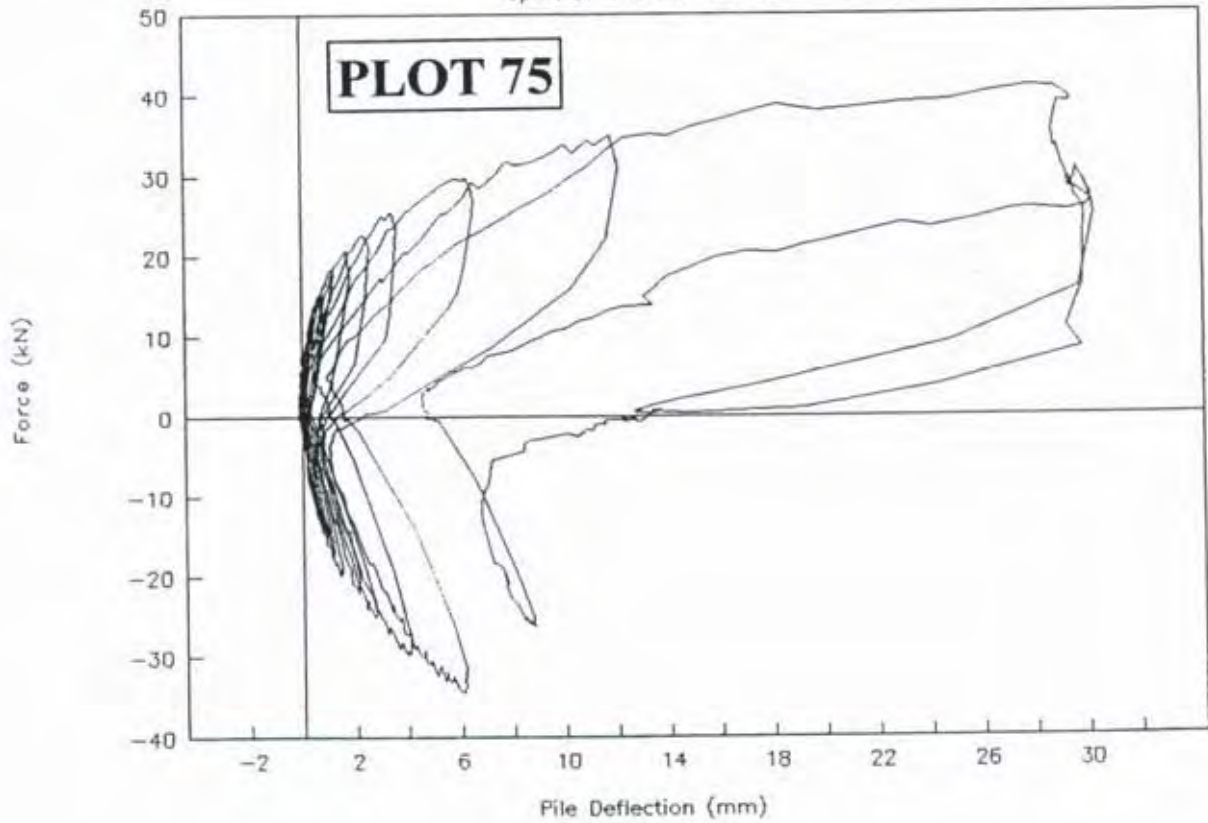
Shear Piles C2-F2 GROUP 1

Bottom of Pile C2. Plot 74



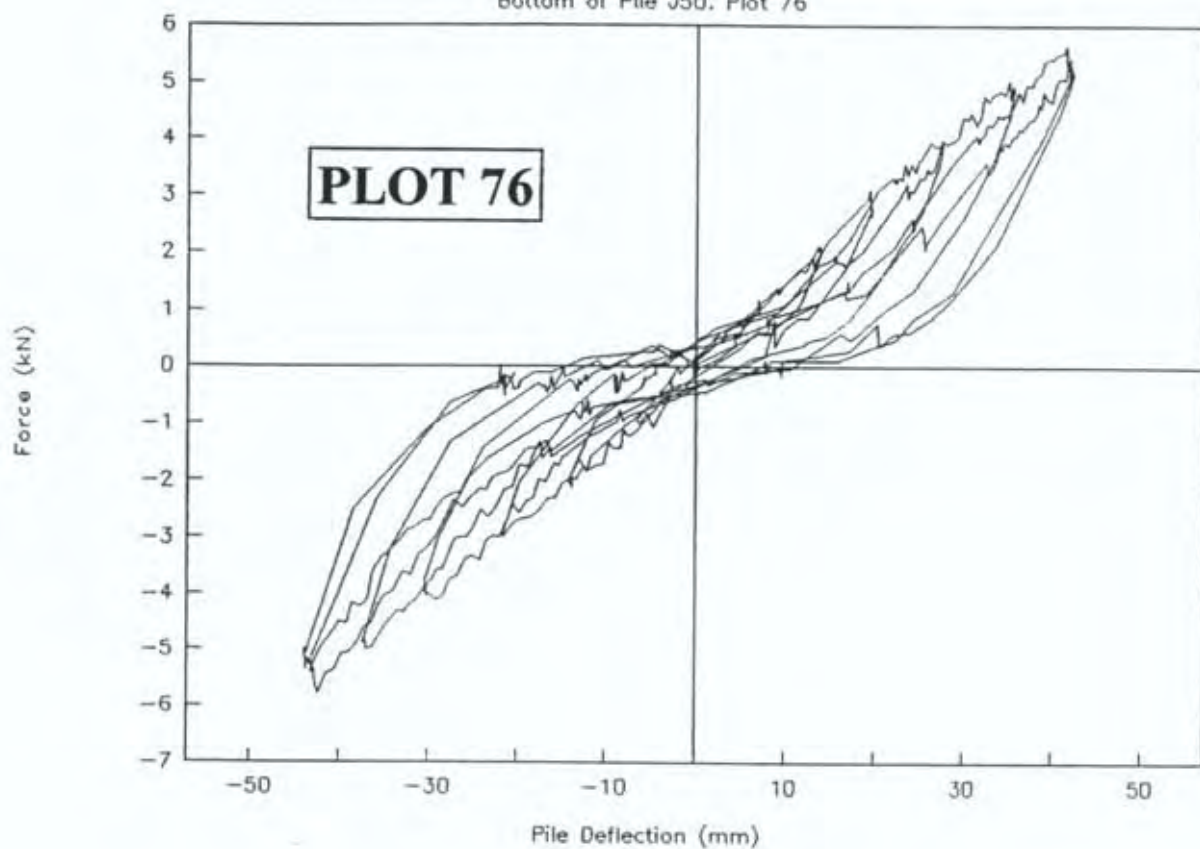
Shear Piles C2-F2 GROUP 1

Uplift of Pile E2. Plot 75



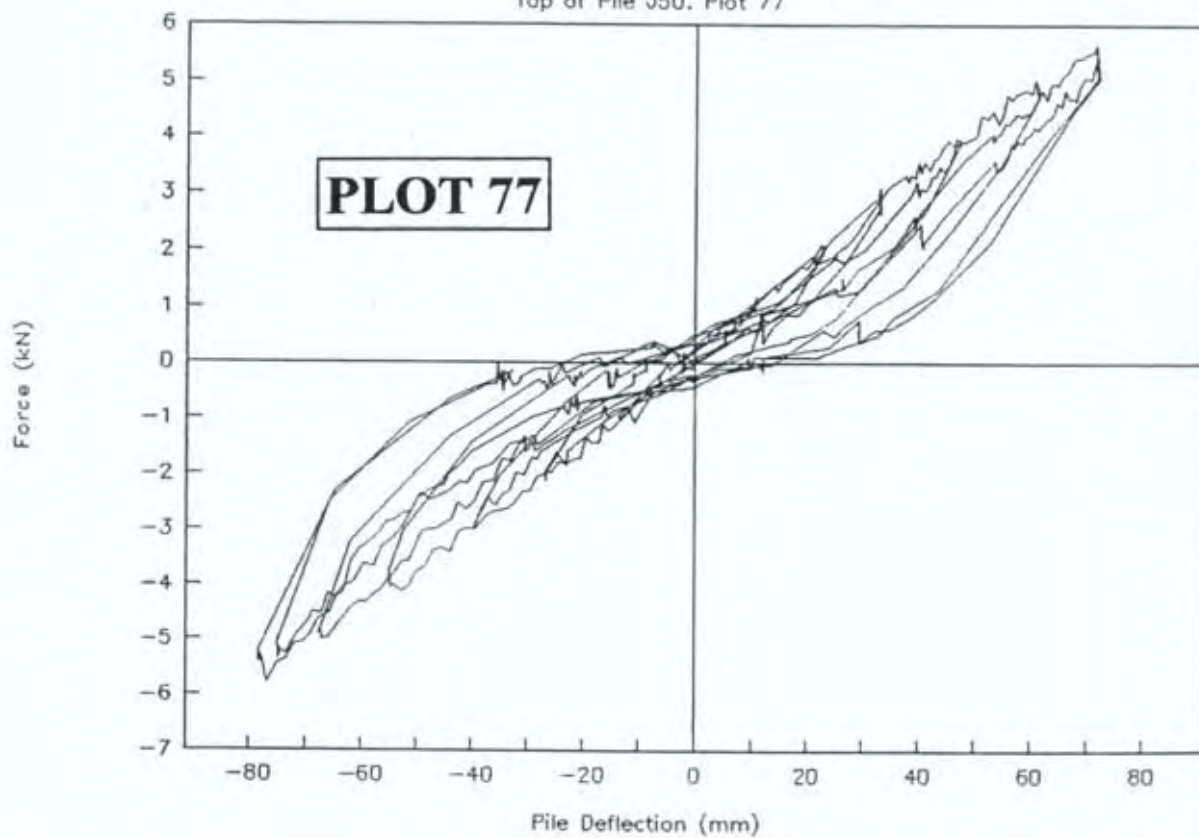
Driven Piles 150-J50 GROUP 3

Bottom of Pile J50. Plot 76



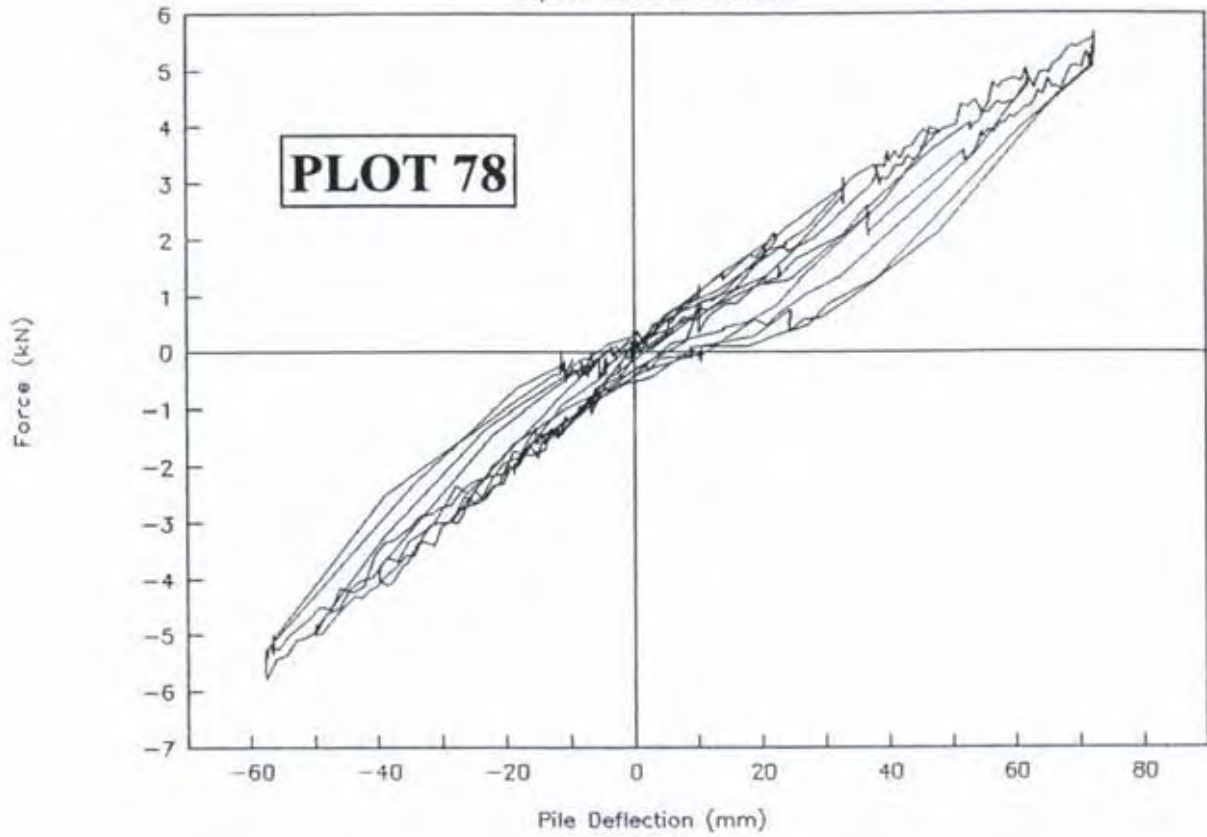
Driven Piles 150-J50 GROUP 3

Top of Pile J50. Plot 77



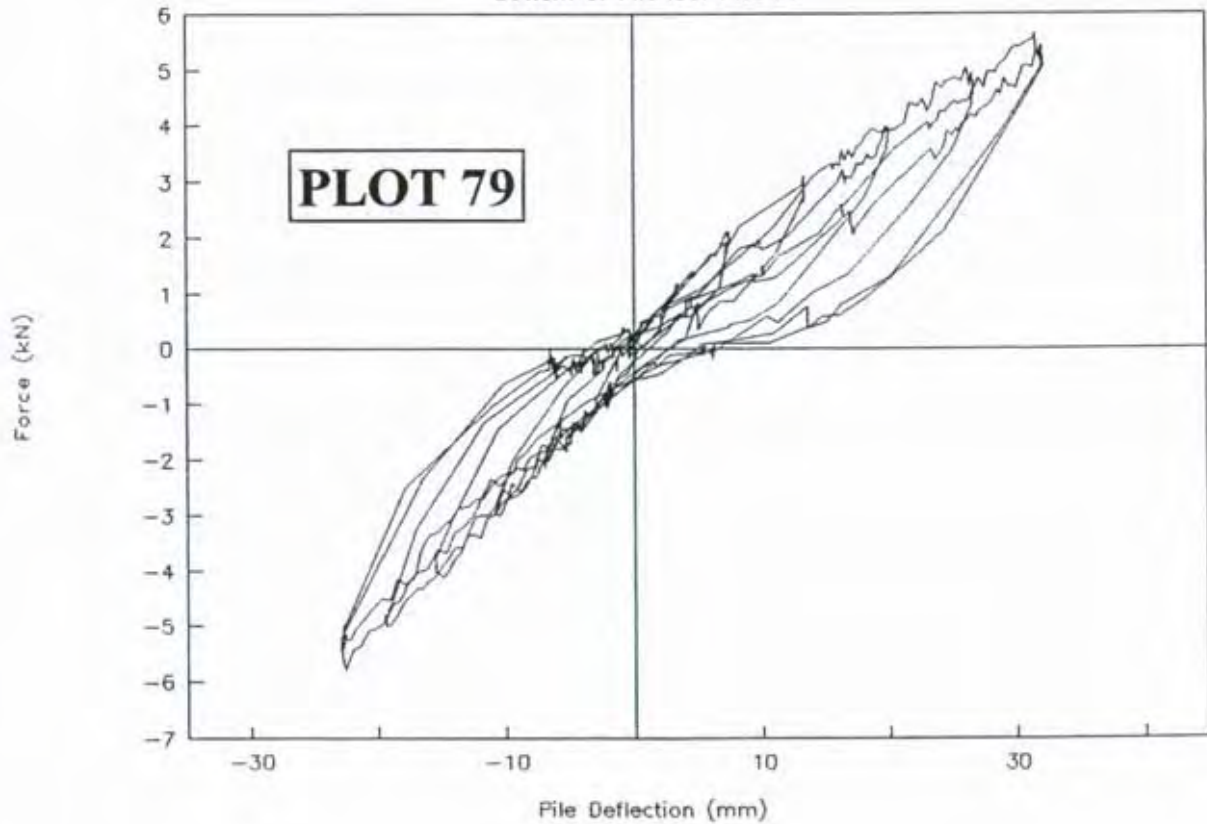
Driven Piles 150-J50 GROUP 3

Top of Pile 150. Plot 78



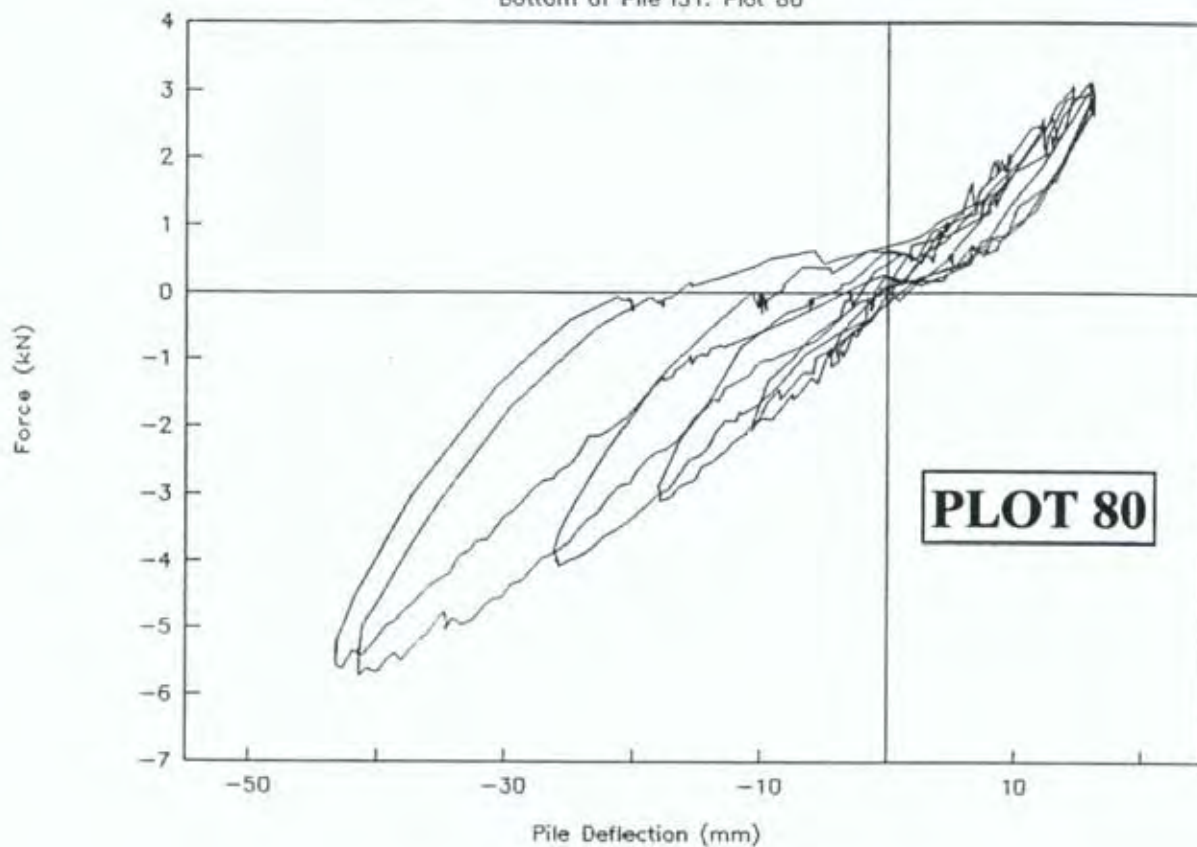
Driven Piles 150-J50 GROUP 3

Bottom of Pile 150. Plot 79



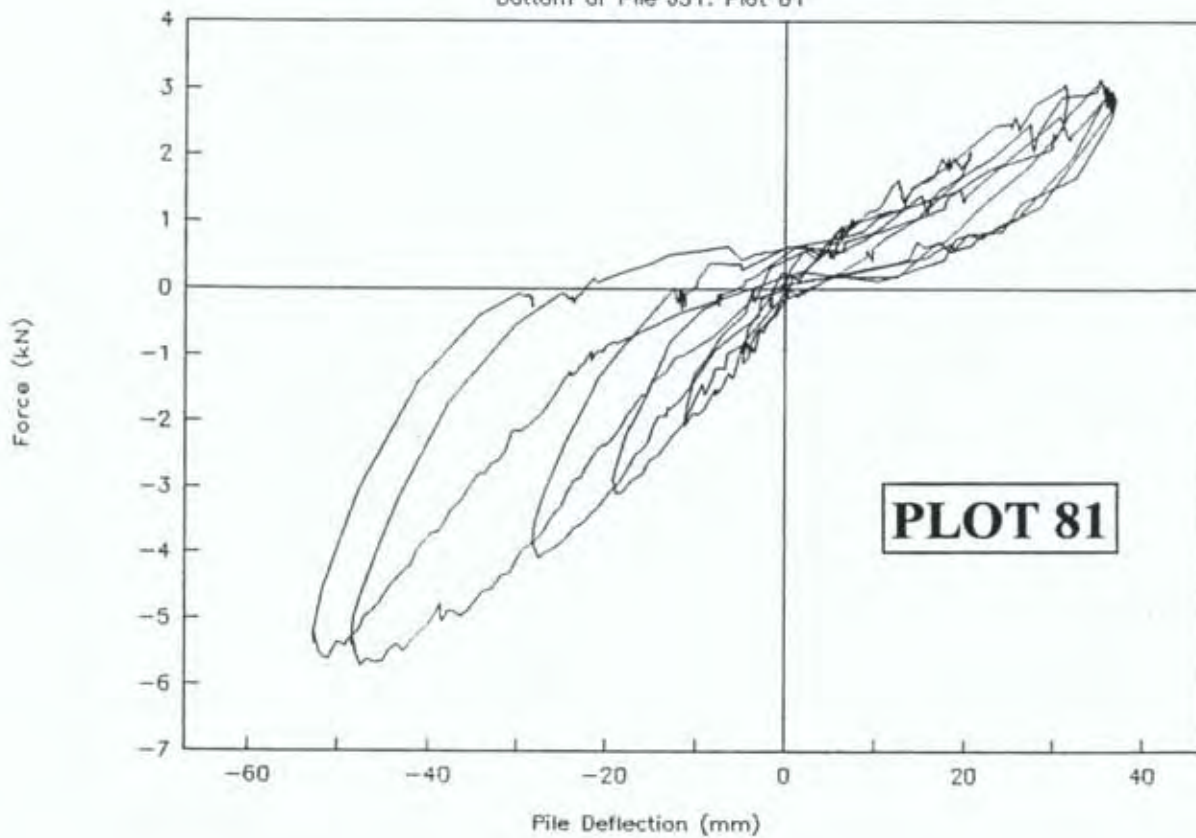
Driven Piles I51-J51 GROUP 3

Bottom of Pile I51. Plot 80



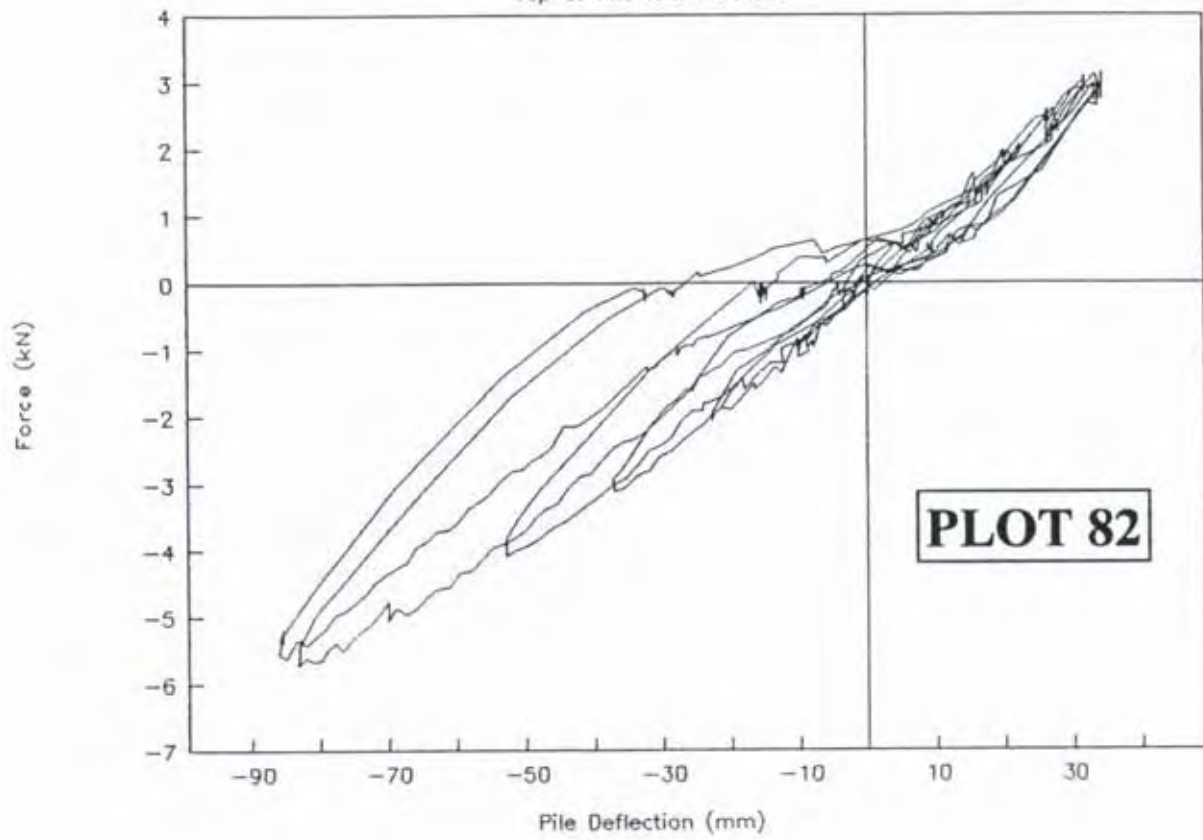
Driven Piles I51-J51 GROUP 3

Bottom of Pile J51. Plot 81



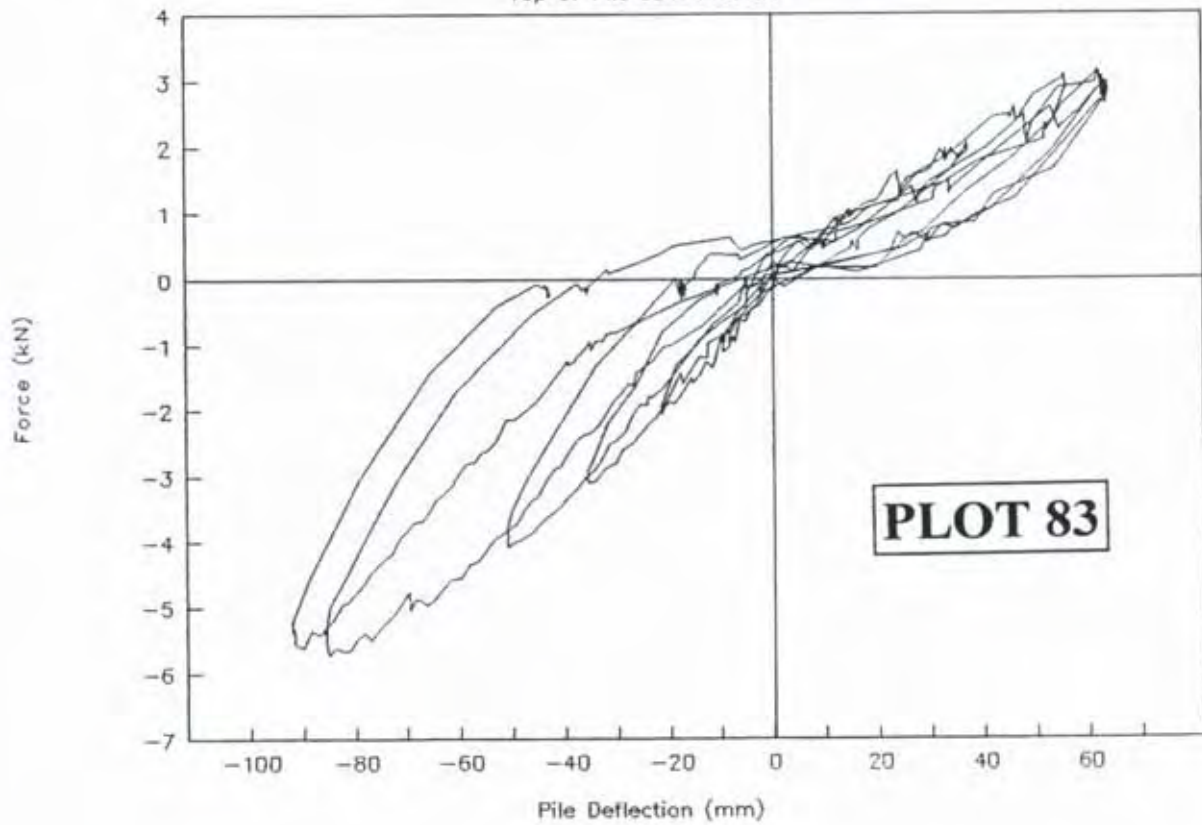
Driven Piles I51-J51 GROUP 3

Top of Pile I51. Plot 82



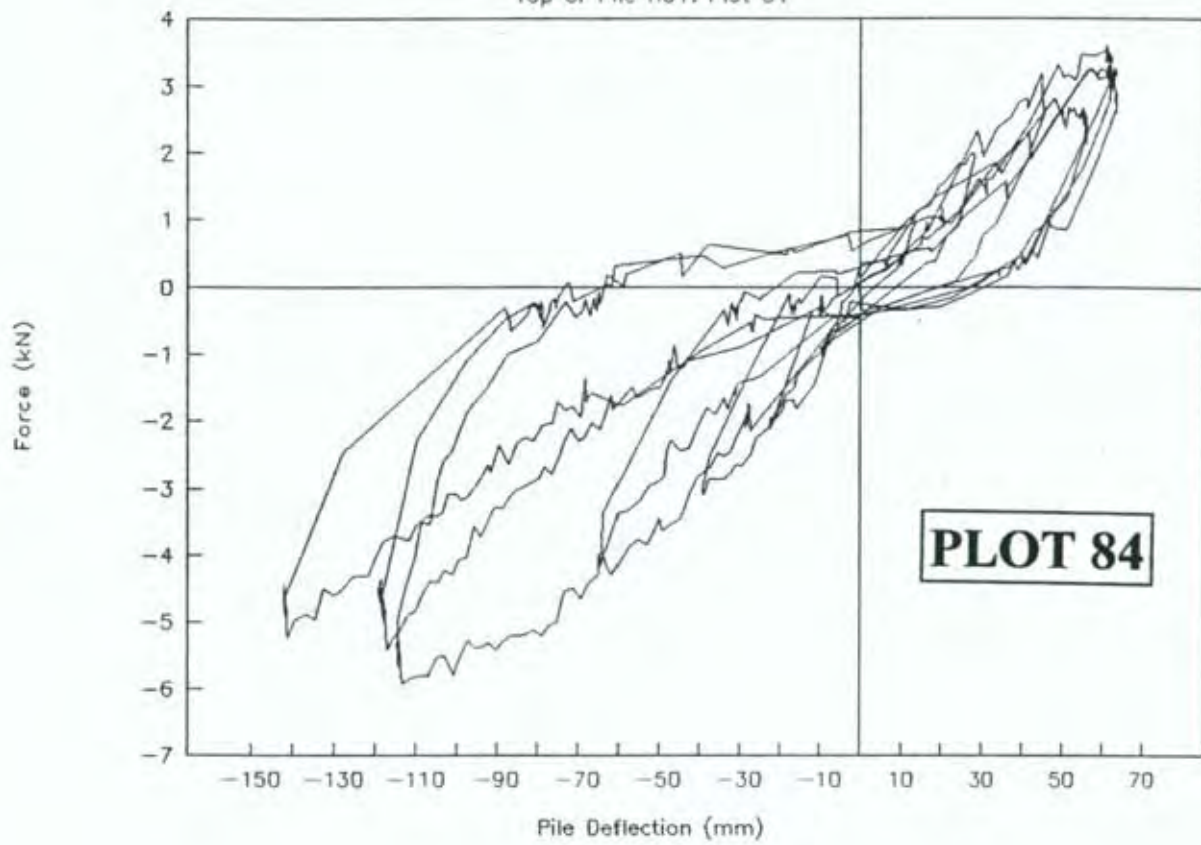
Driven Piles I51-J51 GROUP 3

Top of Pile J51. Plot 83



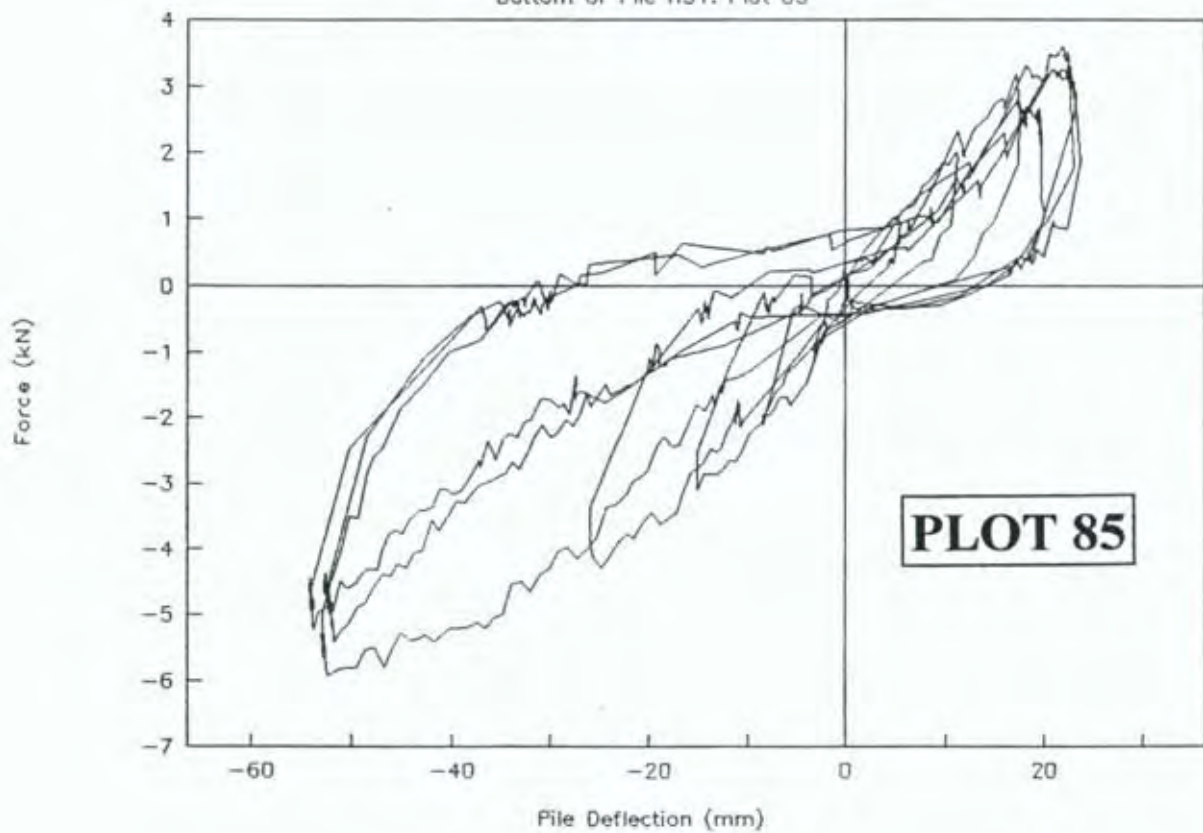
Anchor Pile H51 GROUP 3

Top of Pile H51. Plot 84



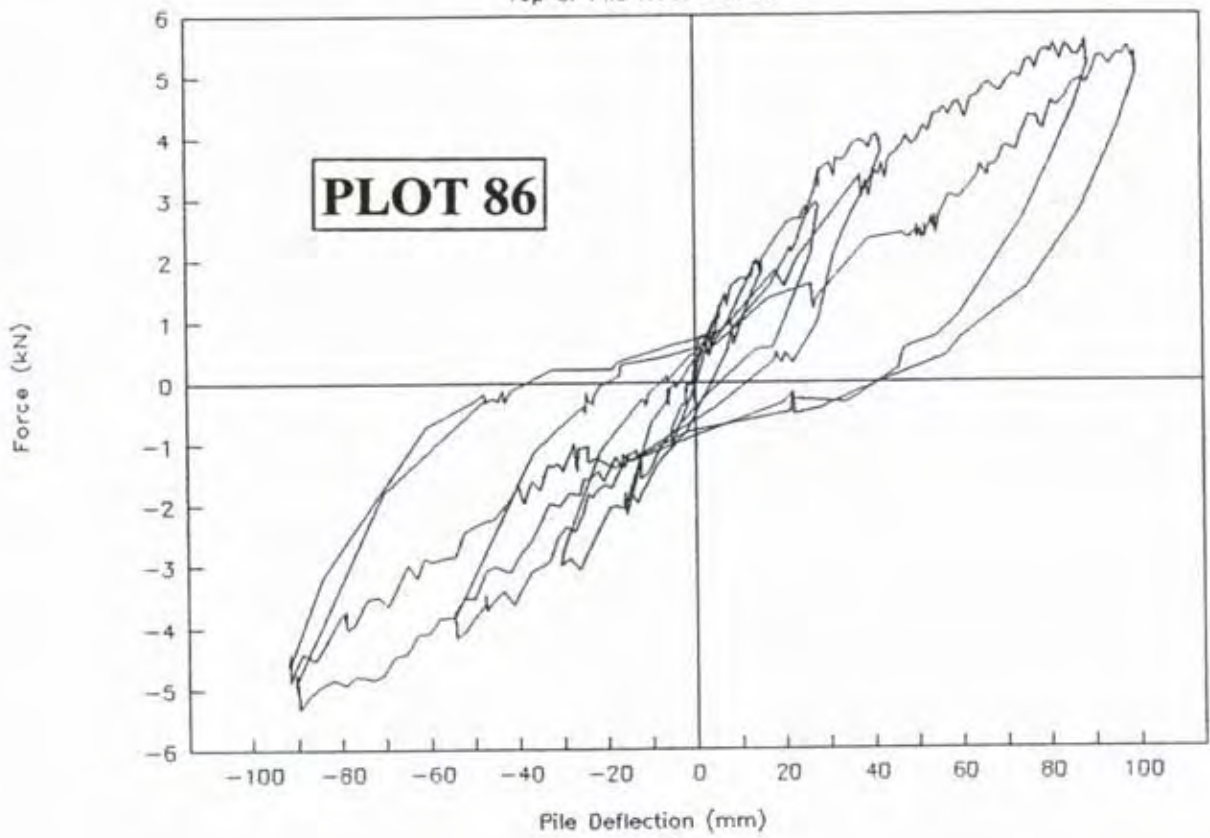
Anchor Pile H51 GROUP 3

Bottom of Pile H51. Plot 85



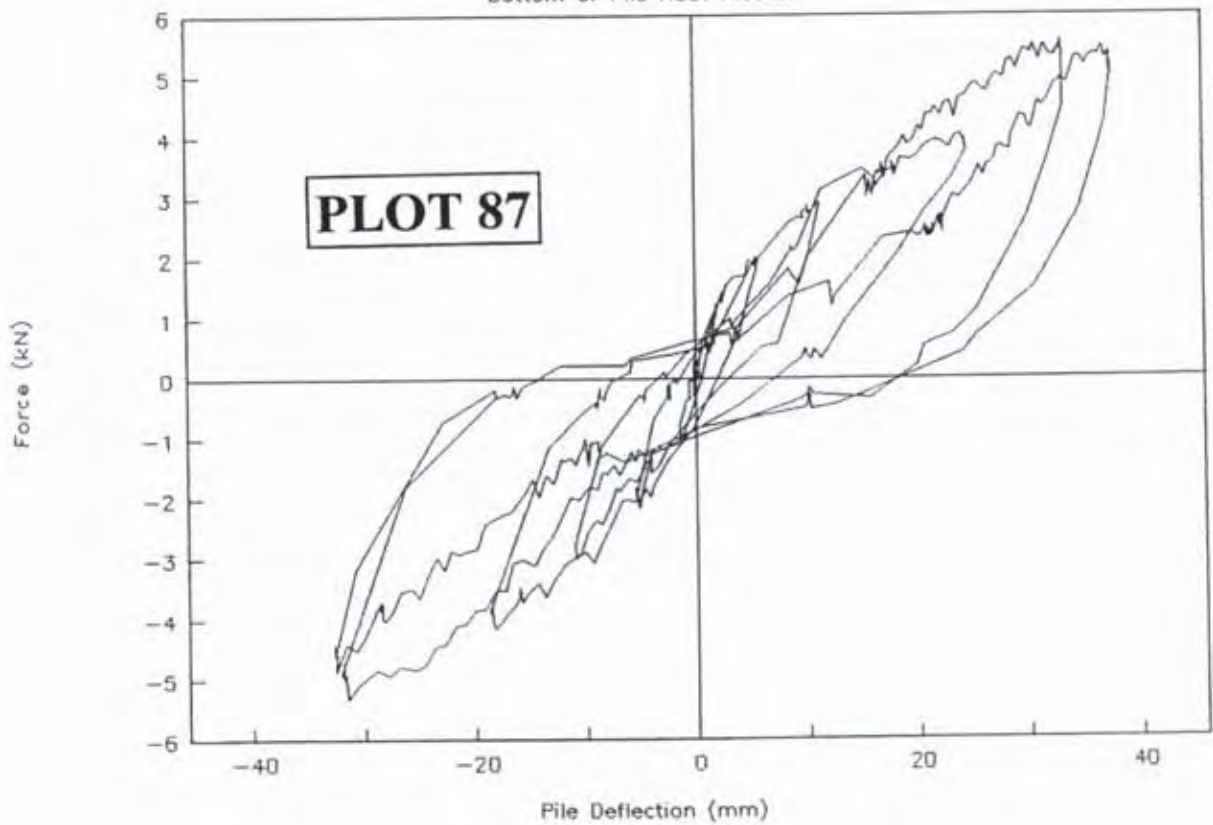
Anchor Pile H50 GROUP 3

Top of Pile H50. Plot 86



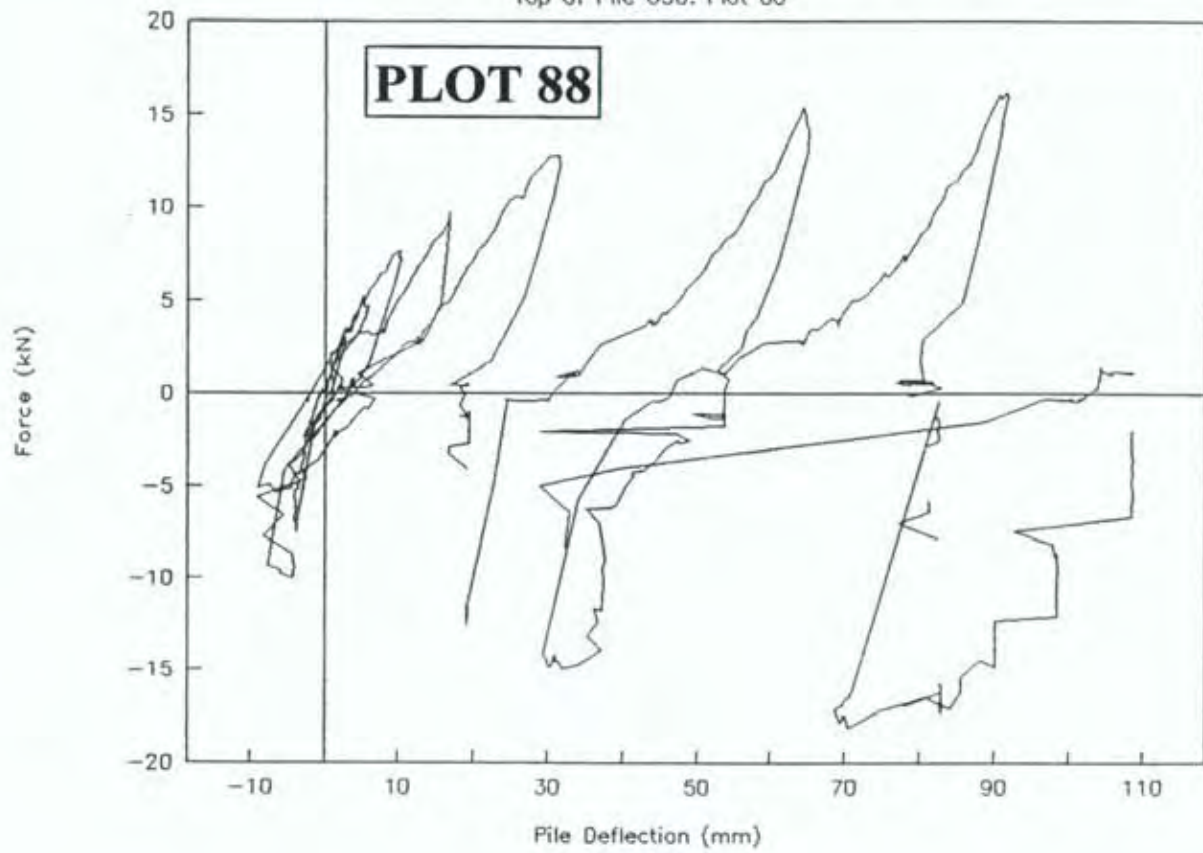
Anchor Pile H50 GROUP 3

Bottom of Pile H50. Plot 87



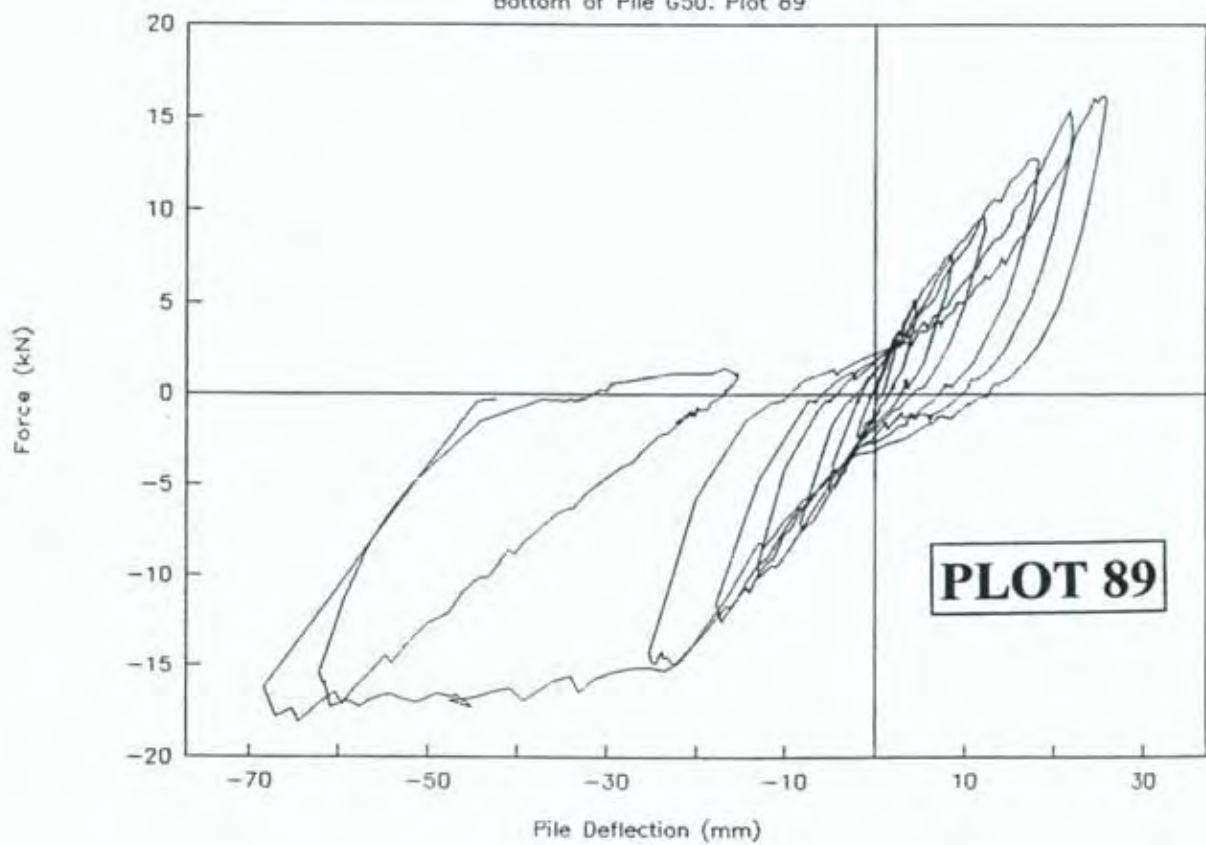
Shear Piles F50-G50 GROUP 3

Top of Pile G50. Plot 88



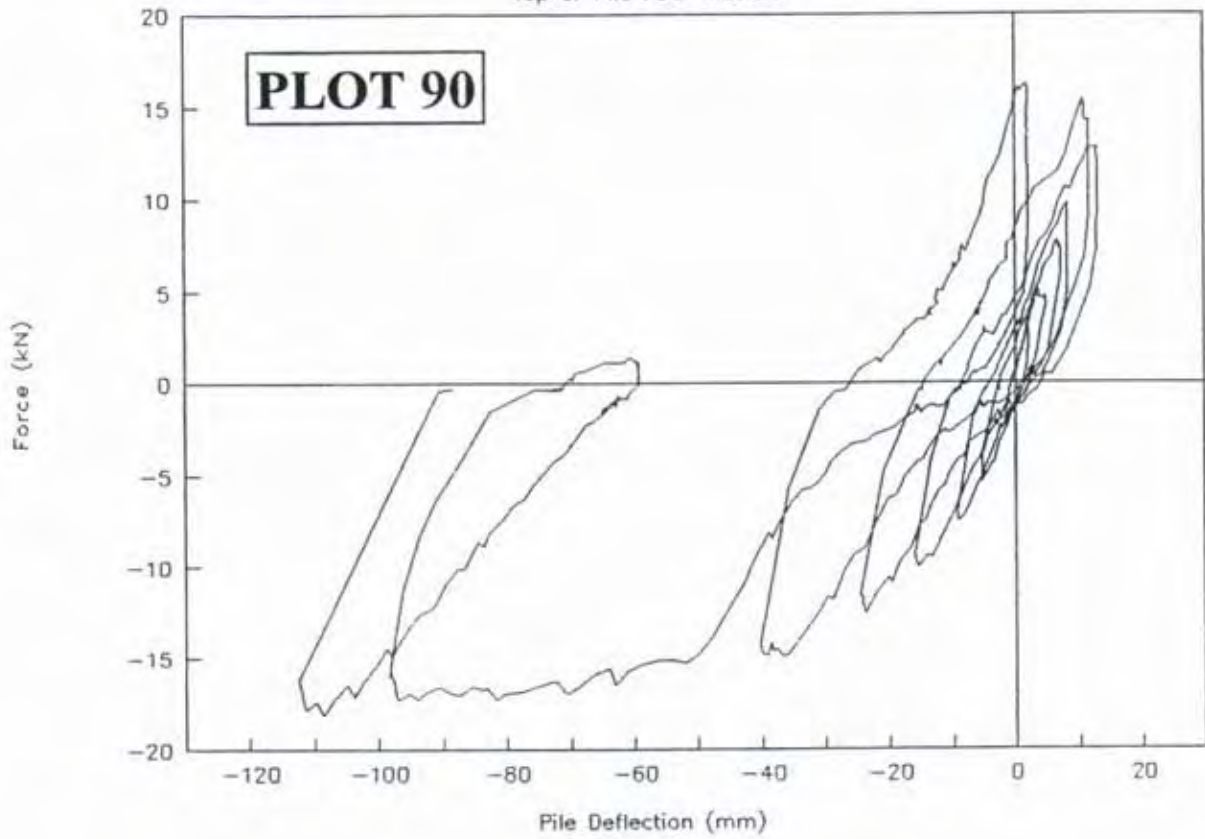
Shear Piles F50-G50 GROUP 3

Bottom of Pile G50. Plot 89



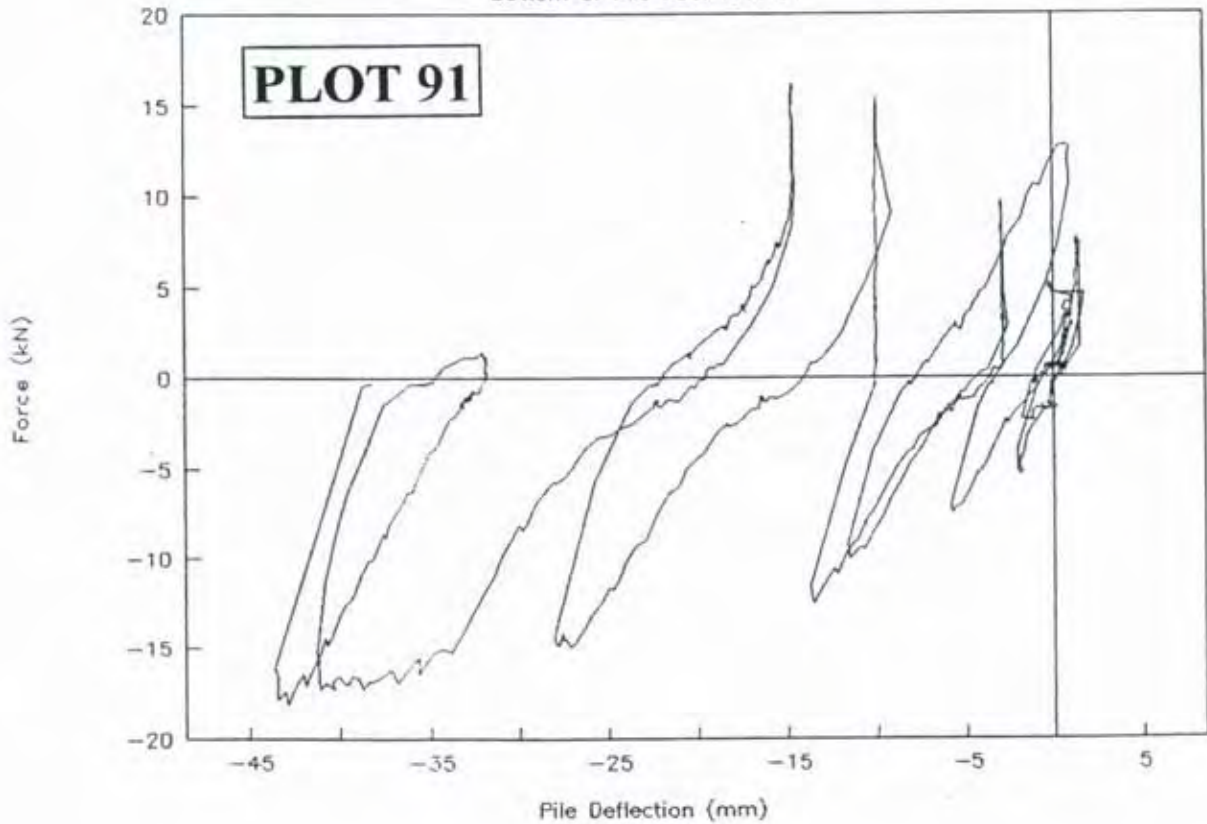
Shear Piles F50-G50 GROUP 3

Top of Pile F50. Plot 90



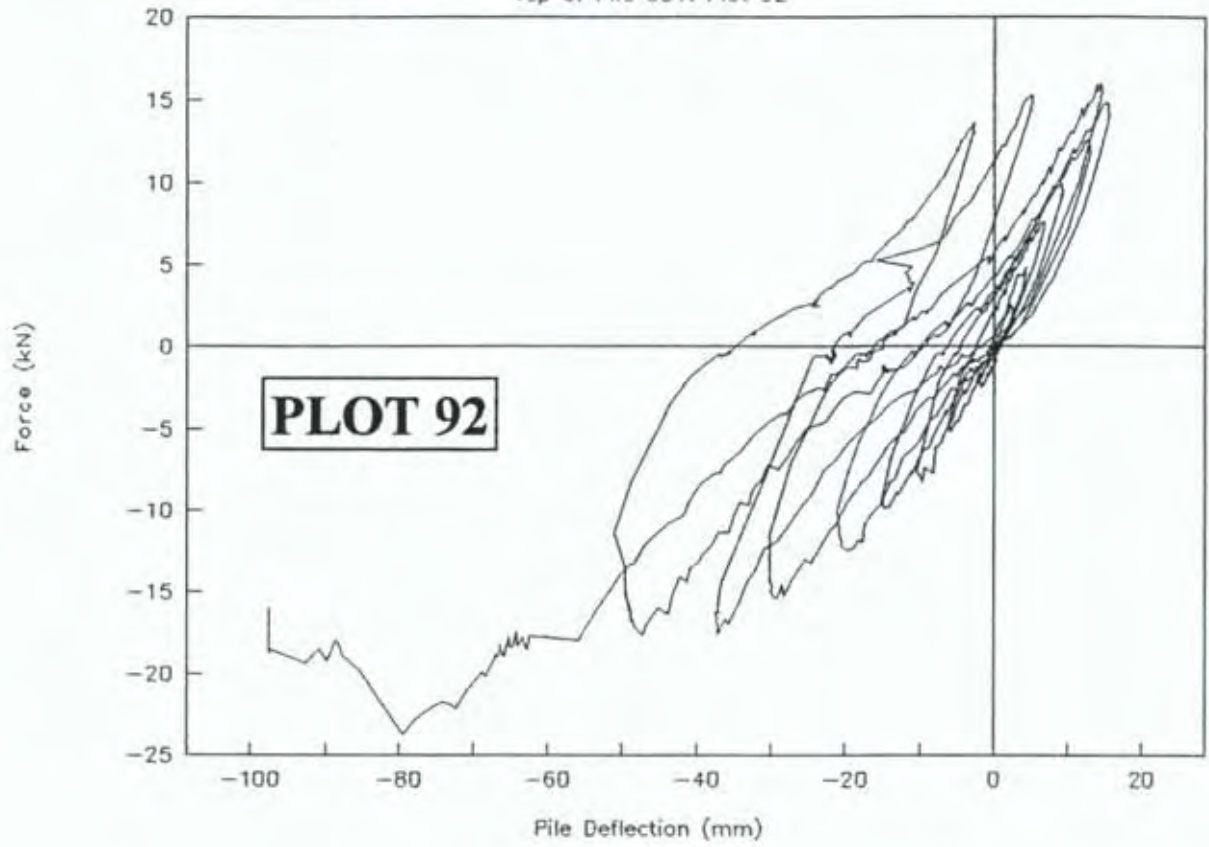
Shear Piles F50-G50 GROUP 3

Bottom of Pile F50. Plot 91



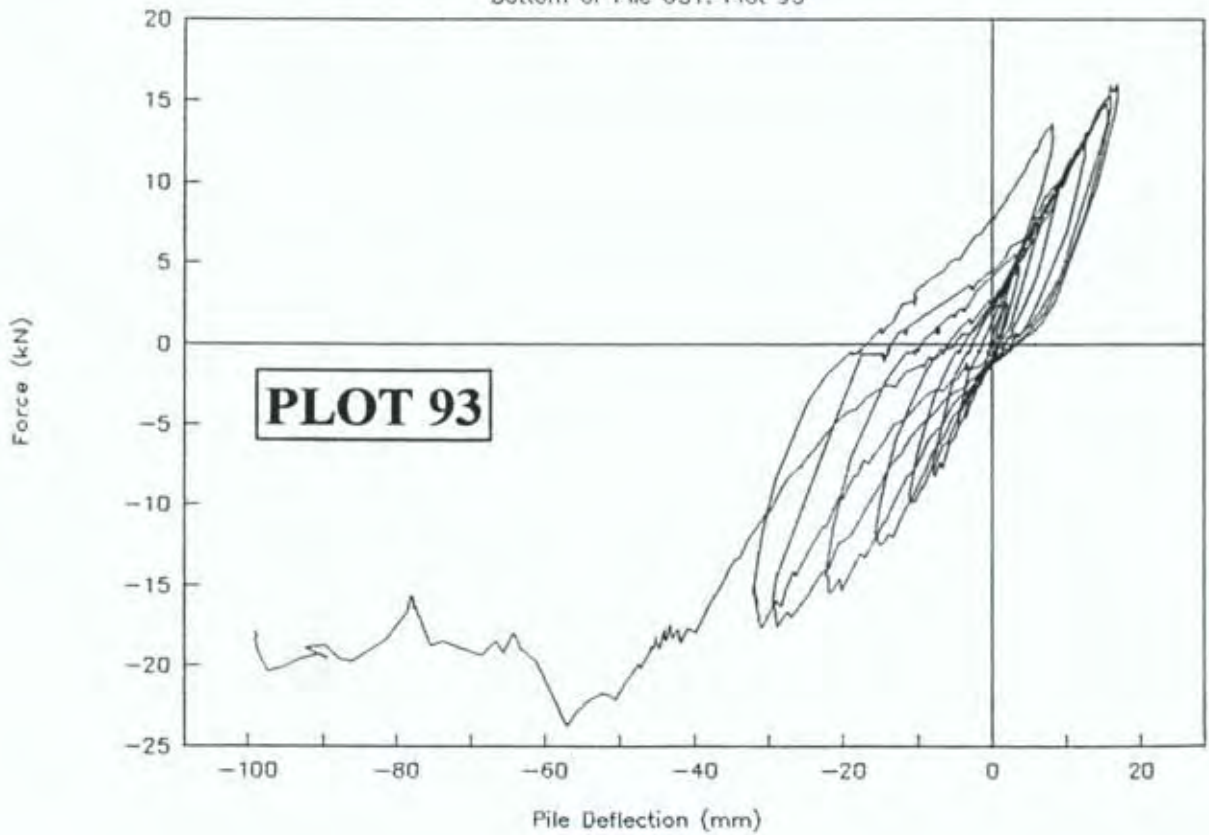
Shear Piles F51-G51 GROUP 3

Top of Pile G51. Plot 92



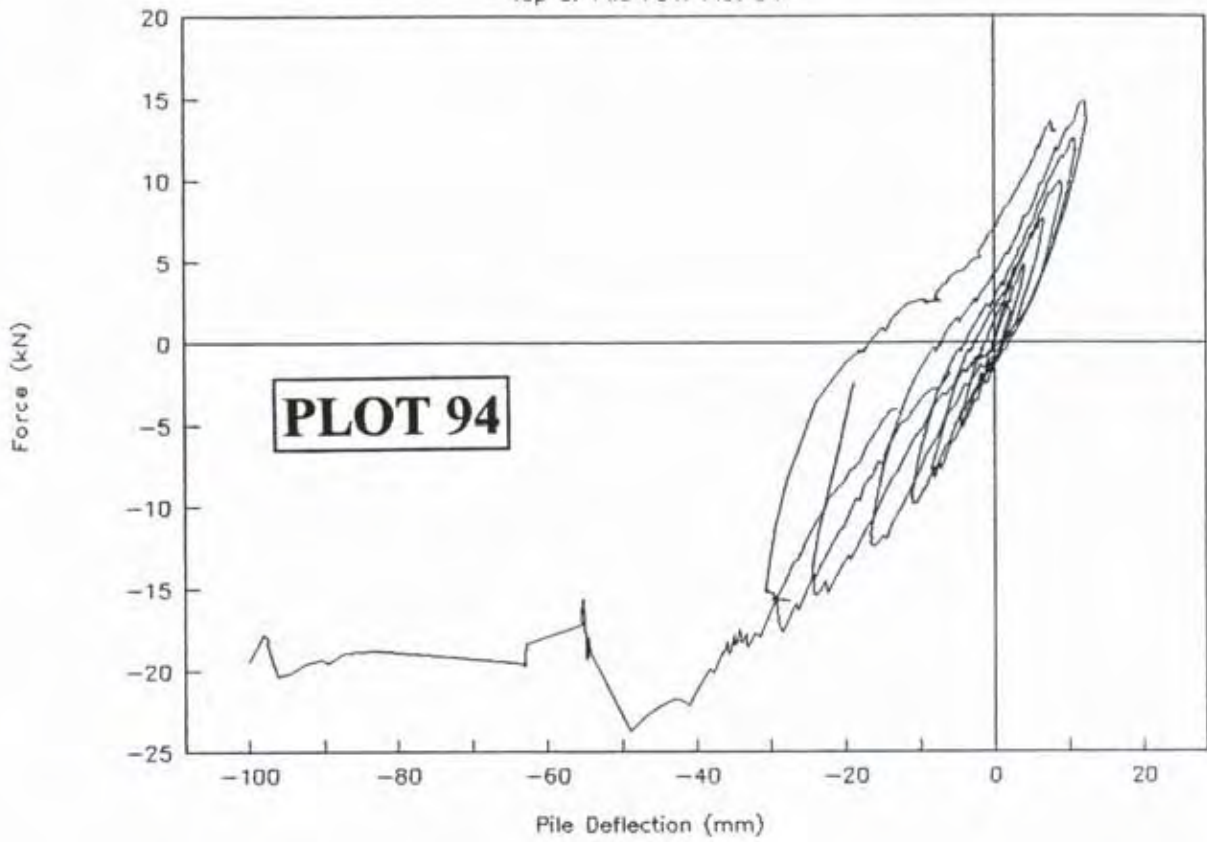
Shear Piles F51-G51 GROUP 3

Bottom of Pile G51. Plot 93



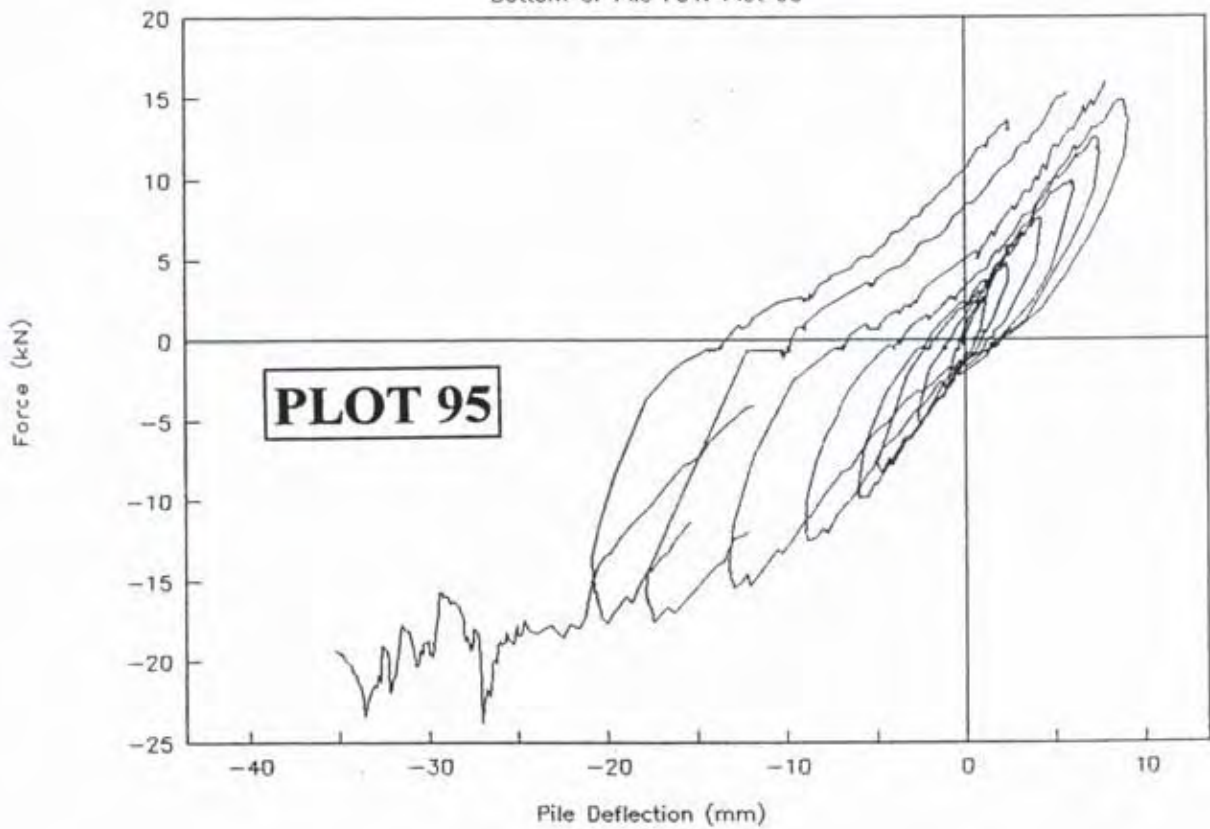
Shear Piles F51-G51 GROUP 3

Top of Pile F51. Plot 94



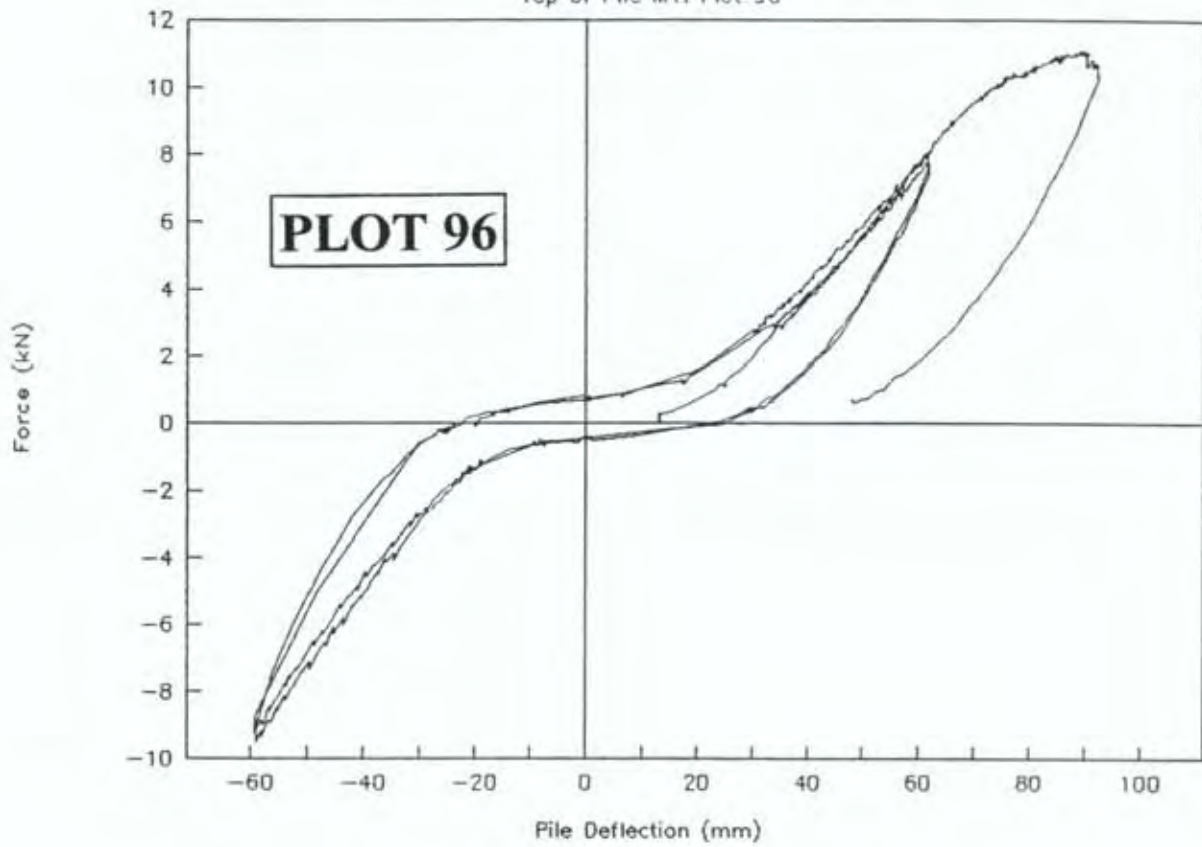
Shear Piles F51-G51 GROUP 3

Bottom of Pile F51. Plot 95



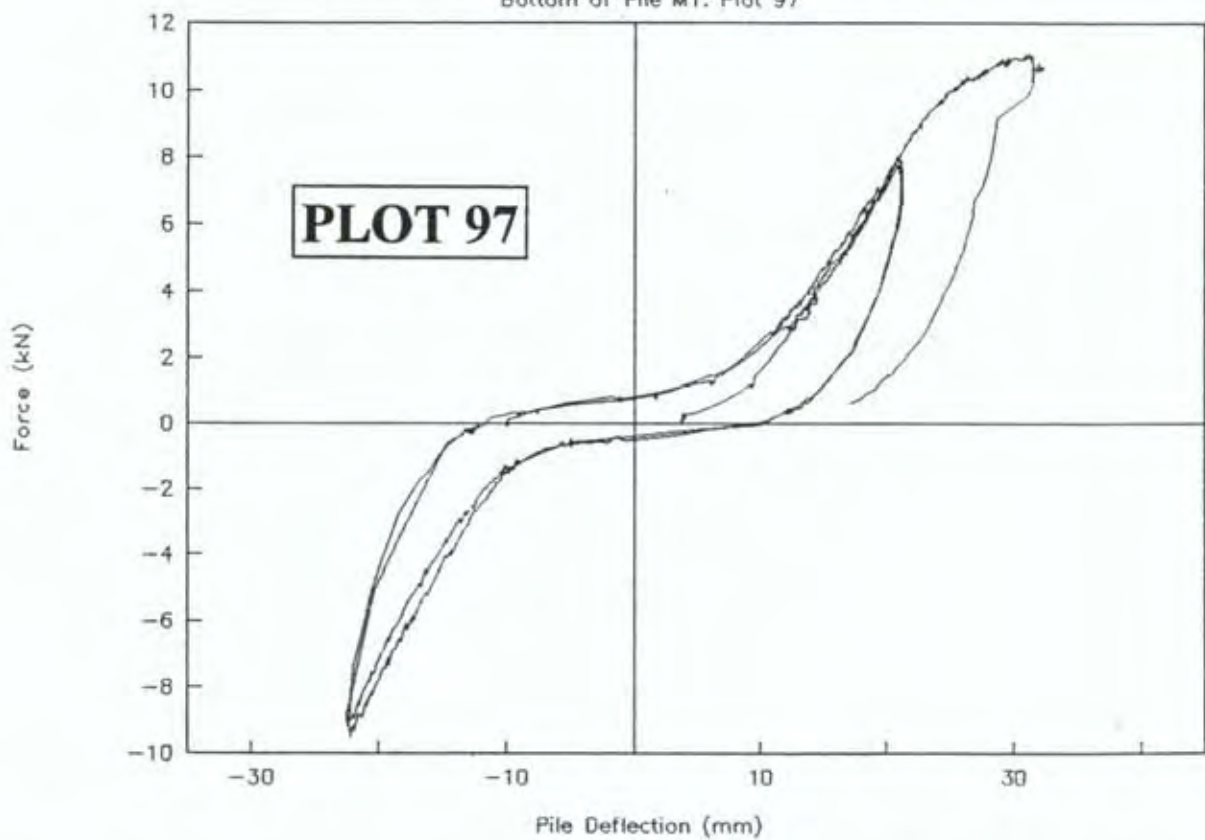
Anchor Piles M1-M2 GROUP 4

Top of Pile M1. Plot 96



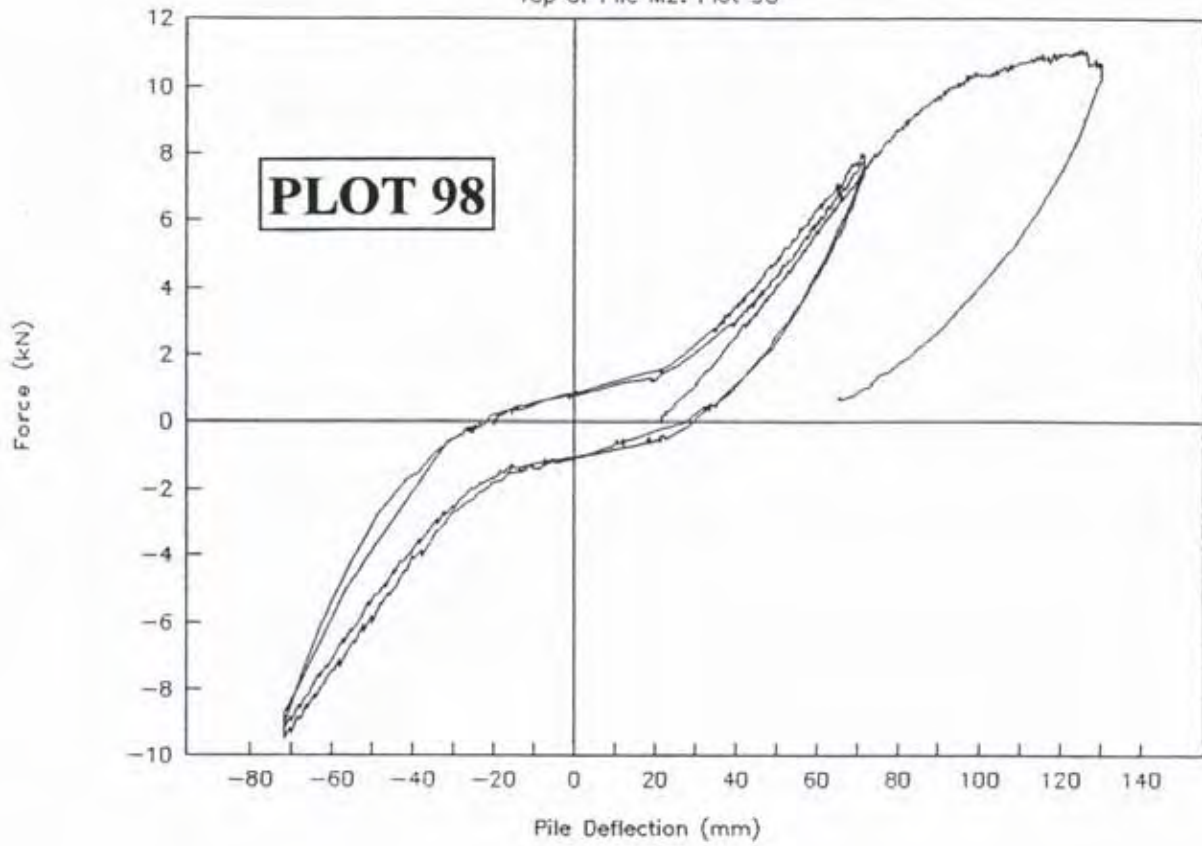
Anchor Piles M1-M2 GROUP 4

Bottom of Pile M1. Plot 97



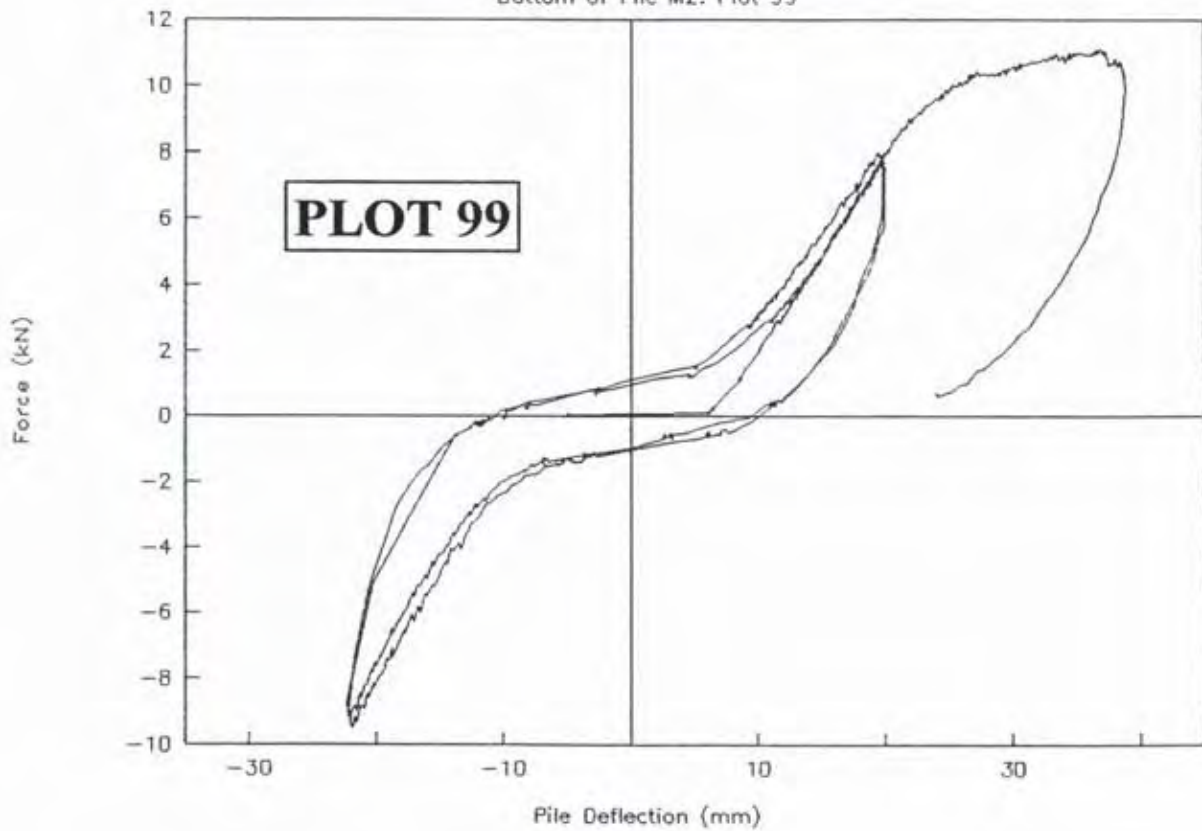
Anchor Piles M1-M2 GROUP 4

Top of Pile M2. Plot 98



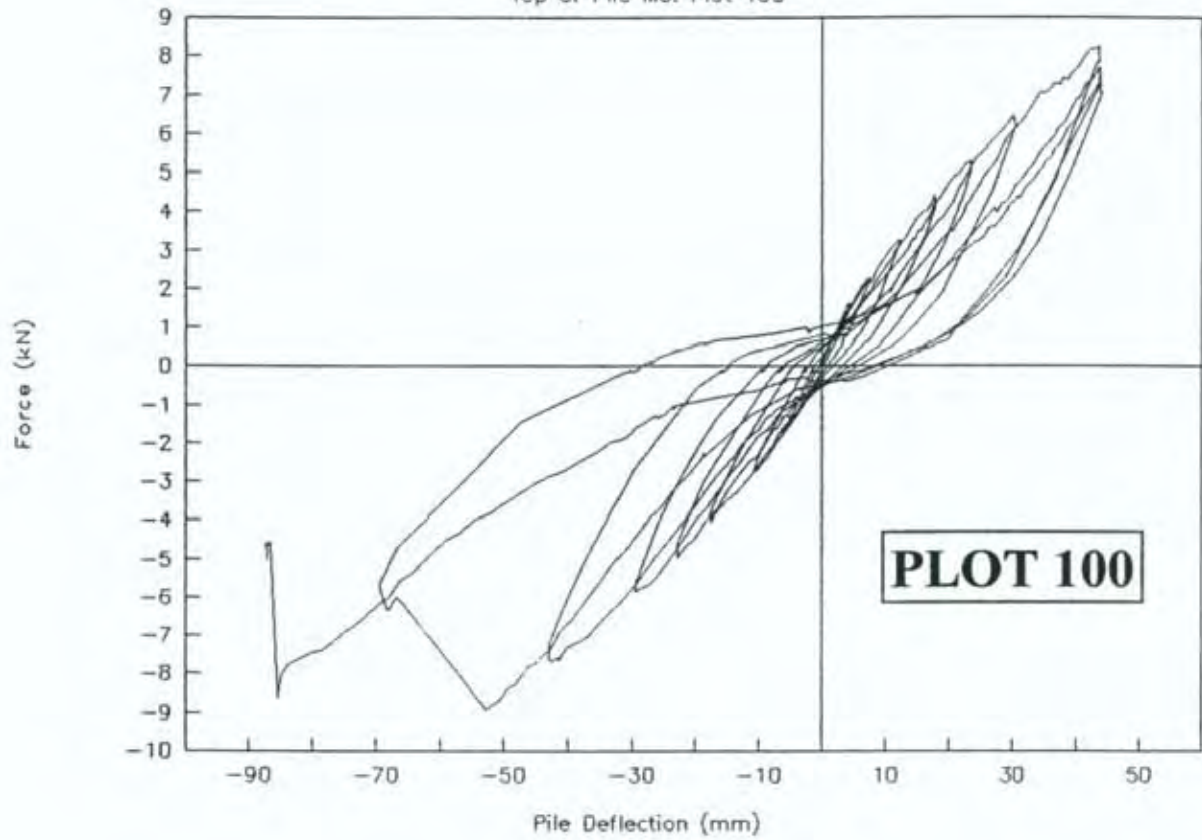
Anchor Piles M1-M2 GROUP 4

Bottom of Pile M2. Plot 99



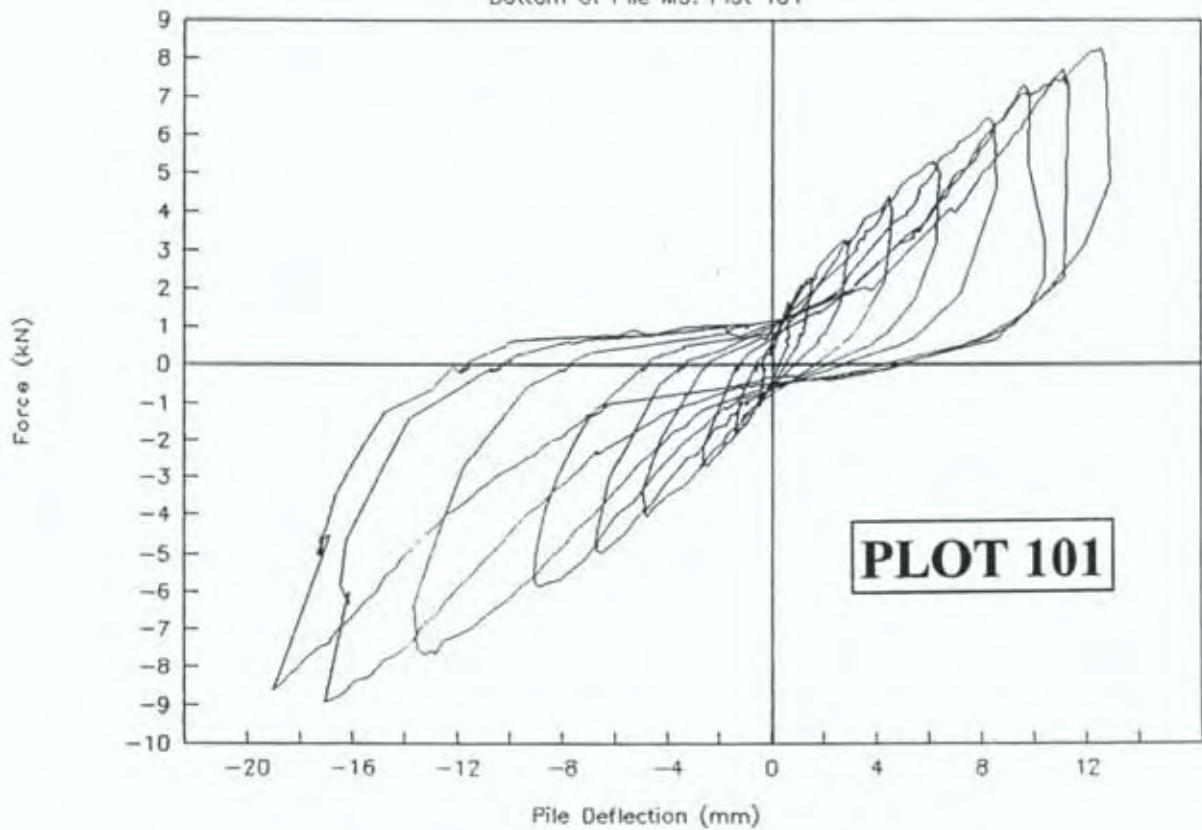
Anchor Piles M3-M4 GROUP 4

Top of Pile M3. Plot 100



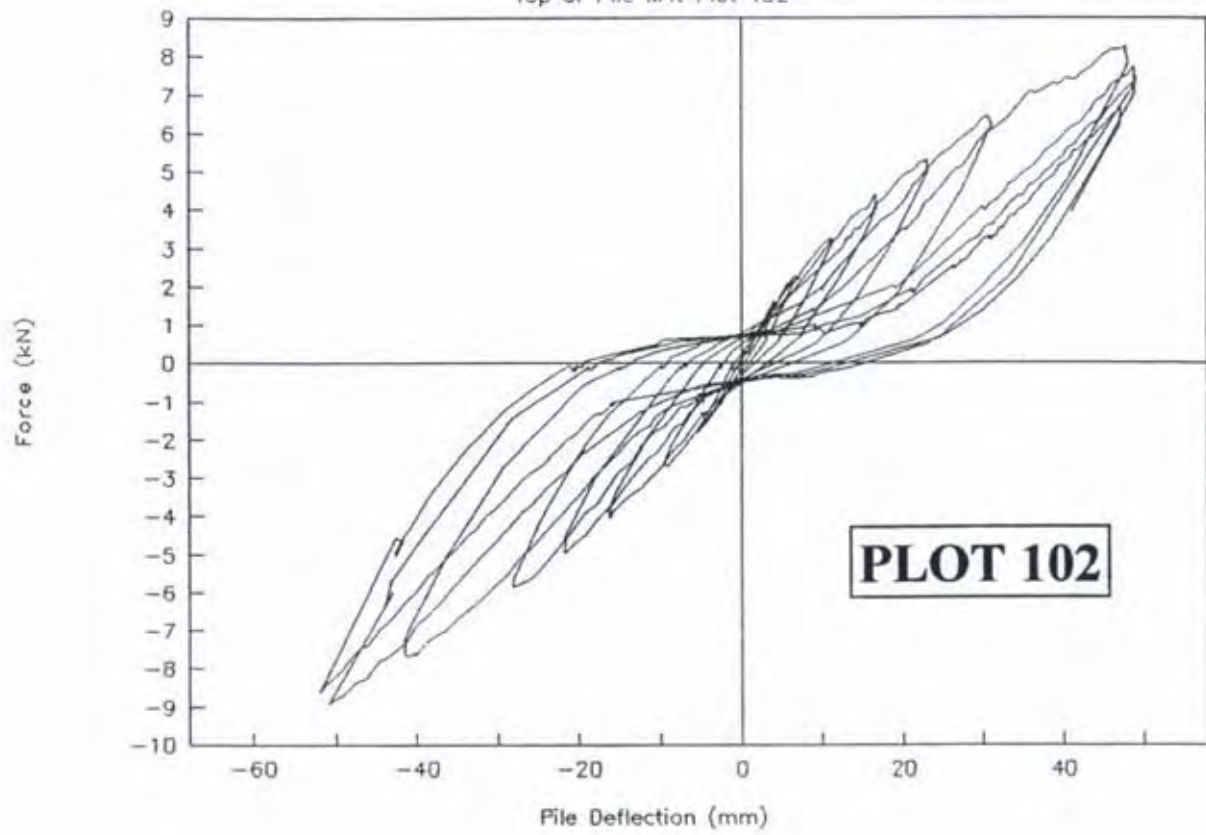
Anchor Piles M3-M4 GROUP 4

Bottom of Pile M3. Plot 101



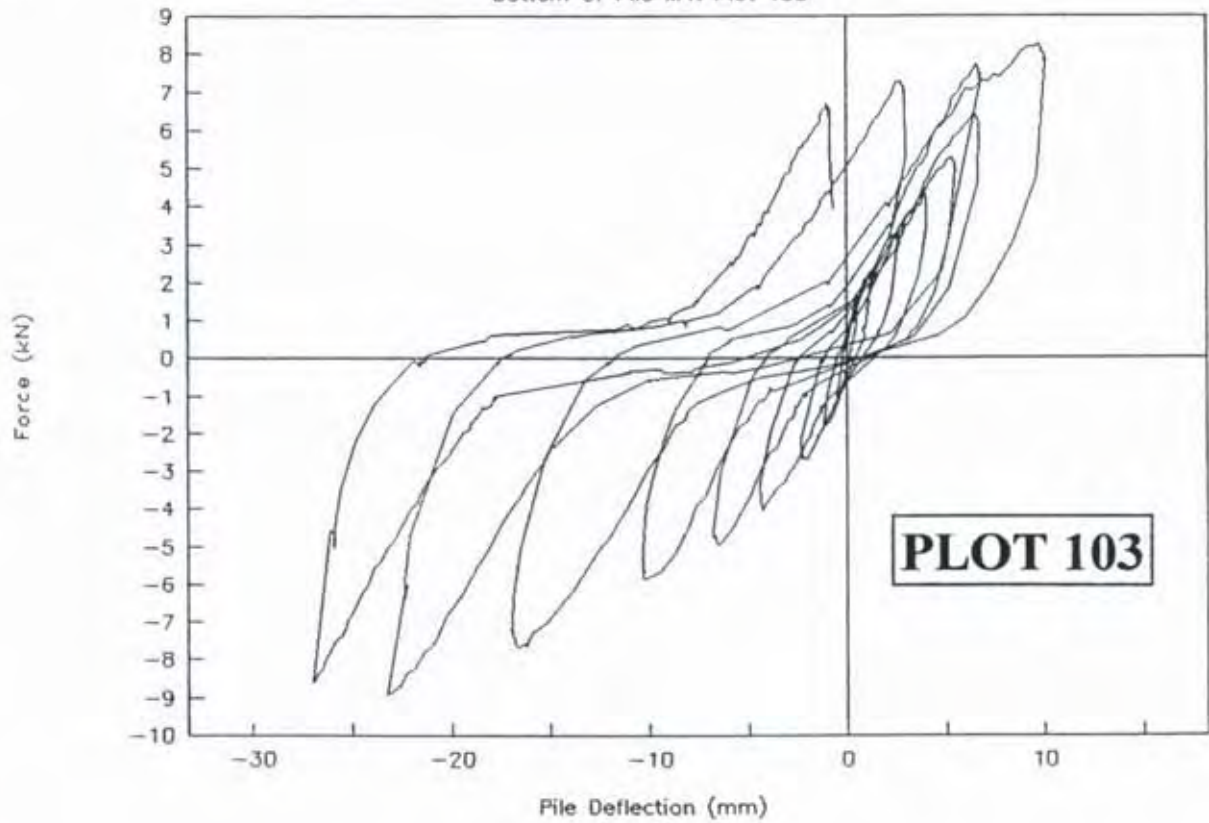
Anchor Piles M3-M4 GROUP 4

Top of Pile M4. Plot 102



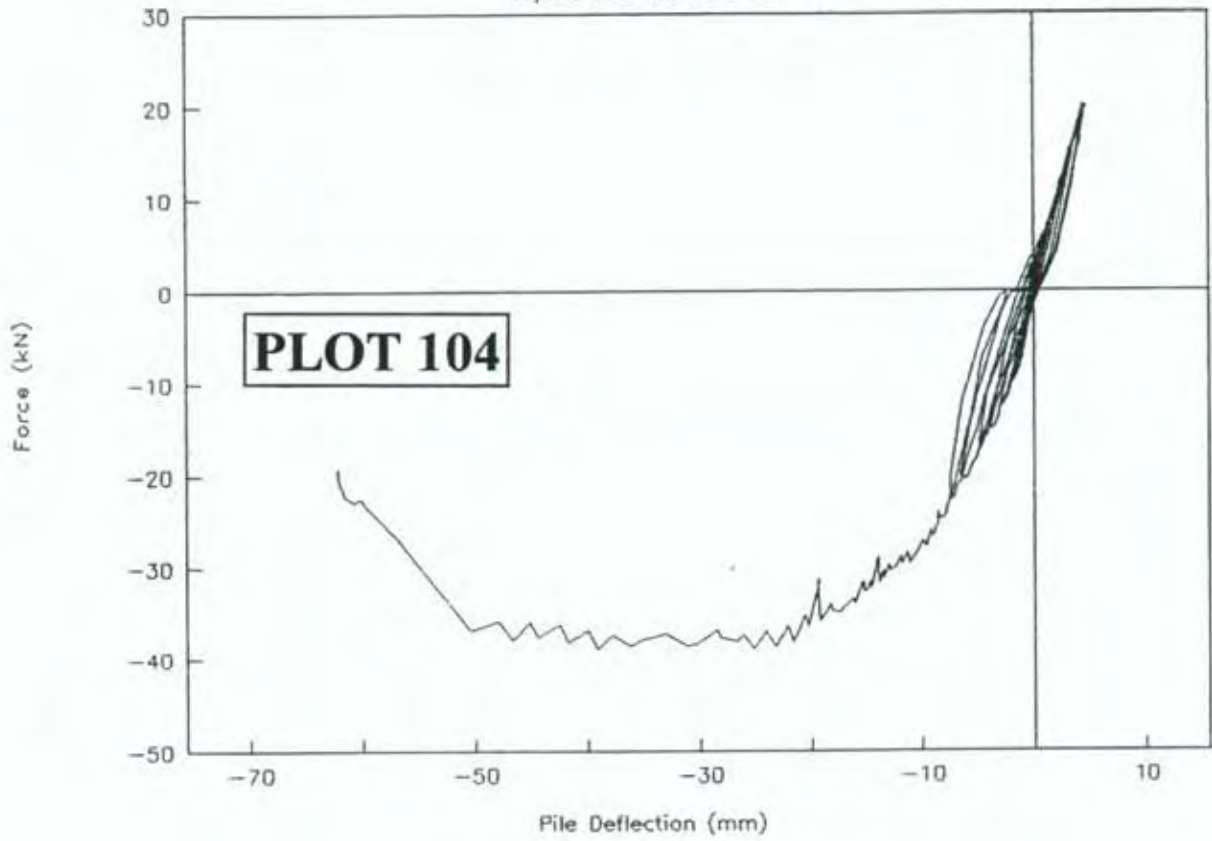
Anchor Piles M3-M4 GROUP 4

Bottom of Pile M4. Plot 103



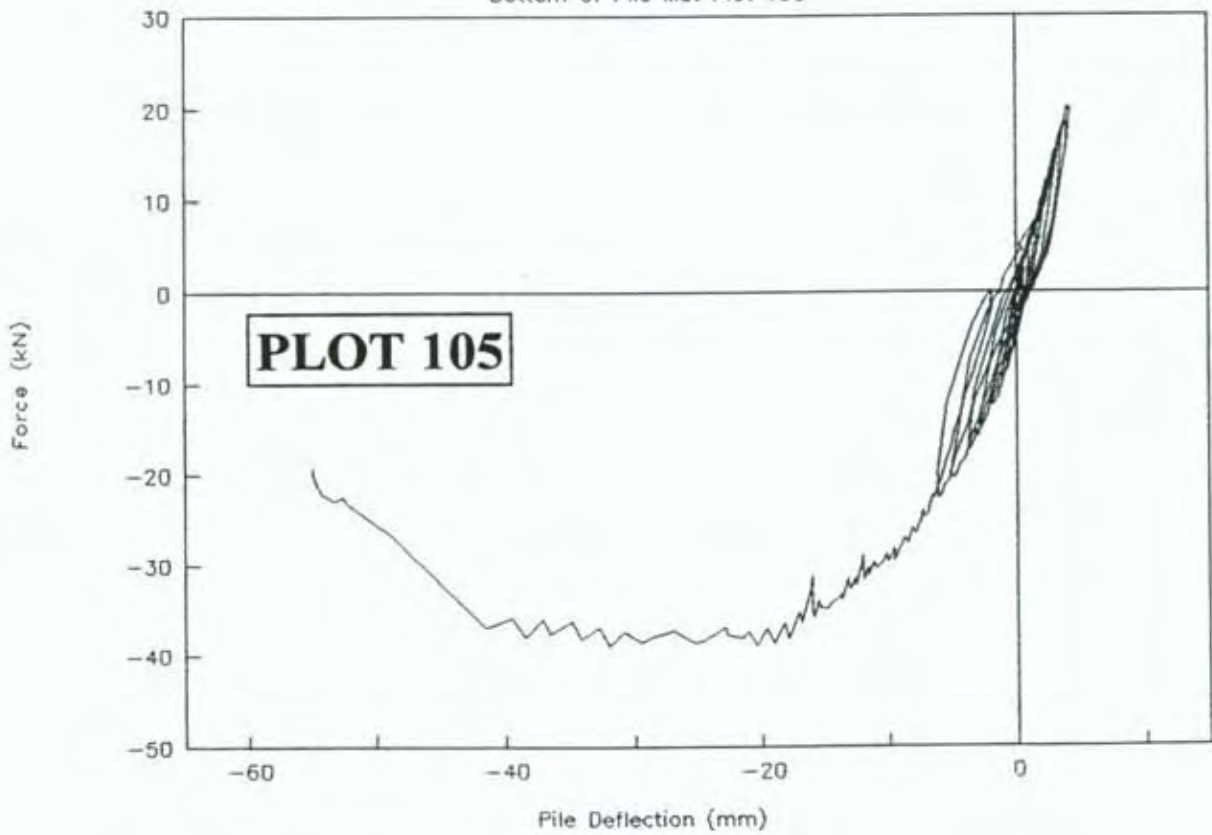
Shear Piles M5-M6 GROUP 4

Top of Pile M5. Plot 104



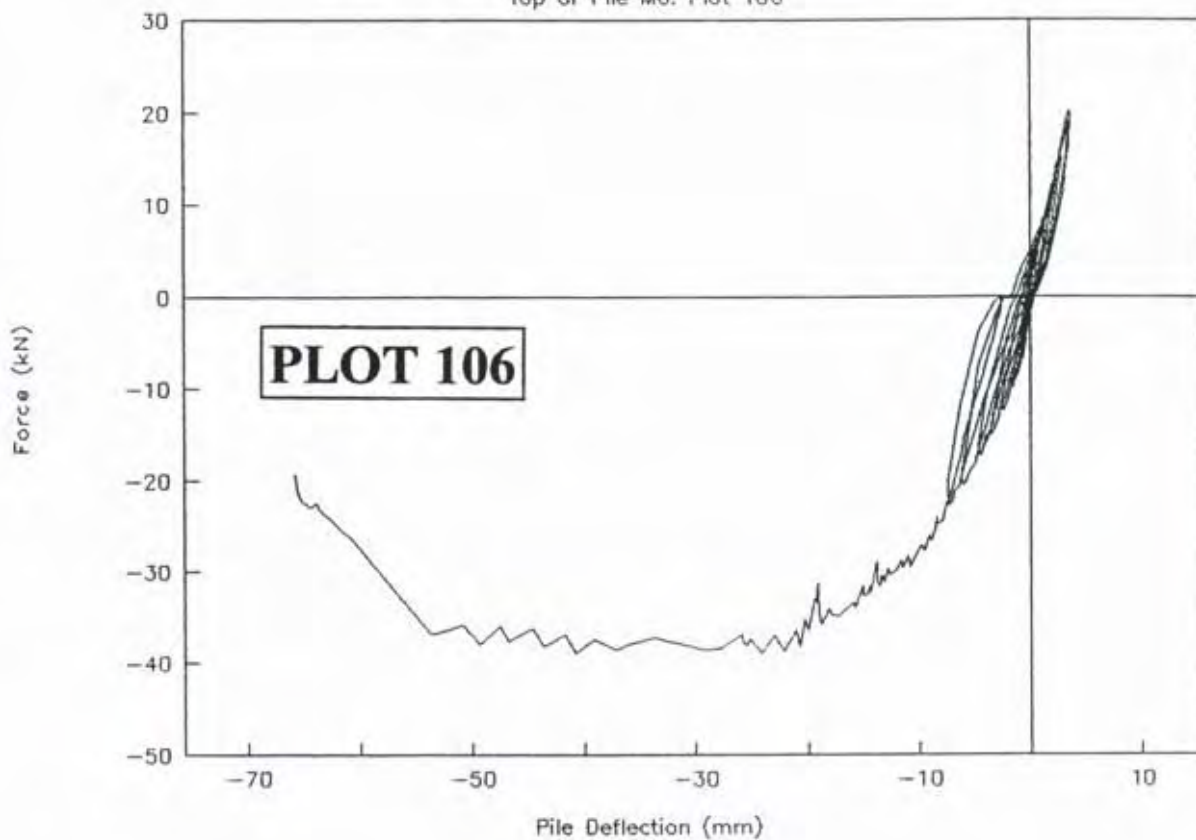
Shear Piles M5-M6 GROUP 4

Bottom of Pile M5. Plot 105



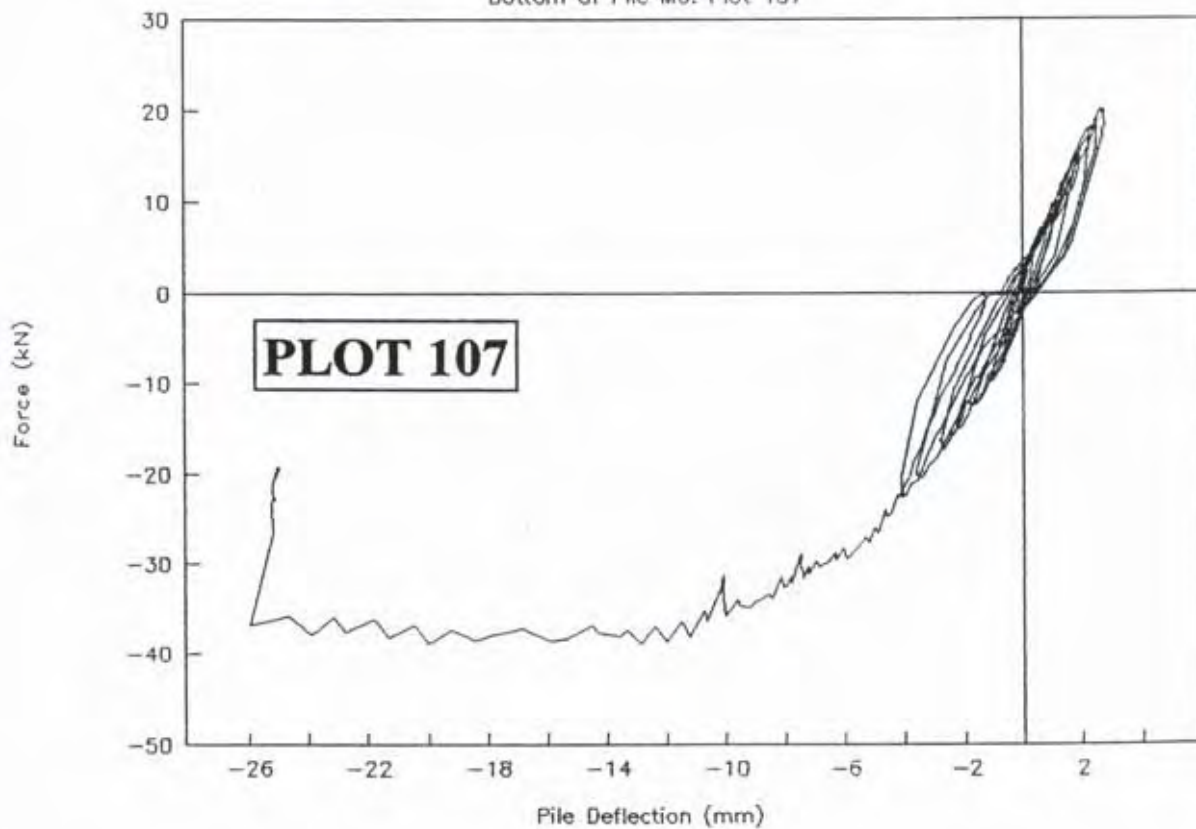
Shear Piles M5-M6 GROUP 4

Top of Pile M6. Plot 106



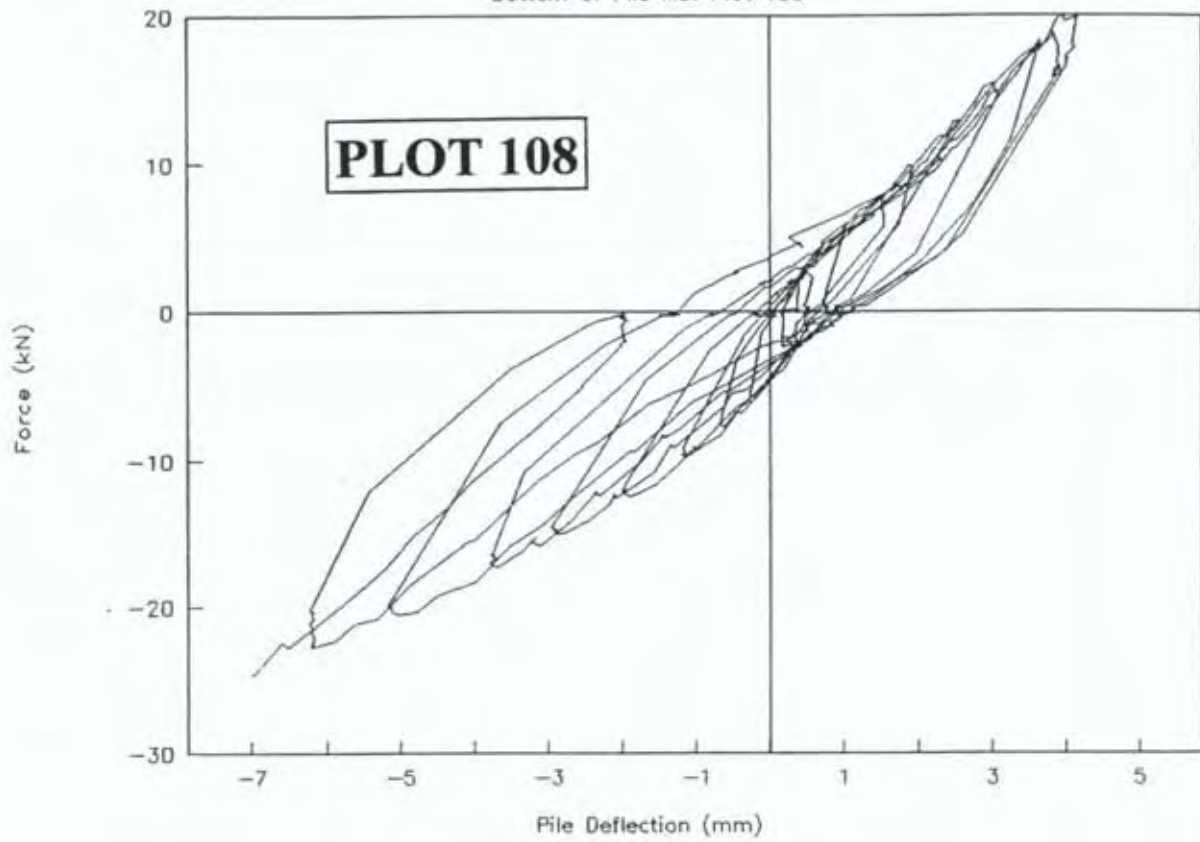
Shear Piles M5-M6 GROUP 4

Bottom of Pile M6. Plot 107



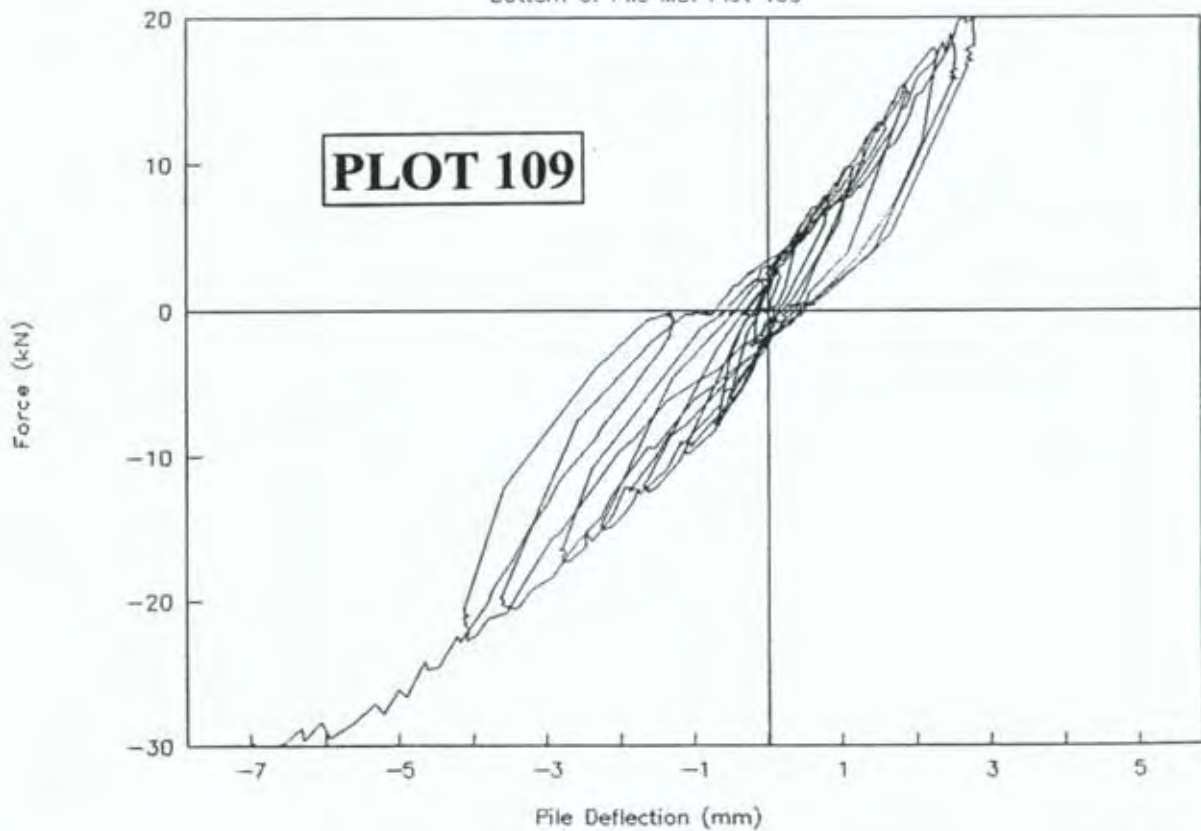
Shear Piles M5-M6 GROUP 4

Bottom of Pile M5. Plot 108



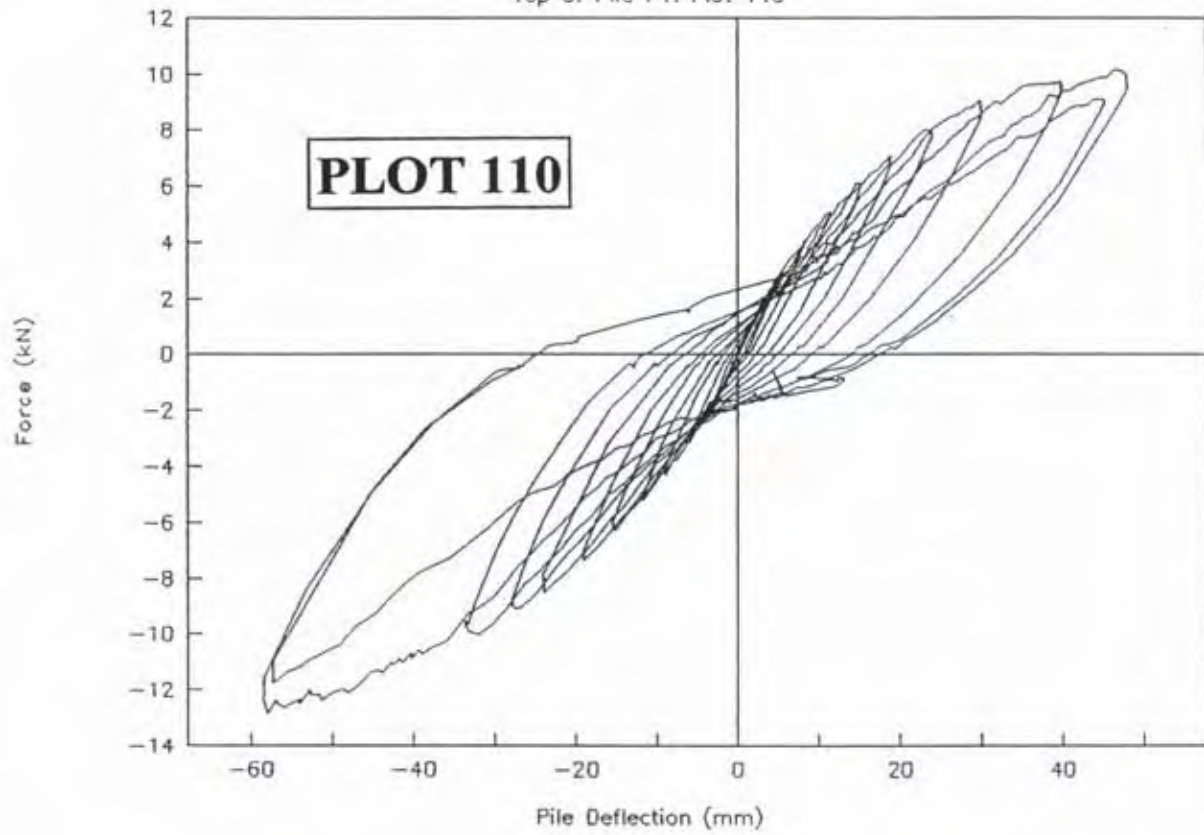
Shear Piles M5-M6 GROUP 4

Bottom of Pile M5. Plot 109



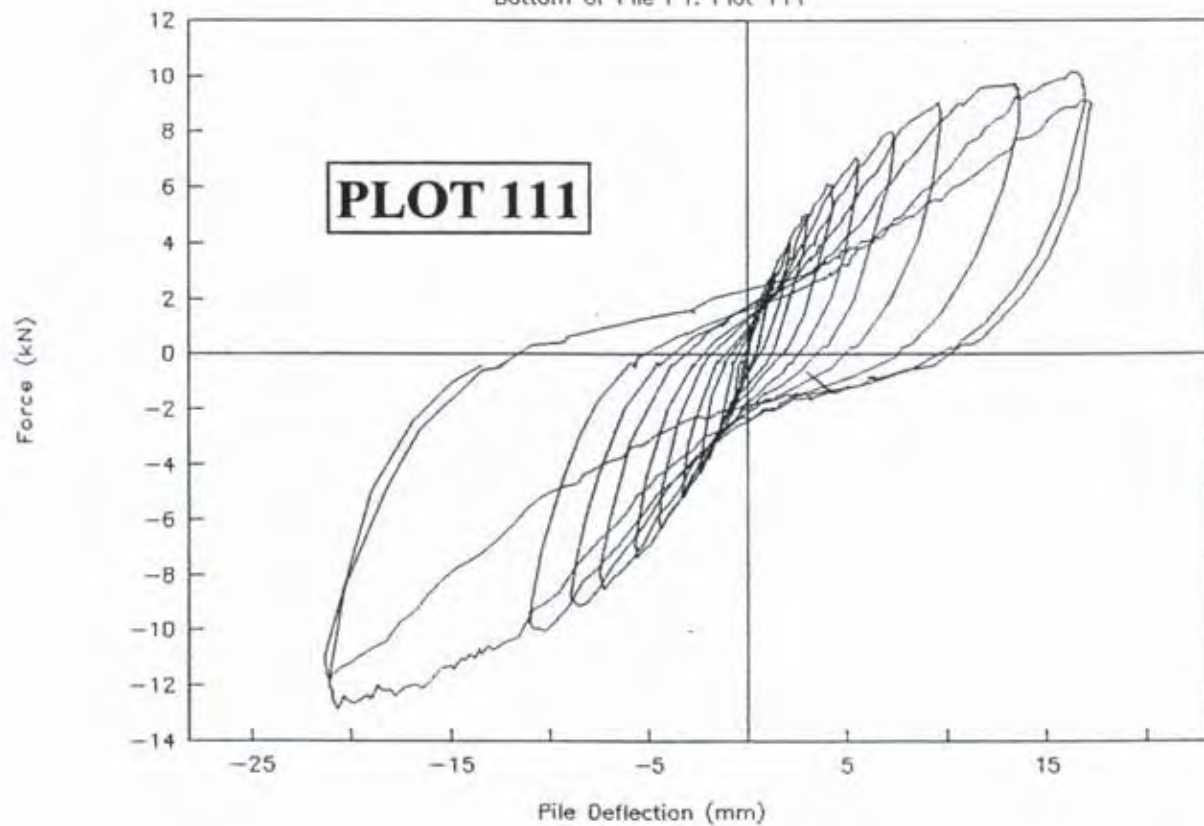
Anchor Piles P1-P2 GROUP 5

Top of Pile P1. Plot 110



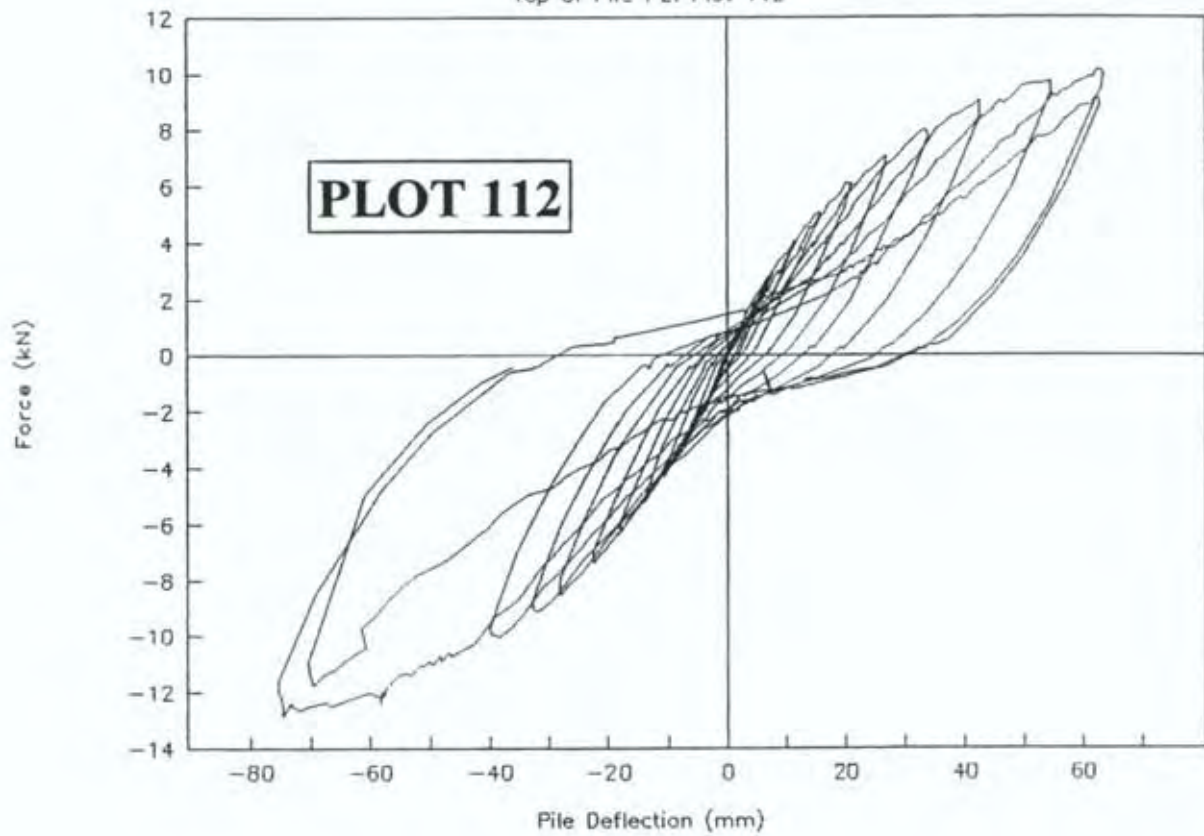
Anchor Piles P1-P2 GROUP 5

Bottom of Pile P1. Plot 111



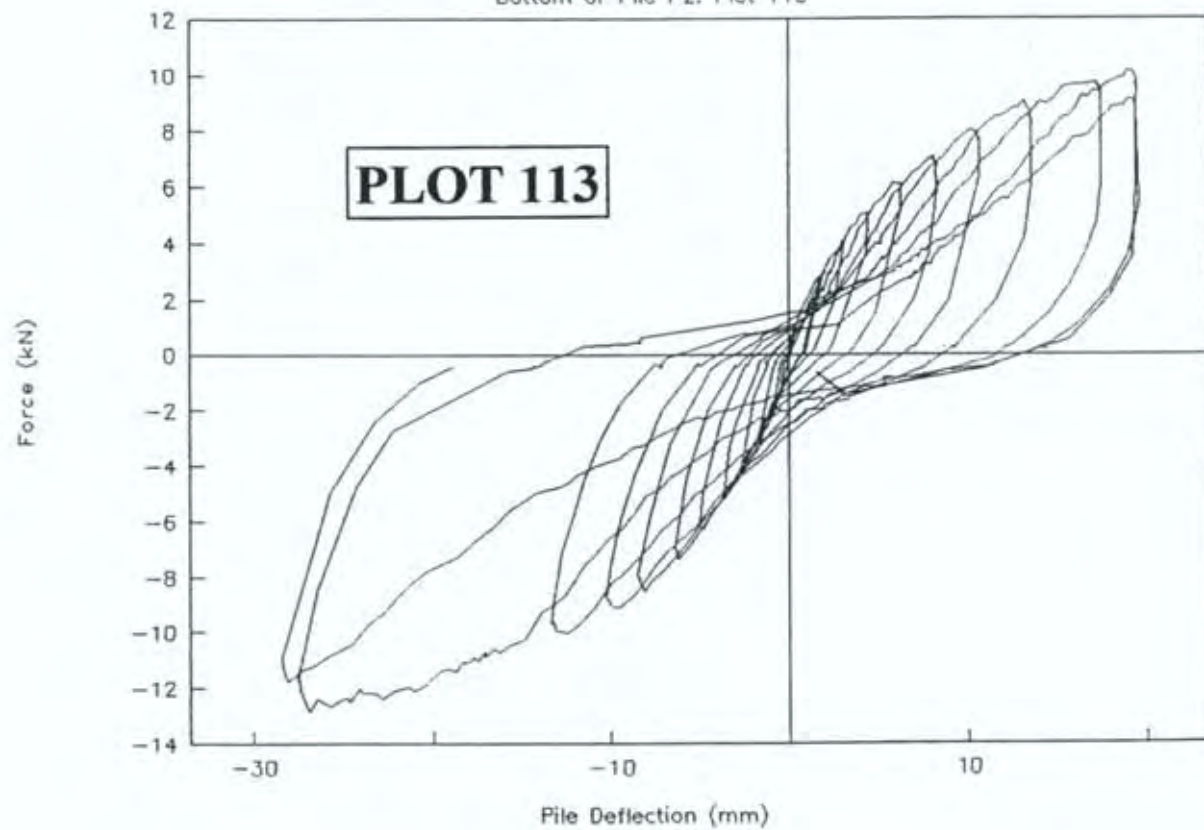
Anchor Piles P1-P2 GROUP 5

Top of Pile P2. Plot 112



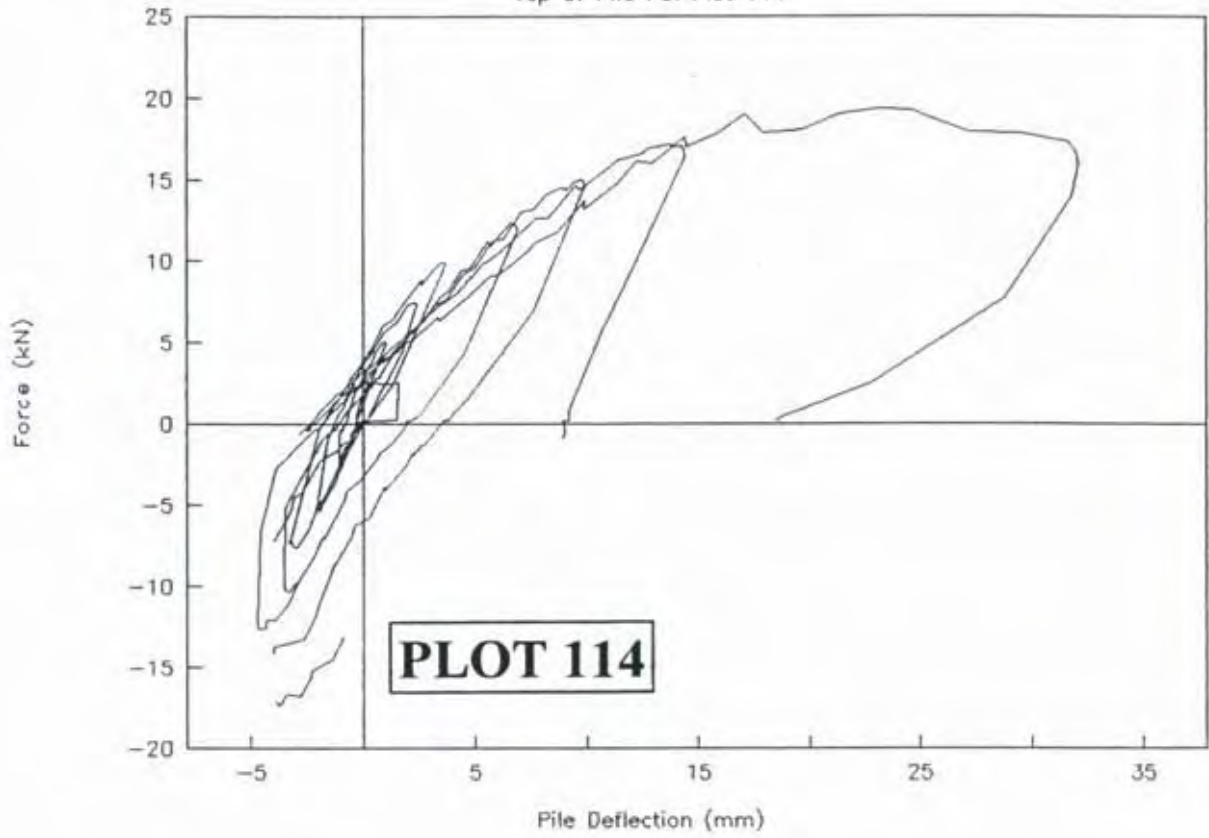
Anchor Piles P1-P2 GROUP 5

Bottom of Pile P2. Plot 113



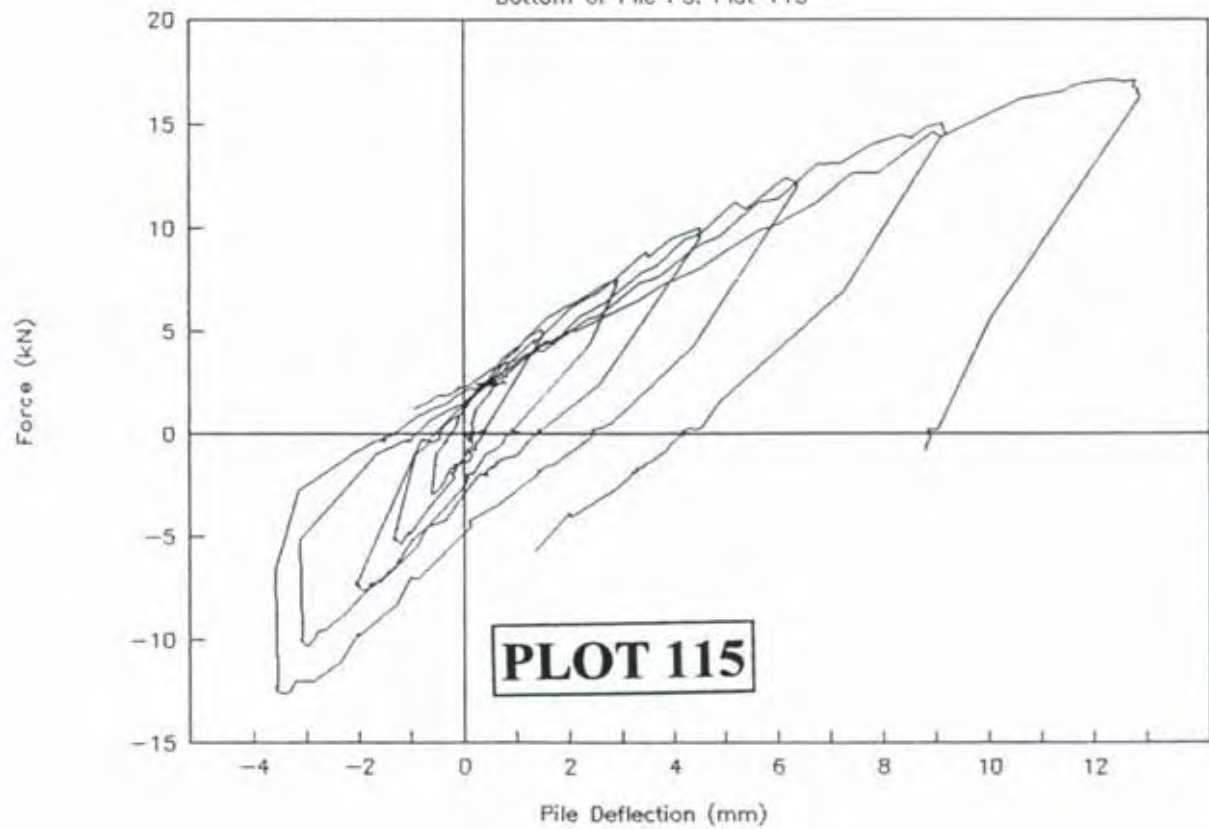
Shear Piles P3-P4 GROUP 5

Top of Pile P3. Plot 114



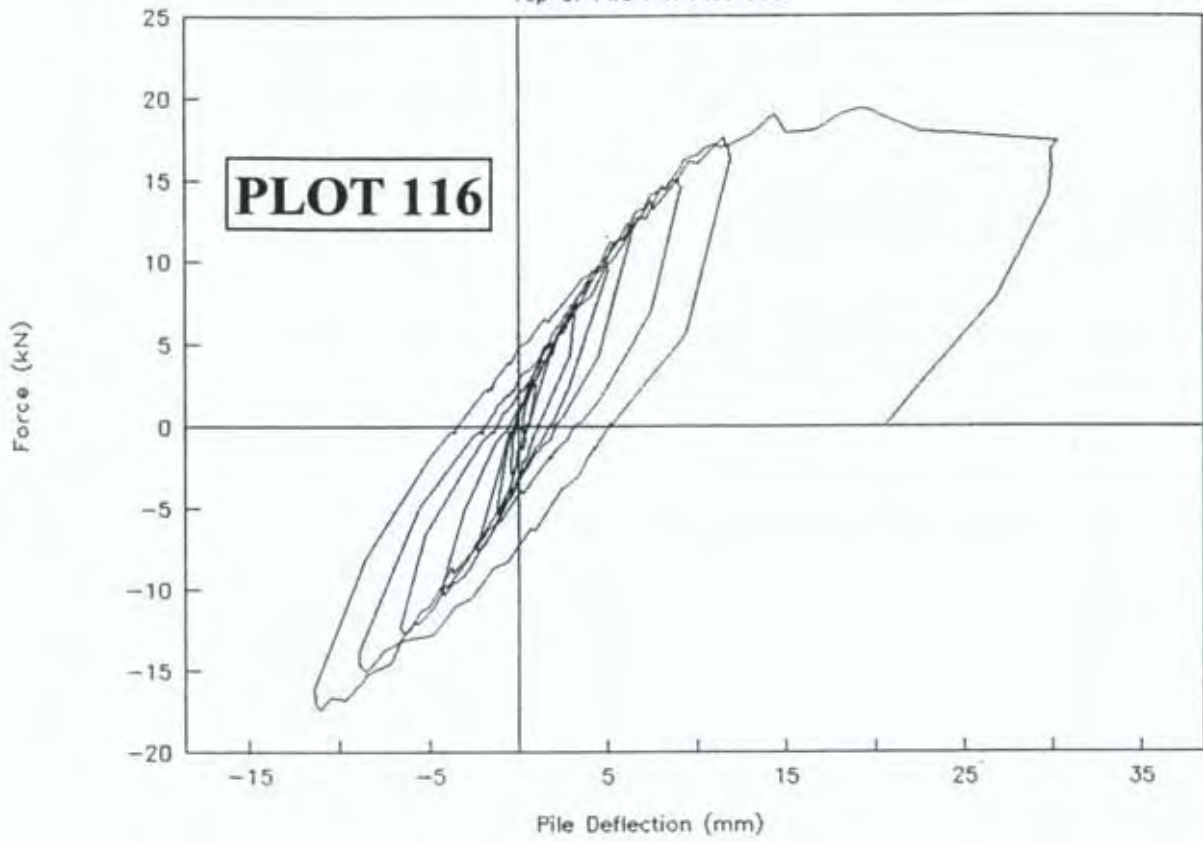
Shear Piles P3-P4 GROUP 5

Bottom of Pile P3. Plot 115



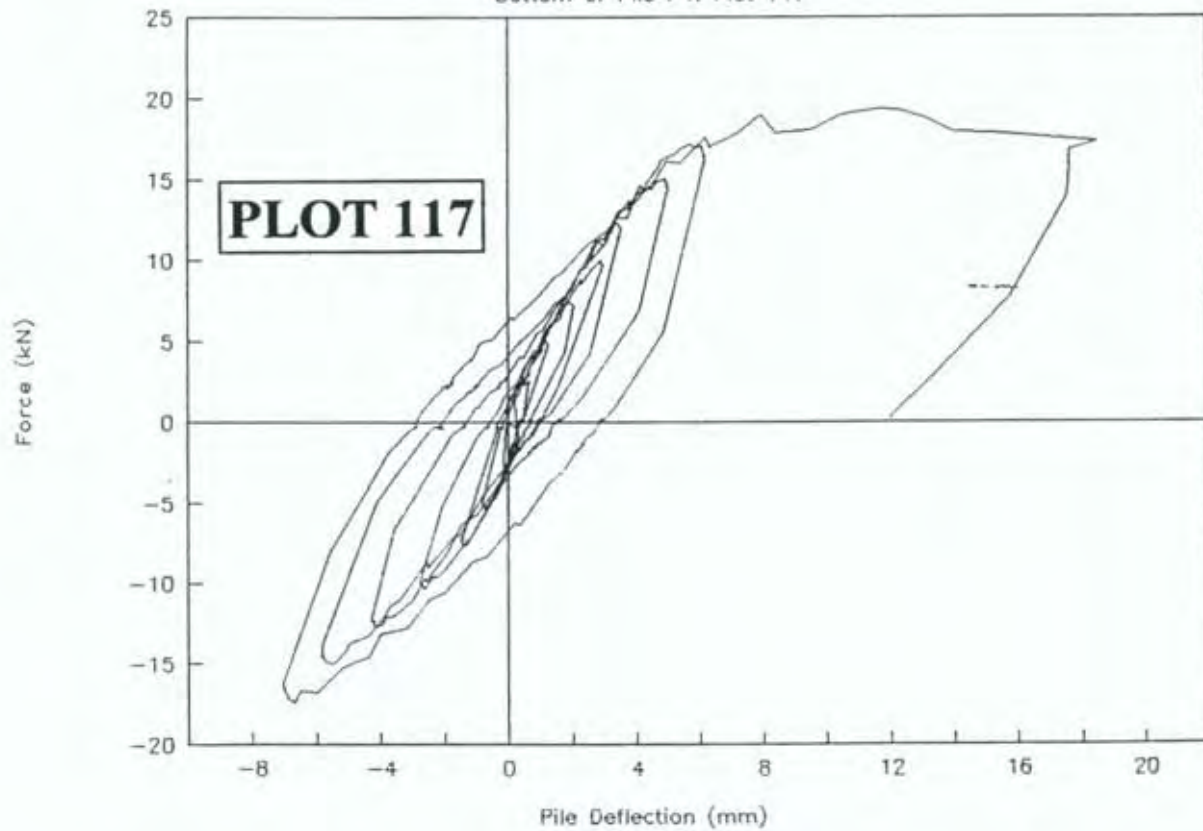
Shear Piles P3-P4 GROUP 5

Top of Pile P4. Plot 116



Shear Piles P3-P4 GROUP 5

Bottom of Pile P4. Plot 117





BRANZ MISSION

To be the leading resource for the development of the building and construction industry.

HEAD OFFICE AND RESEARCH CENTRE

Moonshine Road, Judgeford
Postal Address - Private Bag 50908, Porirua
Telephone - (04) 235-7600, FAX - (04) 235-6070

REGIONAL ADVISORY OFFICES

AUCKLAND

Telephone - (09) 526 4880
FAX - (09) 526 4881
419 Church Street, Penrose
PO Box 112-069, Penrose

WELLINGTON

Telephone - (04) 235-7600
FAX - (04) 235- 6070
Moonshine Road, Judgeford

CHRISTCHURCH

Telephone - (03) 366-3435
FAX (03) 366-8552
GRE Building
79-83 Hereford Street
PO Box 496

